THE APPLICATION OF OPTIMISING CONTROL TO AN HYDRAULIC DRIVE

Thesis submitted for the degree of Doctor of Philosophy of The University of Aston in Birmingham by,

GERALD KIRTON STEEL

October 1968

SUMMARY

An optimising control system has been designed for application to an hydraulic transmission. Optimisation is achieved by an extremum control system which seeks continuously to adjust the transmission to a point of maximum efficiency. The form of extremum control system employed was one developed from the technique of using a periodic perturbation as a probing signal. In these particular circumstances a number of distinctive features have been introduced as modifications of the technique.

The performance of the system was investigated theoretically and it was shown that an optimum design exists. In this the need for rapid adaptation was weighed against the sensitivity of the system to changes of the operating conditions. A system designed to this optimum requirement has been tested experimentally. The results obtained have indicated that the extremum control system is capable of competing only with slow changes in the operating conditions. This is seen to be an inherent limitation of the technique, but some features of the particular form of hydraulic system used were shown to be disadvantageous to this type of control.

In the design of the experimental equipment two significant subsidiary problems have been studied in detail. It was necessary to develop a novel form of control system to regulate the output speed of the transmission. There was also the need to obtain a continuous measurement of the mechanical efficiency and this was met by the development of a unique form of measuring system.

INDEX

	Page
1. Introduction	1
2. Review of extremum control techniques	3
3. Feasibility of an optimising adjustment	9
4. Design of the test rig	23
4.1 Introduction	23
4.2 Choice of control variable	24
4.3 Pump cam control characteristics	24
4.4 Hydraulic system control characteristics	40
4.4.1 Theoretical considerations	40
4.4.2 Experimental results	45
4.4.3 Conclusions	55
4.5 Speed control by feedback	57
4.6 Evolution of the feedforward control arrangement	62
4.7 Feedforward leading to non-interacting control	66
4.7.1 Non-interacting control	66
4.7.2 Non-linear compensation	68
4.7.3 Interaction test	73
4.8 Dynamical characteristics of the variable gain network	75
4.8.1 The problem of gain variation	75
4.8.2 Compensating network	76
4.8.3 Final response characteristics	83
4.9 Evaluation of the results of feedforward control	89

	Page
4.10 Design of the speed control feedback loop	90
4.10.1 General considerations	90
4.10.2 Choice of data for analysis	95
4.10.3 Compensation	98
4.11 Overall characteristics of the speed control system	120
4.11.1 Pump speed variations	121
4.11.2 Transmitted load variations	123
4.11.3 Motor stroke variations	127
4.12 Conclusions on the design of the test rig	131
5. Choice of optimising system	133
6. Design of the optimising system	140
6.1 Measurement of performance curves	140
6.2 Requirements of the perturbation signal	149
6.3 Multiplier - demodulator	154
6.4 Filtering requirements	158
6.5 Further consideration of the overall system	169
6.6 Progress in one cycle	171
6.7 Effect of disturbances	179
6.8 Optimum gain setting	183
6.9 Theoretical performance	193
6.10 Constraints	196
6.11 Choice of perturbation period	198
7. Implementation of the optimising system	200
7.1 General system arrangement	200
7.2 Detail of the integrator	206
7.3 Limit circuit	208
7.4 Multivibrator circuits	213
7.5 Chopper amplifier	215

Page

7.6 Gain setting for the control loop 222
7.7 Setting up procedure 224
7.8 Operating characteristics of the system 225
7.8.1 Fixed operating conditions 225
7.8.2 Varying load conditions 234
8. Review of the system performance 241
9. Conclusion 246
10. Acknowledgements 249
11. References 250

Appendix 252
1. Electrical drive arrangements 252
1.1 Loading generator 252
1.2 Drive motor 253
2. Control of the electrical machines 255
2.1 Characteristics of the speed control system 255
2.2 Generator current control system 260
3. Hydraulic system 265
3.1 Machines 265
3.2 Hydraulic circuit 265
3.3 Stroke control arrangements 267
4. Feedforward amplifier 272
5. Measurement of efficiency 272
5.1 Torque measurement 274
5.2 Mechanical design of the torque tube 278
5.3 Electrical design 280
5.4 Efficiency computation 282
5.5 Servo-balancing system 286
5.6 Speed signal amplifiers 292
5.7 Setting-up procedure 294
5.8 General observations 296

LIST OF PRINCIPAL SYMBOLS

A	Chopper amplifier gain	p.222
a	Potentiometer ratio	p.284
a_1, a_2, etc.	Frequency response angle curves	
C	Compliance	Fig.4.9
C_o, C_1, ., C_n	Components of filter output	p.162
$E\omega$	Feedforward voltage signal	Fig.4.20, Eq.4.22
F_1	Function of $\alpha\tau$	Eq.6.30
F_2	Function of $\alpha\tau$	Eq.6.32
$F(j\omega)$	Response function	Eq.4.4
$f(s)$, $f(j\omega)$	Response function	Fig.4.4
G, g	Slope of performance curves	Eq.6.7
$G(j\omega)$	Hydraulic system response function	Eq.4.36, Fig.4.31
H	Perturbation signal	p.173
h	Amplitude of perturbation signal	p.173
$h(j\omega)$	Response function	Fig.4.7
J	Moment of inertia	Fig.4.9
J_o	Moment of inertia	Eq.4.8
j	Imaginary operator	

K	Gain constant	Eq.4.9
	Demodulator gain	p.155
k	Potentiometer constant	Fig.4.4
K_g	Gain constant	Fig.4.31
K_f	Gain constant	Eq.4.5
m_1, m_2, etc.	Frequency response modulus curves	
$N(j\omega)$	Compensating network response	Fig.4.31
P_p	Pump output pressure	Fig.3.2
P_m	Motor input pressure	Fig.3.3
Q	Generalised disturbance	p.179
q	Fluid displacement per revolution	Eq.3.5
R_p	Leakage resistance	Fig.3.2
R_s	Series resistance	Fig.3.2
R_1	Input resistance	Fig.4.20
R_2	Feedforward resistance element	Fig.4.20 Eq.4.20
R	Input resistance	p.222
r	Damping resistance	Fig.4.9
s	Complex frequency variable	
T	Time constant of hydraulic system	Eq.4.9
T	Integrator time constant	Fig.6.16
T_f	Time constant	Eq.4.5
T_m	Load torque	Eq.3.7
U	Parameter of performance curves	Eq.6.27
V_r	Reference voltage	Fig.4.19
V_e	Voltage error	Fig.4.1
V_ω	Speed feedback voltage	Fig.4.1
v	Position pick-off voltage	Fig.4.4

W_l	Power loss	Eq.3.2
W_t	Transmitted power	Eq.3.2
w	Power loss function	Eq.3.8
w_o	Constant power component	Eq.3.8
Y_1, Y_2	Transfer admittance	Fig.4.24
$Y(j\omega)$	Response to disturbance	Eq.4.37
$y(j\omega)$	Inverse of open loop response	Eq.4.38
Z	Efficiency Performance measure	
Z_o	Sampled value of Z	p.159
$Z(s)$	Input to sampling filter	p.161
$Z^*(s)$	Sampled signal	p.161
z	Damping ratio	Eq.4.9
α	Gain constant	Eq.6.10
ΔZ	Output of sampling filter	p.161
$\delta(V\omega)$	Effect of load change	Fig.4.31
μ	Potentiometer constant	Eq.4.16
ψ	Motor stroke	Sec.6
ψ_m	Motor stroke	Sec.3
ψ_p	Pump stroke	Fig.3.1
ψ_{opt}	Optimum stroke setting	p.185
ψ_H	Progress in one cycle	Eq.6.17
ψ_Q	Effect of disturbance	Eq.6.26
ψ_a	Perturbation amplitude	p.155
λ	Interval between samples	p.161
$\bar{\phi}_1$, $\bar{\phi}_2$	Perturbation signals	Fig.7.1
ϕ_1, ϕ_2	Demodulator output signals	Fig.7.1

$\bar{\phi}_p$	Pump flow	Fig.3.2
$\bar{\phi}_m$	Motor flow	Fig.3.2
$\bar{\phi}_{mo}$	Motor flow for minimum loss	Eq.3.4
ϕ_p	Leakage flow	Fig.3.2
τ	Period of perturbation signal	p.171
ω	Angular frequency	
ω_i	Input speed	Fig.4.9
ω_o	Output speed	Fig.4.9
	Sampling frequency	p.161
ω_m	Motor speed	p.10
ω_p	Pump speed	Fig.3.1

(1) INTRODUCTION.

The philosophy of continuous optimisation has attracted considerable attention over the past fifteen years. In that time a number of different forms of system have been studied. Of these the ones which seek to hold a performance measure at its maximum, or minimum, value are of particular interest. These systems are sometimes called "extremum control systems". The great majority of the published work has been concerned with the theoretical appraisal of the different forms of system. In some cases analogue computer studies have been used to reveal aspects of the system performance in a simulated environment. But there remains a considerable gap between the theoretical possibilities and the achievement of fully engineered applications.

Some of the reasons for this are immediately obvious. The first requirement is that the optimum setting of the process must be continually changing. It is also to be presumed that the setting is not predictable from measurements on the variable conditions. The fact that extremum control is technically possible is by no means the justification for its use. In the majority of cases the economic value of the arrangement is the ultimate justification. In this the capital value of the improved performance must be off-set against the cost of the control system. It follows then that extremum control systems will normally only find application where the capital value of the performance improvement is great. These restrictions are sufficient to ensure that there are few practical cases where this form

of control system may be successfully applied.

Tha capabilities of extremum control systems are also restricted. There are inherent limitations to what can be achieved. Some forms of system are better than others in particular circumstances. The ability to maintain adequate control is then by no means assured without careful attention to the particular characteristics of the controlled process.

In the work described here the objective has been to apply an optimising system to the particular case of a hydraulic transmission. The form of transmission used was one providing a constant speed drive from a variable speed prime mover. One application for this type of transmission is found in the drive for an alternator from an aircraft engine [14]. Hydraulic transmission offers an effective means of obtaining an accurately controlled speed, but in many applications it is not used because the efficiency can be low. The possibility of improving the efficiency provides the motive for applying an optimising system. In this the efficiency is used as a performance measure. An adjustment of the efficiency is possible when a hydraulic motor with variable stroke is used. The setting required to give maximum efficiency changes with the operating conditions and the optimising system is designed to follow the maximum point as it moves.

(2) REVIEW OF EXTREMUM CONTROL TECHNIQUES

The distinctive problem of controlling a process to maintain a performance measure at its maximum or minimum value was recognised as early as 1950. Up to that time closed loop control had been considered only in terms of systems in which a prescribed value of the performance measure was to be maintained. In this conventional control technique a determination of the performance measure at a given instant in time is used to give an error signal. This signal indicates the difference between the desired value and the current value of the performance measure. It is important to note that the error signal is defined by a single measurement of the performance measure at the required instant. In contrast, extremum control depends on determination of the way in which the performance measure changes with adjustment of the controlled variable. A measure of the slope of the performance curve is required. The slope of the curve cannot be obtained from a single observation of the performance measure. In principle no less than two observations must be made at different values of the controlled variable. This need to extend the measurements over a range of values of the controlled variable is the main distinctive feature of extremum control. Subsequent closed loop control action, based on the slope measurement, is required to drive the controlled variable to the point of zero slope and hence the extreme of the performance measure. Such control action is subject to the same

considerations as in conventional control technique. The essential problem of extremum control therefore resides in the determination of the slope of the performance curve.

A variety of solutions to the problem have been proposed. Other terms such as 'optimising control', 'optimalising control', 'adaptive control' and 'hill-climber' have been used to describe the general category of extremum control systems. The broad principles of operation of these systems were identified in the first ten years of development, from 1950 to 1960. There have been several papers devoted to giving a review of these principles, of which Eveleigh[1], Blackman[2], Grensted[3] and Will[4] are typical. These authors are not agreed on the way in which the various forms of system should be categorised and an alternative view will be developed here. There also remain some distinctions of terminology which have not been entirely resolved. The chief point of distinction lies in the use of the term 'adaptive control'. For instance Eveleigh[1] takes as his definition, 'An adaptive system is one which is provided with a means of continuously monitoring its own performance in relation to a given figure of merit or optimum condition and a means of modifying its own parameters by closed loop action so as to approach this optimum'. This definition is in such broad terms as to admit conventional control systems as well as extremum control systems. Others have taken a more restricted view. Will[4] requires that in an adaptive system the performance measure must be based on the

dynamical characteristics of the controlled process, e.g. the impulse response. In this case not all extremum control systems would be classified as 'adaptive systems'. It remains that the features of the extremum control system are quite distinctive in principle and we may agree to describe these as adaptive in character.

That some extremum control systems depend on a measurement of the dynamical characteristics of the controlled plant is an important distinction. Dynamical response can only be measured over an extended period of observation. This requirement places restrictions on the hill-climbing system. In the type of application considered here the performance measure is not a measure of the system dynamics. Therefore in the discussion which follows this will be presumed to be the case.

In categorising the various forms of system under consideration it will be assumed that in all cases the performance measure is available continuously. Attention will also be confined to optimisation with respect to a single controlled variable.

Systems differ in their mode of search in determining the slope of the performance curve. A distinction will first be drawn between two broad groups. In one group the search technique is based on a deterministic sequence of changes in the controlled variable. In the other group the sequence of changes is made to depend on the performance measure and ultimately becomes stochastic in nature. Typical of the first category

are systems which use a periodic perturbation of the controlled variable e.g. a sinusoidal wave-form and a square wave-form. Everleigh[5], Jelonek[6] and Roberts[7] have written at length on the general theory of the operation of systems with a sinusoidal perturbation. Douce[8] has taken up the case of the square wave-form. A further refinement uses a pseudo-random sequence as test signal[9].

Aperiodic systems which have been described fall into two categories. Firstly there are those which make step changes in the controlled variable[6]. The step may be of fixed length but the direction controlled by the success or failure of the previous steps in moving up the performance curve. Other arrangements provide for an adjustment of the step length in relation to estimates of the gradient of the performance curve. The alternative to the stepping system is to use a ramp function adjustment of the controlled variable. The adjustment becomes aperiodic when the point of reversal of the ramp movement is chosen to depend on the performance measure. The 'peak-holding' system of Tsien[10] is of this form. Systems of this type have been analysed by Morosanov[11] and with some refinements have been applied by Perret[12].

Recent work has been done on systems which combine periodic and aperiodic elements in the search technique[8],[9]. In these systems a periodic perturbation is used to obtain a good estimate of the slope of the performance curve at a given setting of the controlled variable. Step adjustments are then

made at the end of the test period on the basis of the slope estimates obtained. This type of system is distinguished by the fact that the process of slope measurement is separated from that of movement towards the optimum setting. In other systems the search action and the movement towards the optimum are superimposed.

With this variety of forms of system available it becomes a fundamental problem to decide which system will be best for a given application. In making this choice it has been recognised[3],[7] that measurement noise is one of the chief factors to be considered. This noise has been broadly defined to be fluctuations in the performance measure due to causes other than the controlled variable. Roberts[7] has shown, under broad assumptions, that the type of system using a sinusoidal perturbation is best when measurement noise is significant. Jelonek[6] has compared this type of system with some aperiodic stepping systems and reached similar conclusions. This comparison is not conclusive however and there are reservations depending on the particular form of system design.[6]

The fundamental problem is that of compromise between two conflicting requirements. On the one hand there is the need to obtain an accurate measurement of the slope of the performance curve. But on the other hand there is the requirement for rapid control action to persue a moving optimum point. Measurement noise makes it necessary to extend the observation time in order to obtain an accurate slope measurement and this is not consistent with the need for rapid control action.

The final choice of the best system for a given application is therefore very much dependent on the extent of measurement noise in the performance measure.

It is notable that the attention given to the broad theoretical justification for using extremum control, greatly exceeds that given to the application to industrial equipment. Perret [12] has made reference to tests conducted in applying an aperiodic ramp perturbation in the control system for an alternator. The system seeks the point of minimum reactive volt-amperes by adjustment of the excitation. These tests gave no attention to the problem of measurement noise and the need to track a moving optimum point. Moran [13] has made a thorough investigation of the application to optimisation of steam generating plant. The special problems of this situation required that the system used a digital computer, connected 'on-line' to the plant. In this work the problem of making an assessment of the overall performance of an optimising system has been exemplified.

The results of these application studies do not contribute directly to an understanding of the case considered here. Neither is it possible, on the basis of the published literature, to decide on the best form of system to be used in this case. In these

circumstances it was decided to design a system to best exploit the particular situation as it emerged. The resulting system was basically one using a periodic perturbation but it differs in detail and performance from what has previously been described. In the design of this system emphasis is given to the need to track a moving optimum point and it is shown that there is an optimum choice of design parameters in this case.

(3) FEASIBILITY OF AN OPTIMISING ADJUSTMENT.

The form of transmission system chosen for this work was one required to provide a constant output speed while the input speed, from the prime mover, was varied. Normally a variable stroke pump, feeding a fixed stroke motor is used for this purpose. The output speed is then controlled by a feedback system manipulating the pump stroke[14]. In this case variable stroke machines were used for both the pump and the motor. The adjustment of motor stroke provides a means of changing the pressure and flow conditions in the hydraulic circuit. This feature then offers the possibility of locating a point of maximum efficiency. The optimising control system is required to adjust to the point of maximum efficiency automatically.

In the first instance the feasibility of making this optimising adjustment is studied. It is required to assess the range of operating conditions over which

an optimising adjustment can be made. This depends on being able to show that the efficiency will pass through a maximum as the flow and pressure in the hydraulic circuit are changed. For the hydraulic machines available it is then possible to define the range of operating conditions within which the optimising system must work. This in turn indicates the appropriate choice of machines for driving and loading the transmission.

A simplified diagram of the transmission is shown in Fig.(3.1). Rotation of the drive shaft causes a fluid displacement in the pump which must be balanced by a flow through the motor. A differential pressure between the inlet and outlet ports of the motor is set up to meet the torque requirements of the load. If the leakage of fluid past the pistons in the machines is neglected, the balance of fluid flow between pump and motor demands that,

$$\Psi_m \omega_m = \Psi_p \omega_p \quad \ldots\ldots\ldots\ldots\ldots\ldots\ldots (1.1)$$

when the pump and motor are identical machines. If the input and output speeds are fixed the ratio of the strokes Ψ_m and Ψ_p is fixed. But there is room for varying the value of each while keeping the ratio constant. The effect of changing the stroke settings is to alter the pressure and flow in the hydraulic circuit. When the load torque and speed are held constant the transmmitted power is constant and the product of pressure and flow is constant.

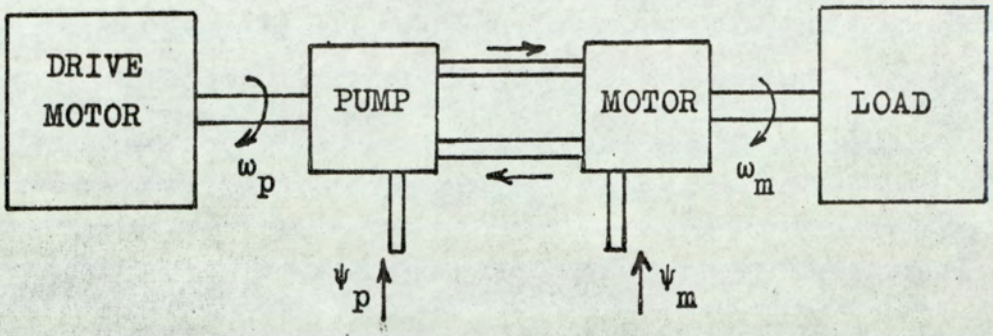

FIG.(3.1)

BLOCK DIAGRAM

A reduction of motor stroke ψ_m requires a corresponding reduction of the pump stroke ψ_p to keep the speed constant. At the same time there is a reduction in the fluid flow with a corresponding increase in the pressure. Thus flow can be exchanged for pressure. Some of the loss of energy in the system is attributable to the flow and some to the pressure and thus the possibility exists in principle, of finding an optimum setting of motor stroke which minimises the loss in the system.

The following analysis shows more precisely how this exchange takes place. M.K.S. units are used.

The pump is regarded as a source of flow $\mathbb{Q}_p$ (m^3/sec) which is diminished by leakage flow ϕ'_l. The leakage is presumed proportional to pressure to simplify the analysis. There is also a drop of pressure, as a result of the fluid flow, leading to a nett output pressure P_p (N/m^2). On the assumption of linearity we may regard the relationship between these variables as represented by the "equivalent circuit" of Fig.(3.2). The resistance elements are defined by the ratio of pressure to flow ($N.m^{-5}.s$). It might be argued that the element R_p should be connected across the output terminals of the equivalent circuit, rather than across the source. The distinction is unimportant however in this case because the series resistance is expected to be very much less than the parallel resistance. If a better approximation is required it

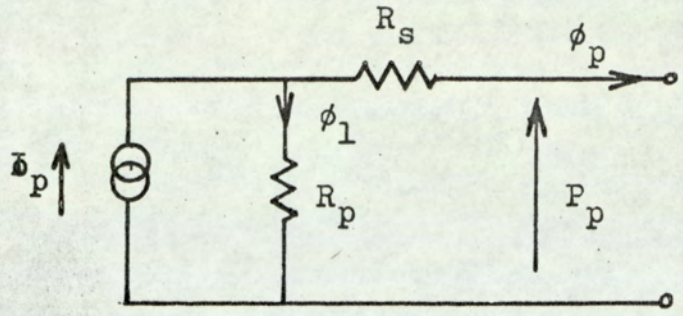

FIG.(3.2)

EQUIVALENT CIRCUIT OF PUMP

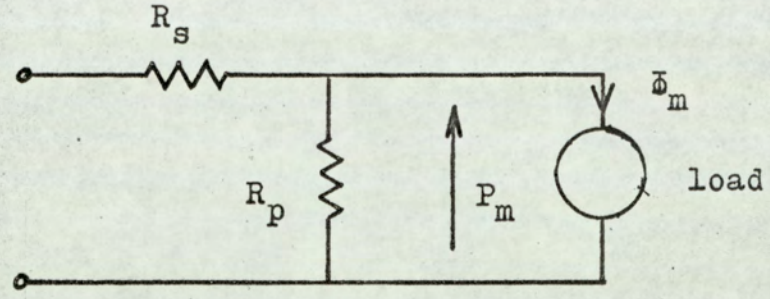

FIG.(3.3)

EQUIVALENT CIRCUIT OF MOTOR

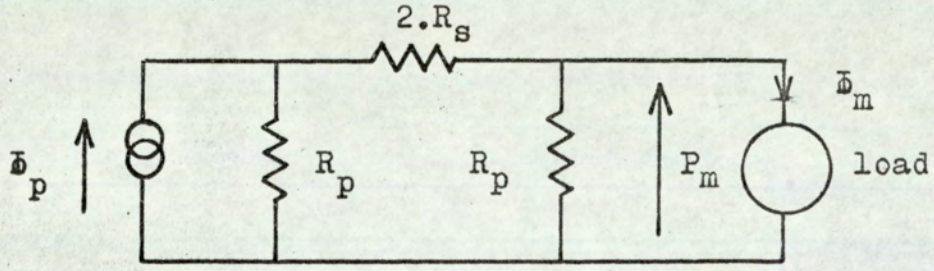

FIG.(3.4)

COMBINED EQUIVALENT CIRCUIT

would be appropriate to place two series elements, $R_{s/2}$, on either side of R_p.

The motor used in the transmission system is a similar machine to the pump. It will be assumed that the machines are identical so that the equivalent circuit of the motor may be drawn as shown in Fig.(3.3).

When the pump and motor are combined the complete equivalent circuit becomes as shown in Fig.(3.4).

Now, assuming that R_s is very much less than R_p, the power loss in the system is,

$$W_l = 2 R_s \Phi_m^2 + 2 \frac{P_m^2}{R_p} \quad \ldots\ldots\ldots\ldots\ldots(3.2)$$

The power transmitted by the drive is W_t, equal to $P_m \Phi_m$ (W), so that equation (3.2) may be written,

$$W_l = 2 R_s \Phi_m^2 + 2 \frac{W_t^2}{\Phi_m^2 R_p} \quad \ldots\ldots\ldots\ldots(3.3)$$

If the power transmitted is constant we get the condition for minimum loss when $dW_l/d\Phi_m = 0$ which gives,

$$\Phi_{mo} = \sqrt{\frac{W_t}{\sqrt{R_s R_p}}} \quad \ldots\ldots\ldots\ldots\ldots\ldots\ldots(3.4)$$

as the value of the flow for minimum loss.

This flow condition is to be set by adjustment of the motor stroke Ψ_m. If the variable Ψ_m is defined

to be proportional to the motor stroke and take the value of unity at full stroke, then

$$\Phi_m = \frac{\omega_m \Psi_m q}{60} \qquad \ldots\ldots\ldots\ldots\ldots\ldots\ldots\ldots (3.5)$$

where q is the fluid displacement per revolution at maximum stroke and ω_m is in r.p.m..
Substitution from equation (3.5) into equation (3.4) gives the optimum motor stroke,

$$\Psi_{mo} = \frac{360\ W_t}{\omega_m^2\ q^2 \sqrt{R_s\ R_p}} \qquad \ldots\ldots\ldots\ldots\ldots\ldots (3.6)$$

It should now be noted that for the purpose of this work it is the efficiency of the complete transmission which is the object of consideration. The analysis must therefore include the frictional losses in the pump and motor. The above results are based on an approximate view of the hydraulic circuit alone. In order to accommodate the frictional losses it will be assumed that they can be related to the pressure and flow in the hydraulic circuit. This is justified in that a large proportion of the frictional loss will be due to the piston mechanism, in which the loading is proportional to pressure and the movement proportional to stroke. It is therefore proposed to include the loss attributable to pressure by modifying R_p. Similarly the effect of stroke changes on the friction will be included in R_s. The circuit of Fig.(3.2) may then be regarded as representing the overall terminal properties of the pump rather than

the fluid system alone.

In view of this we may now recognise that the transmitted power W_t can be equated to the mechanical output power of the motor. Taking T_m as the load torque, the output power becomes $\omega_m T_m/60$. On placing this in equation (3.6) we have the optimum motor stroke as,

$$\psi_{mo} = \frac{60\ T_m}{\omega_m\ q^2 \sqrt{R_s\ R_p}} \qquad \ldots\ldots\ldots\ldots\ldots\ldots (3.7)$$

This indicates that when the motor speed ω_m is constant the optimum stroke setting increases in proportion to the load torque. It is significant that the pump speed does not appear to affect the result. This analysis cannot be relied upon to indicate this conclusively however since broad approximations have been made. It is to be expected that the input speed will have some influence on the optimum stroke position but that the load torque is the dominant variable. The effect of changes in the fluid temperature may be inferred from equation (3.7). A rise in temperature will reduce the viscosity of the fluid . This will reduce the effective values of R_s and R_p. The result will be to move the optimum stroke setting to a larger stroke.

It is now proposed to use equation (3.7) to define the range of operating conditions over which the transmission system may usefully be tested. We require

to find appropriate values of R_s and R_p for the machines to be used. The data available from the manufacturer are given on Fig.(3.5) and Fig.(3.6). The curves refer to the pump and motor characteristics at maximum stroke. Data on the characteristics at other stroke values were not available so that the effect of stroke changes cannot be assessed with great confidence.

The change in the loss with pressure can be found from Fig.(3.5) as follows. Along the fixed speed line at say 1500 r.p.m., we can extract values of efficiency for corresponding pressure values. Calculating the power loss in each case and plotting this against pressure gave the curve (a) on Fig.(3.7). The change of flow along the 1500 r.p.m. line is small enough for the loss to be attributed entirely to pressure changes. From the equivalent circuit of Fig.(3.2) we would expect the power loss at constant flow to follow the law,

$$w = w_o + \frac{P_p^2}{R_p} \quad \ldots\ldots\ldots\ldots\ldots\ldots\ldots\ldots (3.8)$$

where w_o is the constant loss in R_s.
To find R_p we plot w against P_p^2 to obtain curve (b) on Fig.(3.7). The slope of this curve gives the result $R_p = 1.485 \times 10^{12}$ (N m^{-5} s). The intercept of curve (b) on the power axis gives w_o, the loss at zero pressure. In accordance with the previous argument this is entirely attributed to the flow ϕ_p.

HYDRAULIC PUMP TYPE IP.125

TYPICAL PERFORMANCE CHARACTERISTICS AT 50° C. INLET TEMPERATURE ON 21 CENTISTOKES OIL

CURVE No. S.6410

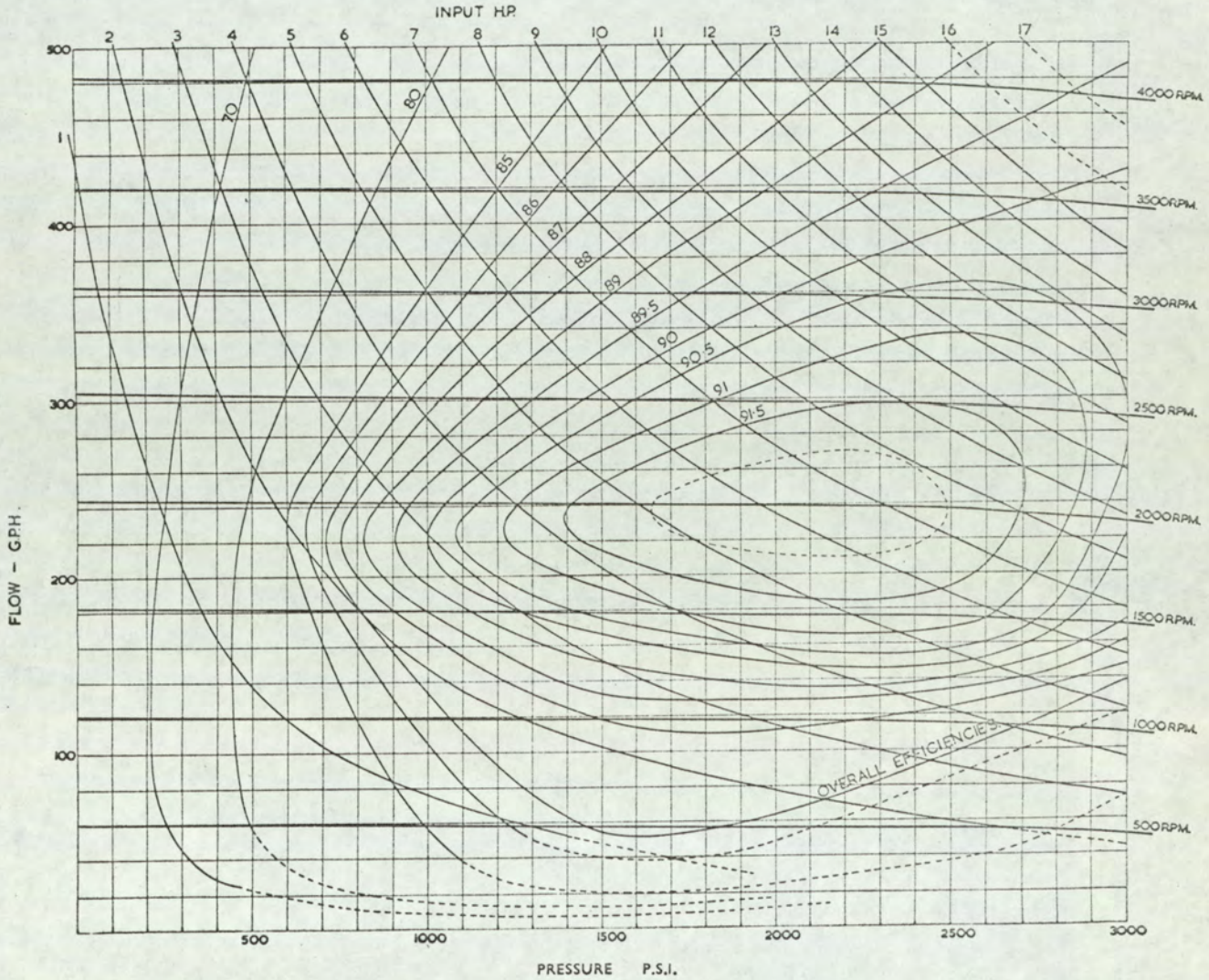

FIG.(3.5)

HYDRAULIC MOTOR TYPE IM.125

TYPICAL PERFORMANCE CHARACTERISTICS ON TELLUS 27 OIL AT 50°C. INLET TEMPERATURE

CURVE No. S.6601

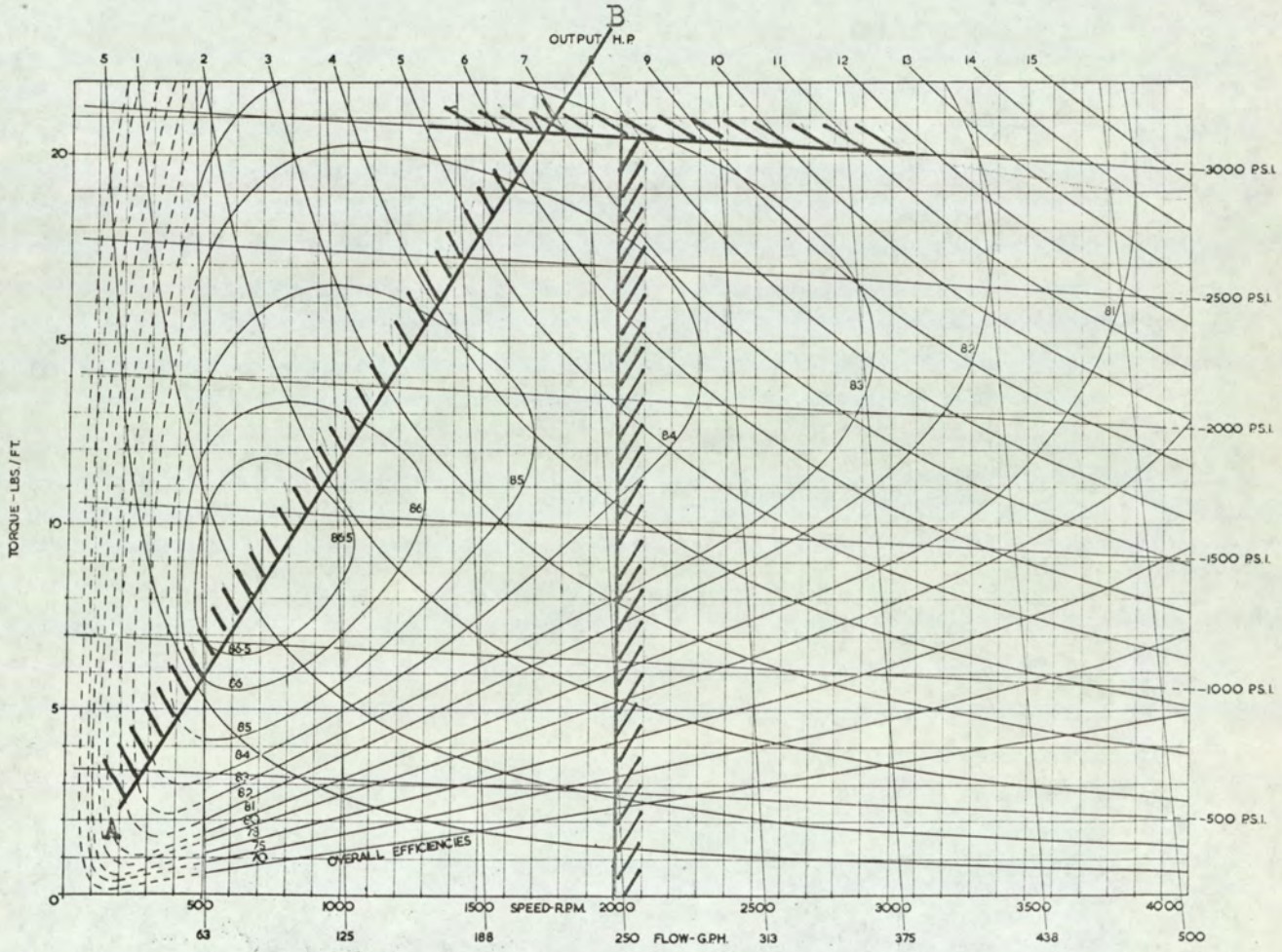

FIG.(3.6)

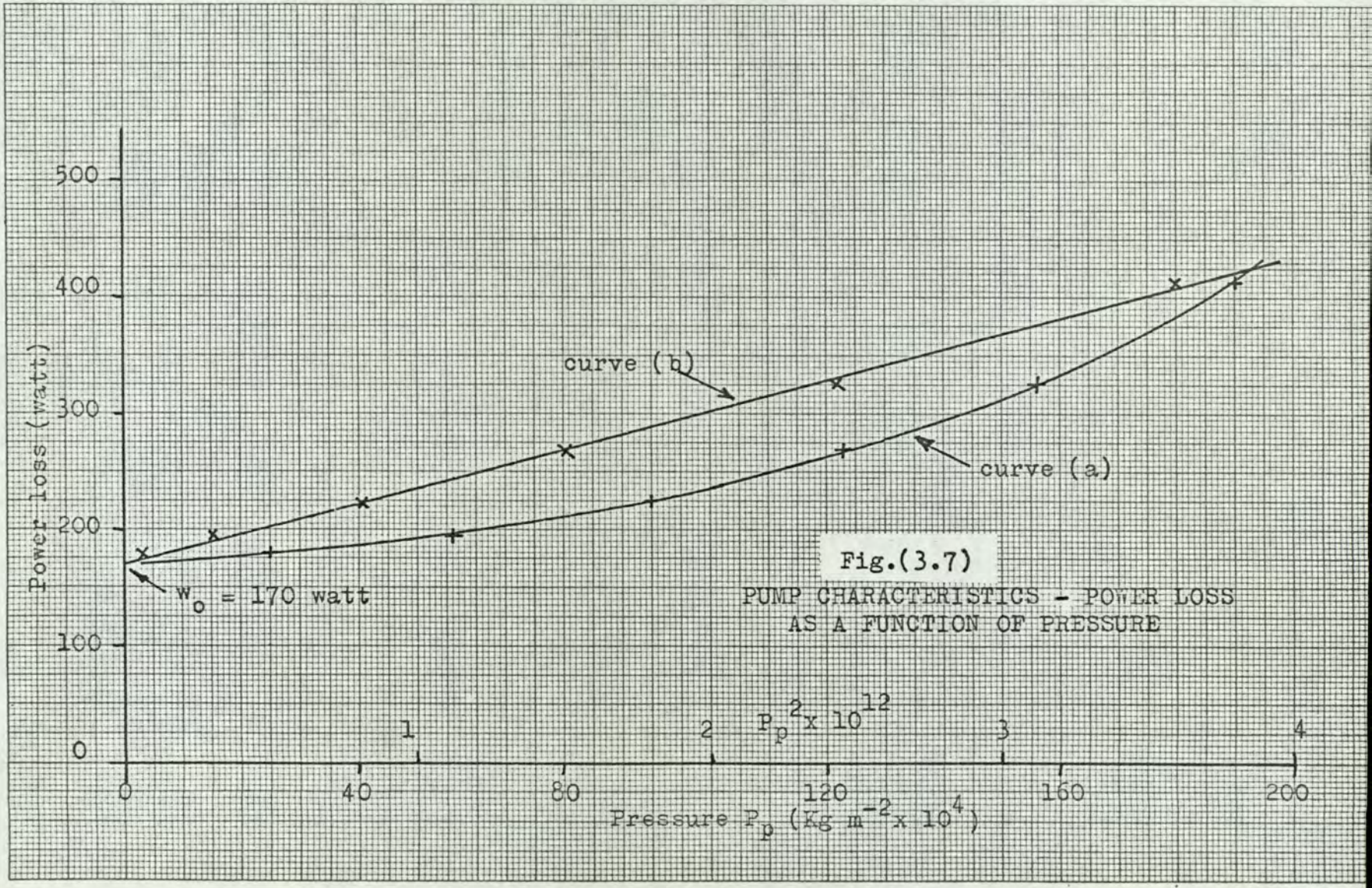

Fig.(3.7)
PUMP CHARACTERISTICS - POWER LOSS AS A FUNCTION OF PRESSURE

We may then write,

$$w_o = \phi_p^2 R_s \quad \ldots\ldots\ldots\ldots\ldots\ldots\ldots\ldots\ldots\ldots (3.9)$$

and using the nominal flow at 1500 r.p.m. we get $R_s = 3.13 \times 10^9$ (N m^{-5} s). This amounts to neglecting the power required to turn the pump at zero stroke. These figures justify the assumption that R_s is small compared with R_p. A repetition of this procedure at speeds of 1000 r.p.m. and 500 r.p.m. gave substantially the same values of R_s and R_p.

Returning to the general result in equation (3.6) we note that the optimum motor stroke varies in proportion to the transmitted power W_t. It is useful to enquire what is the maximum power which can be transmitted under optimum conditions with the available adjustment of Ψ_m. This can be found from equation (3.4) by solving for W_t. We then get,

$$W_t = \Phi_{mo}^2 \sqrt{R_s R_p} \quad \ldots\ldots\ldots\ldots\ldots\ldots\ldots\ldots (3.10)$$

which gives the maximum power transmitted when Φ_{mo} takes the maximum flow value available at a chosen speed. When W_t is evaluated in this way for several values of motor speed a line A-B is defined on the motor performance curves of Fig.(3.6). The significance of this line is that if a combination of torque and speed moves the operating point above this line the optimum flow exceeds what can be obtained with maximum stroke. The absolute optimum cannot then be reached and the best setting is at maximum stroke.

If the operating point falls below the line A-B an optimum stroke setting will be found at less than maximum stroke. The region in which the optimising control system will operate is then seen to be that below the line A-B.

In assessing the significance of this limiting condition it is useful to note the following points. The minimum loss condition of equation (3.4) corresponds to equal power loss in the series resistance and the combined parallel resistances of Fig.(3.4). This also implies a fixed ratio of pressure to flow equal to $\sqrt{R_s R_p}$. The line A-B is then almost a straight line, since pressure is approximately proportional to torque as also is flow to speed.

Apart from the line A-B further limitations must be imposed on the operating region. One limitation is the maximum working pressure of 3000 p.s.i. and a second is the maximum speed at which the motor may be run. A maximum speed of 2000 r.p.m. was chosen in order that a standard d.c. generator could be used to load the transmission.

In conclusion it should be noted that the results of the above analysis are somewhat speculative. Broad assumptions have necessarily been made but it has been shown that in principle an optimum stroke setting will exist. It is also clear that the optimum setting is chiefly set by the load on the drive but the input speed and the fluid temperature will also have an effect. The main result is that the operating region has been defined and this is useful in the selection of machines to drive and load the transmission.

4. DESIGN OF THE TEST RIG.

4.1 INTRODUCTION.

The form of transmission system, adopted as the basis of this work, was one in which the requirement was to maintain a constant output speed. This requirement is met by incorporating a speed control system [14]. It was found to be convenient to make this control system an electro-hydraulic arrangement. A number of problems were encountered in the design of the system, chiefly in the characteristics of the electro-hydraulic control valves which it was necessary to use. The resulting non-linearity of the system makes the theoretical analysis difficult. The other major difficulty lies in the variation of the dynamical characteristics of the transmission. Over the range of possible stroke settings there is a considerable change in the response to control action. The normal technique of feedback control was found to be inadequate in dealing with this situation and it was necessary to devise a novel form of control system. To this end the control characteristics of the system were studied in detail.

The theoretical treatment of this non-linear system was based on the use of frequency response characteristics of the elements. Data for the analysis were obtained from measurements made with a transfer function analyser*. The instrument used was of the type which measures

* Short Brothers and Harland Ltd. Mark I

only the fundamental component of the response wave-form. The approximations involved in using data obtained in this way are those normally made in the general analytical technique of describing function analysis[16].

4.2 CHOICE OF CONTROL VARIABLE.

The speed of the motor can be varied by changing either the motor stroke or the pump stroke and a choice between them must be made. When fluid leakage is neglected we have, from equation (3.1),

$$\omega_m = \frac{\psi_p \omega_p}{\psi_m} \quad \ldots\ldots\ldots\ldots\ldots\ldots\ldots\ldots (4.1)$$

which shows that the motor speed is proportional to the pump stroke ψ_p and inversely proportional to the motor stroke ψ_m. It is therefore best to control the motor speed by adjustment of the pump stroke as the control law is then linear.

The motor stroke is then available as a controlled variable for making the optimising adjustment.

The speed control loop employing feedback control can be identified with the block diagram of Fig.(4.1). There are two main blocks, representing the pump cam control elements and the hydraulic elements. These are first analysed separately.

4.3 PUMP CAM CONTROL CHARACTERISTICS

The mechanism by means of which the tilt angle of the cam plate is adjusted is shown diagramatically on Fig.(4.2). A movement of the servo piston positions the cam plate and responds to the action

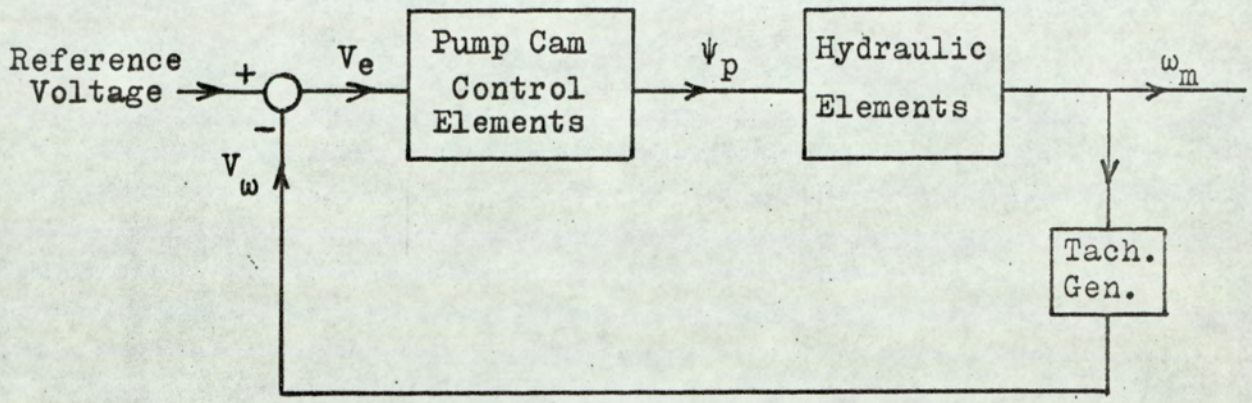

FIG.(4.1)

BLOCK DIAGRAM OF SPEED CONTROL LOOP

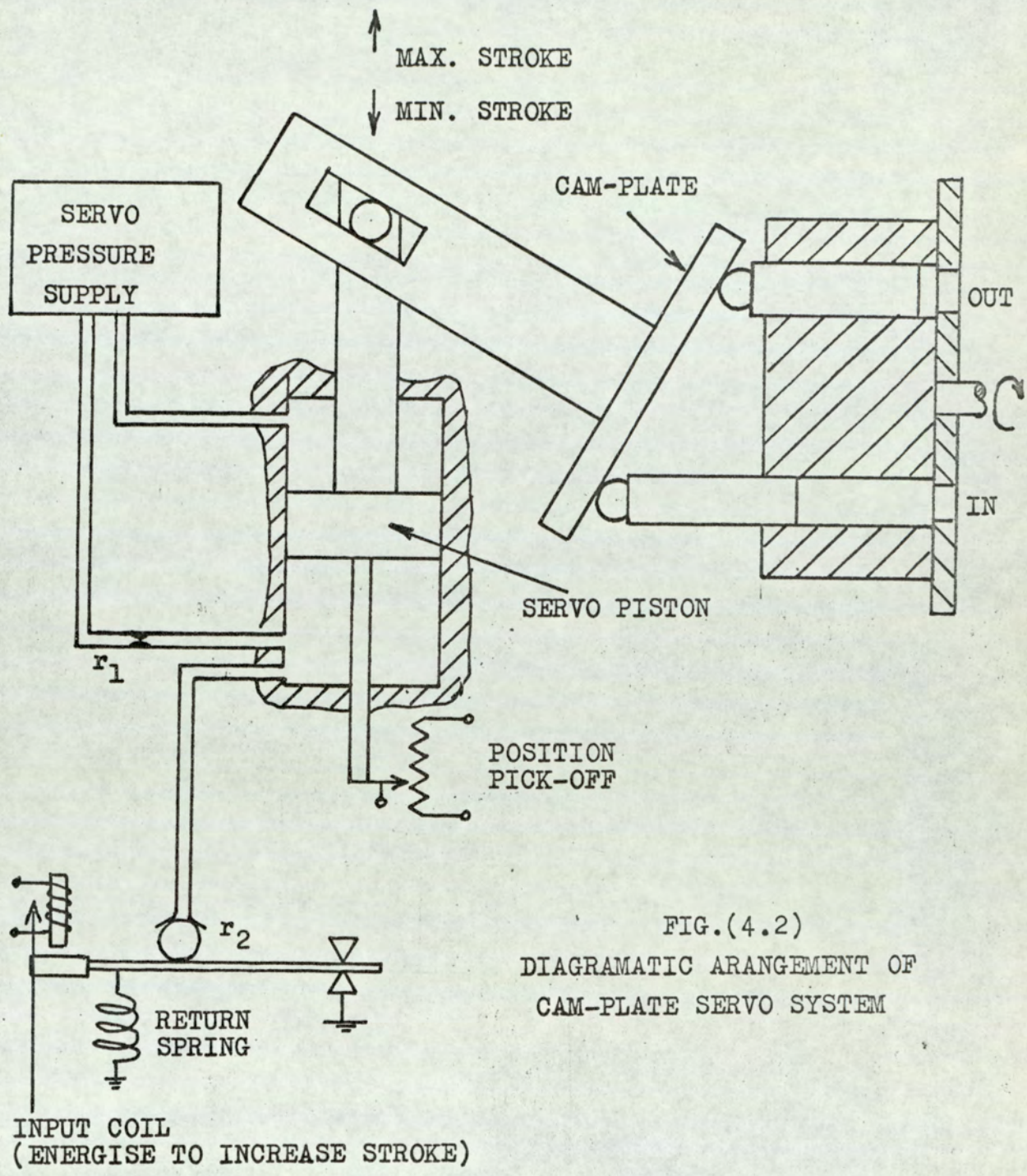

FIG.(4.2)
DIAGRAMATIC ARANGEMENT OF
CAM-PLATE SERVO SYSTEM

of the electrically controlled ball valve. The action is as follows.

The servo piston is subjected to hydraulic pressure at both ends. It is necessary that the area under pressure at the top end is less than that at the bottom. This being so, the servo piston is held stationary when the pressure at the bottom is less than that at the top. The pressure at the bottom is determined by the pressure drop in the restrictor r_1 and this in turn depends on the flow taken from the lower chamber. The restriction r_2, formed by the ball valve, controls the flow and hence sets the pressure in the lower chamber. An electromagnet is used to set the position of the ball valve.

When the electromagnet is energised the ball valve closes, cutting off the flow from the lower chamber. This causes the pressure to rise in the lower chamber so that the piston travels upwards continuously. To reverse the motion the ball valve is allowed to open sufficiently to let the pressure in the lower chamber fall below the value which will support the piston. In this reverse movement the fluid in the lower chamber is expelled through the ball valve and in the upward movement the chamber is filled through the restrictor r_1. This displacement of fluid introduces a feedback effect in which the rate of movement of the servo piston influences the pressure in the lower chamber. In the design of this type of control mechanism it is difficult to arrange that the maximum

rate of travel is the same in each direction of movement. Also the speed of response is slow, due to the fact that it is uneconomical to allow a large flow to drain continuously through the ball valve. This limits the rate at which fluid can enter or leave the lower chamber.

To hold a fixed stroke setting the ball valve must be kept partly open. This requires that the current in the electromagnet be set to give this valve setting. The electromagnet is not polarised so that the current flows in one direction through the coil and the valve responds to changes about the static setting. To a first approximation the control action gives a rate of change of stroke proportional to the change of current in the electromagnet.

An amplifier designed to energise the coil of the electromagnet is described in Section (3.3) of the Appendix. With an input current in the range $\pm$ 2 μA, this amplifier gives control of the rate of movement of the cam plate up to the maximum rate in either direction. The input resistance of the amplifier is approximately 1 kΩ so that the amplifier is to be regarded as a current amplifier of low input resistance.

In the first instance it is of interest to obtain the dynamical relationship between the position of the servo piston and the input current to the amplifier. The position of the servo pistion was therefore measured by means of a linear potentiometer connected to an extension from the piston. It was ultimately desired to

use this same potentiometer pick-off as a measure of the stroke. There is a possibility of some non-linearity in the linkage mechanism between the servo piston and the stroke setting. To assess the linearity of this relationship a test was conducted. The motor speed was measured over a range of settings of the pump stroke with the motor at maximum stroke. The result of plotting motor speed against the indicated position of the servo piston is shown on Fig.(4.3). Under these conditions the motor speed gives a good indication of the fluid flow from the pump and hence the pump stroke. A straight line approximation has been drawn through the points plotted and it is clear that the departure from linearity is slight. For all further purposes the indicated position of the servo piston was taken as a measure of the stroke. The stroke variables Ψ_p and Ψ_m were defined to take unit value at full stroke and the measurements on the servo pistons were scaled accordingly.

In order to investigate the dynamical characteristics of the cam positioning mechanism it is necessary to establish control over the position of the servo piston using a position feedback loop. This avoids the difficulty of a possible drift in the stroke setting during a frequency response test. The circuit arrangement of the position feedback system is shown in Fig.(4.4), together with the corresponding block diagram. The element f(s) here represents the transfer function combining the amplifier and the electro-hydraulic system i.e. f(s) relates the stroke Ψ_p

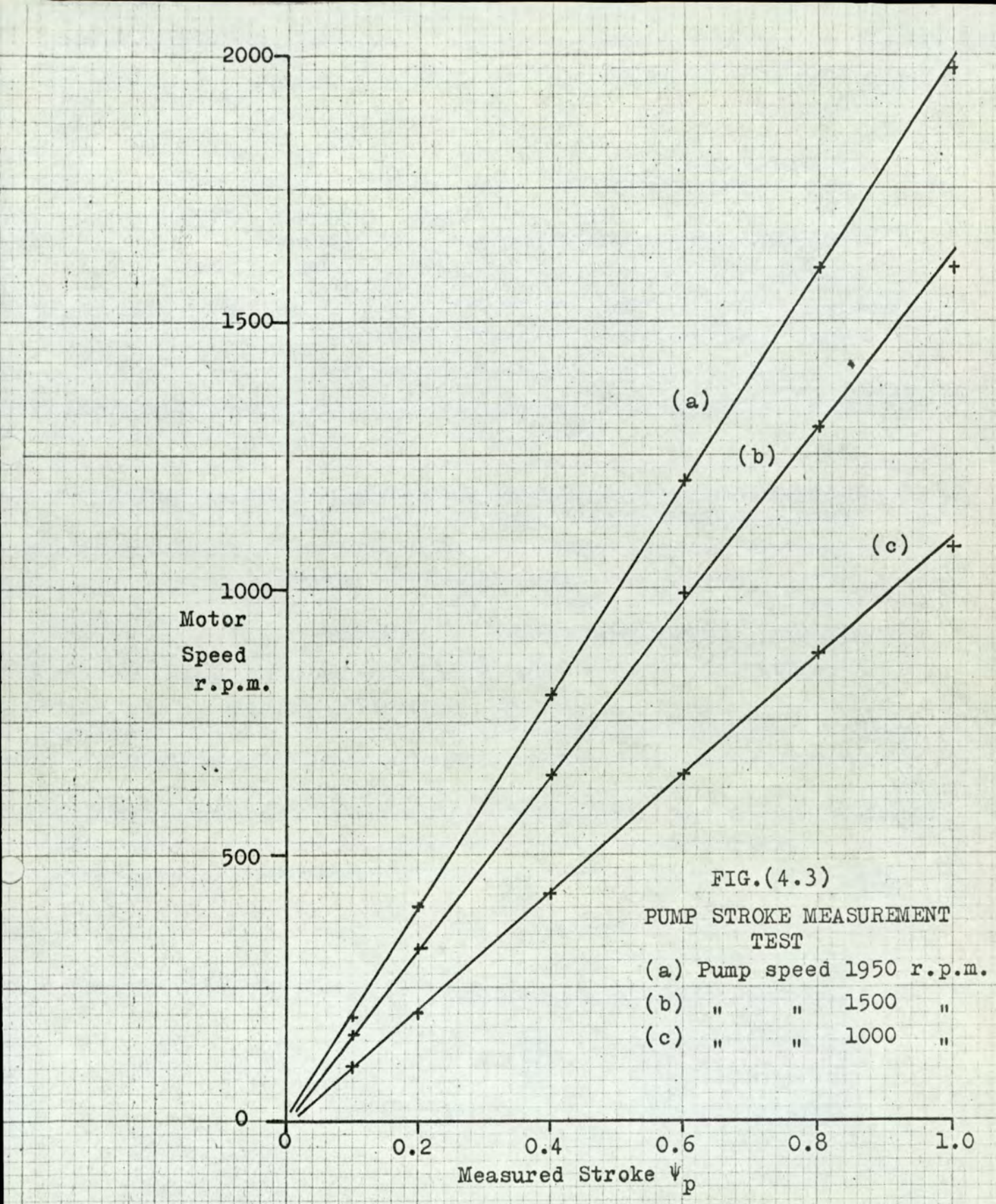

FIG.(4.3)

PUMP STROKE MEASUREMENT TEST

(a) Pump speed 1950 r.p.m.
(b) " " 1500 "
(c) " " 1000 "

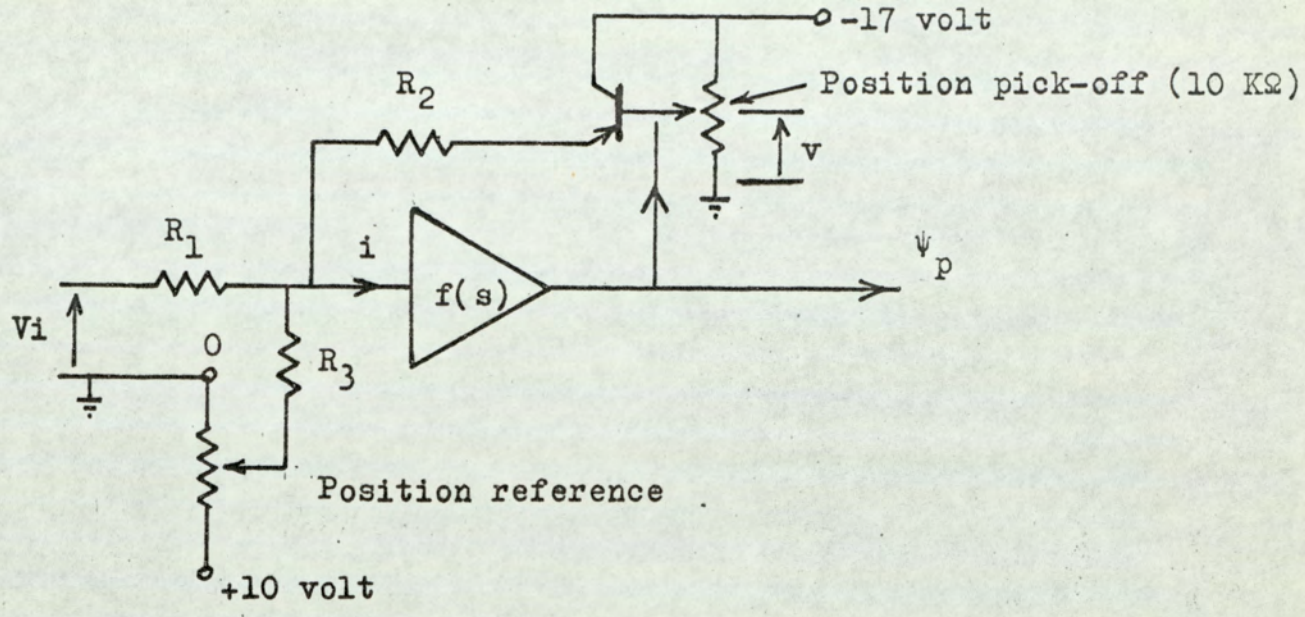

CIRCUIT ARRANGEMENT

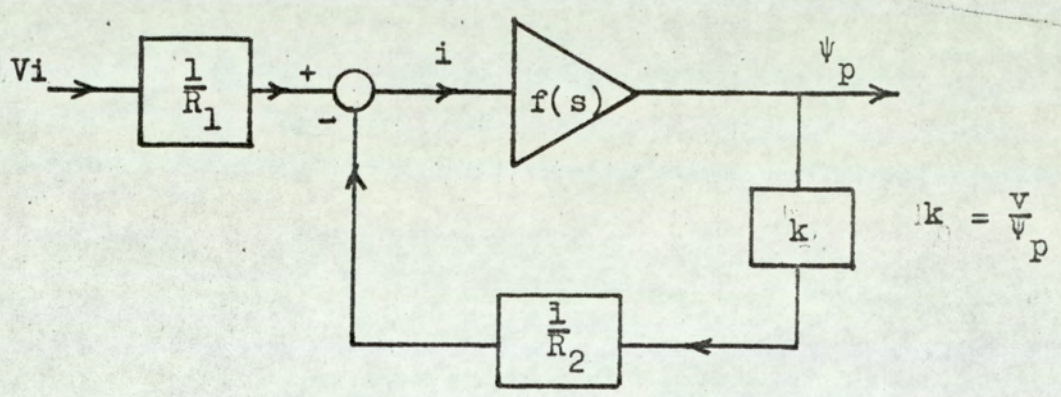

BLOCK DIAGRAM (REFERENCE OMITTED)

FIG.(4.4)
PUMP CAM POSITION CONTROL LOOP

to the current at the input to the amplifier. The block diagram is derived on the assumption that the voltage at the input to the amplifier is zero since the amplifier gain is high and the input resistance is low.

It is required to identify the response function f(s), but this must be done from a measurement of the overall response of the position control system. From the block diagram of Fig.(4.4) we obtain the closed loop frequency response as,

$$\frac{\psi_p}{Vi} = \frac{f(j\omega)}{R_1(1 + \frac{k\, f(j\omega)}{R_2})} \qquad \ldots\ldots\ldots\ldots\ldots\ldots (4.2)$$

or

$$\frac{\psi_p}{Vi} = \frac{R_2}{k\, R_1}\left(\frac{F(j\omega)}{1 + F(j\omega)}\right) \qquad \ldots\ldots\ldots\ldots\ldots\ldots (4.3)$$

where $F(j\omega) = \frac{k\, f(j\omega)}{R_2}$ $\ldots\ldots\ldots\ldots\ldots\ldots (4.4)$

Measurement of the closed loop frequency response gave the results shown on Fig.(4.5). The curves designated m_1 to m_5 indicate the change of the modulus of the response with different values of the test signal amplitude. The corresponding phase characteristics appear as shown in the curves a_1 to a_5. There is clearly a considerable change in the response with variations in the signal amplitude. The signal amplitude is here specified in terms of the percentage movement of the servo piston at zero frequency. With reference to Fig.(4.4) the

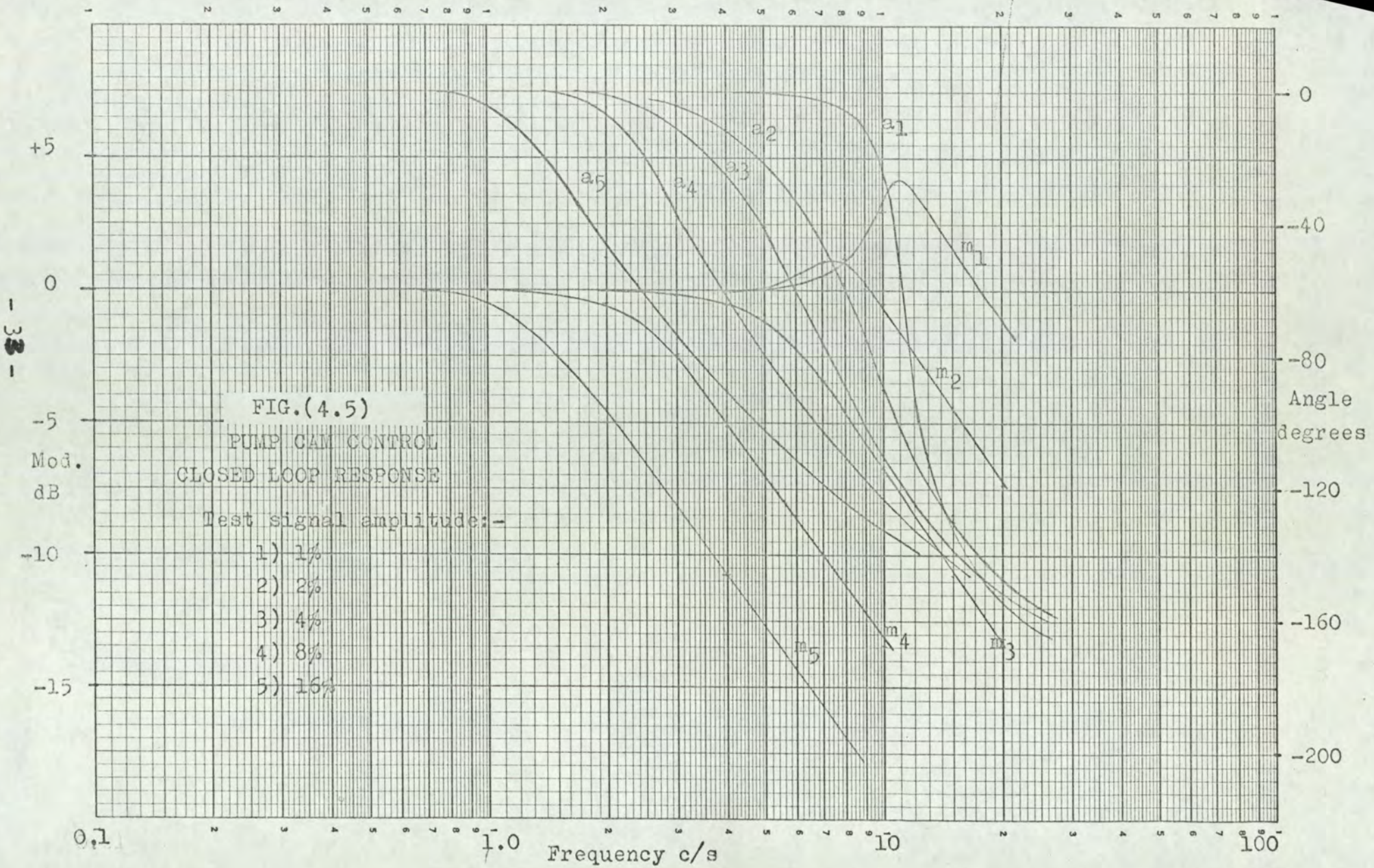

FIG.(4.5)

PUMP CAM CONTROL

CLOSED LOOP RESPONSE

Test signal amplitude:-

1) 1%
2) 2%
3) 4%
4) 8%
5) 16%

circuit parameters for this test were,

$$R_1 = 47\ k\Omega$$

$$R_2 = 6.8\ k\Omega$$

and the constant k takes the value 8.9 Volt. These measurements were made with the pump stationary. A further test with the machine rotating, and on load, showed negligible change in the response from the results given above.

The amplitude scale of Fig.(4.5) has been set to read zero dB at zero frequency. This has the effect of removing the constant multiplier in equation (4.3) so that the curves actually show the factor $\frac{F(j\omega)}{1 + F(j\omega)}$ alone. These results may then be used to obtain the function $F(j\omega)$ by transferring the data to a Nichols Chart[17]. This chart is normally used to evaluate functions of the form $\frac{F(j\omega)}{1 + F(j\omega)}$ when $F(j\omega)$ is given. We require the inverse process here. To do this the closed loop response data of Fig.(4.5) are plotted with reference to the parametric curves of constant amplitude and constant phase. The open loop response $F(j\omega)$ is then read from the ordinate and abscissa of the chart. The Nichols Chart is shown on Fig.(4.6) with the data plotted from Fig.(4.5).

The effect of changes in the amplitude of the test signal on $F(j\omega)$ is large but we note that the curves plotted on Fig.(4.6) are displaced by a vertical shift for the most part. This implies that it is the modulus rather than the phase of $F(j\omega)$ which is affected by changes in the signal amplitude. This effect is

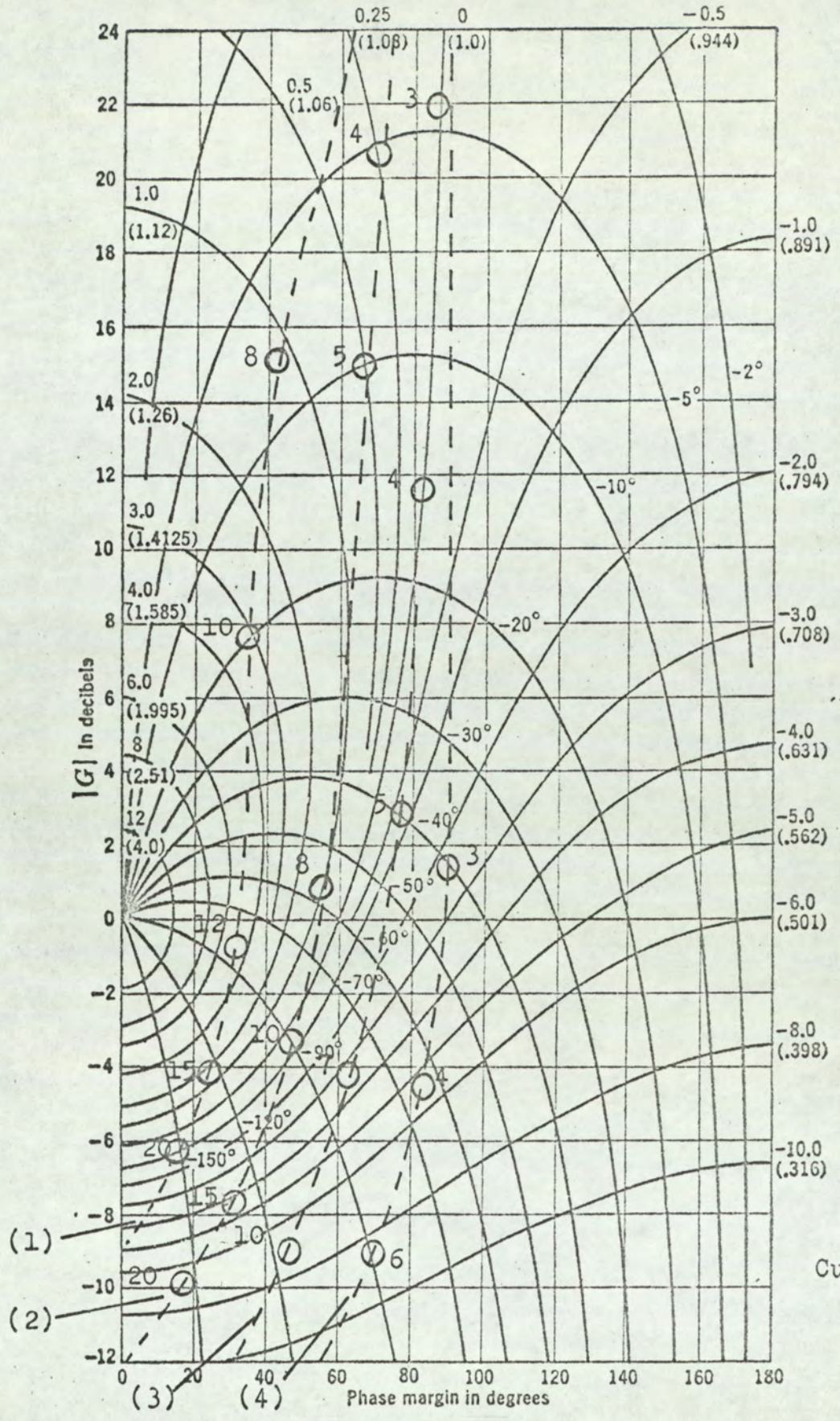

Amplitude

Curve (1) 1%

" (2) 2%

" (3) 4%

" (4) 8%

FIG.(4.6)

NICHOLS CHART

what would be expected when the non-linearity is due to a pronounced saturation. This suggests that a model of the function $F(j\omega)$ would take the form shown in Fig.(4.7), where $h(j\omega)$ is a linear element. At small amplitudes the response approaches that of $h(j\omega)$ so that this factor can be estimated by plotting the magnitude and phase curves of $F(j\omega)$ at small signal amplitude. This leads to the results given on Fig.(4.8). These curves are not consistent in detail with a linear form of transfer function, indicating that even at this small amplitude of 1% the saturation has an effect. However it is sufficient for the present purposes to make an approximation to Fig.(4.8) using the function,

$$F(j\omega) = \frac{k}{R_2}\, h(j\omega) = \frac{K_f}{j\omega(1 + j\omega T_f)} \quad \ldots(4.5)$$

When the constants K_f and T_f are chosen to fit the function to the phase curve of Fig.(4.8) we get,

$$K_f = 8.2 \times 10^2 \ s^{-1}$$

$$T_f = 0.023 \ s$$

These values then lead to,

$$h(j\omega) = \frac{6.25 \times 10^5}{j\omega(1 + 0.023j\omega)} \ Amp^{-1} \ s^{-1} \quad \ldots(4.6)$$

In conjunction with the block diagram of Fig.(4.7) this formally identifies the response characteristics of the stroke control mechanism and the associated amplifier.

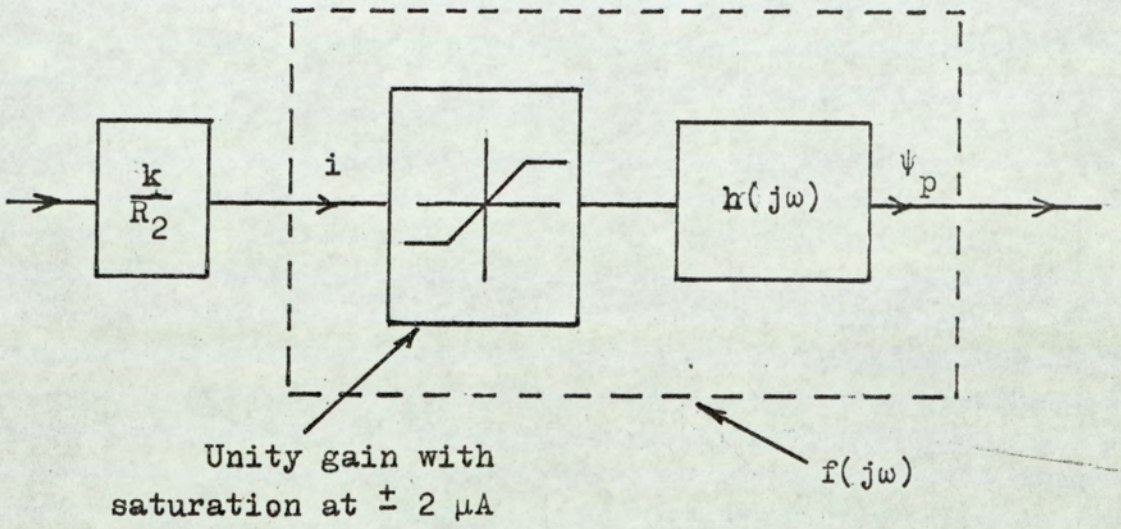

FIG.(4.7)
APPROXIMATE MODEL OF PUMP CAM
RESPONSE FUNCTION F(jω)

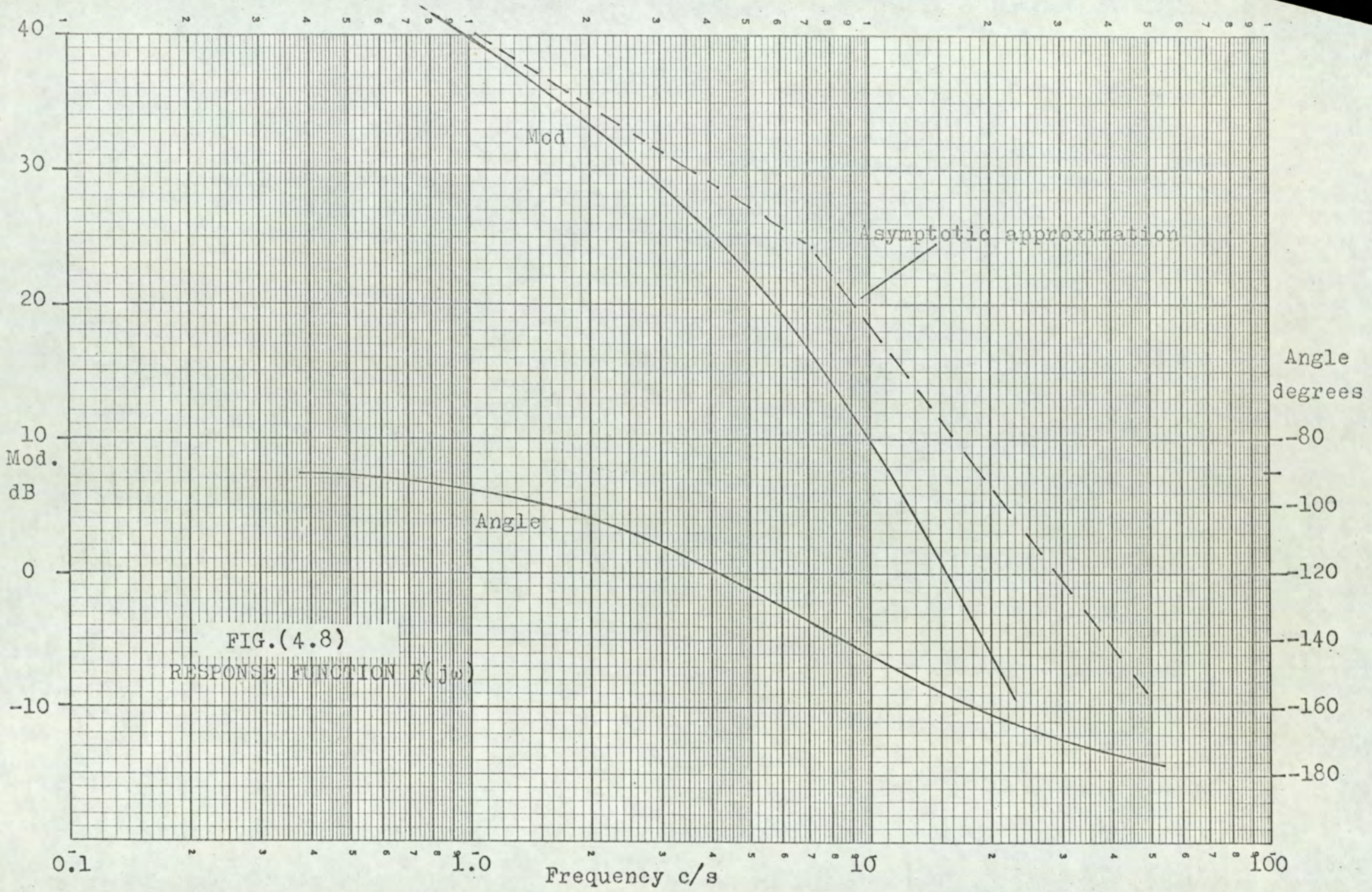

FIG.(4.8)
RESPONSE FUNCTION F(jω)

4.4 HYDRAULIC SYSTEM CONTROL CHARACTERISTICS

The dynamical characteristics relating the speed of the motor to the pump stroke are to be investigated. The results presented here give a brief theoretical account of the expected performance, followed by an analysis of the results of measurement on the system.

4.4.1 THEORETICAL CONSIDERATIONS

Variable speed drives of the type used here have normally been subjected to theoretical analysis under conditions of fixed motor stroke [14],[18]. In order to appreciate how the observed response characteristics arise it is necessary to develop the analysis to show clearly the effects of changes in the motor stroke. A simplified view of the system in terms of linear approximations is sufficient for the present purposes.

Two factors influence the general behaviour of the hydraulic circuit. There is the compressibility of the fluid and pipework which gives the system an elastic property, and the leakage of fluid in the machines which contributes energy dissipation. The dynamical characteristics of the load on the motor combine with those of the hydraulic circuit. When the load has a large moment on inertia a resonant mode is set up between the compliance of the hydraulic circuit and the load. This mode is damped by the dissipation in fluid leakage.

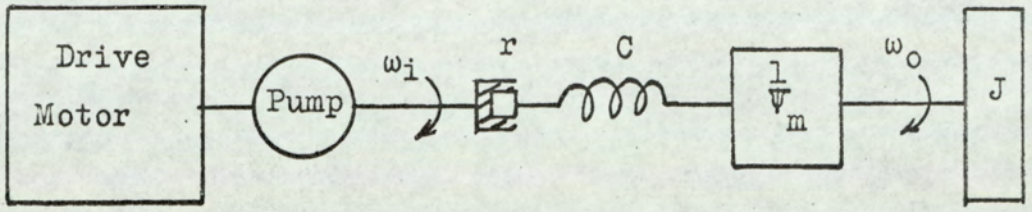

MECHANICAL LINKAGE DIAGRAM

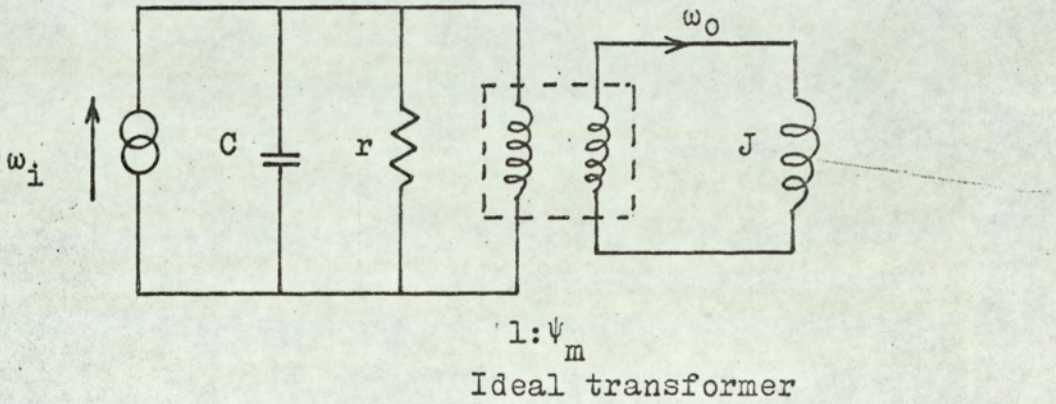

EQUIVALENT CIRCUIT

FIG.(4.9)

MECHANICAL SYSTEM

Energy dissipation in the load also contributes damping to this natural mode. In the following work the system was studied with the loading generator on open circuit; this is the condition of minimum damping which presents the worst condition from the point of view of closed loop control.

The dynamical properties of the prime mover also affect the response of the transmission to load changes. When the load is transmitted back to the prime mover it may give rise to transient changes in the input pump speed. In this case it is possible to approximate the drive motor to a constant speed source in view of three effects,

(a) high moment of inertia of the motor armature.
(b) shunt motor characteristics due to constant armature supply voltage.
(c) action of the motor speed control loop.

The mechanical linkage diagram is shown in Fig.(4.9) for the complete transmission system. Taking the drive motor speed to be constant allows us to regard the pump and drive motor as one element. Variations in the pump stroke are equivalent to changes of the input speed and are imagined as a speed disturbance ω_i. The element C in the linkage diagram is a compliance representing the elasticity of the hydraulic circuit, J is the moment of inertia of the load and r is a viscous damping element due to fluid leakage. A coupling of velocity ratio $\frac{1}{\Psi_m}$ introduces the effect of changes in the motor stroke. This mechanical arrangement has the same response characteristics as the equivalent

circuit shown on Fig.(4.9). An analysis of the equivalent circuit shows that the transfer function relating the load speed change ω_o to the input speed change ω_i is given by,

$$\frac{\omega_o}{\omega_i} = \frac{1}{\psi_m (J_o C s^2 + \frac{J_o}{r} s + 1)} \quad \ldots\ldots\ldots\ldots\ldots (4.7)$$

where J_o is the reflected moment of inertia of the load i.e.,

$$J_o = \frac{J}{\psi_m^2} \quad \ldots\ldots\ldots\ldots\ldots\ldots\ldots\ldots (4.8)$$

The change of input speed ω_i is proportional to the change of pump stroke so that the overall response of the transmission system will be governed by the transfer function,

$$\frac{\omega_m}{\psi_p} = \frac{K}{T^2 s^2 + 2 z T s + 1} \quad \ldots\ldots\ldots\ldots\ldots (4.9)$$

The quadratic factor here is the same as in equation (4.7) so that the time constant T is given by,

$$T = \frac{1}{\psi_m} \sqrt{J C} \quad \ldots\ldots\ldots\ldots\ldots\ldots\ldots\ldots (4.10)$$

and the damping ratio z is,

$$z = \frac{1}{2 \psi_m} \sqrt{\frac{J}{C r}} \quad \ldots\ldots\ldots\ldots\ldots\ldots\ldots\ldots (4.11)$$

The important conclusion at this stage is that the response characteristics of the system will vary as a function of the motor stroke. This is due to the change in the reflected moment of inertia of the load. The time constant and the damping ratio in the transfer function are both inversely proportional to the motor stroke.

A further important observation is that the constant K in equation (4.9) is also variable. This constant represents the gain at zero frequency and it can be evaluated by taking the steady state condition of flow balance,

pump flow = motor flow + leakage

$$\psi_p \omega_p q = \psi_m \omega_m q + \phi \quad \text{.....(4.12)}$$

If the leakage is neglected we then have,

$$\omega_m = \frac{\psi_p}{\psi_m} \omega_p \quad \text{.....(4.13)}$$

and the steady state gain for a small change of ψ_p is given by,

$$K = \frac{d\omega_m}{d\psi_p} \quad \text{.....(4.14)}$$

i.e.
$$K = \frac{\omega_p}{\psi_m} \quad \text{.....(4.15)}$$

These results may now be used to interpret the experimental observations in a frequency response test on the transmission.

4.4.2. EXPERIMENTAL RESULTS.

In Section (3) the operating conditions leading to a maximum efficiency in the transmission system were identified. In reviewing the range of operating conditions likely to be of interest in the optimisation study, the area of interest was defined on Fig.(3.6). This suggests that the load speed be kept within the range 750 to 2000 r.p.m.. The effect of increasing the speed is to increase the flow at any given setting of the motor stroke. It is expected that the change of flow will have only a second order effect on the dynamical characteristics of the system. The lower speed limit was therefore chosen as a condition for these experimental tests as this allows the widest range of operating conditions resulting from pump speed changes.

The behaviour of the motor speed as a function of pump stroke variations was investigated by measuring the frequency response. An a.c. tachometer generator connected to the motor shaft was used to measure the speed and the linear potentiometer, measuring the movement of the servo piston of the pump, was used to indicate the stroke. The position of the cam plate of the pump was controlled by using the position control system described in Section (4.3). A sinusoidal test signal was then applied to the input of the control circuit to produce a controlled oscillation of pump stroke. This is the same condition as was used in the tests to determine the pump cam control characteristics. The results of Fig.(4.5) give the

response amplitude and phase of the stroke oscillation. The overall frequency response was measured first, relating the motor speed to the input to the pump cam control circuit. These results were then corrected to give the true response, relating motor speed to pump stroke, by removing the amplitude and phase changes due to the cam control circuit, Fig.(4.5).

It is important to note that in these tests the speed control system was in operation on the motor driving the pump. This is necessary so that the dynamical characteristics of the prime mover are the same as in normal operation. The drive motor characteristics affect the response of the transmission since changes in the input speed contribute to changes in the output speed. These effects must be taken into account in the design of the speed control system controlling output speed.

A series of tests was conducted with pump speed and motor stroke as parameters. The results are shown on Fig.(4.10) to Fig.(4.16) in sequence. The choice of test conditions was carefully made to explore the extremes of variation of the characteristics and the trend of intermediate conditions. The response curves are consistent with the transfer function represented by equation (4.9) and a view of the mode of variation of the response with operating conditions may be obtained as follows.

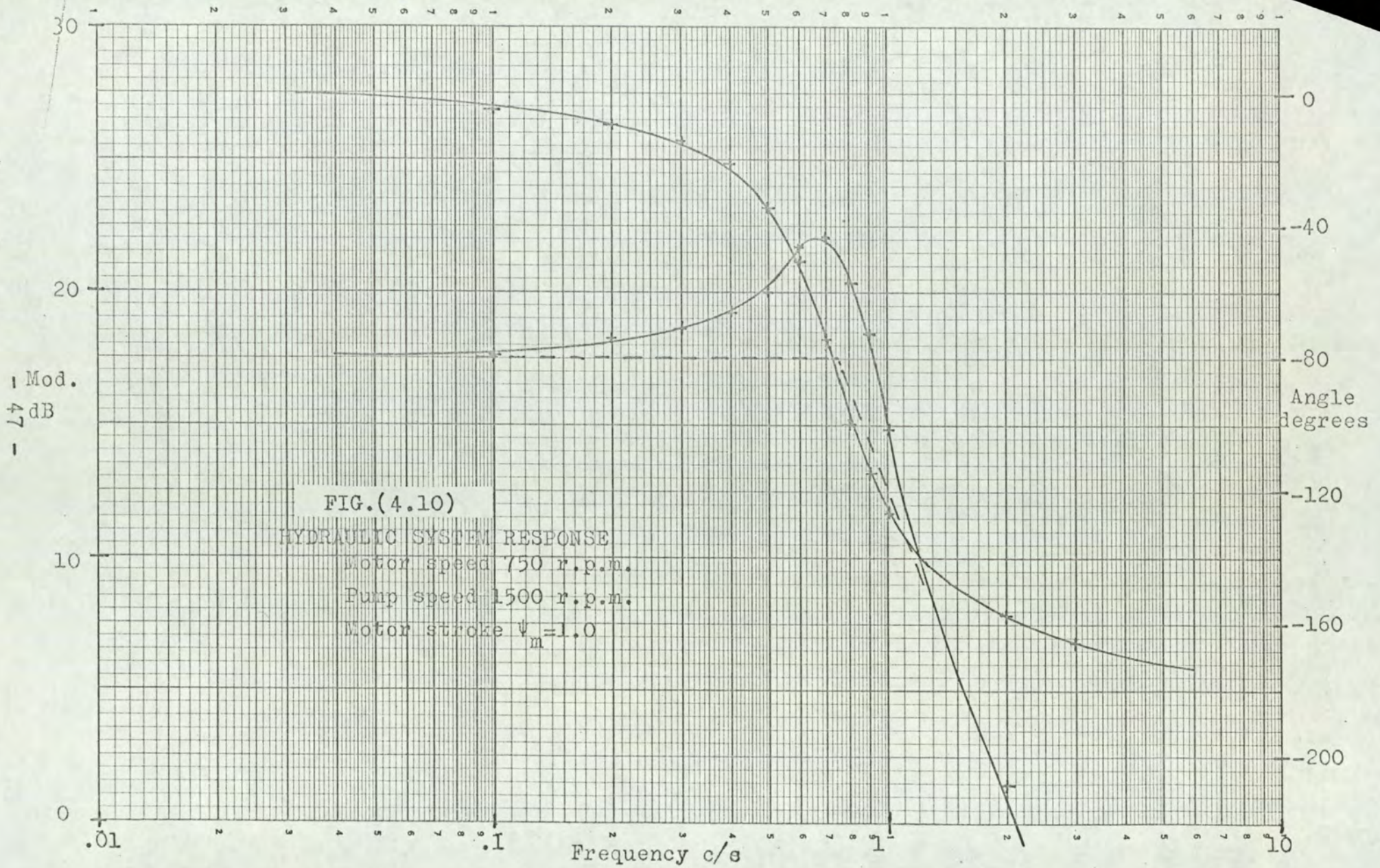

FIG.(4.10)

HYDRAULIC SYSTEM RESPONSE

Motor speed 750 r.p.m.

Pump speed 1500 r.p.m.

Motor stroke ψ_m=1.0

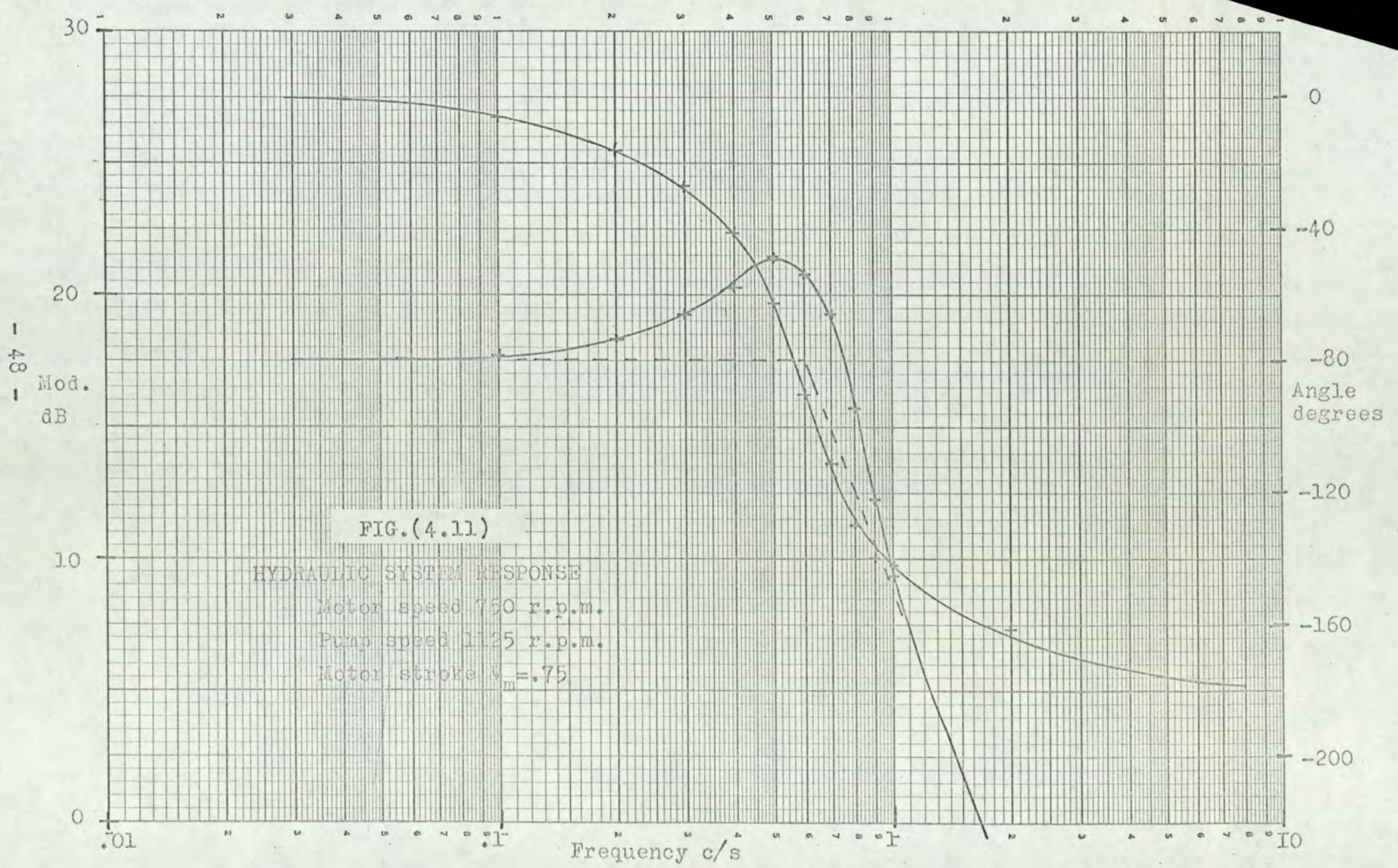

FIG.(4.11)

HYDRAULIC SYSTEM RESPONSE

Motor speed 750 r.p.m.

Pump speed 1125 r.p.m.

Motor stroke $\%_m$=.75

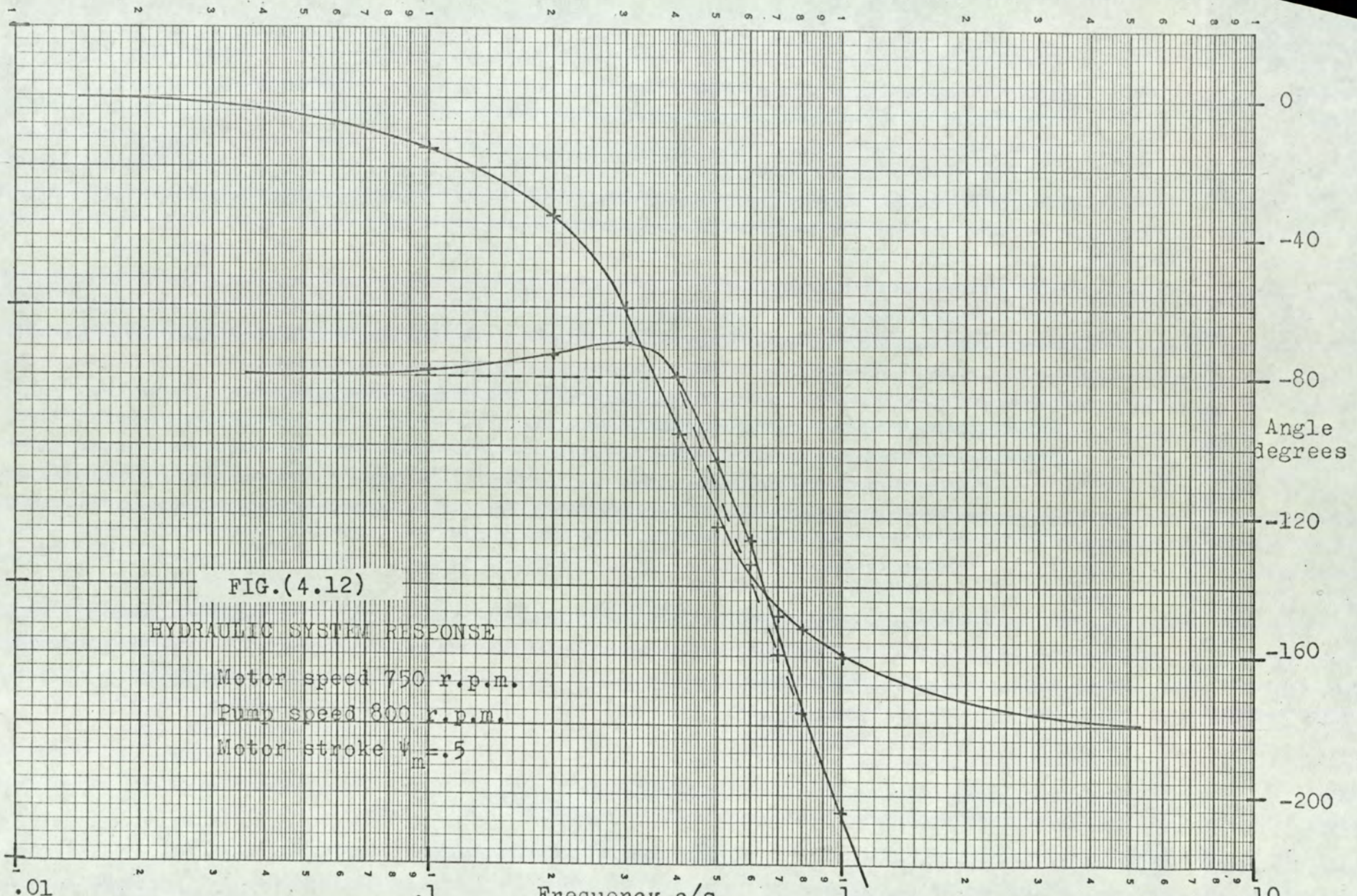

FIG.(4.12)

HYDRAULIC SYSTEM RESPONSE

Motor speed 750 r.p.m.

Pump speed 800 r.p.m.

Motor stroke $\Psi_m = .5$

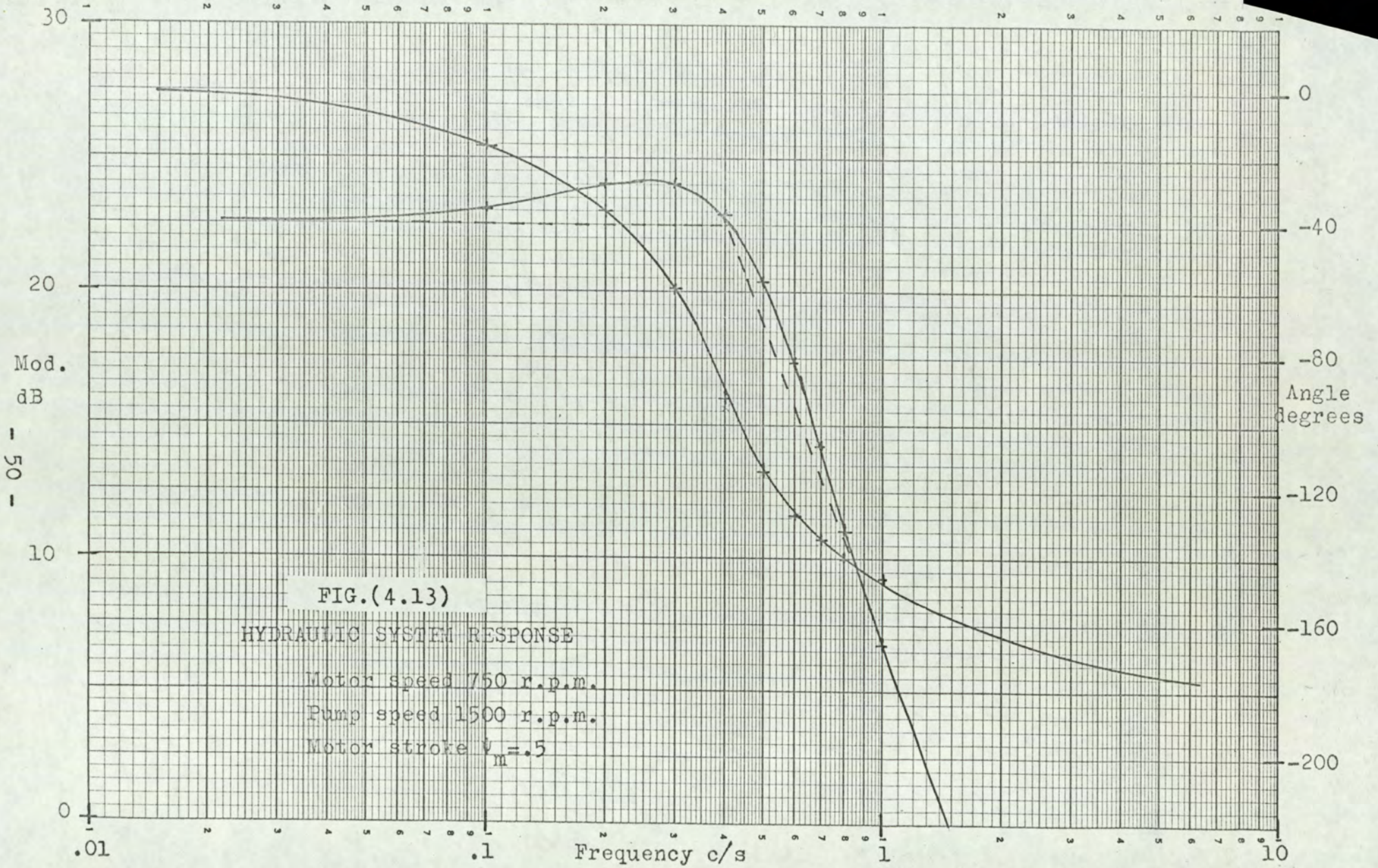

FIG.(4.13)

HYDRAULIC SYSTEM RESPONSE

Motor speed 750 r.p.m.

Pump speed 1500 r.p.m.

Motor stroke $V_m = .5$

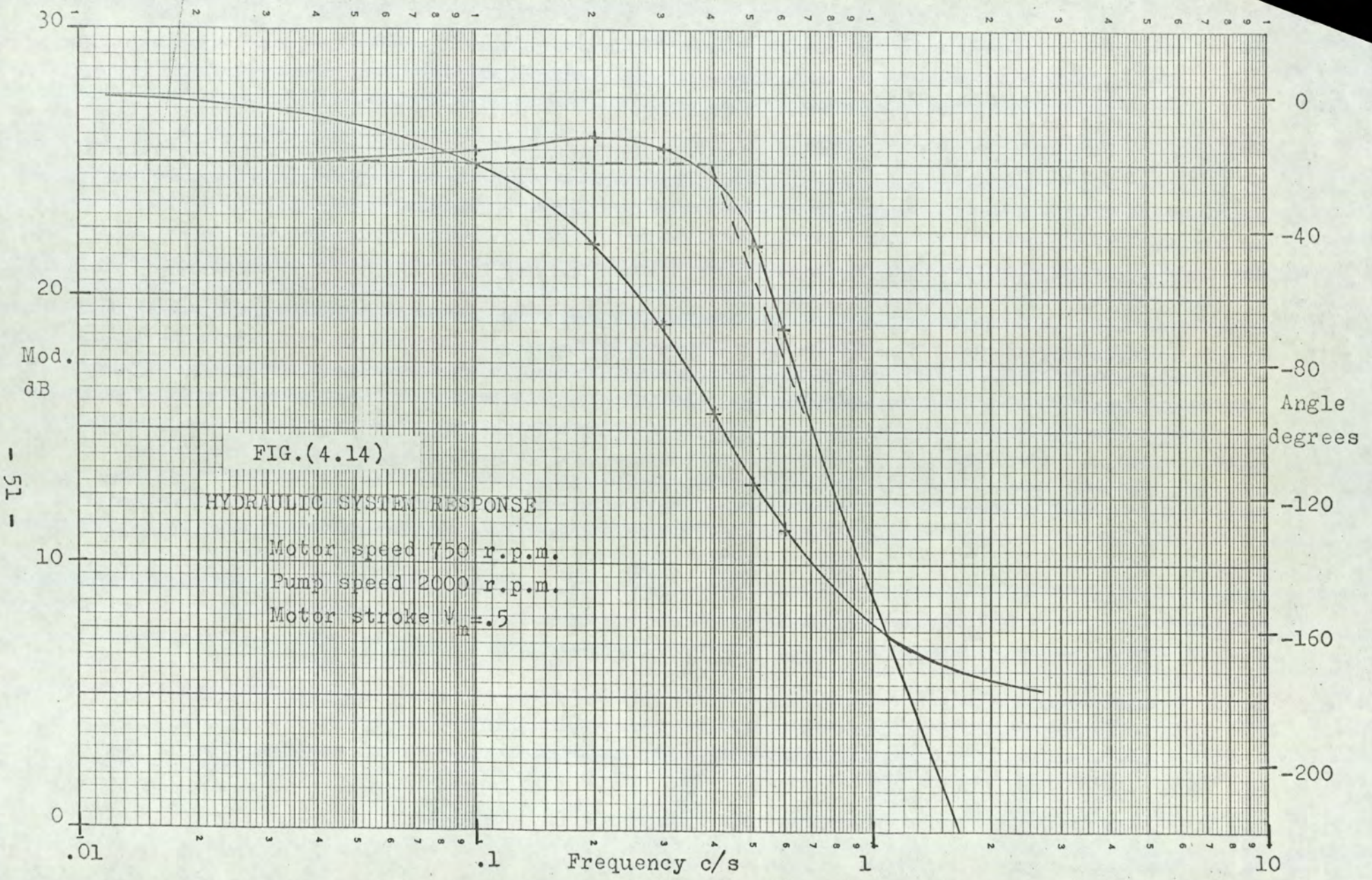

FIG.(4.14)

HYDRAULIC SYSTEM RESPONSE

Motor speed 750 r.p.m.

Pump speed 2000 r.p.m.

Motor stroke V_n =.5

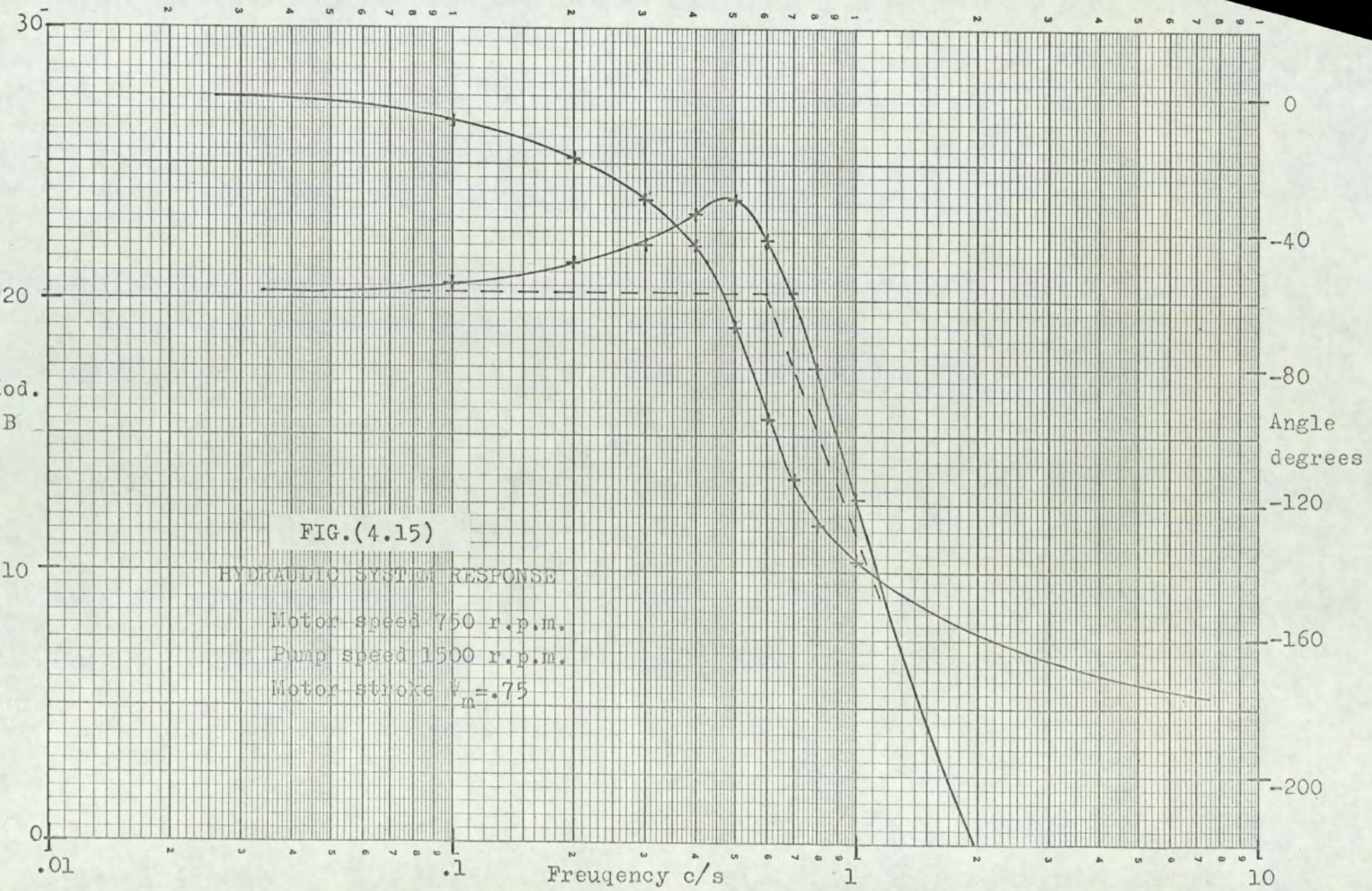

FIG.(4.15)

HYDRAULIC SYSTEM RESPONSE

Motor speed 750 r.p.m.

Pump speed 1500 r.p.m.

Motor stroke V_m=.75

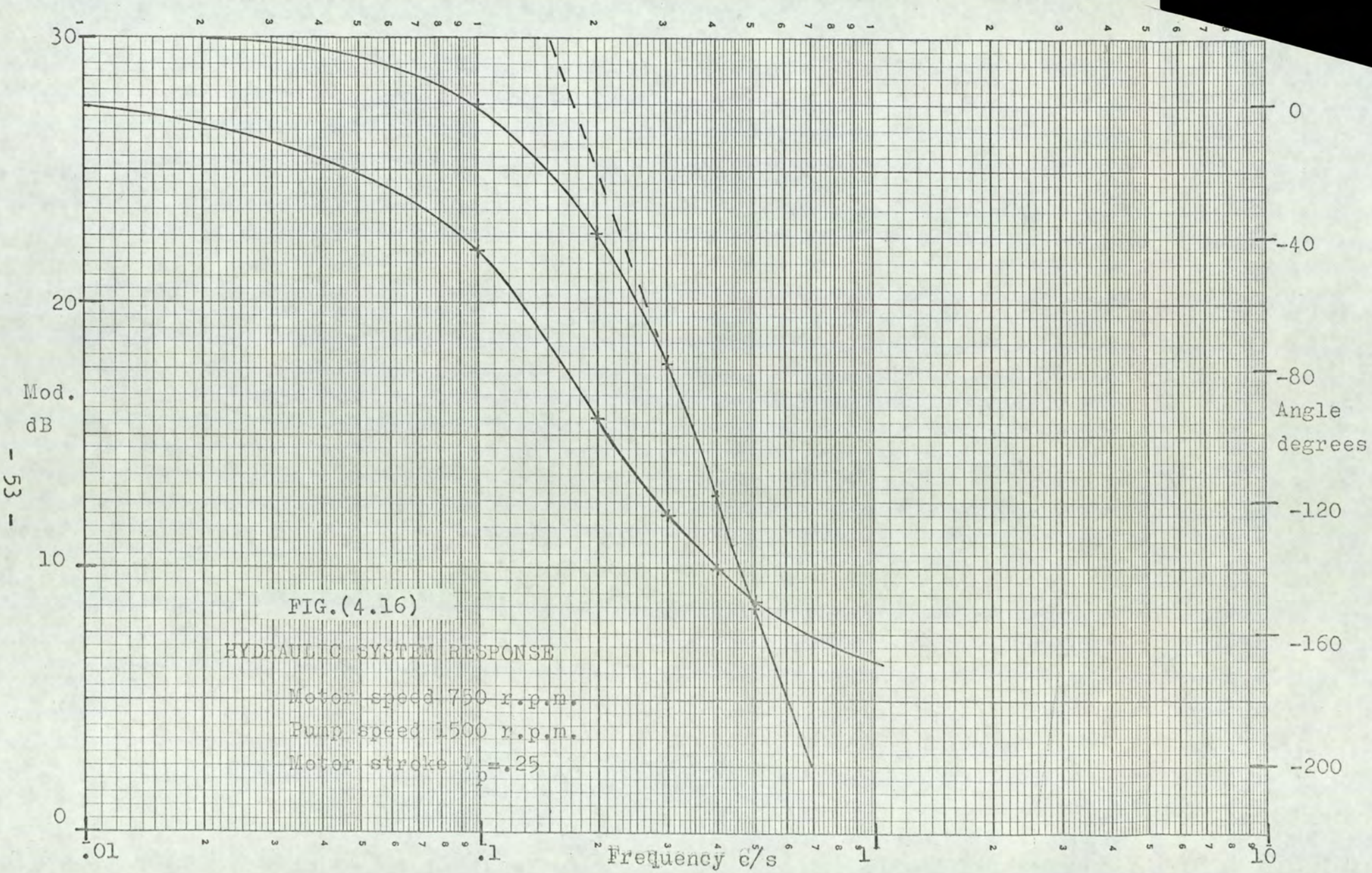

FIG.(4.16)

HYDRAULIC SYSTEM RESPONSE

Motor speed 750 r.p.m.

Pump speed 1500 r.p.m.

Motor stroke Y_p =.25

The gain of the system at zero frequency is defined by equation (4.15) and is constant when ω_p/ψ_m is constant. The results of Fig.(4.10), Fig.(4.11) and Fig.(4.12) are obtained for three conditions having the same gain at zero frequency. There is seen to be an increase in both the time constant and damping ratio as the motor stroke is reduced and this is consistent with what would be expected from equations (4.10) and (4.11).

The variations due to a change of pump speed alone are seen in Fig.(4.12), Fig.(4.13) and Fig.(4.14), the motor stroke is here fixed at 0.5. There is a slight increase in the damping ratio as the pump speed is increased. This is due to the increased proportion of the leakage flow in the pump as a result of the reduction of stroke at the higher speeds. There is a negligible variation in the time constant which suggests that the assumption of constant drive motor speed is valid over the frequency range involved. The most significant effect seen in these results is the change of gain at zero frequency. The corresponding change in the gain constant K is consistent with equation (4.15).

The variations due to changes of motor stroke alone are evident from Fig.(4.15), Fig.(4.16) and Fig.(4.10). The pump speed is then held constant. The trend is again that of increase in the time constant and damping ratio with decreasing motor stroke. There is also a change of gain which does not, however, entirely follow equation (4.15). There is a noticeable loss of

gain when the stroke is small which may be attributed to the increased leakage of fluid at small stroke settings.

These results show little variation with a change of the amplitude of the test signal, provided that the fluid pressure in the system does not exceed the limit set by the relief valve.

4.4.3. CONCLUSIONS ON THE HYDRAULIC SYSTEM CHARACTERISTICS.

The tests results show that the theoretical analysis of Section (4.4.1) is broadly satisfactory. The response characteristics of the system vary with the pump speed and the motor stroke. These variations amount to changes in the time constant, damping ratio and gain constant in the transfer function. The time constant and damping ratio are determined by the motor stroke setting alone while the gain constant is affected by both the stroke and pump speed.

Some observations can now be made on the prospects of controlling the motor speed. The speed control system is required to adjust the pump stroke in order to hold the motor speed constant. In this it must counteract three sources of variation in speed,

(1) pump speed changes
(2) motor stroke changes
(3) load changes

As far as the steady state effects of these changes are concerned the balance of fluid flow, given by equation (4.12), will determine the required setting

of the pump stroke ψ_p. Consider the extent to which ψ_p must be manipulated to counteract the effect of changes in each of the three variables. When the pump speed is changed ψ_p must change in inverse proportion, and when the prime mover changes speed over the range 750 to 2000 r.p.m. this means that the movement of pump stroke must cover a range of 2.67 : 1. A change of motor stroke ψ_m requires, to a first approximation, a proportional change in ψ_p. If the motor stroke is allowed to change from full stroke down to 0.25 this will require a 4 : 1 change in ψ_p. Load on the transmission increases the hydraulic pressure without much effect on the flow, such effect as there is will be due to increased leakage. The performance curves of Fig.(3.5) refer to the pump characteristics at maximum stroke. These show that the total leakage could amount to 15% of the flow when the pressure is raised to 3000 p.s.i. at 1500 r.p.m.. At reduced stroke the proportion of leakage flow is greater and may be as high as 50% but even so the effect of load on the output speed is small compared with the other two variables. For completeness it should be added that a change of load may also affect the pump speed and this would then contribute to the change of output speed. It has been shown that the prime mover gives a constant speed in this case so that this effect is insignificant.

The variation in the transfer function of the system is to be accommodated in the design of the speed control system. The extremes of variation are seen in Fig.(4.10) and Fig.(4.16). In Fig.(4.10) the time

constant and damping ratio are small while in Fig.(4.16) the opposite extreme is evident. These variations must be taken together with a gain change which will amount to 10.65 : 1, or 20 dB, over a pump speed range of 750 to 2000 r.p.m., combined with a motor stroke change down to a quarter of full stroke.

4.5 SPEED CONTROL BY FEEDBACK.

Consideration is now given to the possibility of using a simple feedback system to control the motor speed. The form of the system is outlined in Fig.(4.2). The pump cam control elements in this diagram comprise the electro-hydraulic servo system and the current amplifier described in Section (4.3). To implement the arrangement of Fig.(4.2) the voltage Ve, representing the speed error, must be converted into a proportional current i at the input to the current amplifier. This is done as shown in Fig.(4.17), where also a more detailed block diagram of the complete control loop is developed.

The general control characteristics of this system are those of a Type (1) system [19], i.e. a system with one integration in the forward path. The integrating action is provided by the pump cam control elements. This means that in principle the steady state accuracy of control should be high. The error current i will be brought to zero in the steady state, giving complete cancellation of the effects which might otherwise change the motor speed.

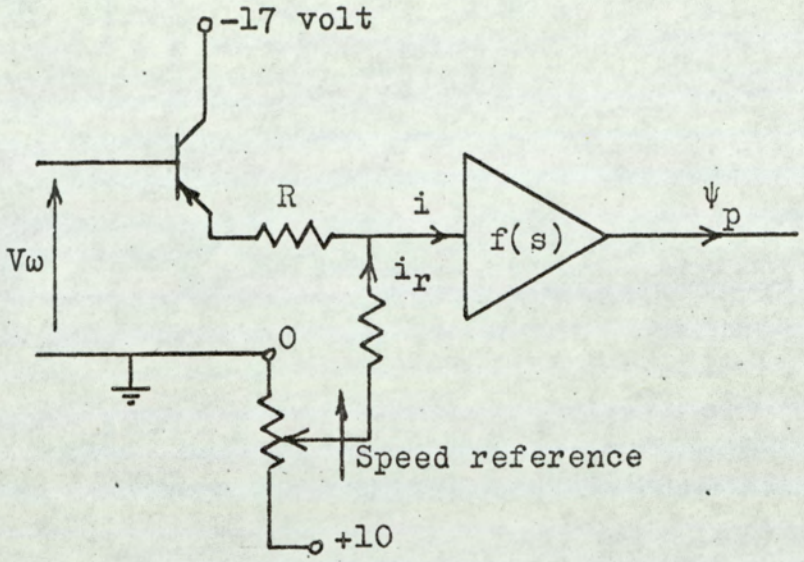

INPUT CIRCUIT

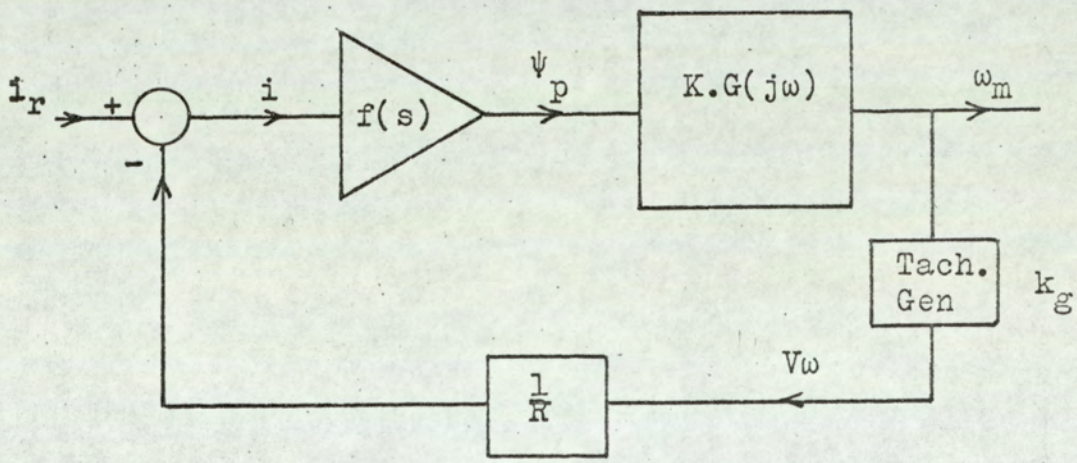

BLOCK DIAGRAM

FIG.(4.17)
SPEED CONTROL FEEDBACK SYSTEM

In the block diagram of Fig.(4.17) the frequency response of the hydraulic system is designated $K.G(j\omega)$. This is subject to the variations described in Section (4.4.2.), resulting from changes in the pump speed and the motor stroke. Following the conclusions reached in Section (4.4.3.) the response characteristics of Fig.(4.10) and Fig.(4.16) are taken to indicate two extremes of variation. The conditions of Fig.(4.10) are those of low gain constant, wide bandwidth and small damping ratio, while in Fig.(4.16) the same three factors are all at the opposite extreme.

The element $f(s)$ in the block diagram represents the pump cam control system. It combines the electro-hydraulic servo system and the current amplifier preceding it. In Section (4.3) the form of $f(s)$ was identified and shown to be as indicated on Fig.(4.7), with $h(j\omega)$ given by equation (4.6). This element is non-linear due to the effect of amplitude saturation.

In considering the stability of the complete control loop we can simplify the analysis as follows. The saturation effect produces a gain change without a change of phase and the maximum gain is seen in the central linear segment. The stability of the control loop is therefore least when the non-linear element is operated in this range. It is then sufficient to design the control loop for stable operation when the frequency response $h(j\omega)$ is allocated to $f(s)$.

When the frequency response of the hydraulic system is combined with $h(j\omega)$ the result is obtained as shown on Fig.(4.18). Curves m_1, representing the modulus and a_1, representing the phase, are derived from the response of Fig.(4.10). The corresponding curves m_2 and a_2 follow from Fig.(4.16). In both cases the phase curves pass beyond 180° so that the open loop gain is limited by instability. The worst condition in this respect is seen when the motor stroke is small. The open loop gain can be set to 65 dB on the amplitude scale for a phase margin of 35°. This would mean that the closed loop bandwidth will be 0.15 Hz which is so low that the system could only compensate for slow changes in the operating conditions. With this gain setting the conditions of curves (1) show an even lower bandwidth of 0.09 Hz.

There is of course some possibility of improving the bandwidth by adding a compensating network but one would be looking for a ten times increase in bandwidth and this does not appear to be possible. The effect of saturation in this case can be regarded as giving a reduction of loop gain as the signal amplitude increases. Although the system stability is not impaired the effective bandwidth will be reduced still further.

The general conclusion from this is that the control of speed by feedback alone cannot give anything but an unreasonably slow response. This is due to the

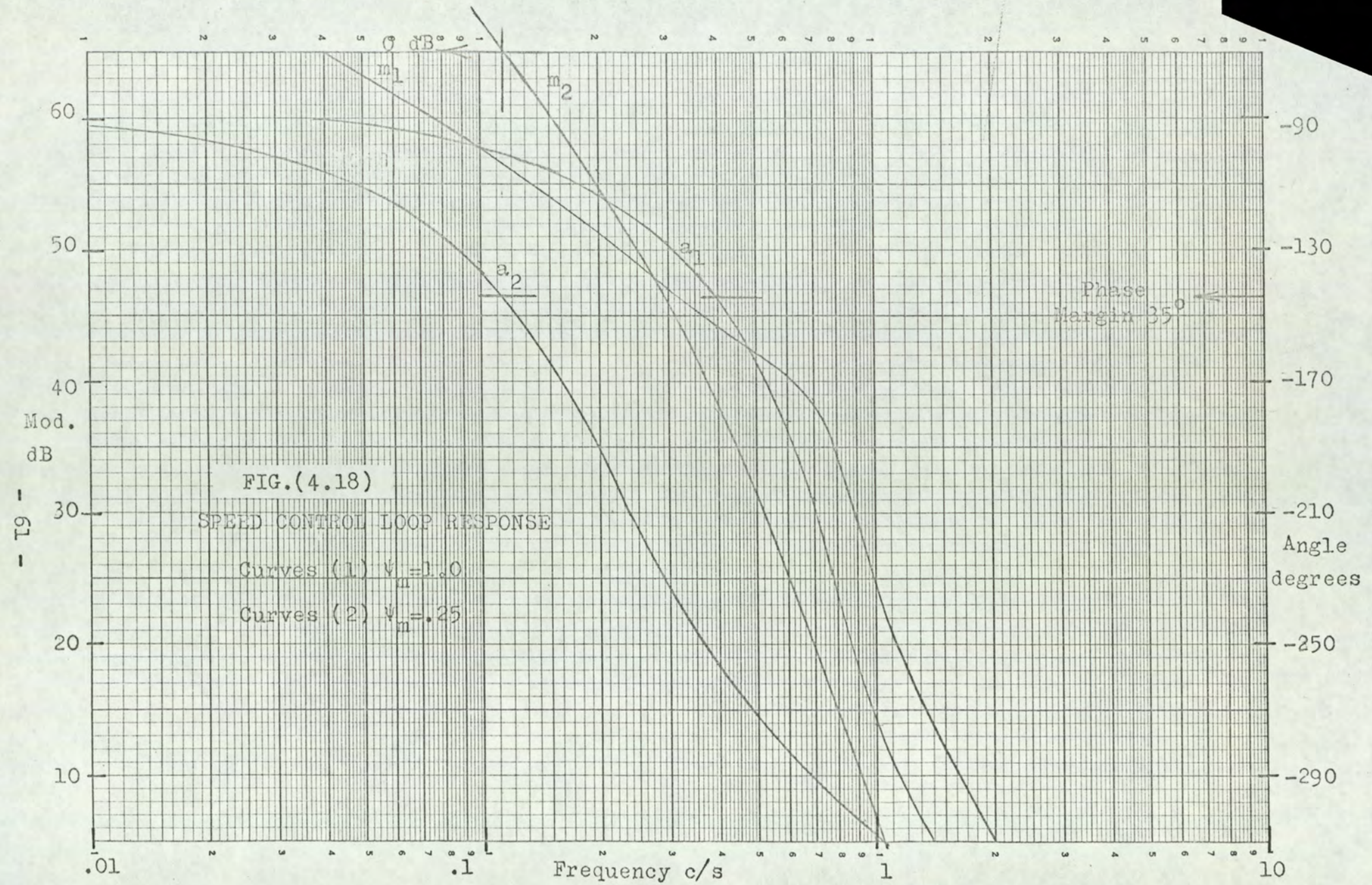

FIG.(4.18)

SPEED CONTROL LOOP RESPONSE

Curves (1) $\forall_m$=1.0

Curves (2) $\forall_m$=.25

need to accommodate a large variation in the characteristics of the hydraulic system. Another factor is the low natural frequency of the hydraulic system. This is due to the high moment of inertia of the generator armature, which is driven by the hydraulic motor, combined with a large compliance of the flexible hose in the hydraulic circuit.

4.6 EVOLUTION OF THE FEEDFORWARD CONTROL ARRANGEMENT.

The following line of thought was followed in developing an alternative to the feedback control system.

(1) The variation in the gain of the hydraulic system is a obstacle to obtaining stable control over the whole range of operating conditions. The change in the gain constant amounts to 20 dB. This could be avoided if the gain could be kept constant by inserting a network having a gain which varies in the opposite sense from that of the hydraulic system.

(2) If the compensation of the gain was complete there would be no need to have a Type (1) system, with an integration in the forward path. A Type (0) system would give adequate steady state accuracy. The block diagram of Fig.(4.19) makes this clear. Here the network N has a finite zero frequency gain which is varied to keep the loop gain $\frac{V\omega}{Ve}$ constant. Thus, in the steady

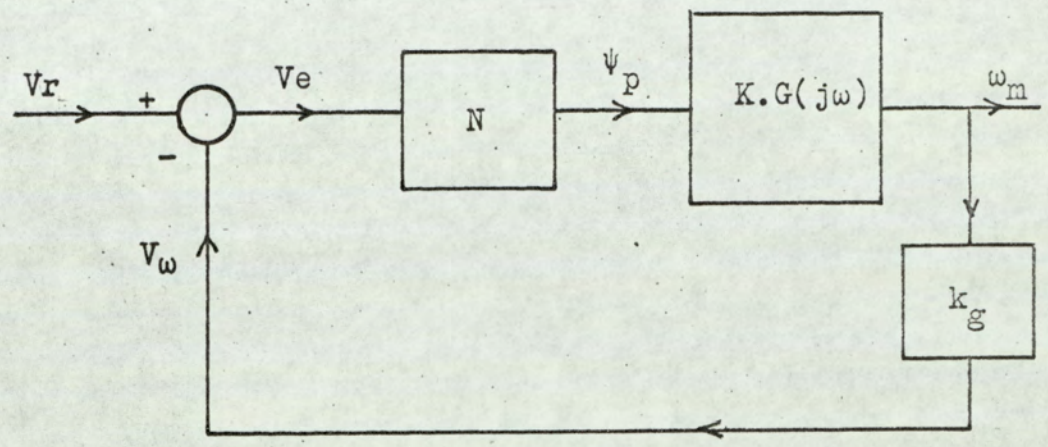

FIG.(4.19)

SPEED CONTROL LOOP WITH GAIN COMPENSATION

state, Ve and the output speed ω_m will both remain constant. The voltage error Ve will not be zero but this is not important as the system is a regulator, with fixed reference Vr which can be set to give the required output speed.

(3) In order to introduce the network N the integrating action of the pump cam control element must be replaced by a system of finite zero frequency gain. To do this it is sufficient to introduce a position feedback loop round the integrating element. A position controlled arrangement of this type was studied in Section (4.3) which gives an indication of what can be expected.

(4) It is necessary to devise a means of varying the closed loop gain of the pump cam position control system to compensate for the gain variations in the hydraulic system. The variation of the gain constant K for the hydraulic system is given by equation (4.15). This means that the gain of the compensating network must be proportional to $\frac{\psi_m}{\omega_p}$.

(5) A solution to this problem is shown in Fig.(4.20). The integrating action in the element f(s) will reduce the current i to zero in the steady state, so that the steady state gain becomes,

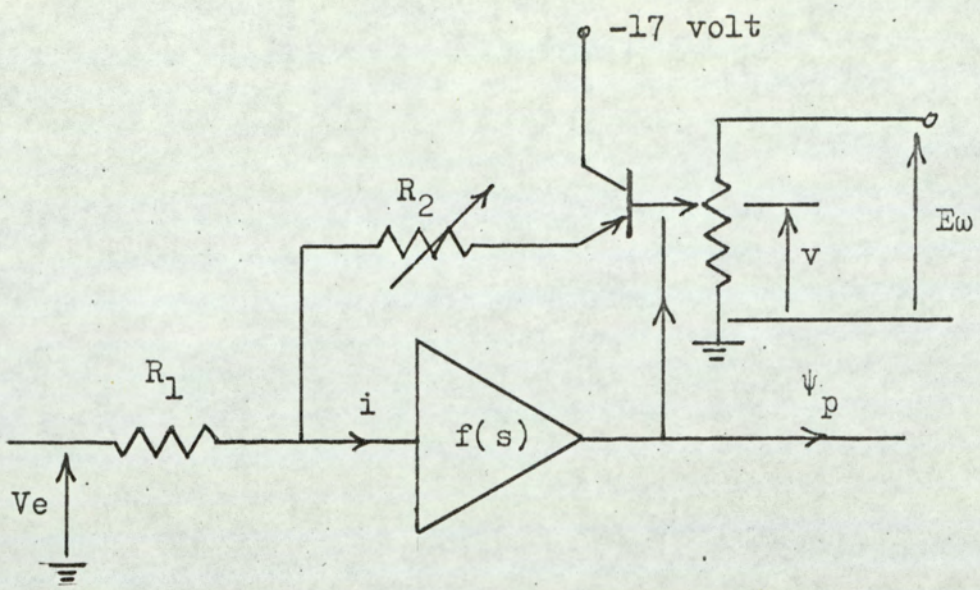

FIG.(4.20)

VARIABLE GAIN NETWORK

$$\frac{\psi_p}{Ve} = \frac{R_2}{R_1 \, E\omega \, \mu} \quad \ldots\ldots\ldots\ldots\ldots\ldots\ldots\ldots\ldots\ldots (4.16)$$

where μ is the fractional movement of the pick-off potentiometer over the range of variation of ψ_p.

Thus if R_2 is made proportional to ψ_m and $E\omega$ proportional to ω_p we get the desired result,

$$\frac{\psi_p}{Ve} \propto \frac{\psi_m}{\omega_p} \quad \ldots\ldots\ldots\ldots\ldots\ldots\ldots\ldots\ldots\ldots (4.17)$$

The further consequences of using this arrangement are investigated in the following section.

4.7 FEEDFORWARD LEADING TO NON-INTERACTING CONTROL.

The line of thought pursued in the preceding section was that of introducing a variable gain element in the speed control loop to keep the loop gain constant. It is now desirable to take a different point of view on the objectives of this arrangement.

4.7.1 NON-INTERACTING CONTROL.

When the pump speed is increased the control action applied to the pump stroke must reduce the stroke by the amount required to keep the motor speed constant. The action of applying the signal $E\omega$, proportional to pump speed, to the variable gain network of Fig.(4.20), may be

regarded as a feedforward operation. Ideally this feedforward action should compensate completely for the change of pump speed, no further control action would then be required from the speed control feedback loop. The pump speed changes would then not interact with the motor speed.

Similarly the adjustment of the motor stroke requires a compensating adjustment of the pump stroke. The action of adjusting R_2 in Fig.(4.20), in proportion to the motor stroke, should ideally set up the required pump stroke. Thus both these variables may be rendered non-interacting with the motor speed by the feedforward action.

Some advantages of this technique are immediately obvious. The speed of response which can be obtained when controlling a load of high moment of inertia is much greater than with feedback control. In the feedback system no control action can be initiated until the load speed has changed. But the feedforward system anticipates the change of load speed and gives control action before the speed has changed. The high inertia of the load can even be an advantage under these conditions. Against this advantage there is the disadvantage that the feedforward system is essentially an 'open loop' arrangement in that the control action is not based on a direct measurement of the controlled variable.

The success of feedforward control depends on maintaining accurately defined characteristics in the feedforward path. This is one of the considerations leading to the decision to use a feedback control loop as well as the feedforward system.

4.7.2. NON-LINEAR COMPENSATION.

The idea of gain compensation was used in Section (4.6) to establish that the voltage $E\omega$ should be proportional to the pump speed ω_p. Similarly it was shown that R_2 should be proportional to the motor stroke Ψ_m. This is based on the somewhat idealised analysis leading to equation (4.15) in which leakage is neglected in the hydraulic system. In order to determine more precisely how the feedforward effect should be related to the primary variables it is better to use the notion of non-interacting control. To do this a test was conducted as follows.

The motor stroke and the pump speed were varied over a range of values and at each setting the motor speed was brought to the same value (750 r.p.m.) by adjustment of the pump stroke. The test was conducted with the loading generator on open circuit. The values of pump stroke obtained in this way should be set up by the feedforward action if complete non-interaction is to be achieved.

We require to decide how the pump stroke Ψ_p should be related to the motor stroke Ψ_m and the pump speed ω_p. If Ψ_p is plotted against Ψ_m at constant ω_p the result is as shown in Fig.(4.21). The relationship is non-linear but a straight line approximation is adequate. For a given value of ω_p we then approximate with,

$$\Psi_p = a + b\,\Psi_m \qquad \ldots\ldots\ldots\ldots\ldots\ldots (4.18)$$

In the variable gain network of Fig.(4.20) we see from equation (4.16) how Ψ_p is related to R_2. This suggests that R_2 should be made to follow the function given in equation (4.18).

Also from equation (4.16) we note that Ψ_p is inversely proportional to $E\omega$. Thus on plotting $\frac{1}{\Psi_p}$ against ω_p we find how $E\omega$ is to be related to ω_p. This results in Fig.(4.22) and a straight line approximation is again used to establish the relationship,

$$\frac{1}{\Psi_p} = c + d\,\omega_p \qquad \ldots\ldots\ldots\ldots\ldots\ldots (4.19)$$

Hence $E\omega$ must follow this same relationship.

Equation (4.18), giving the motor stroke function, is implemented as follows. If R_2 is made up of a fixed resistor r in series with a resistance proportional to Ψ_m we get,

$$R_2 = R\left(\frac{r}{R} + \Psi_m\right) \qquad \ldots\ldots\ldots\ldots\ldots\ldots (4.20)$$

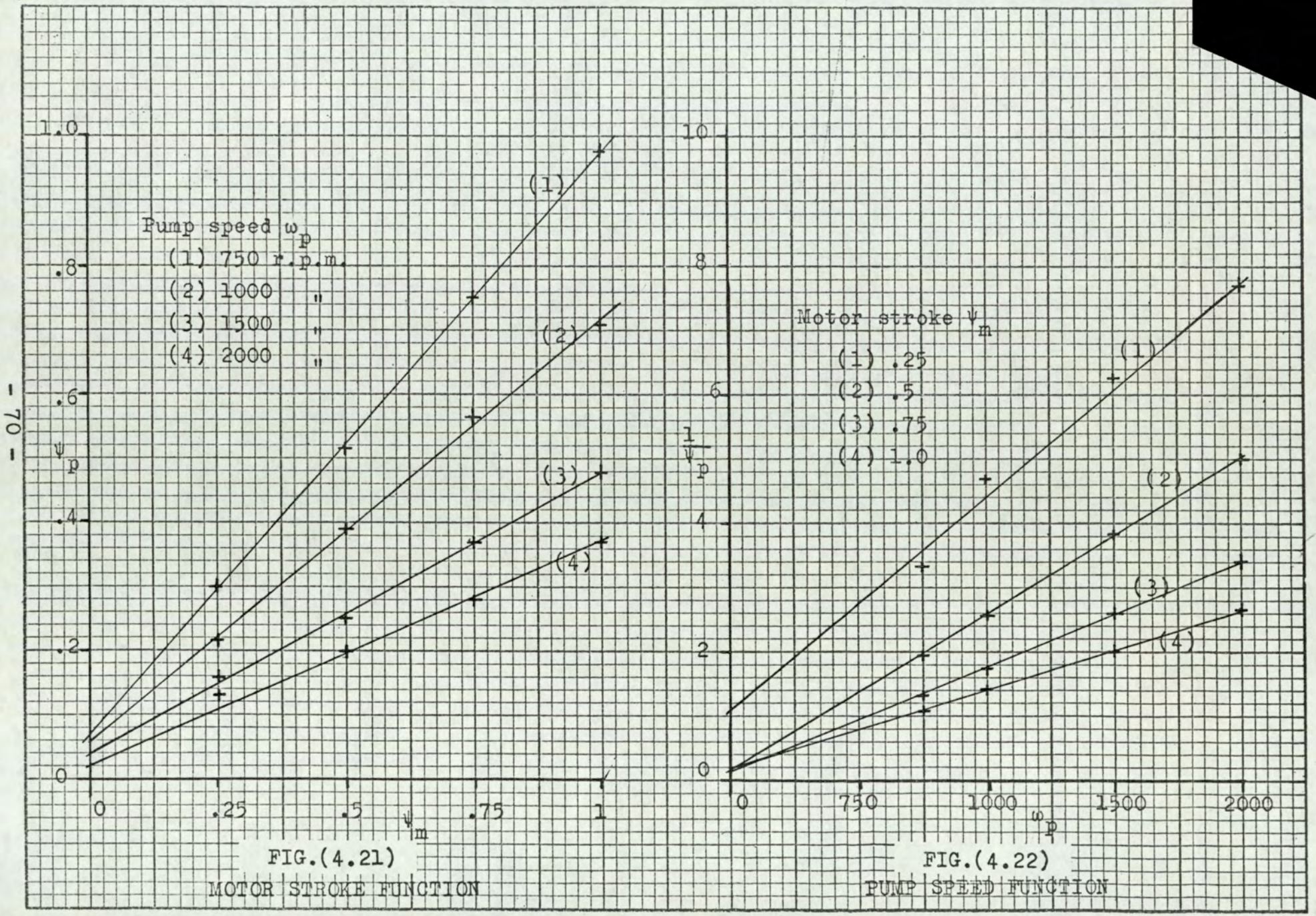

FIG.(4.21)
MOTOR STROKE FUNCTION

FIG.(4.22)
PUMP SPEED FUNCTION

and when this is inserted in equation (4.16) we have, for constant Eω,

$$\frac{\psi_p}{Ve} = k_1 \left(\frac{r}{R} + \psi_m \right) \quad \ldots\ldots\ldots\ldots\ldots (4.21)$$

The magnitude of $\frac{r}{R} = \frac{a}{b}$ may be determined for each line on Fig.(4.21) to give the results shown in Table (1).

ω_p r.p.m.	$\frac{r}{R}$
750	0.0775
1000	0.083
1500	0.092
2000	0.104

TABLE (1)

VALUES OF $\frac{r}{R}$

There is a variation of the required ratio with the pump speed and an average value of 0.087 is taken as a suitable approximation. When R = 10 kΩ this gives r = 870 Ω.

Similarly to implement the pump speed function in equation (4.20) we give Eω a fixed component e and a component proportional to ω_p. We can then write,

$$E\omega = E \left(\frac{e}{E} + \frac{\omega_p}{2000} \right) \quad \ldots\ldots\ldots\ldots\ldots (4.22)$$

and for a constant value of R_2 equation (4.16) then

gives,

$$\frac{Ve}{\psi_p} = k_2 \left(\frac{e}{E} + \frac{\omega_p}{2000} \right) \quad \ldots\ldots\ldots\ldots (4.23)$$

The ratio $\frac{e}{E} = \frac{c}{2000\ d}$ can be evaluated for each line on Fig.(4.22) to give the results shown in Table (2).

ψ_m	$\frac{e}{E}$
0.25	0.167
0.5	0.0345
0.75	0.0625
1.0	0.082

TABLE (2)

VALUES OF $\frac{e}{E}$

There is a variation in the ratio with motor stroke and an approximation is necessary. A value of 0.125 was taken.

The final requirements for implementing these two relationships were met as follows. In the optimising system it is convenient to use an electro-mechanical integrator and set the motor stroke by means of a position control servo loop. The input to the position control loop is taken from a rotary potentiometer and it is convenient to couple a second potentiometer to the same shaft. The resistance of this potentiometer is then proportional

to the motor stroke.

To generate the relationship given in equation (4.22) it was necessary to design an amplifier, the circuit details of which are given in Section (4) of the Appendix. The relationship between voltage and speed produced in this way is shown in Fig.(4.23).

4.7.3. INTERACTION TEST

The degree of interaction remaining after the feedforward system had been applied, was measured by subjecting the overall system to changes of pump speed and motor stroke. The speed control feedback system was not connected in this test. The results are given in Table (3). The figures presented here represent the percentage change from the base speed of 750 r.p.m., as set initially at ω_p = 750 r.p.m. with Ψ_m = 1.0.

ω_p \ Ψ_m	1.0	0.25
750	0	+2
1000	0	+1
1500	+1	-4
2000	+2	-6

TABLE (3)
INTERACTION TEST

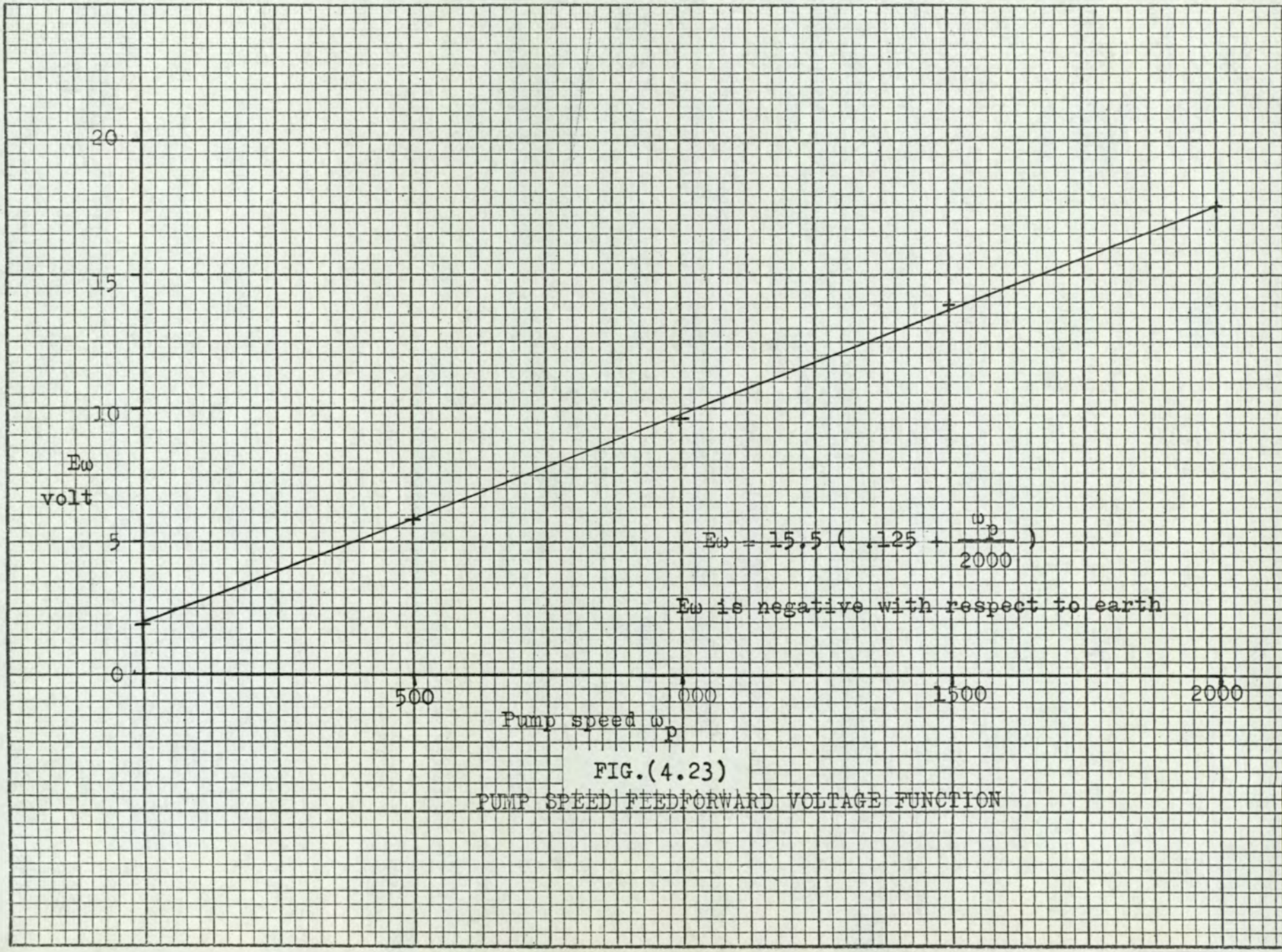

FIG.(4.23)
PUMP SPEED FEEDFORWARD VOLTAGE FUNCTION

The results of Table (3) indicate that when the pump speed is low the motor speed increases as the motor stroke is reduced. This would imply that the fixed component of R_2 is too large. However when the pump speed is high the opposite effect is seen and the setting achieved is therefore a compromise between these two states. When the motor stroke is held constant at the maximum value an increase in the pump speed gives an increase in the motor speed. This would suggest that $\frac{e}{E}$ is too large. Again the trend is opposite when the stroke is set to 0.25 and a compromise must be accepted. It is concluded that the settings achieved offer a reasonable compromise, within the limitations of what can be obtained with linear approximations.

4.8 DYNAMICAL CHARACTERISTICS OF THE VARIABLE GAIN NETWORK.

The analysis of the compensating function of the variable gain network, in Section (4.7), has been based on the steady state response of the system. It is now required to look more closely at the dynamical properties of the system, bearing in mind that it is proposed to operate a feedback control loop round the complete system.

4.8.1. THE PROBLEM OF GAIN VARIATION.

The closed loop gain of the variable gain network, shown in Fig.(4.20), is changed by adjustment of the gain in the feedback path. This changes the open loop gain of the subsidiary loop round f(s) and

the dynamical response of the closed loop will therefore change as well. It is important that the subsidiary loop should not become unstable at the maximum gain condition. But equally at the condition of low loop gain the gain should be high enough to prevent the lag between Ψ_p and Ve becoming too large. A compromise must be found which must take account of a variation of loop gain amounting to 20 dB.

The closed loop characteristics of this system were studied in Section (4.3), in order then to measure the frequency response of the element f(s). The results presented on Fig.(4.5) indicate what is to be expected in the closed loop response. There is a marked peak in the modulus curves at high frequency when the signal amplitude is small. This indicates that the system is not far from instability. A further test was conducted in which R_2 was reduced (Fig.(4.4)). It was then clear that the gain could not be increased more than 6 dB without instability appearing. Hence therewas a need to increase the stability margin of the loop to accommodate a 20 dB change of loop gain.

4.8.2. COMPENSATING NETWORK.

The requirements for an increased stability margin may be met by introducing a compensating network. Reference to the Nichols Chart of Fig.(4.6) suggests that phase advance compensation is required in the region of 20 Hz. It is convenient to obtain this

by adding components C and R_3 as shown in Fig.(4.24). The resistor R_3 is included to limit the current fed to the input of the current amplifier at high frequencies. This is necessary because the signal $E\omega$ contains high frequency components due to rectification of the a.c. tachometer signal which is used to measure the pump speed.

The fact that R_2 is variable must be taken into account in making the choice of the value of C. Furthermore we should enquire whether this means of improving the stability margin of the loop will adversely affect the transfer functions relating Ψ_p to Ve, $E\omega$ and Ψ_m.

A block diagram of the system is shown on Fig.(4.24). The component Y_2 is the transfer admittance of the feedback network and is given by,

$$Y_2 = \frac{1 + sC(R_2 + R_3)}{R_2(1 + sCR_3)} \qquad \ldots\ldots\ldots\ldots (4.24)$$

The varying gain representing the transfer ratio of the pick-off potentiometer is designated k,

$$k = \frac{V}{\Psi_p} = \mu E\omega \qquad \ldots\ldots\ldots\ldots\ldots\ldots (4.25)$$

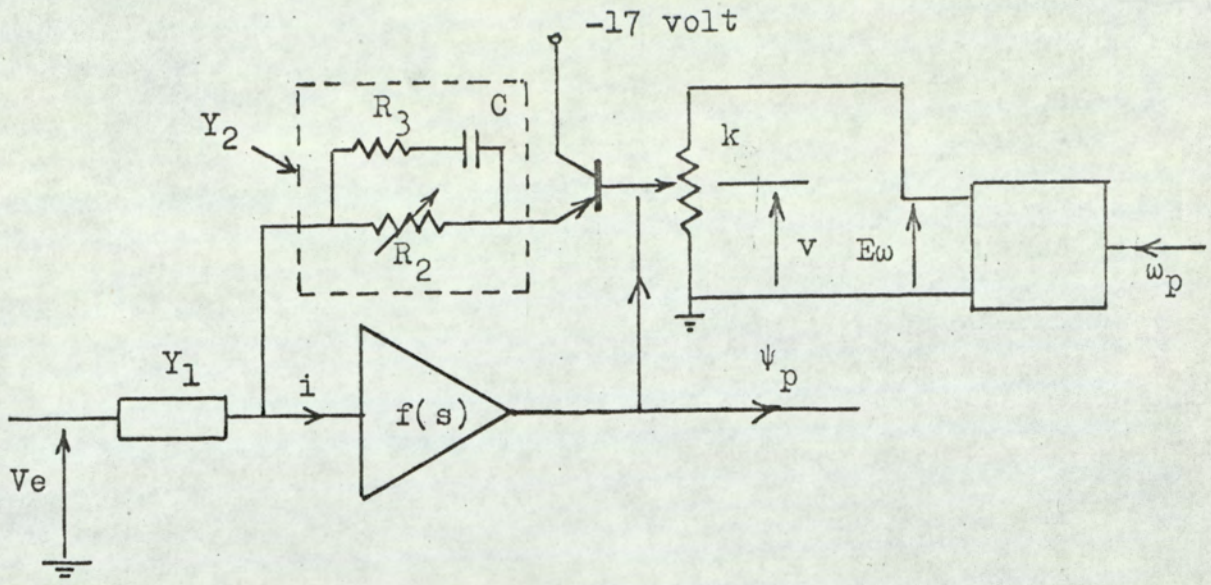

CIRCUIT WITH COMPENSATING NETWORK

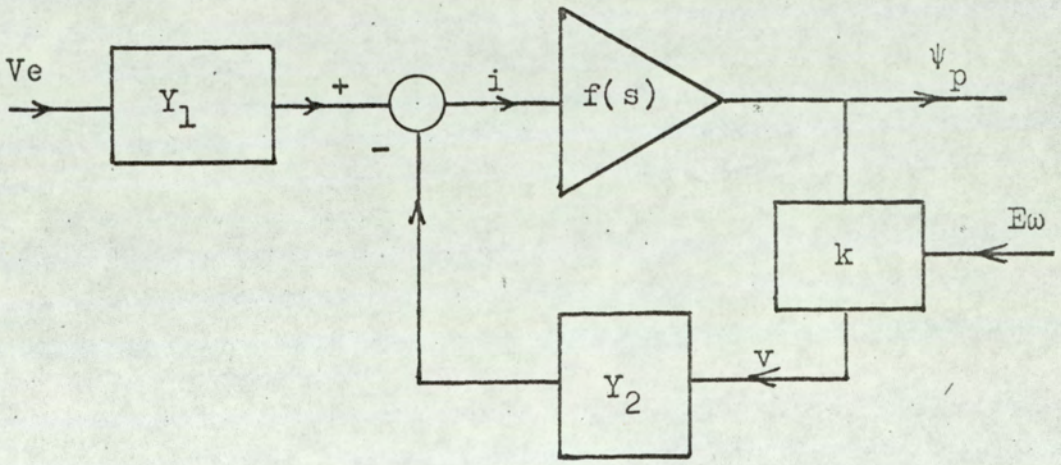

BLOCK DIAGRAM

FIG.(4.24)

PUMP CAM POSITION CONTROL LOOP

The transfer function $\frac{\psi_p}{Ve}$ is obtained from the block diagram as,

$$\frac{\psi_p}{Ve} = \frac{Y_1 f(s)}{1 + Y_2 k f(s)} \quad \text{.....(4.26)}$$

Since Y_2 operates in the feedback path it appears only in the denominator of this transfer function. A phase advance in Y_2 will therefore contribute a lag in the response of ψ_p to changes of Ve.

The transfer function relating ψ_p to $E\omega$ varies with $E\omega$, i.e. the system is non-linear. For small changes we can find a linear approximation as follows. The pick-off voltage v in Fig.(4.24) is given by,

$$v = \mu E\omega \psi_p \quad \text{.....(4.27)}$$

then, for small changes,

$$dv = \mu E\omega \, d\psi_p + \mu \psi_p \, dE\omega \quad \text{.....(4.28)}$$

and using this result, in conjunction with the block diagram of Fig.(4.24), we can draw the block diagram shown in Fig.(4.25). From this latter diagram the transfer function is seen to be,

$$\frac{d\psi_p}{dE\omega} = \psi_p \left(\frac{-\mu Y_2 f(s)}{1 + \mu Y_2 E\omega f(s)} \right) \quad \text{.....(4.29)}$$

Here Y_2 appears in both numerator and denominator and the effect of phase advance in Y_2 is then to

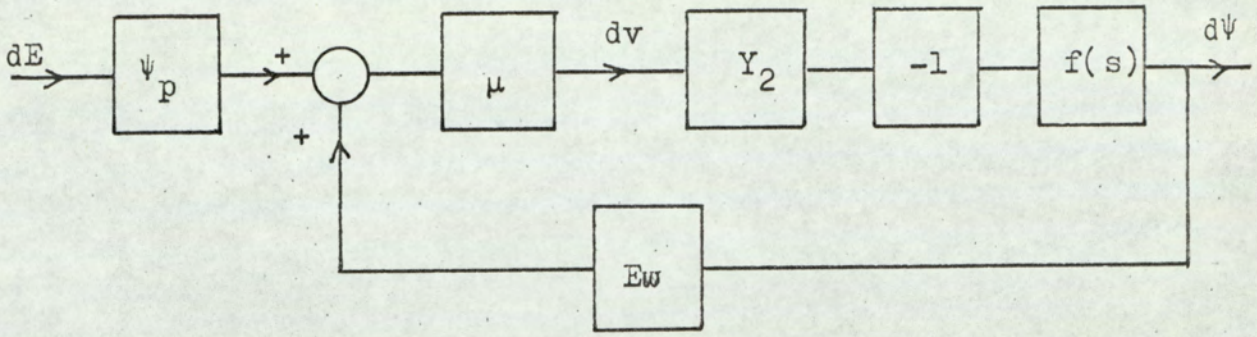

FIG.(4.25)

RESPONSE TO CHANGES IN Eω

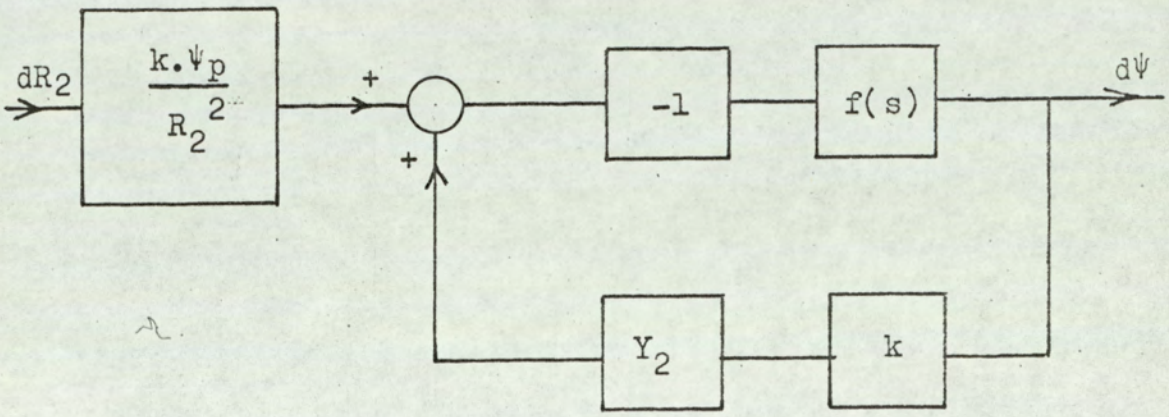

FIG.(4.26)

RESPONSE TO CHANGES IN R_2

reduce the lag in the response of Ψ_p to $E\omega$.

The motor stroke controls Ψ_p through the feedback resistor R_2. The transfer function relating Ψ_p to changes in R_2 depends on the value of R_2. Again we may linearise the transfer function for small changes. The current in R_2 is seen from Fig.(4.24) to be,

$$i_2 = \frac{v}{R_2} = \frac{k\,\Psi_p}{R_2} \qquad \text{.....(4.30)}$$

and hence,

$$\frac{di_2}{dR_2} = \frac{-k\,\Psi_p}{R_2^2} \qquad \text{.....(4.31)}$$

For small changes in R_2 the block diagram of Fig.(4.26) can be developed and from this the transfer function is seen to be,

$$\frac{d\Psi_p}{dR_2} = \frac{k\,\Psi_p}{R_2^2}\left(\frac{-f(s)}{1 + Y_2\,k\,f(s)}\right) \qquad \text{.....(4.32)}$$

Because Y_2 is present in the denominator only a phase advance in Y_2 will increase the lag of Ψ_p in following changes of R_2.

The overall assessment of these effects is that by advancing the phase of Y_2 the stability margin of the loop may be increased but at the same time there are detrimental effects. The lag of Ψ_p

on Ve and ψ_m is increased while the lag of ψ_p on ω_p is reduced. It is therefore unwise to use more than the minimum phase advance necessary to give an adequate stability margin.

The phase characteristics of the function Y_2 given by equation (4.24) have been analysed [20]. It is sufficient to make R_3 470 Ω to limit the high frequency response. The maximum loop gain occurs when R_2 is small and we therefore take the value for $\psi_m = 0.25$. Equation (4.20) then gives the value $R_2 = 3.37$ kΩ. The time constant ratio in Y_2 sets the maximum value of the phase advance and this is determined by the ratio $\frac{R_3}{R_2 + R_3}$ which becomes 0.122. The results of D'Azzo and Houpis then show that the maximum phase advance will be 50^o. To position the advance at the correct point on the frequency response characteristics involves a choice of capacitor C. In view of the response shown on Fig.(4.6) we make the lower break frequency of the network occur at 20 Hz and thereby fix the value of C as 2.07 μF.

At the minimum loop gain $\psi_m = 1.0$ and $R_2 = 10.87$ kΩ, so that the lower break frequency of the network then moves to 7.6 Hz. This frequency is still sufficiently high for the effects of Y_2 to be outside the frequency range of interest in the overall speed control system and is therefore satisfactory.

4.8.3. FINAL RESPONSE CHARACTERSITICS.

With the addition of the network designed in the preceding section the response of Fig.(4.5) is modified and becomes as shown on Fig.(4.27). The improved stability margin is apparent. In assessing the response characteristics it should be noted that this variable gain network will operate as the element N in the speed control loop shown on Fig.(4.19). The gain of the network is changed to compensate for the change of zero frequency gain of the hydraulic system, $K.G(j\omega)$. However, as the gain changes take place the dynamical characteristics of both N and $K.G(j\omega)$. alter. In order to design the speed control loop it is necessary to combine the response of the variable gain network with that of the hydraulic system. From the range of possible response characteristics for each of these it is necessary to select those which relate to conditions of extreme variation. In order to make it more easy to assess the trend of variation of the loop response it is helpful to identify an operating region defined by Ψ_m and ω_p. The response of the variable gain network and the hydraulic system may then be associated with points in this region.

Taking first the variable gain network. The steady state gain in the feedback path gives a guide to the form of closed loop response to be expected. The feedback gain at zero frequency is proportional to the factor g given by,

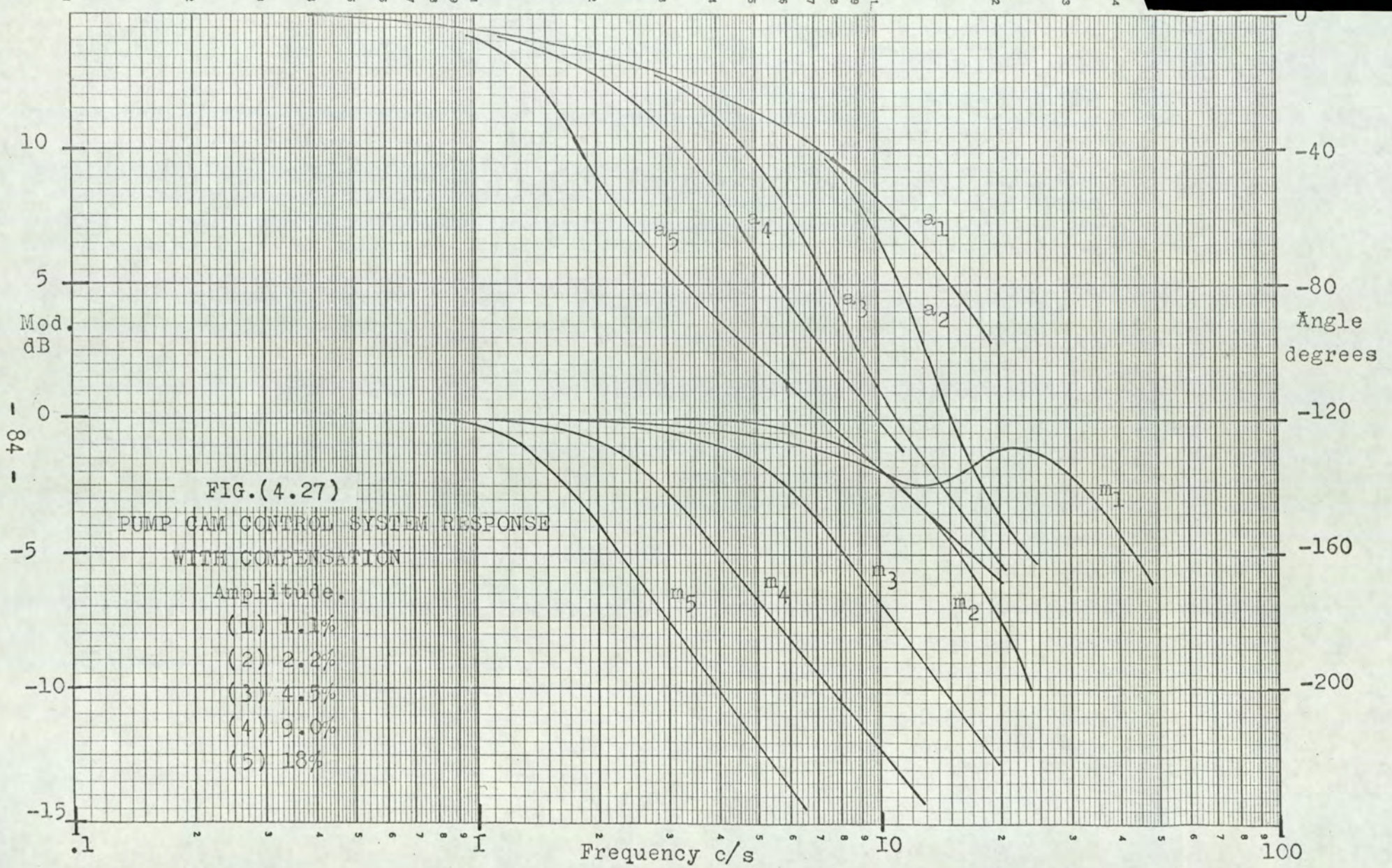
10
5
0
-5
-10
-15
Mod. dB
0
-40
-80
-120
-160
-200
Angle degrees
.1
1
10
100
Frequency c/s
a_1
a_2
a_3
a_4
a_5
m_1
m_2
m_3
m_4
m_5
FIG.(4.27)
PUMP CAM CONTROL SYSTEM RESPONSE
WITH COMPENSATION
Amplitude.
(1) 1.1%
(2) 2.2%
(3) 4.5%
(4) 9.0%
(5) 18%

$$g = \frac{E\omega}{R_2} \quad \text{.....(4.33)}$$

From equation (4.20) we have R_2 and from equation (4.22), $E\omega$. Hence,

$$g = \frac{E}{R}\left(\frac{\frac{e}{E} + \frac{\omega_p}{2000}}{\frac{r}{R} + \Psi_m}\right) \quad \text{.....(4.34)}$$

Lines of constant g can be drawn over the operating region by solving equation (4.34) for Ψ_m i.e.

$$\Psi_m = \frac{E\,\omega_p}{2000\,R\,g} + \left(\frac{e}{R\,g} - \frac{r}{R}\right) \quad \text{.....(4.35)}$$

The lines of constant g are thus straight lines which appear as shown on Fig.(4.28). The zero dB value of g is taken as 2.61, the condition leading to the results of Fig.(4.27). Further tests conducted at operating points X (Ψ_m=1.0, ω_p=500) and Y (Ψ_m=0.25, ω_p=2000) in the region, define the extremes of variation of the response and the results are given on Fig.(4.29) and Fig.(4.30). Together with the results of Fig.(4.27), taken at point Z, a general view of the variation of the response over the operating region is obtained.

Also indicated in the operating region on Fig.(4.28) are the seven points at which the response of the hydraulic system has been measured. These are numbered (1) to (7).

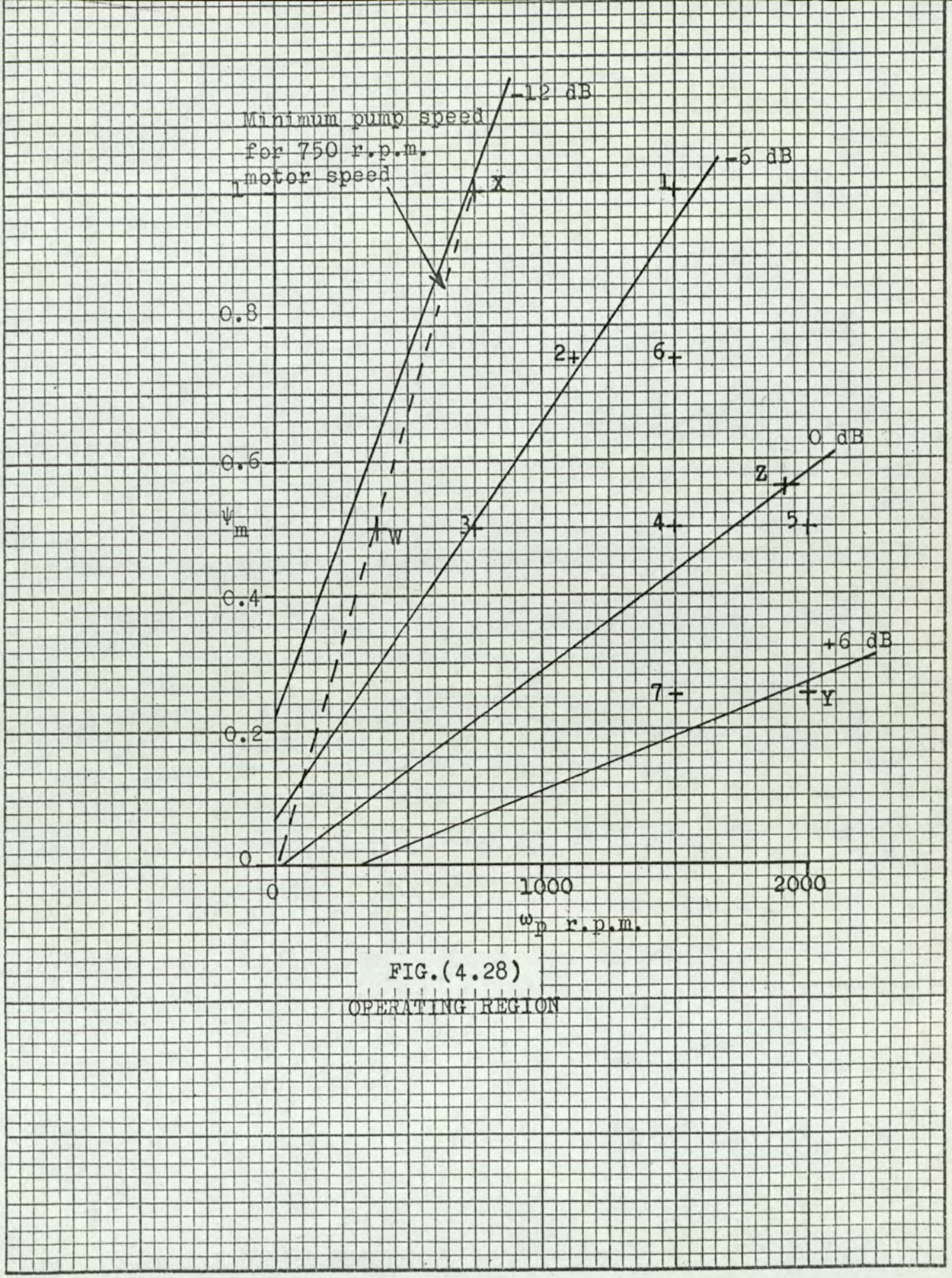

FIG.(4.28)
OPERATING REGION

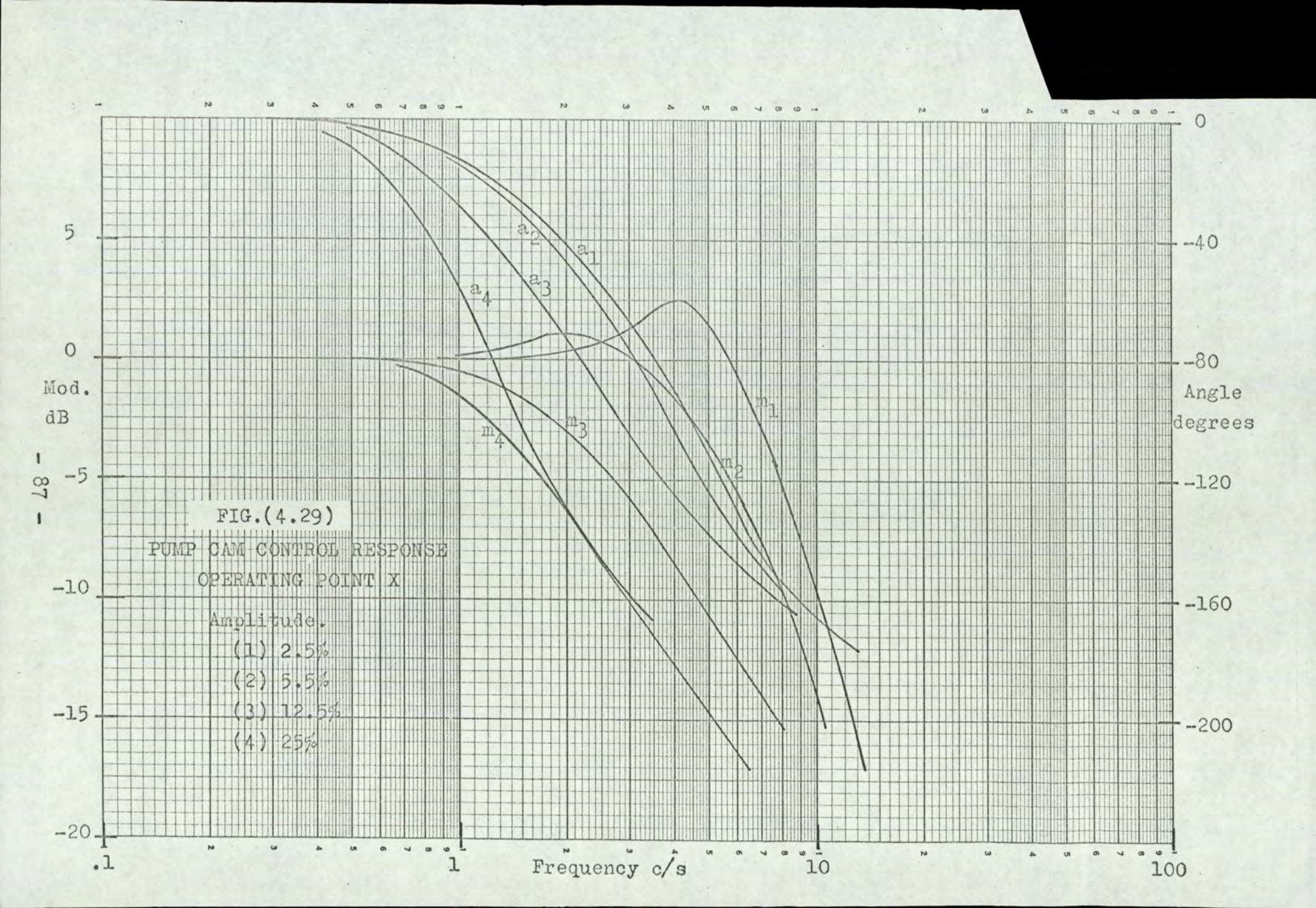
5
0
-5
-10
-15
-20
Mod.
dB
0
-40
-80
-120
-160
-200
Angle
degrees
.1
1
10
100
Frequency c/s
a_1
a_2
a_3
a_4
m_1
m_2
m_3
m_4
FIG.(4.29)
PUMP CAM CONTROL RESPONSE
OPERATING POINT X
Amplitude.
(1) 2.5%
(2) 5.5%
(3) 12.5%
(4) 25%

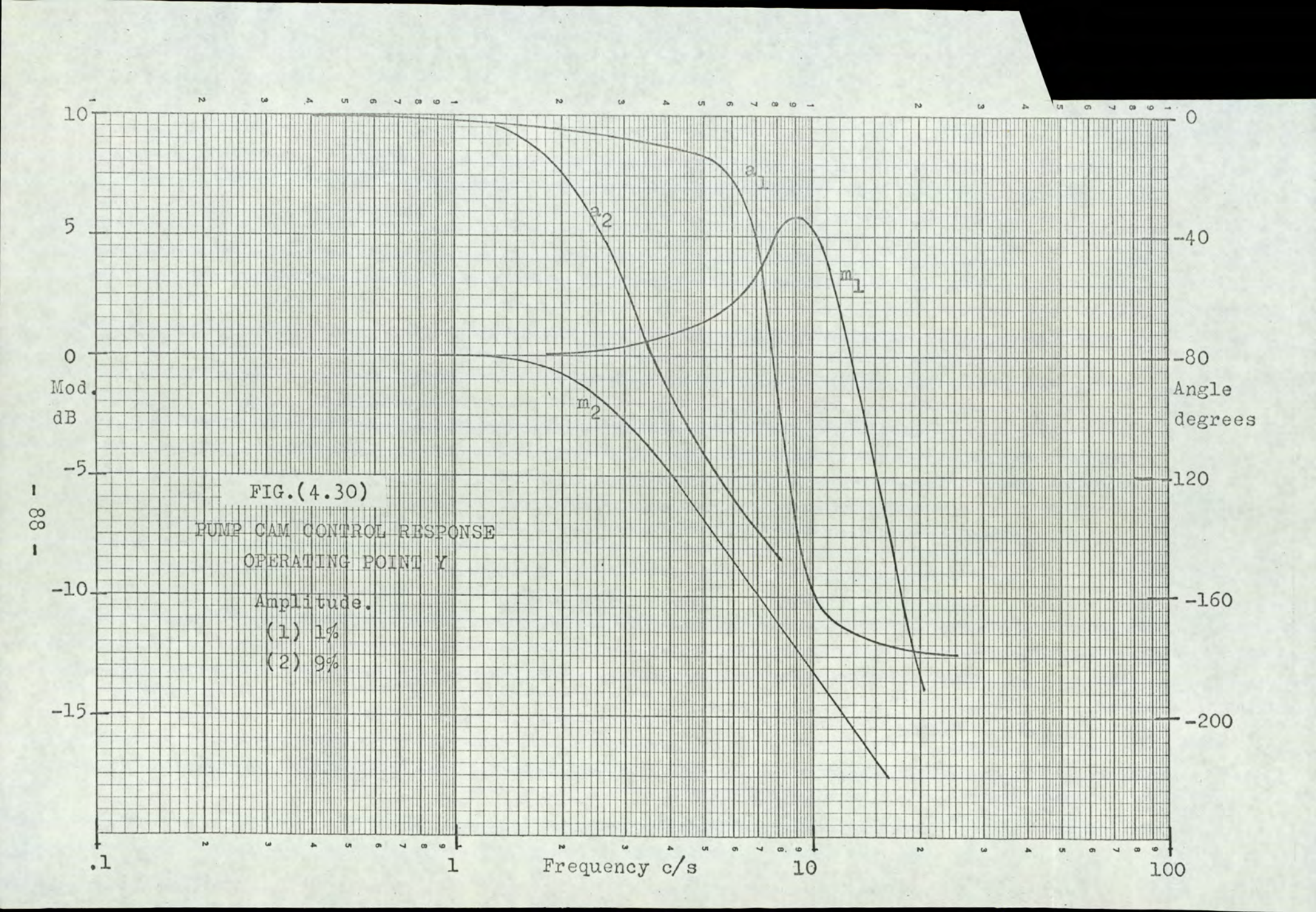
10
5
0
-5
-10
-15
Mod.
dB
0
-40
-80
-120
-160
-200
Angle
degrees
.1
1
10
100
Frequency c/s
a_1
a_2
m_1
m_2
FIG.(4.30)
PUMP CAM CONTROL RESPONSE
OPERATING POINT Y
Amplitude.
(1) 1%
(2) 9%

4.9 EVALUATION OF THE RESULTS OF FEEDFORWARD CONTROL.

The general result of controlling the pump stroke by feeding forward signals derived from the pump speed and the motor stroke has been studied. It has been shown to be capable of reducing the motor speed variations to less than 6% in the steady state. This corresponding to a change of pump speed of 8.5 dB, or 2.67 : 1, combined with a motor stroke change of 12 dB, or 4 : 1. To reduce the interaction to this low level it was necessary to apply non-linear shaping to the feedforward signals. Straight line approximations were used in this to simplify the circuit design. A further reduction of the interaction could be made by more attention to the choice of non-linear shaping functions, but this development is regarded as being beyond the scope of the present study.

Another interesting problem arises when the dynamical interaction of the system is considered. If the pump speed is changing the lag in the feedforward control action is important. This will cause the change of pump stroke to lag behind the change of pump speed and will result in a transient change of the motor speed. There is a prospect of improving the situation by designing a network to operate on the feedforward signal, $E\omega$, before passing it to the variable gain network. Similarly with the feedforward of motor stroke

changes, dynamical compensation could improve the response. These developments are considered to be outside the scope of the present work. An assessment of the dynamical charactersitics of the system, as designed at present, will be made following the design of the speed control feedback system.

The response of the system as a variable gain network has been studied here. In this, the response to changes in the voltage error Ve has been measured. Non-linearity is a dominant feature of this response and is due to velocity saturation of the cam-plate control mechanism. This can only be improved by modifying the hydraulic system, which controls the servo piston movement, to give a higher maximum rate of travel of the piston. Some advantage is gained in using the mechanism as the basis of the variable gain network. This introduces a position feedback round the non-linear element which has the effect of improving the linearity of the overall speed control loop.

4.10 DESIGN OF THE SPEED CONTROL FEEDBACK LOOP.

4.10.1 GENERAL CONSIDERATIONS.

The use of feedforward control of the pump stroke eliminates most of the variation of motor speed due to pump speed and motor stroke changes. The remaining variation is confined to the range +2% to -6% about the nominal speed setting. While the speed control feedback loop will further reduce these variations, its primary purpose is to compensate for changes of speed which result from load on the transmission. The design will be based

therefore on the point of view of rejecting the effects of load changes.

The block diagram of Fig.(4.31) shows the control loop with a signal $\delta(V\omega)$ representing the effect of a load change. Thus the speed change is indicated as a small change in the speed feedback voltage $V\omega$. The change $\delta(V\omega)$ is what would be seen if the load is applied to the transmission without the feedback control loop connected. If $\varepsilon(V\omega)$ is the nett change in $V\omega$, as a result of the same disturbance, when the feedback is operating, its value is given by the transfer function,

$$\frac{\varepsilon(V\omega)}{\delta(V\omega)} = \frac{1}{1 + N(j\omega)\, KG(j\omega)\, k_g} \qquad \ldots\ldots\ldots(4.36)$$

The performance of the feedback control system is then to be assessed on the basis that this ratio should be as small as possible, over the frequency range of interest. A compensating network will be introduced to modify the response $N(j\omega)$ so that the performance is improved.

In order conveniently to evaluate equation (4.36) it is best to write it in the form,

$$\frac{\varepsilon(V\omega)}{\delta(V\omega)} = Y(j\omega) = \frac{y(j\omega)}{1 + y(j\omega)} \qquad \ldots\ldots\ldots(4.37)$$

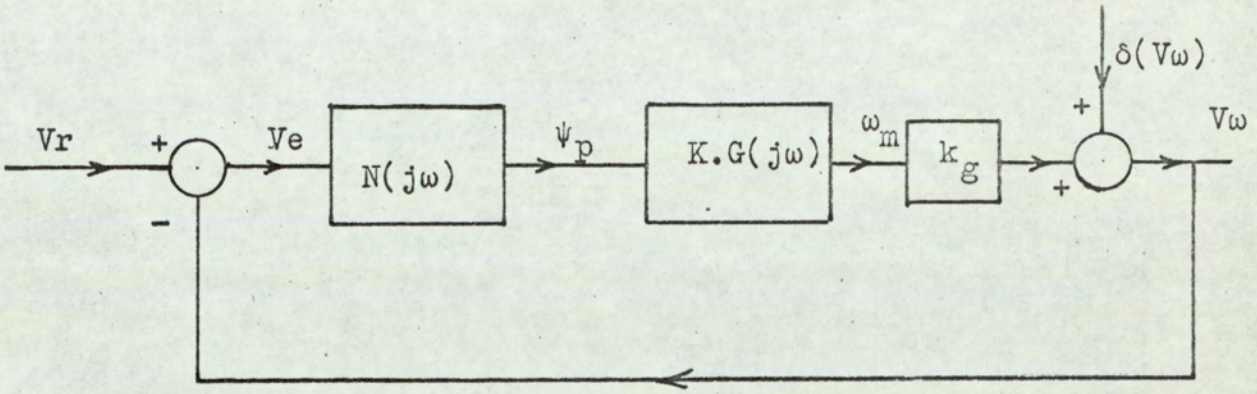

FIG.(4.31)

BLOCK DIAGRAM WITH LOAD DISTURBANCE

where,

$$y(j\omega) = \frac{1}{N(j\omega)\ K\ G(j\omega)\ k_g} \qquad \ldots\ldots\ldots(4.38)$$

The response function $y(j\omega)$ is then the inverse of the open loop response. Equation (4.37) may now be evaluated using a Nichols Chart [17]. As this is not the usual way in which the chart is used, some explanation of the mode of application here is necessary.

A Nichols Chart is presented on Fig.(4.32). If the values of $y(j\omega)$ are plotted against the ordinate and abscissa scales, the lines of constant magnitude and constant phase give values of $Y(j\omega)$. When the magnitude of $Y(j\omega)$ is zero dB the effect of the disturbance is the same in magintude with the feedback connected as it would be on open loop. More significantly, if the modulus of $Y(j\omega)$ is greater than zero dB the effect of the disturbance is increased in magnitude by the feedback action. This is clearly most undesirable and therefore the locus of $y(j\omega)$ should, as far as possible, be confined to the region outside the shaded area on Fig.(4.32).

The need for stability also places restrictions on the locus. Any system having a stable open loop response, i.e. with no poles of the open loop transfer function in the right hand half of the s-plane, will be stable only if the locus of $y(j\omega)$ passes above the critical point (0 dB, zero phase margin) as frequency increases. This means that

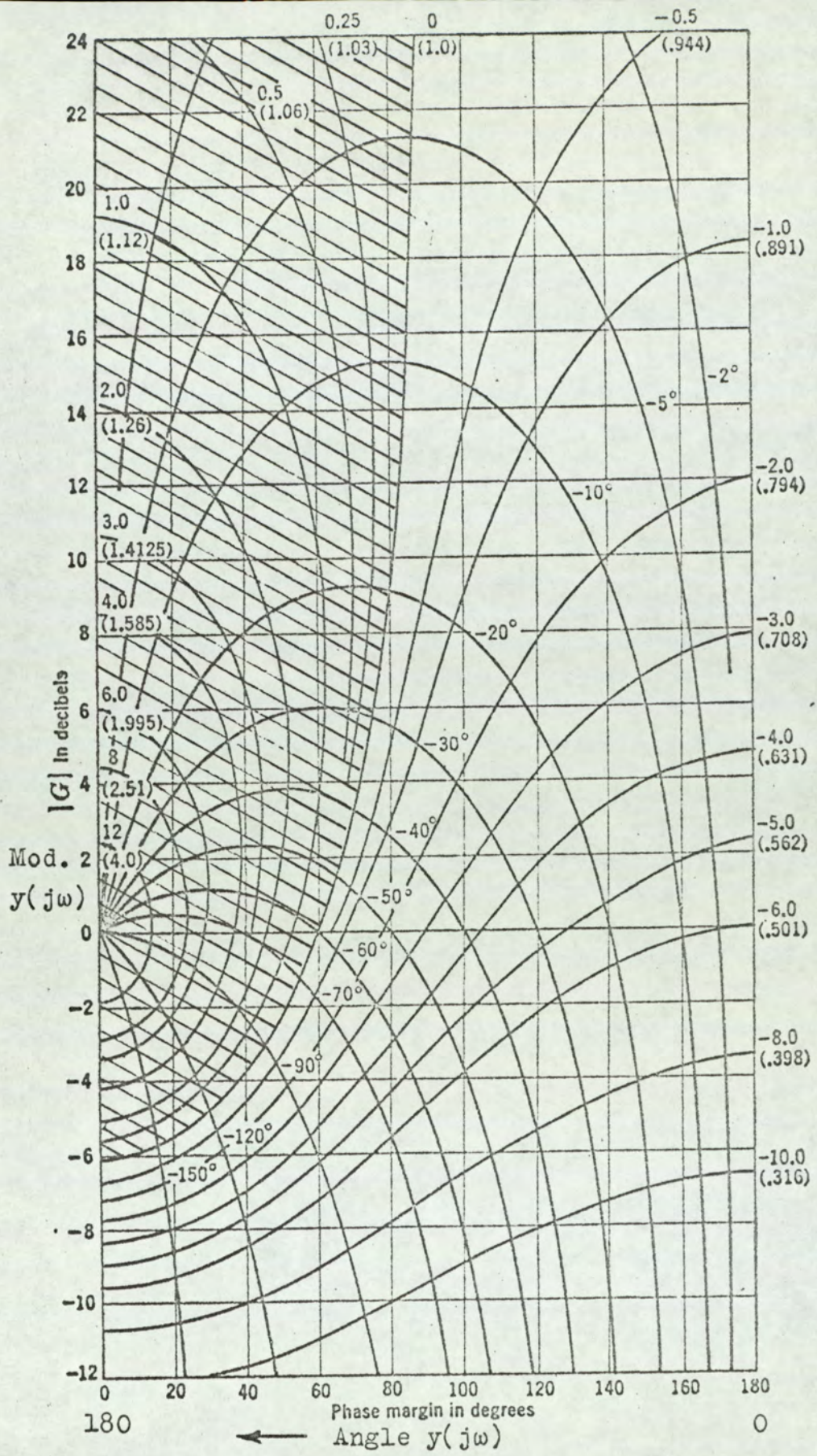
0.25
0
−0.5
(1.03)
(1.0)
(.944)
0.5
(1.06)
1.0
(1.12)
−1.0
(.891)
−2°
−5°
2.0
(1.26)
−2.0
(.794)
−10°
3.0
(1.4125)
4.0
(1.585)
−3.0
(.708)
−20°
6.0
(1.995)
−30°
8
(2.51)
−4.0
(.631)
−40°
12
(4.0)
−5.0
(.562)
−50°
−6.0
(.501)
−60°
−70°
−8.0
(.398)
−90°
−120°
−150°
−10.0
(.316)
Mod. y(jω)
|G| In decibels
24
22
20
18
16
14
12
10
8
6
4
2
0
−2
−4
−6
−8
−10
−12
0
20
40
60
80
100
120
140
160
180
Phase margin in degrees
180
Angle y(jω)
0

FIG.(4.32)

ideally the phase angle of $y(j\omega)$ should not exceed 90° at high frequencies if both these requirements are to be met completely.

4.10.2 CHOICE OF DATA FOR ANALYSIS.

In designing the speed control feedback loop it is first necessary to obtain the open loop frequency response. The loop is made up of two sub-systems, the hydraulic system and the variable gain network. Both of these have response charactersitics which vary with the operating conditions. A choice must be made from the data giving the response of each of the sub-systems. The diagram of Fig.(4.28) assists in making this choice as it is necessary to associate the two sets of response data as they vary over the operating region. On this diagram the points numbered (1) to (7) indicate the conditions under which the response of the hydraulic system has been tested. The results of these tests are given in Section (4.4.2) and correspond to the points indicated as follows,

Point (1) corresponds to Fig.(4.10)
" (2) " " Fig.(4.11)
" (3) " " Fig.(4.12)
" (4) " " Fig.(4.13)
" (5) " " Fig.(4.14)
" (6) " " Fig.(4.15)
" (7) " " Fig.(4.16)

It was observed in Section (4.4.2) the response of the hydraulic system is only slightly affected by changes of the pump speed but varies considerably with the motor stroke setting. The extremes are are therefore seen at $\Psi_m = 1.0$ and $\Psi_m = 0.25$; the results under these conditions are given on Fig.(4.10) and Fig.(4.16).

The lines of constant loop gain in the variable gain network are also shown on Fig.(4.28). It then becomes clear that points X and Y represent the operating conditions which set the extremes of variation of the complete open loop response of the speed control loop. In addition it is also advisable to look at the conditions at point W and this represents an intermediate state.

An initial review of these three conditions shows that the response at point X sets the limit to the zero frequency gain required for stable operation. At this point the data from Fig.(4.10) are combined with those of Fig.(4.29) and their inverse is plotted on Fig.(4.33). Here Curve (1) is obtained using the response of the hydraulic system alone as a basis for comparison. Curve (2) includes the response of the variable gain network with a signal amplitude of 2.5% and Curve (3) uses the results at an amplitude of 25%. The curves have been given a vertical shift to place the zero frequency gain at zero dB for convenience. It is clear that the curves pass well into the undesired region. What is more the control loop

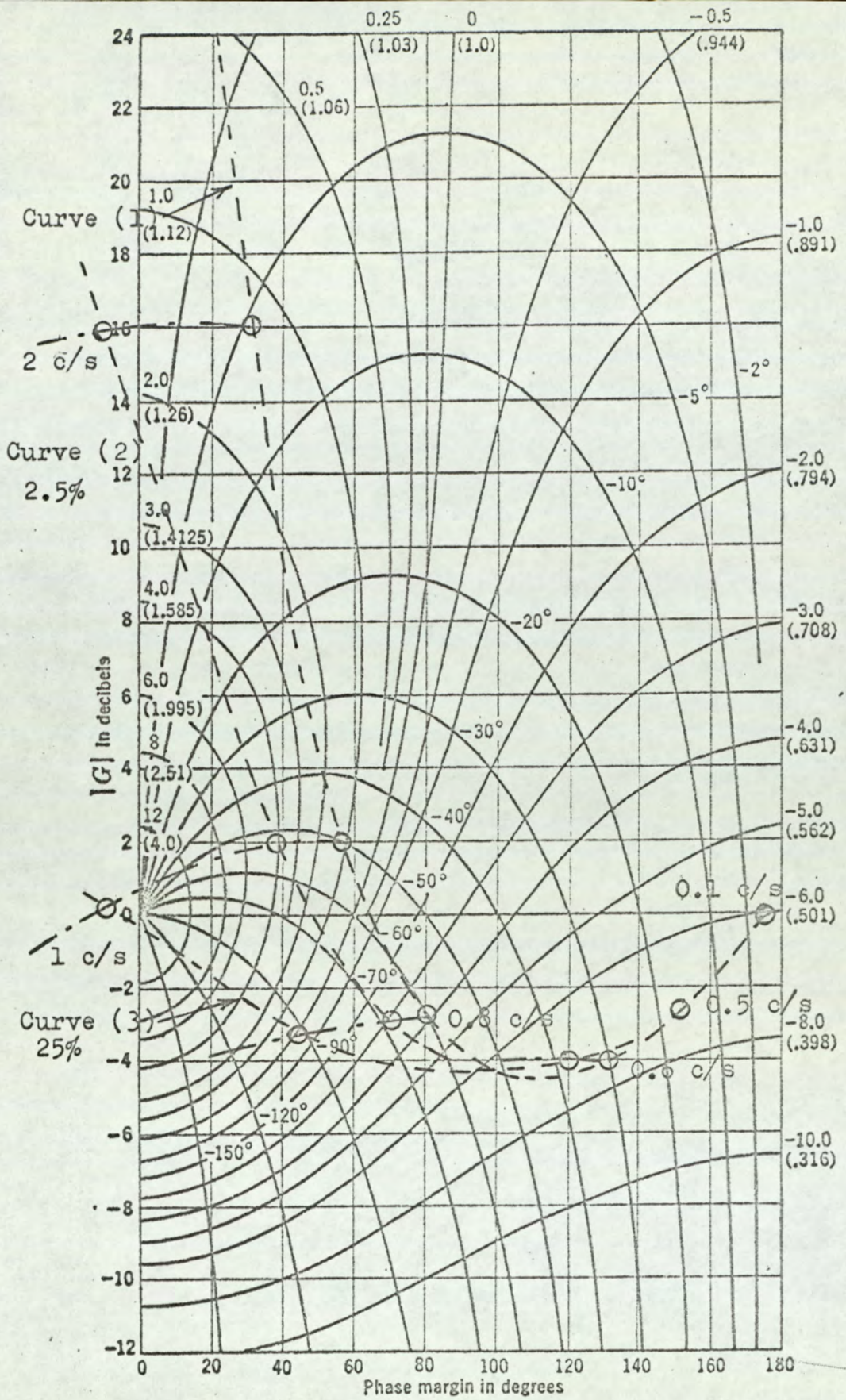

FIG.(4.33)

UNCOMPENSATED RESPONSE

will become unstable at this gain setting when the amplitude of oscillation is large, i.e. the locus Curve (3) passes below the critical point. In this condition the system will be stable in response to small disturbances but will diverge into oscillation following a large disturbance. The oscillation will eventually carry the pump stroke between zero and maximum stroke with a frequency of about 1 Hz.

There is clearly a need to make a compensating adjustment to shape the frequency response so that this effect is avoided.

4.10.3 COMPENSATION.

The instability identified above may be removed by reducing the loop gain and thereby moving the locus curves upwards on the Nichols Chart. However the resulting control action would be quite ineffective as the loop gain will be too low. The compensating adjustment must move the locus to the right i.e. to advance the phase if the reduction of loop gain is to be avoided. The method of introducing compensation is to set up the appropriate transfer admittance Y_1 as shown on Fig.(4.24).

The simplest form of phase advance network would be that shown on Fig.(4.34). For this network the transfer admittance $\frac{i}{v}$ is,

$$Y_1 = \frac{1}{R_1} (1 + s T_1) \quad \ldots\ldots\ldots\ldots (4.39)$$

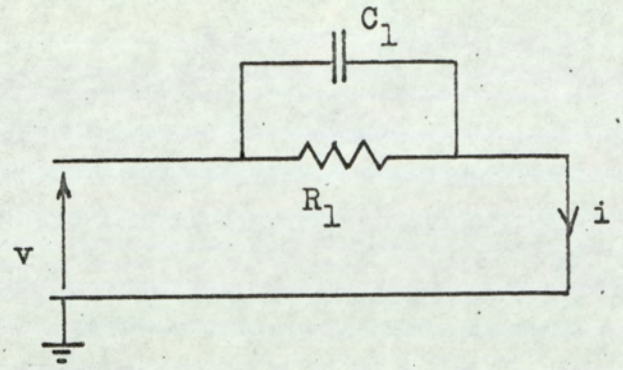

FIG.(4.34)

SIMPLE PHASE ADVANCE NETWORK

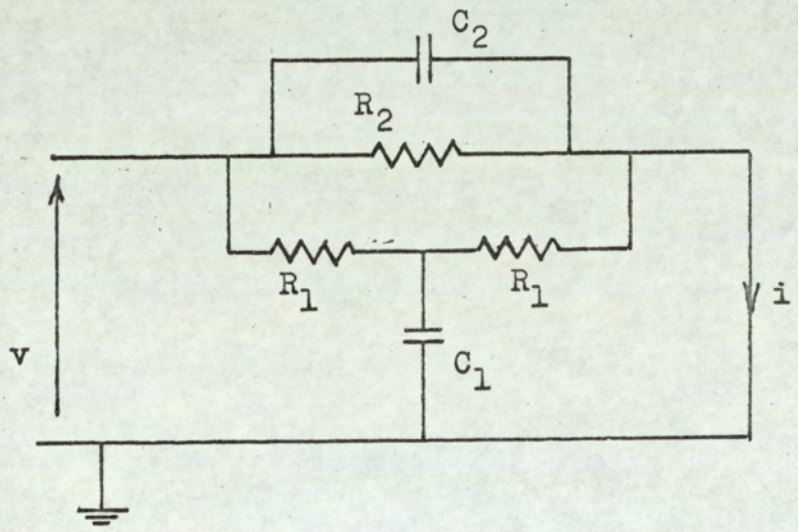

FIG.(4.35)

PHASE ADVANCE NETWORK WITH COMPLEX ZEROS

where $T_1 = C_1 R_1$ .....(4.40)

This network does not prove to be satisfactory. It gives 90^o phase advance at high frequencies but the rise of gain with frequency brings the locus curve downwards on the Nichols Chart to counteract the advantageous effect of the phase advance.

The large increase of phase shift in the variable gain network at about 1 Hz is largely responsible for the difficulty. That the peak of the response of the hydraulic system also comes at about 1 Hz exaggerates this effect. With this in mind a second view of the choice of compensating network may be taken. The objective in this is to cancel the peak response of the hydraulic system and at the same time to introduce the phase advance effect.

It was shown in Section (4.4.1) that the response of the hydraulic system may be closely approximated by the transfer function given in equation (4.9). The complete open loop response is then given by,

$$\frac{1}{y(j\omega)} = \frac{N(j\omega)\ K\ k_g}{(j\omega T)^2 + 2\ z\ j\omega T + 1} \quad .....(4.41)$$

where $N(j\omega)$ is presumed to embrace the compensating function of the transfer admittance Y_1. The peak due to the quadratic factor in equation (4.41) may be removed by cancelling it in $N(j\omega)$ and substituting a simple lag. The form required in

$N(j\omega)$ is then,

$$N(j\omega) = \frac{Ko}{K\,k_g}\left(\frac{(j\omega T)^2 + 2\,z\,j\omega T + 1}{j\omega T_o + 1}\right) \quad ....(4.42)$$

The values of the time constant T and the damping ratio z are to match those of the hydraulic system. For the response given on Fig.(4.10) we have,

$$T = 0.213 \text{ s}$$
$$z = 0.3$$
$$K\,k_g = 17.5 \text{ dB} = 7.5$$

The choice of T_o and K_o may now be made so that under large signal conditions the combined locus falls in a satisfactory position on the Nichols Chart.

Of the networks which can produce a transfer admittance as required by equation (4.42), the one shown on Fig.(4.35) was chosen because it contains only RC elements. It gives the transfer admittance,

$$Y_1 = \frac{1}{A}\left(\frac{s^2T_1T_2 + sT_1 + 1}{sT_3 + 1}\right) \quad .....(4.43)$$

and has sufficient degrees of freedom to allow independent adjustment of the three time constants. This is necessary in order that the quadratic factor can have complex zeros as is required in this case. Analysis of the network gives,

$$T_1 = \frac{R_1(R_1C_1 + 2\,R_2C_2)}{2\,R_1 + R_2}$$

$$T_2 = \frac{R_1R_2C_1C_2}{R_1C_1 + 2\,R_2C_2}$$

$$T_3 = \frac{R_1C_1}{2} \qquad \text{.....(4.44)}$$

$$A = \frac{2\,R_1R_2}{2\,R_1 + R_2}$$

In order to design the network for specified values of A and the three time constants, equations (4.44) are solved for the component values,

$$R_1 = \frac{A\,T_3^{\,2}}{2(\,T_3^{\,2} - T_1(T_3 - T_2)\,)}$$

$$R_2 = \frac{A\,T_3^{\,2}}{T_1\,(\,T_3 - T_2\,)} \qquad \text{.....(4.45)}$$

$$C_1 = \frac{4(\,T_3^{\,2} - T_1(T_3 - T_2)\,)}{A\,T_3} = \frac{2\,T_3}{R_1}$$

$$C_2 = \frac{T_1T_2}{A\,T_3}$$

To facilitate the choice of T_o and hence T_3, the form of the response function $Y_1(j\omega)$ is plotted on Fig.(4.36) for two values of T_3. Either of these two conditions would be satisfactory when taken in conjunction with the response data at point X in the operating region. The larger value of T_3 is the best as this allows a higher gain at zero frequency. However the effect on the response at other points in the operating region must be considered. If the conditions at point Y are taken the overall response becomes as shown in Fig.(4.37). Similarly at point W the results are as given on Fig.(4.38). The significant feature of these curves is the depression of the phase towards 180^o. This carries the locus of $y(j\omega)$ towards the critical point on the Nichols Chart. In fact the phase depression is too great even with the smaller value of T_3. The conditions at operating points Y and W thus impose restrictions on what can be achieved at point X. The problem is that of making a compromise over the three conditions.

The phase depression seen on Fig.(4.37) can be reduced by increasing the damping ratio of the quadratic factor in the response of the compensating network. The result of changing the damping ratio to 0.5 is shown on Fig.(4.39). When this compensating response is combined with the response of the hydraulic system at point W the result is as shown on Fig.(4.40). Of the two values of T_3

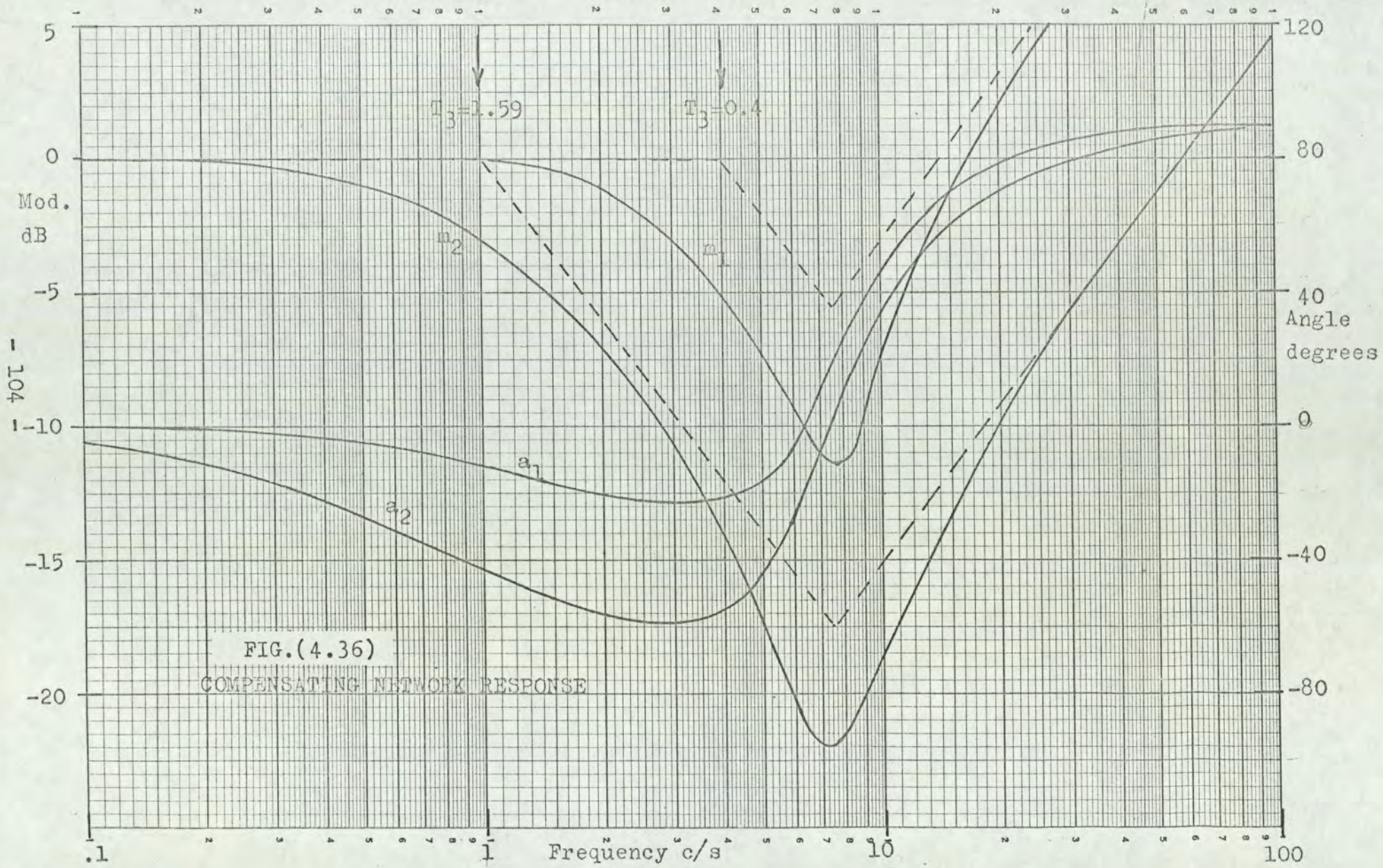

FIG.(4.36)
COMPENSATING NETWORK RESPONSE

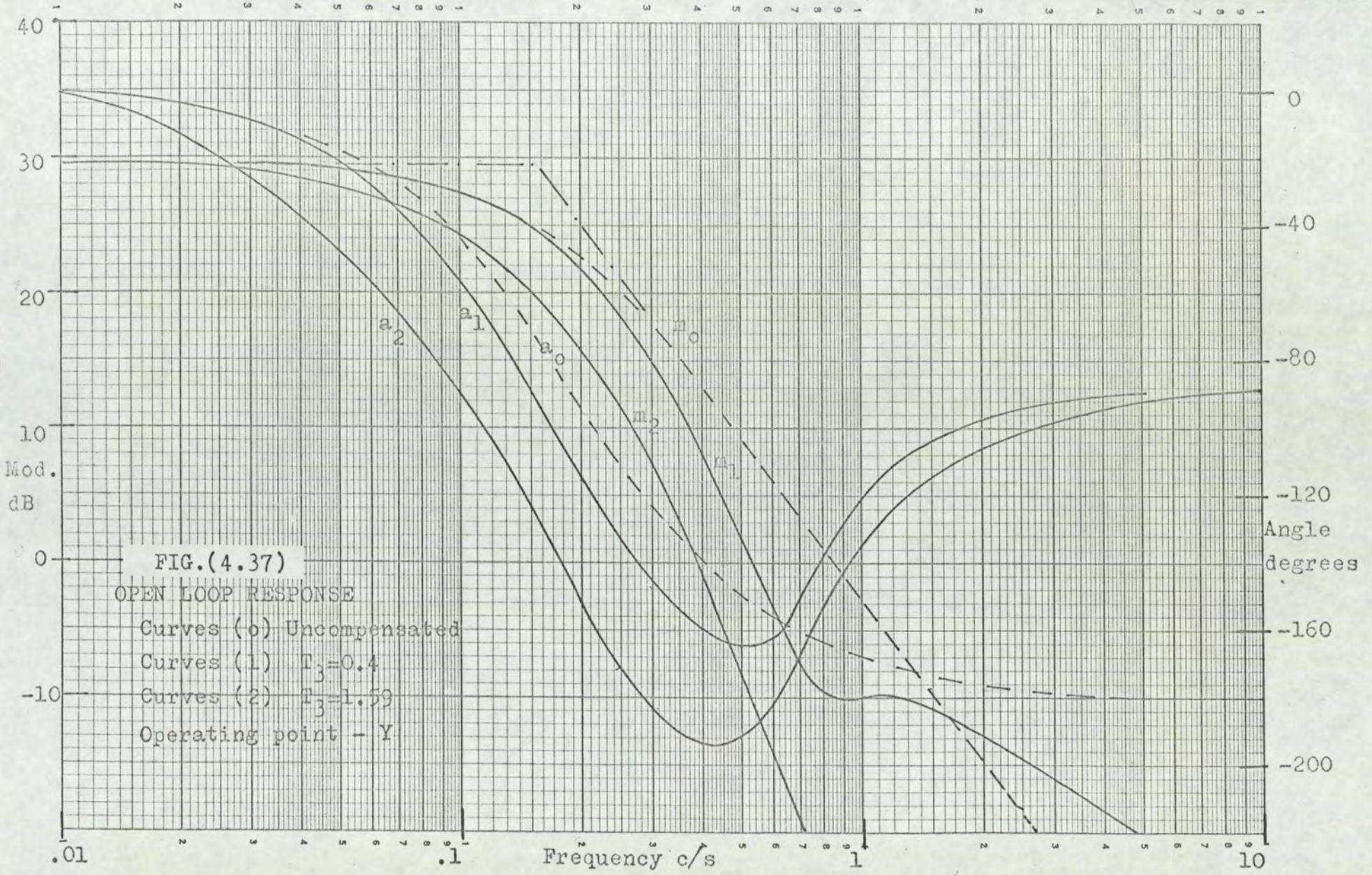

FIG.(4.37)

OPEN LOOP RESPONSE

Curves (o) Uncompensated

Curves (1) T_3=0.4

Curves (2) T_3=1.59

Operating point - Y

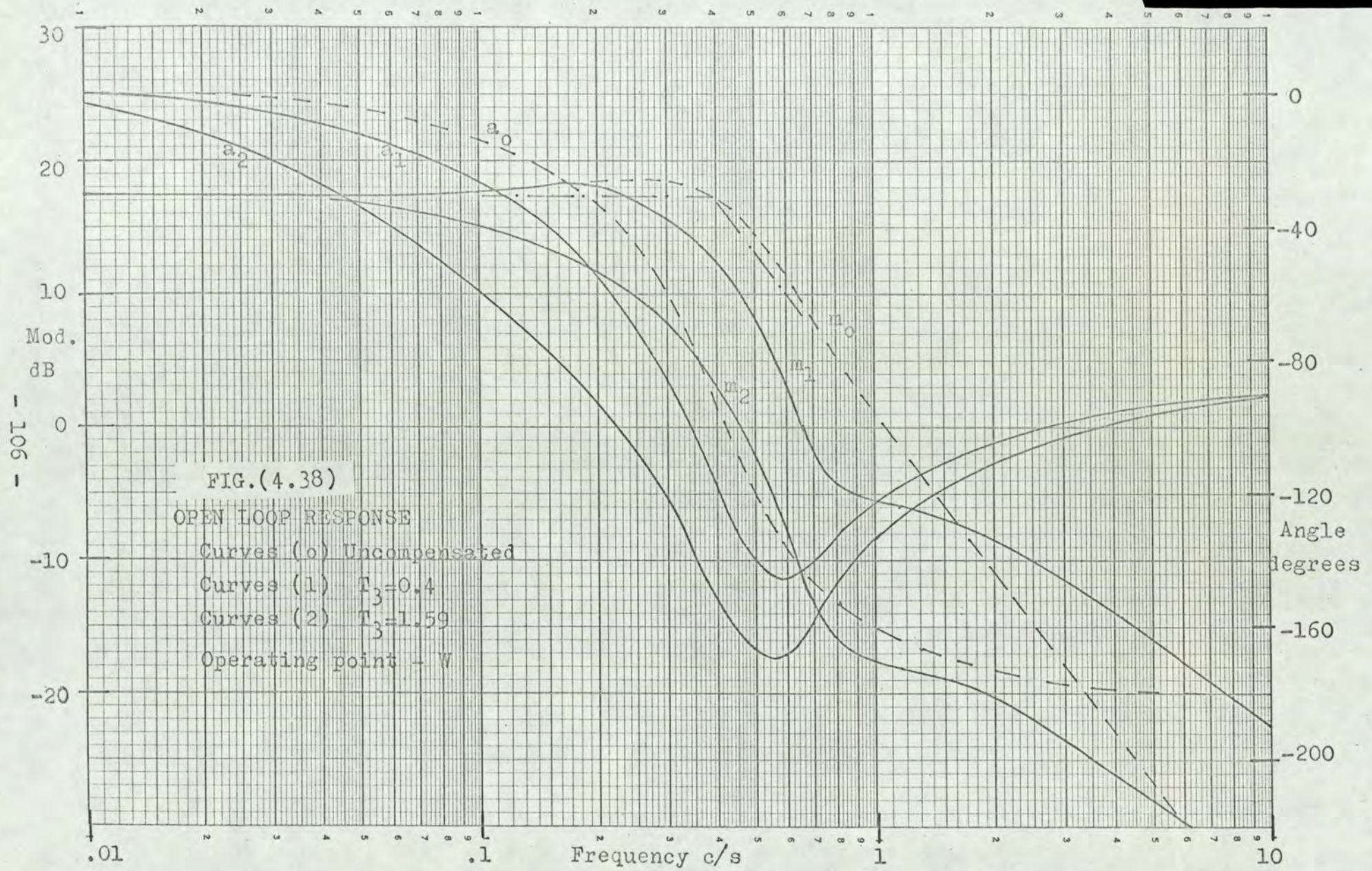

FIG.(4.38)

OPEN LOOP RESPONSE

Curves (o) Uncompensated

Curves (1) T_3=0.4

Curves (2) T_3=1.59

Operating point - W

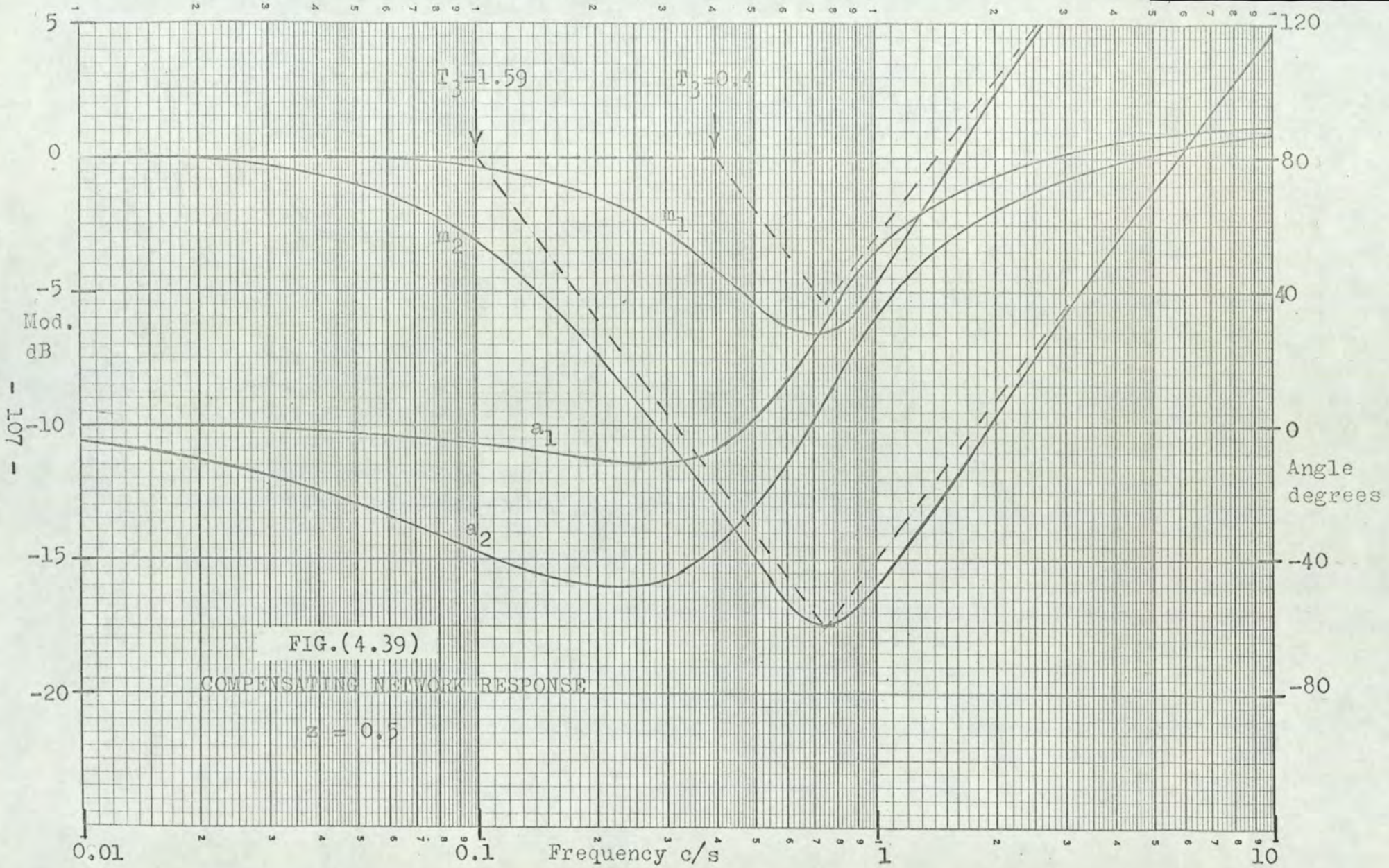

FIG.(4.39)

COMPENSATING NETWORK RESPONSE

$\varepsilon = 0.5$

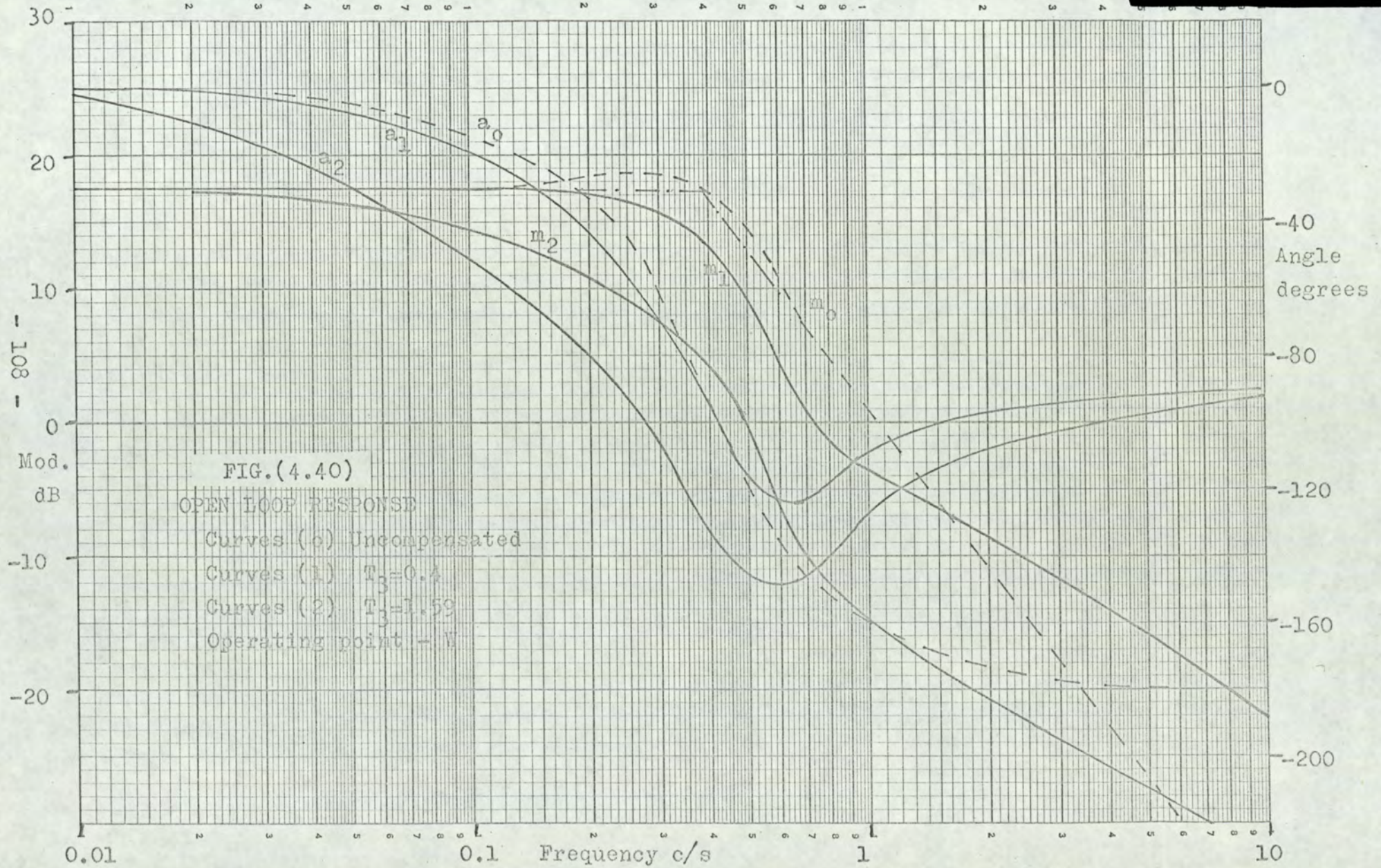
30
20
10
0
-10
-20
Mod. dB
- 108 -
0
-40
-80
-120
-160
-200
Angle degrees
0.01
0.1
1
10
Frequency c/s
a_0
a_1
a_2
m_0
m_1
m_2
FIG.(4.40)
OPEN LOOP RESPONSE
Curves (c) Uncompensated
Curves (1) T_3=0.4
Curves (2) T_3=1.59
Operating point - V

the smaller is taken as the most appropriate value, since the phase angle then never exceeds -130^{o}. With this value of T_3 the combined response curves at operating point X are shown on Fig.(4.41) and at operating point Y on Fig.(4.42).

The response of Fig.(4.42) is transferred to the Nichols Chart on Fig.(4.43) as Curve (1). The effect of an increase in the signal amplitude on the response of the variable gain network is seen in Curves (2) and (3). The zero frequency gain has been set to 6 dB, this being about the maximum allowable in the interests of keeping the locus clear of the critical point.

With the same compensating adjustments the response at operating point W, from Fig.(4.40), gives the results shown on Fig.(4.44). The locus moves into the undesired region and would indicate that more phase advance is required at about 0.6 Hz. However an increased phase advance will be accompanied by an increase in gain at the higher frequencies. This will be detrimental to the conditions of Fig.(4.43), necessitating a reduction of the zero frequency gain. It was therefore decided not to make any further adjustment.

The conditions at operating point Y lead to the locus shown on Fig.(4.45), using the results of Fig.(4.42). At the low frequencies involved the change in the response of the variable gain network with signal amplitude has negligible effect. This locus also passes into the undesired region but

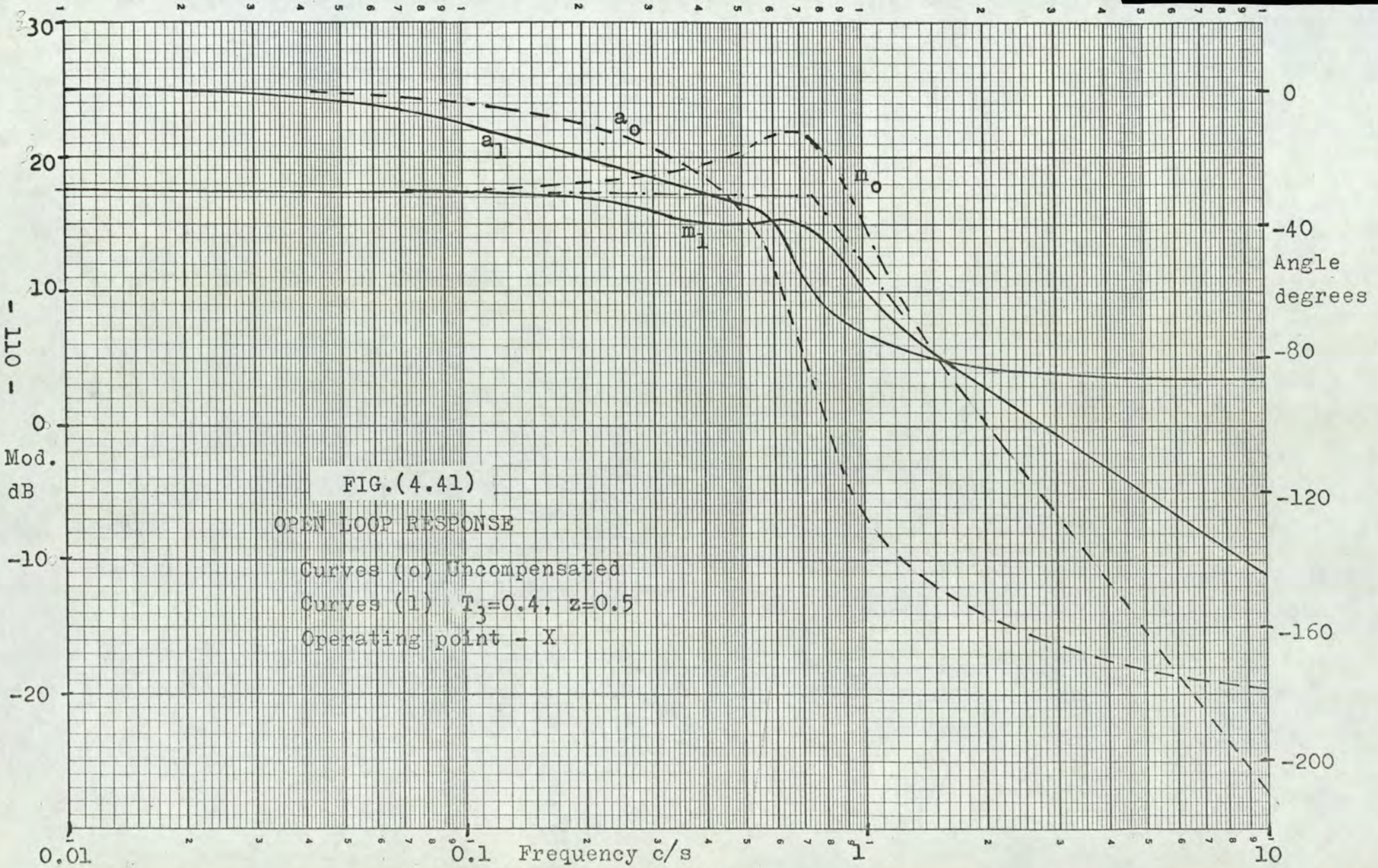

FIG.(4.41)

OPEN LOOP RESPONSE

Curves (o) Uncompensated

Curves (1) T_3=0.4, z=0.5

Operating point - X

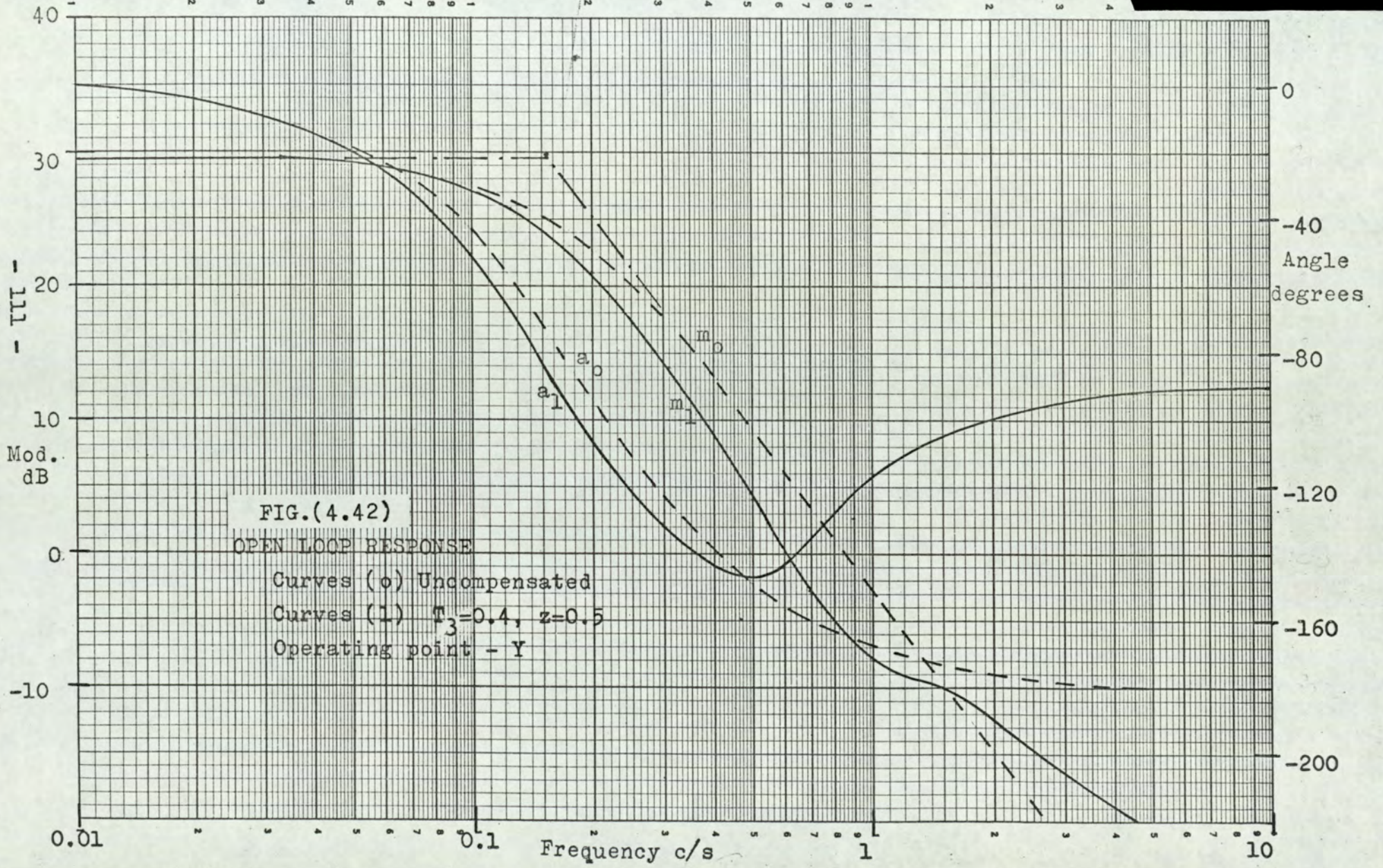

FIG.(4.42)
OPEN LOOP RESPONSE
Curves (o) Uncompensated
Curves (1) T_3=0.4, z=0.5
Operating point - Y

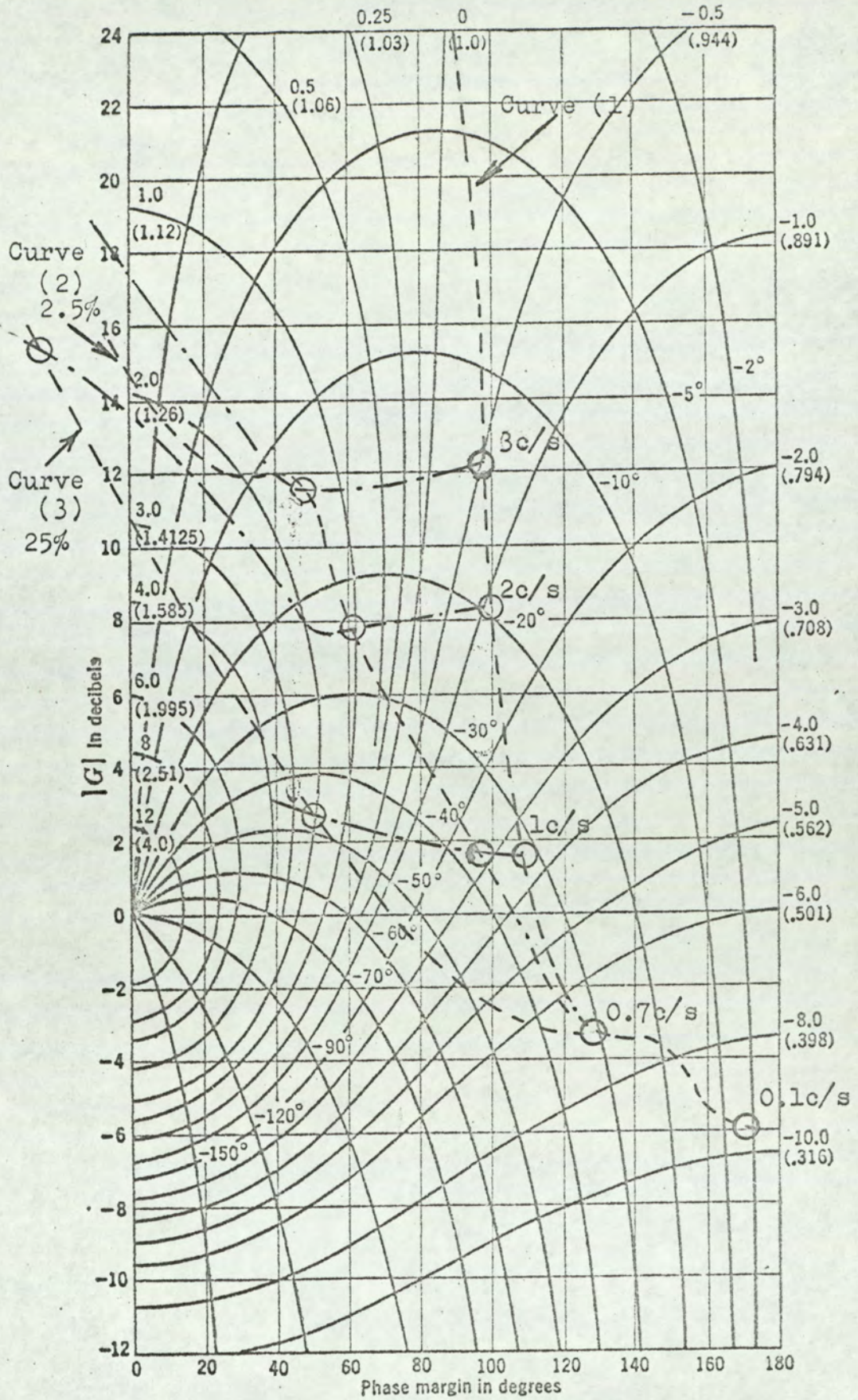

FIG.(4.43)
COMPENSATED RESPONSE

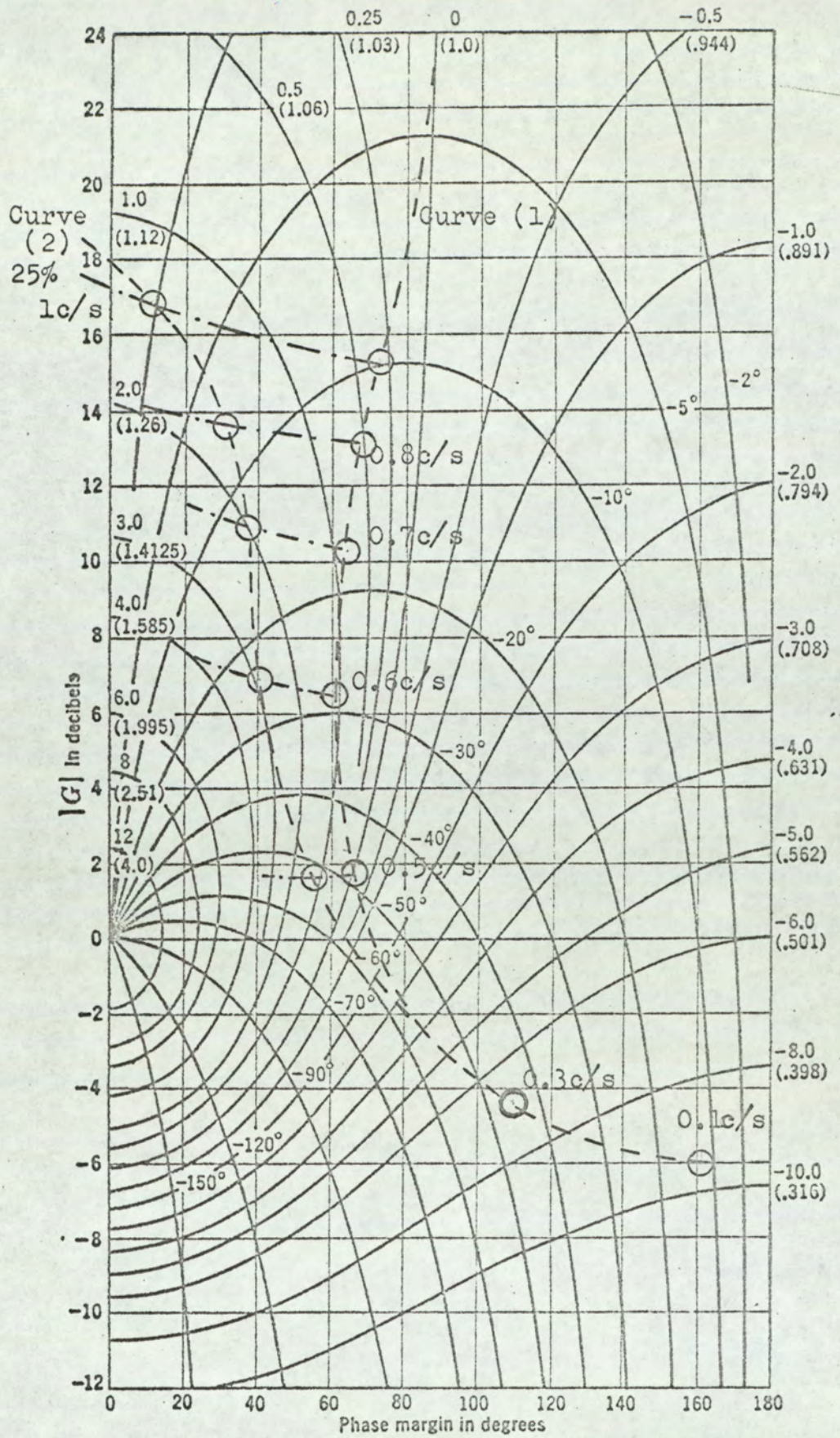

FIG.(4.44)
COMPENSATED RESPONSE

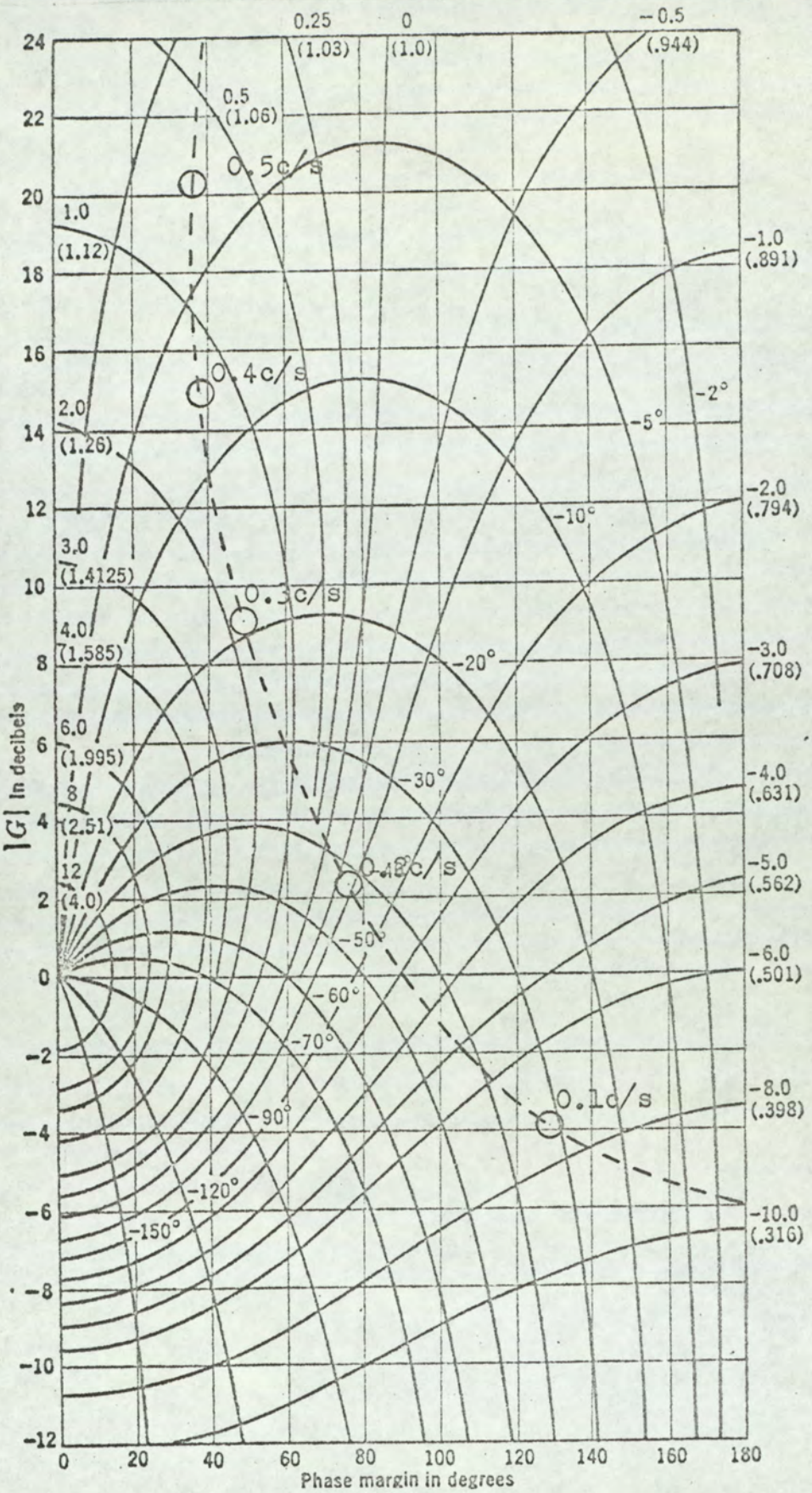

FIG.(4.45)
COMPENSATED RESPONSE

again any adjustment designed to correct this would adversely affect the conditions at points X and Y.

The set of conditions arrived at is judged to be a reasonable compromise in gain and phase compensation over all the operating region. In terms of equation (4.42) the compensating network response is defined by the parameters,

$$\begin{aligned} T &= 0.213 \text{ s} \\ z &= 0.5 \\ T_o &= 0.4 \text{ s} \\ K_o &= 6 \text{ dB} = 2 \end{aligned} \qquad \ldots\ldots\ldots\ldots\ldots\ldots\ldots\ldots (4.46)$$

It remains to design the network to realise these values. Identifying the equation (4.42) with equation (4.43) we calculate the time constants of the network,

$$\begin{aligned} T_1 &= 2\,zT = 0.213 \text{ s} \\ T_2 &= \frac{T^2}{T_1} = 0.213 \text{ s} \\ T_3 &= T_o = 0.4 \text{ s} \end{aligned} \qquad \ldots\ldots\ldots\ldots\ldots\ldots (4.47)$$

The constant A of the network is defined by the zero frequency gain requirement as follows. From Fig.(4.24) we get the zero frequency gain of the variable gain network as,

$$\frac{\psi_p}{Ve}(0) = \frac{Y_1(0)}{k\,Y_2(0)} \qquad \ldots\ldots\ldots\ldots\ldots\ldots (4.48)$$

where $Y_1(0)$ and $Y_2(0)$ are the values of the transfer admittances at zero frequency and $k = \mu E\omega$. With the appropriate values substituted this then gives,

$$\frac{\psi_p}{Ve}(0) = \frac{R_2}{A \mu E\omega} \quad \ldots\ldots\ldots\ldots\ldots\ldots (4.49)$$

The block diagram of Fig.(4.31) shows the zero frequency value of the open loop gain to be,

$$K_o = \frac{V\omega}{Ve}(0) = \frac{R_2 K k_g}{A \mu E\omega} \quad \ldots\ldots\ldots\ldots\ldots (4.50)$$

It is sufficient to set the gain at one point in the operating region as it has been shown that the variable gain network will hold the loop gain constant over the whole operating region. Taking for analysis the conditions at operating point X, we have ω_p = 1500 r.p.m. and ψ_m = 1.0. The voltage $E\omega$ fed forward when ω_p = 1500 is found from Fig.(4.23) as 13.8 volt. Equation (4.20) gives the value of R_2 as 10.87 kΩ when ψ_m = 1.0. The response of the hydraulic system at operating point X is seen on Fig.(4.10), where the zero frequency gain gives the value of $K k_g$ as 17.6 dB or 7.5. We require to set K_o in equation (4.50) to 6 dB or 2.0 by a choice of the constant A. On solving for A we get,

$$A = \frac{R_2 K k_g}{K_o \mu E\omega} \quad \ldots\ldots\ldots\ldots\ldots\ldots (4.51)$$

With the potentiometer ratio μ defined as 0.523 and the values of the other parameters arrived at above, this leads to A = 5.6 kΩ.

This value of A, together with the time constant values given in equations (4.47) determines the component values in the compensating network. Solution of equations (4.45) gives,

$$R_1 = 3.75\ k\Omega \qquad R_2 = 22.3\ k\Omega$$
$$C_1 = 215\ \mu F \qquad C_2 = 20.3\ \mu F$$

The nearest preferred values to these results are,

$$R_1 = 3.6\ k\Omega \qquad R_2 = 22\ k\Omega$$
$$C_1 = 200\ \mu F \qquad C_2 = 20\ \mu F$$

Electrolytic capacitors may be used for C_1 and C_2 if the circuit is arranged as shown in Fig.(4.46). The reference input is connected after the compensating network so that the voltage applied to the network is $V\omega$ and this cannot reverse polarity. The response of the system to a change of the reference will be different from that implied by the block diagram of Fig.(4.31) but this is not important as the reference is fixed for a given output speed setting.

A further refinement of the compensating network is necessary. The voltage $V\omega$ is derived from the rectified output of an a.c. tachometer generator coupled to the loading generator. This signal contains ripple components at 100 Hz and higher harmonics. The large shunt capacitor C_2, provides a low impedance path to the ripple current in $V\omega$.

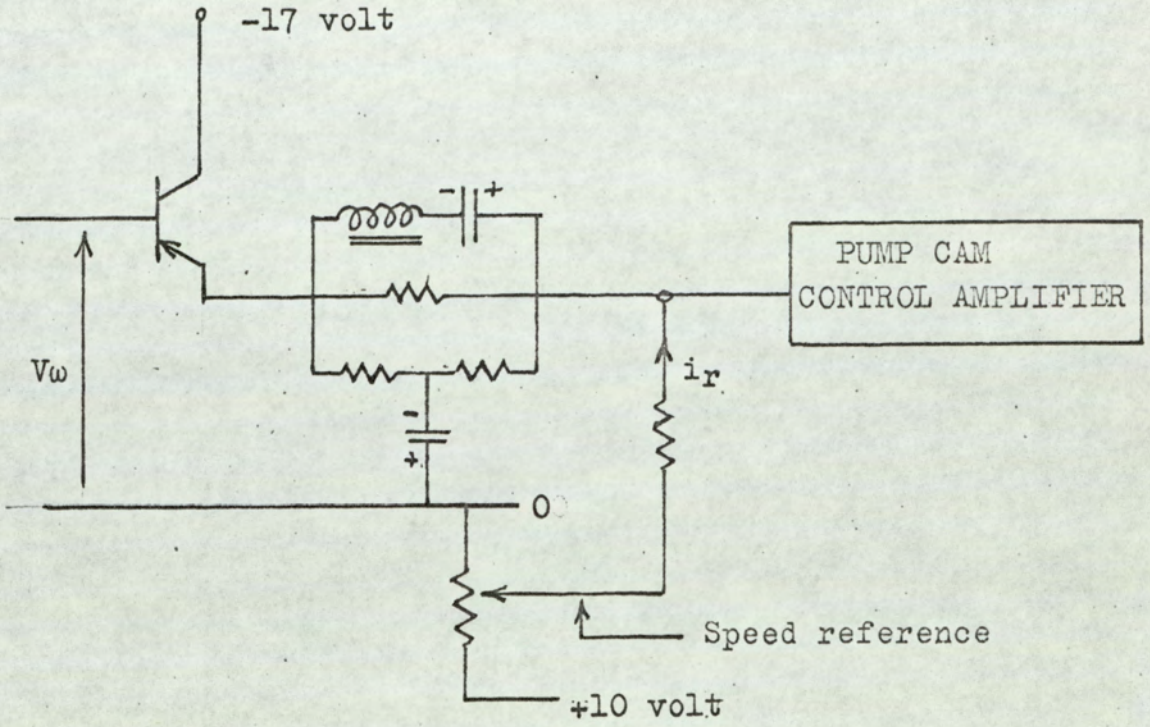

FIG.(4.46)
COMPENSATING NETWORK

As the linear range of the pump cam control amplifier is $\pm 2\,\mu A$ the ripple current must be kept below this level. If this is not done the amplifier will be driven between the saturation limits at high frequency and its average gain will be low. The accuracy of the setting of the pump stroke will then be reduced.

If the smoothing filter following the rectifier is designed to give adequate attenuation of the ripple in $V\omega$, the lag introduced by the filter in the speed control loop is significant. It is better to limit the ripple current in the compensating network. A resistor added in series with C_2 would do this, by setting a maximum limit to the transfer admittance. However the value of resistance necessary is large enough to affect the transfer admittance within the frequency range of the speed control loop. It is therefore preferable to use a choke in series with C_2 as shown on Fig.(4.46). A choke of inductance 2.1 H and resistance 120 Ω was found to be satisfactory. This has an impedance of 1.3 kΩ at 100 Hz. It is resonant with C_2 at 25 Hz, sufficiently above the frequency range of interest in the speed control loop for its effect to be ignored.

4.11 OVERALL CHARACTERISTICS OF THE SPEED CONTROL SYSTEM.

It is now possible to assess the combined performance of the feedforward and feedback sections of the system. The features which are of interest in making this assessment concern the ability of the system to maintain a constant motor speed. There are three variables to be considered; the pump speed, the motor stroke and the transmitted load. In reviewing the effects of these variables in Section (4.4.2) it was revealed that the pump speed and motor stroke changes produce the greatest demand for control action. In the control system evolved here these variations are compensated by the feedforward arrangement. The feedforward action is capable of giving a rapid adjustment of the pump stroke, in contrast with the feedback action which responds more slowly due to the high inertia of the load. A particular advantage of this arrangement is that the largest demand for control action is placed on the section of the system having the fastest response.

In addition to having a slow response, the feedback loop is limited to a low gain. This is chiefly due to the adverse effect of the non-linear characteristics of the pump stroke control mechanism. The compensating effect of the feedback loop is therefore not great. However it provides a measure of compensation for the effects of load on the transmission and gives a monitoring action on the performance of the feedforward system. Some of the residual interaction, due to the

imperfections in the feedforward system, is then removed.

These overall effects were assessed in tests conducted on the complete system. The deviation of the motor speed was measured as a result of sinusoidal disturbances applied to each of the three variables.

4.11.1 PUMP SPEED VARIATIONS.

A controlled oscillation of the pump speed was obtained by applying a sinusoidal voltage to the external input of the drive motor speed control system. The results plotted on Fig.(4.47) show the magnitude (curves m_1 and m_2) and the phase (curves a_1 and a_2) of the output speed oscillation. The zero dB reference level is taken as the amplitude of the pump speed oscillation, then without any control action the response would be at zero dB level. Results are obtained with the motor stroke at the maximum value and also at half stroke, In each case the amplitude of the pump speed oscillation was 7.5% peak. The accuracy of the results is not high as the output speed oscillation was of such small amplitude.

The indications are that the control system is effective in reducing the output speed variations to a small amplitude. The form of the response curves is the result chiefly of the feedforward control action. The output speed changes arise from the incomplete cancellation of the interaction between the pump speed and the motor speed. The precise nature of this effect is difficult to

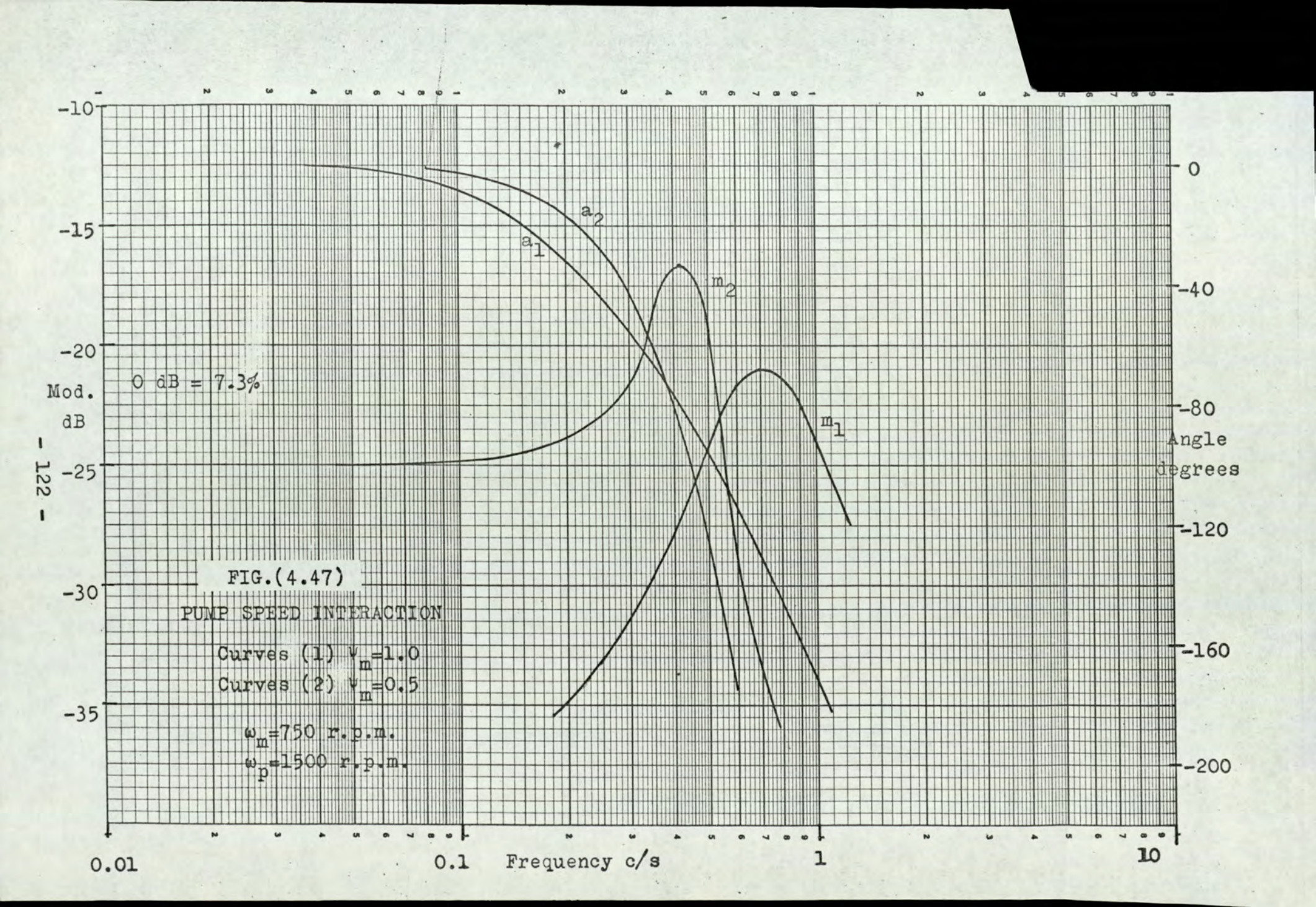
-10
-15
-20
-25
-30
-35
Mod. dB
0 dB = 7.3%
a_2
a_1
m_2
m_1
0
-40
-80
-120
-160
-200
Angle degrees
0.01
0.1
Frequency c/s
1
10
FIG.(4.47)
PUMP SPEED INTERACTION
Curves (1) V_m=1.0
Curves (2) V_m=0.5
ω_m=750 r.p.m.
ω_p=1500 r.p.m.

assess theoretically in view of the fact that the variable gain network is non-linear and the remaining interaction is small. It is to be expected however that a further study of the dynamical effects in the feedforward system could lead to an improved design. This would involve placing a compensating network in the feedforward transfer path with a view to minimising the interaction over a wide frequency range. The system in its present form is adequate for the project in hand and this refinement is left for study elsewhere.

4.11.2 TRANSMITTED LOAD VARIATIONS.

The system was tested with a sinusoidal oscillation of load torque. This is obtained by changing the armature current in the loading generator using the current control system described in Section (2.2) of the Appendix.

The change of load speed produced by this stimulus was measured. A comparison was made between the response without the speed control feedback loop and that with the loop connected. In these tests the torque oscillation was superimposed on a steady load sufficient to prevent reversal of the load torque.

The response with the system under speed control is shown on Fig.(4.48), at maximum motor stroke and half full stroke. Zero dB on the magnitude scale is taken as 1% speed variation about the nominal speed of 750 r.p.m.. The results are consistent with

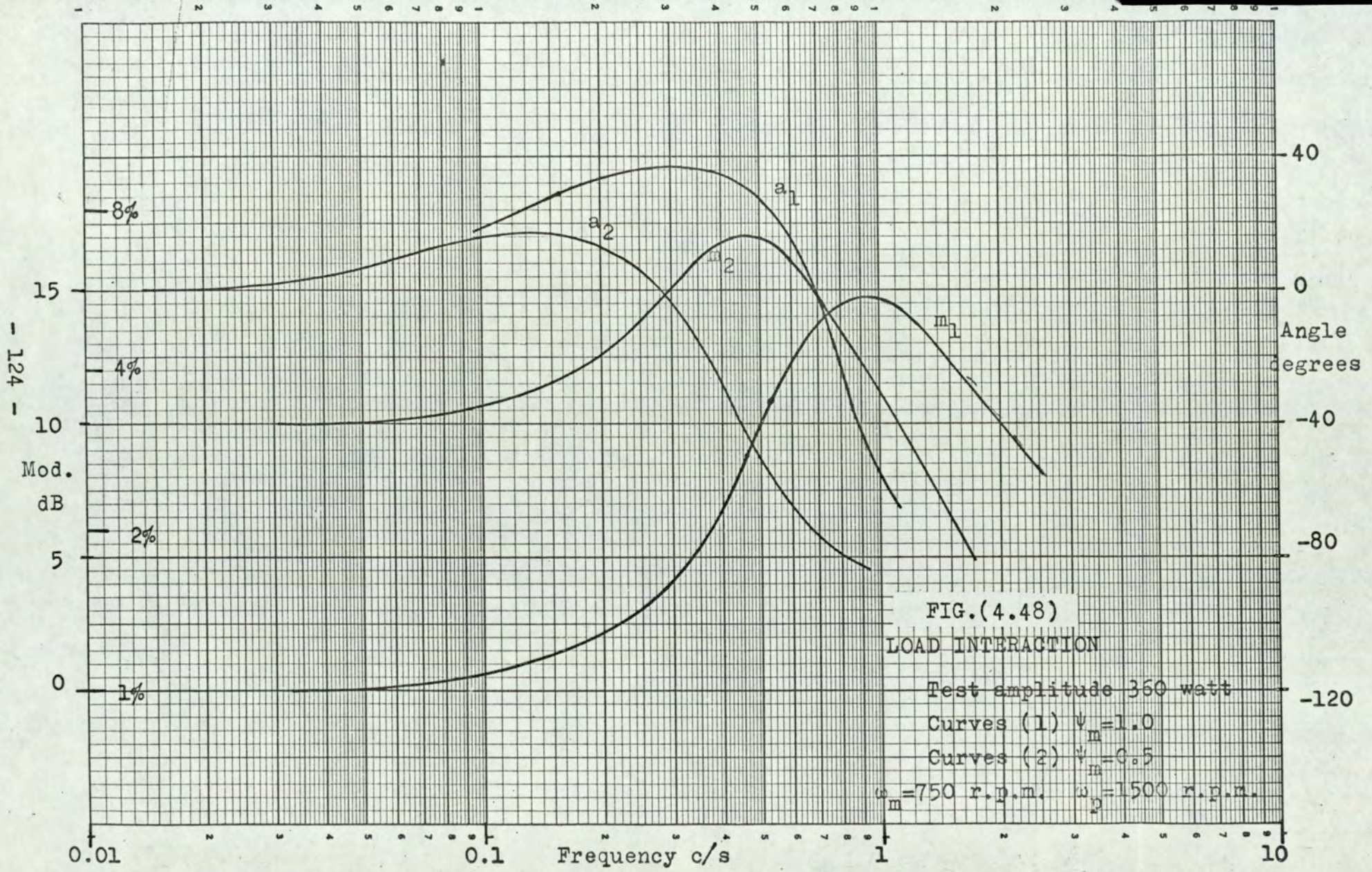

FIG.(4.48)

LOAD INTERACTION

Test amplitude 360 watt

Curves (1) Ψ_m=1.0

Curves (2) Ψ_m=0.5

ω_m=750 r.p.m. ω_p=1500 r.p.m.

what would be expected. The resonant characteristic is again present due to the combination of the compliance of the hydraulic circuit and the load inertia. The progressive increase in attenuation of the disturbance at high frequencies is due to the high load inertia.

The corresponding results when the feedback loop was disconnected have not been plotted separately. It is more informative to plot the ratio of speed variation with control to the speed variation without control. These results are shown on Fig.(4.49). It is this ratio which forms the basis of the design analysis of the speed control feedback system in Section (4.10). The results measured here are consistent with what would be expected from Fig.(4.43) which gives the theoretical response at maximum motor stroke. The corresponding results at half stroke were presented on Fig.(4.44). The precise comparison of the measured results and the theoretical response is very difficult to make, due to the non-linear characteristics of the system.

The overall effect of the speed control feedback loop is to reduce the variations of load speed by 9.5 dB in the steady state i.e. to one third of the value without control. This is consistent with the design based on a loop gain of 6 dB. When the frequency is raised the modulus ratio curves m_1 and m_2 show a progressive rise up to the zero dB level. At zero dB the speed control loop has no effect. This means that when the motor is at full

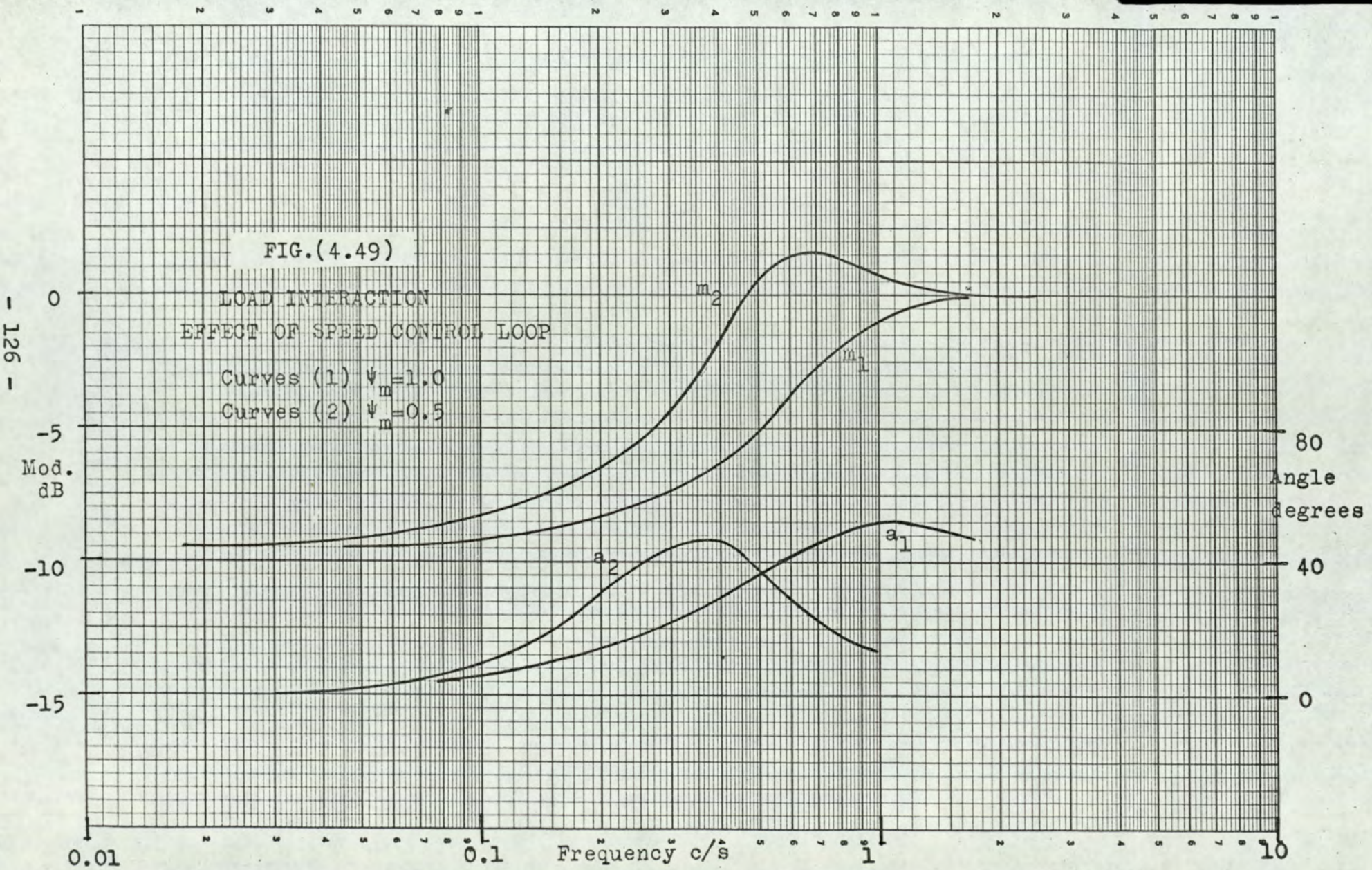
FIG.(4.49)
LOAD INTERACTION
EFFECT OF SPEED CONTROL LOOP
Curves (1) ψ_m=1.0
Curves (2) ψ_m=0.5
m_2
m_1
a_2
a_1
0
-5
-10
-15
Mod. dB
80
40
0
Angle degrees
0.01
0.1
1
10
Frequency c/s

stroke there is no effective control action above about 1 Hz. At half stroke the bandwidth of effective control falls to about 0.5 Hz and infact at higher frequencies the control action increases the effect of the torque oscillation. This is one of the consequences of the difficult compromise which has to be made in the design of the speed control loop, due to the wide variation in the response over the range of operating conditions.

4.11.3 MOTOR STROKE VARIATIONS.

The response to a sinusoidal oscillation of the motor stroke was investigated. To do this it was necessary to control the motor stroke setting using a position control feedback system. The ultimate arrangements for controlling the motor stroke involve using an a.c. servo integrator as part of the optimising control system. The detailed arrangements for this are described in Section (7.2). In this system the motor stroke is set by a feedback control loop which causes the servo piston to follow the rotation of the integrator. The output shaft of the integrator is also used to drive a potentiometer which operates as a feedforward element in the variable gain network. It is therefore important that the changes of motor stroke be produced by working through the servo integrator. Arrangements are made to control the position of the servo integrator by feedback from the output shaft. The oscillation of the motor stroke is then induced by an external input to this position control loop. As the control loop is a 50 Hz a.c. carrier system the input must be in the form of

a sinusoid with suppressed carrier modulation at 50 Hz. This signal was generated by means of a wave form generator *. A variable phase output from the same waveform generator was used to make a phase measurement of the system response.

It is necessary first to obtain the response characteristics relating the motor stroke to the input signal. The curves plotted on Fig.(4.50) as m_1, m_2 and m_3 show the magnitude of the response ratio for three values of signal amplitude. The corresponding phase curves are given as a_1, a_2 and a_3.

Following this the response of motor speed to the stroke oscillation was measured, using the results of Fig.(4.50) to correct the ovarall response measurements.

It was evident that the change of motor speed was negligible when the mean motor stroke was near maximum and the load on the transmission was small. This confirms the success of the feedforward control action. As the mean motor stroke is reduced or the load increased the stroke oscillation gives rise to changes of motor speed. This is shown in the results plotted on Fig.(4.51). In each case shown the amplitude of the test oscillation was the

* Test Waveform Generator Type TWG. 200
Feedback Ltd.

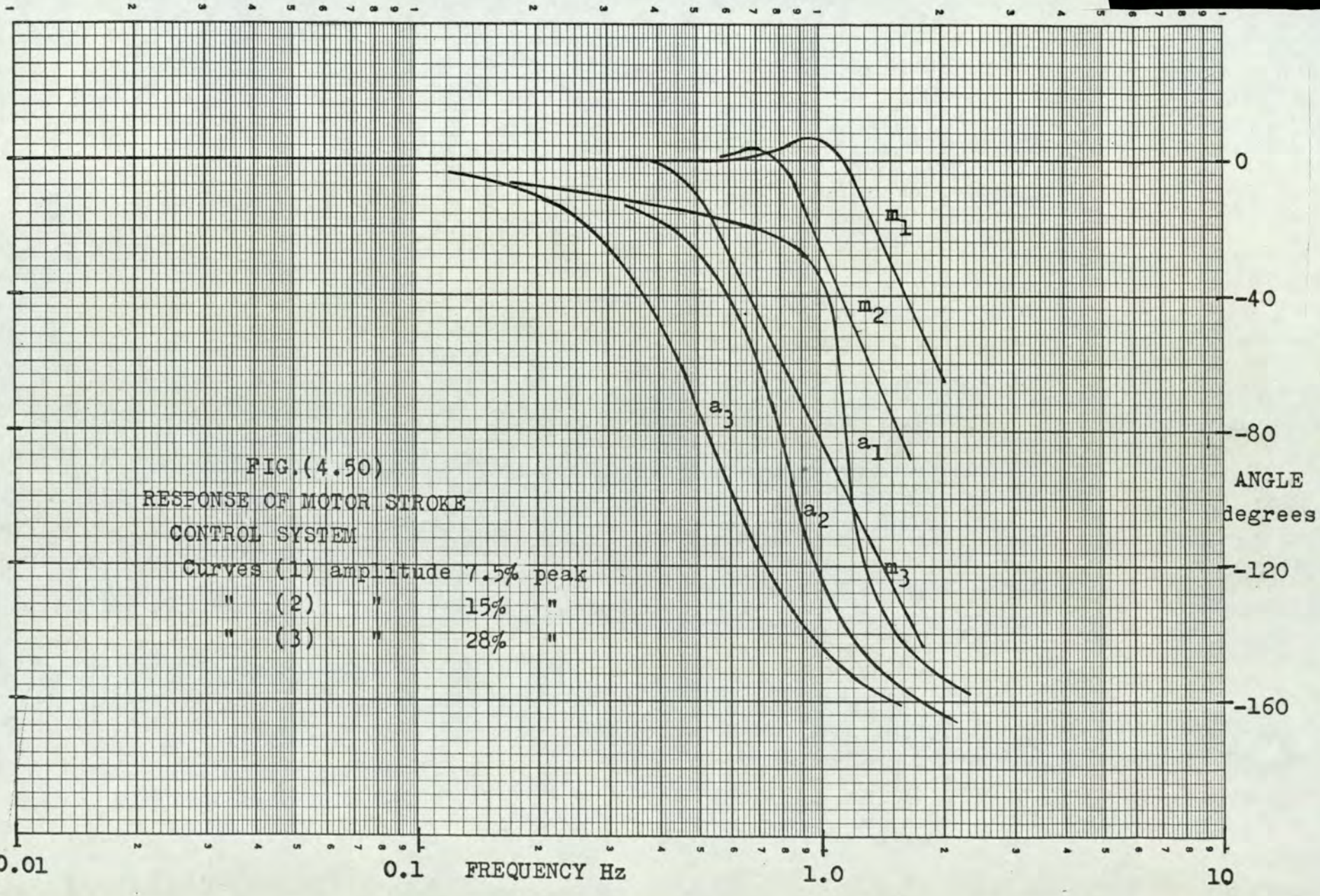

FIG.(4.50)
RESPONSE OF MOTOR STROKE
CONTROL SYSTEM
Curves (1) amplitude 7.5% peak
" (2) " 15% "
" (3) " 28% "

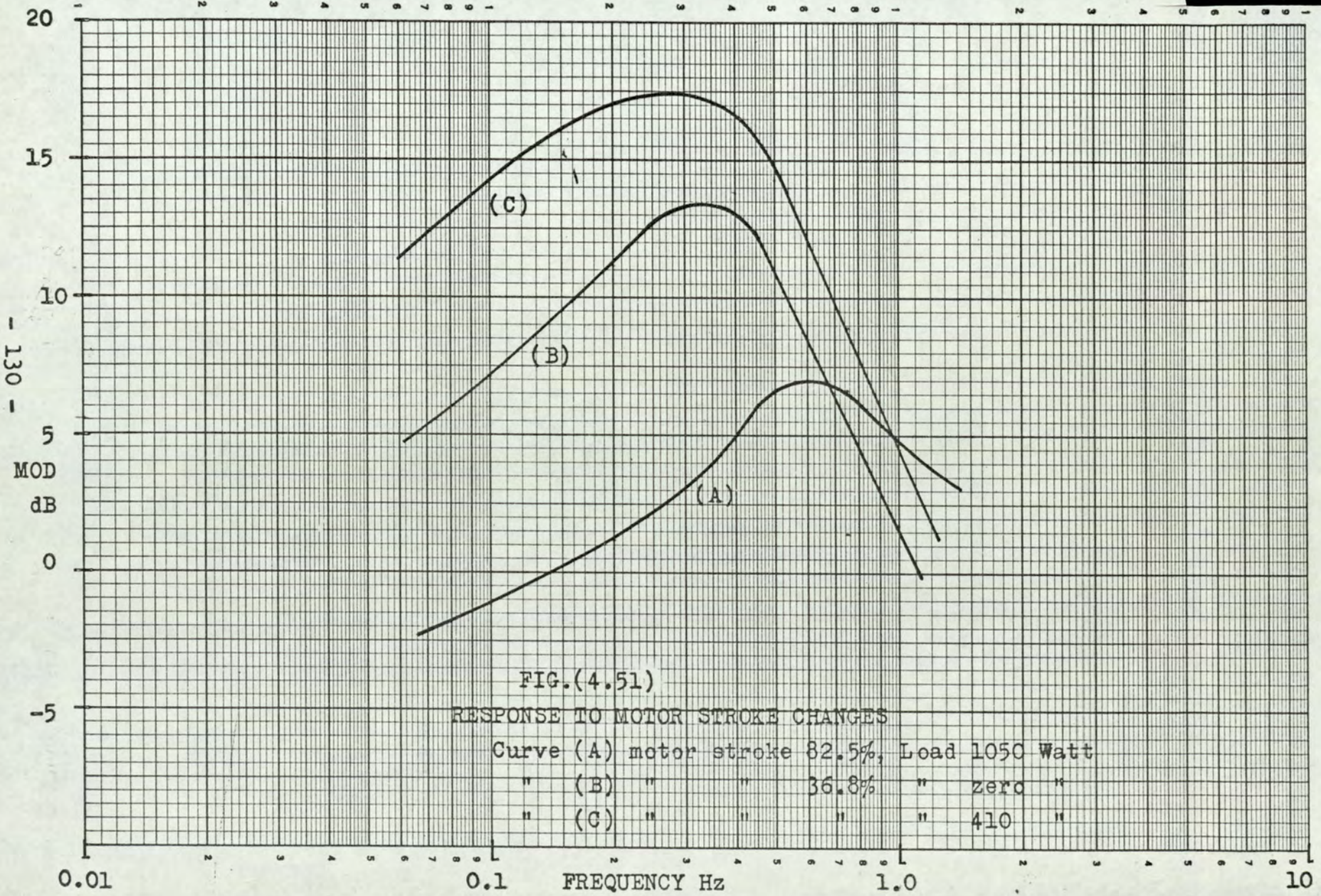

FIG.(4.51)

RESPONSE TO MOTOR STROKE CHANGES

Curve (A) motor stroke 82.5%, Load 1050 Watt

" (B) " " 36.8% " zero "

" (C) " " " " 410 "

same at 12.5% peak. The curve (A) gives the magnitude of the response when the mean motor stroke is near full stroke and the load is raised to the maximum tolerable. The load is limited here by the pressure in the hydraulic circuit, which was not allowed to exceed 3000 p.s.i.. Curves (B) and (C) relate to conditions when the mean motor stroke is small, the change from (B) to (C) is the result of increasing the load to the maximum limit. The magnitude scale against which these curves are plotted is set to zero dB when the amplitude of the motor speed oscillation is 1% of the nominal 750 r.p.m..

The form of these response curves shows that the interaction at low frequencies is small as is to be expected in that the feedforward system has been designed to give a high steady state accuracy. The peak which is developed in the response at the higher frequencies is due to the dynamical interaction remaining. In this respect the response could be improved by further attention to compensation of the transmission characteristics in the feedforward system.

4.12 CONCLUSIONS ON THE DESIGN OF THE TEST RIG.

In this section an outline has been given of the work undertaken in the design of a comprehensive test rig, as a basis for the study of the optimising control problem. The main problem which has been solved is that of the regulation of the output speed of the transmission. This has necessitated the use of a

combination of feedforward and feedback transfer paths. It has been shown in particular that the use of the feedforward arrangement gives substantial improvements over what can be achieved by feedback control alone. To exploit the advantage of this arrangement to the full it has been necessary to design a non-linear feedforward system. This reduces the interacting effect of the pump speed and motor stroke changes on the motor speed.

The feedback control loop adds further refinement to the performance achieved with the feedforward system. The design of this control loop is complicated by the wide variation in the open loop response over the range of operating conditions. The dynamical response of the hydraulic system is variable as also is that of the feedforward system. A significant non-linearity is present too, in the mechanism controlling the pump stroke. The design of this control loop has been facilitated by developing a new way of using a Nichols Chart, in the analysis of the effect of output disturbances on a regulator system.

The design of the system has been carried to a point where the performance is adequate for the further study of optimising control. But a number of features have been shown to be worthy of further investigation. In particular the feedforward system may be improved. This would involve improvements in the form of non-linear transfer characteristic to be used and also

the investigation of the dynamical effects. In this way the steady state and transient interaction, affecting the motor speed, could be reduced still further.

5. CHOICE OF OPTIMISING SYSTEM.

The forms of extremum control system which have been described in the literature were reviewed in Section (2). There is apparently a wide variety of techniques available and the problem in this case was first to select the form of system most appropriate to the case in hand. In making this choice it was felt to be a particular requirement that the resulting system should be as simple in construction as possible. The capital value of the hydraulic transmission equipment which it is usual to find is not large. In such cases the saving, in financial terms, which an optimising system might yield is small. To this extent it is unreasonable to consider a large capital investment in the optimising system. It is, for instance, unreasonable to consider using an on-line digital computer as the optimising controller.

The extent of measurement noise in the performance signal is a major factor affecting the operation of any optimising system. In this case the noise level was low and it was therefore possible to consider using systems which are capable of rapid adaptation, although susceptible to noise.

It was decided that those systems which call for step changes in the controlled variable would not be acceptable. A step change of the motor stroke would impose too great a disturbance on the transmission system. We require to keep the bandwidth of the frequency spectrum of adjustments in the controlled variable as small as possible to avoid this.

In view of these observations, two forms of system were chosen for an initial study. These were a peak-holding system and a system with periodic perturbation.

Peak-holding System.[10]

An outline of this form of system is given on Fig.(5.1). The controlled variable Ψ is adjusted at constant rate by means of an integrator with a fixed input. As the performance measure Z passes through a maximum, the maximum value is retained in the peak clamp unit. Thereafter the output of the peak clamp is the difference between the peak value and the current value of Z. When the current value falls an amount δ below the peak value an amplitude discriminator is triggered. This then causes a bistable circuit to reverse the direction of travel of the controlled variable and resets the peak clamp. Constraints which limit the range of movement of the controlled variable would also have the same effect. The system enters a limit cycle, oscillating about the peak value in the steady state. The motion of this type of system has been analysed by Morosanov[11].

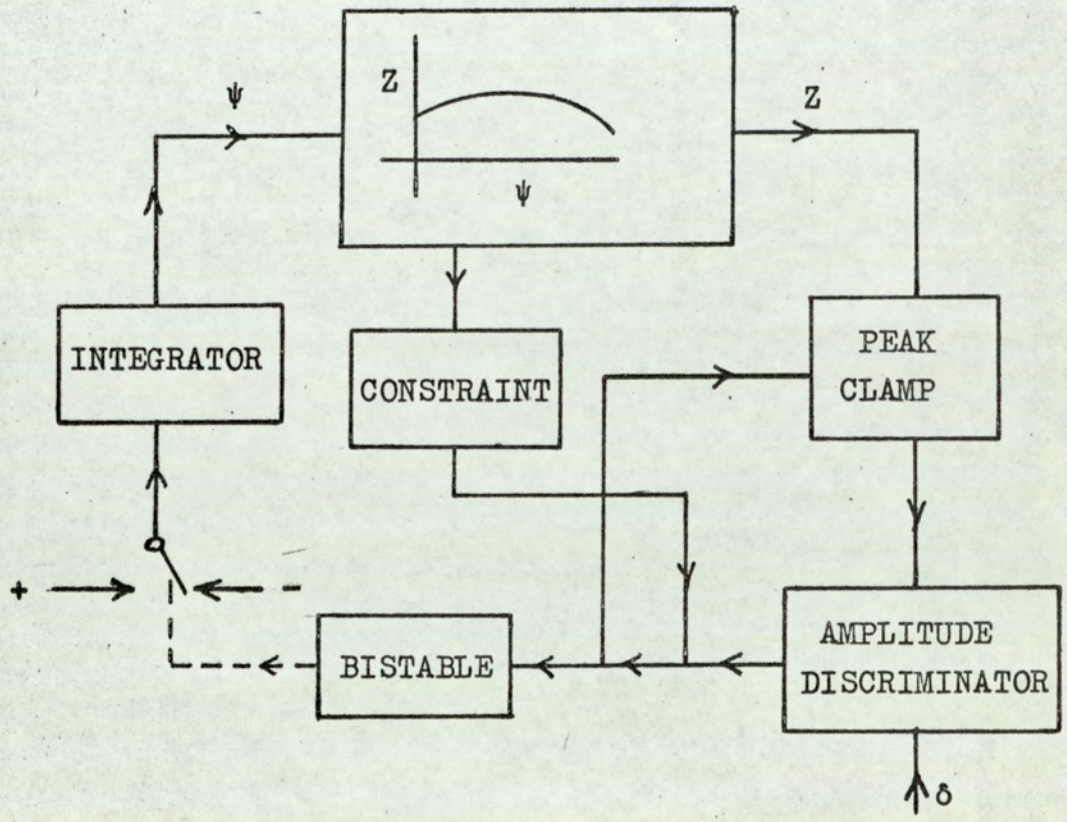

FIG.(5.1)

PEAK-HOLDING SYSTEM

Periodic Perturbation System[5]

The system is outlined in Fig.(5.2) in the form usually advocated. A sinusoidal perturbation is applied to the controlled variable and the same signal is used, with phase correction, to demodulate the variations in the performance measure. The demodulator takes the form of a multiplier. The resulting mean value of the signal from the multiplier then drives the controlled variable through an integrator. Consideration must also be given to applying constraints by interrupting the optimising loop.

In order to make an assessment of these two types of system it is necessary first to have an insight into the performance characteristics of the system to be optimised. The detailed form of these characteristics is reviewed in Section (6),from which the major results may be summarised as follows.

In the transmission system the factors which give rise to a change of efficiency are the load torque, the input speed and the fluid viscosity change with temperature. These three factors together define the operating conditions. The relative importance of each in determining the efficiency is significant. Fluid viscosity changes slowly,as the temperature can only change slowly,and the effect on the efficiency is comparatively slight. The influence of the load torque and the input speed on efficiency is more significant, and on the whole the load torque is more important than the input speed. Furthermore the load torque and

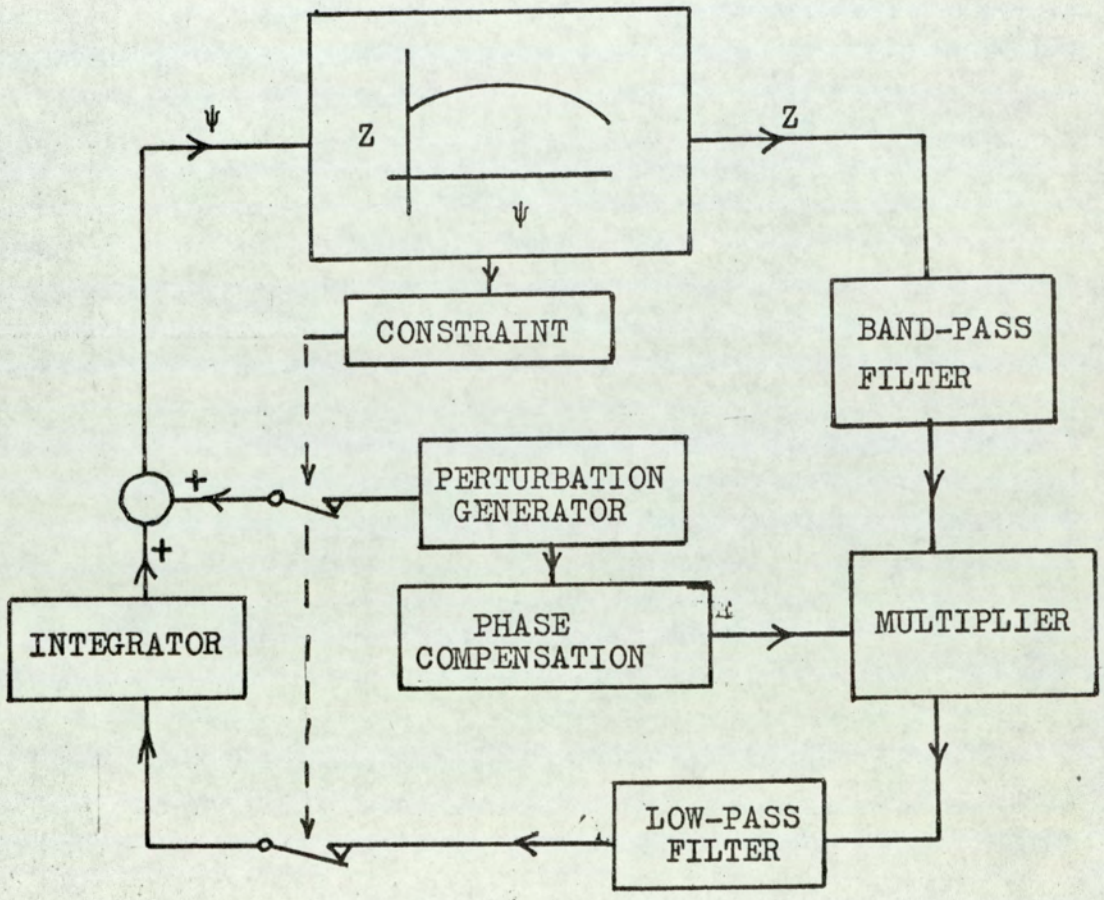

FIG.(5.2)

PERIODIC PERTURBATION SYSTEM

the input speed will change in a manner determined by the situation in which the transmission system is employed. Normally they will fluctuate comparatively rapidly. The most significant factor defining the operating conditions is therefore the load torque.

The motor stroke is to be adjusted as the controlled variable. To study its effects we make reference to the performance curves. These show how the efficiency varies with the motor stroke under different operating conditions. The measurements on the performance curves show that they exhibit a comparatively shallow maximum; the change of efficiency on either side of the peak is small, in relation to the changes produced by the operating conditions. On the basis of this it was concluded that the perturbation system would be preferable to the peak-holding system. The chief reason for this is that the amplitude of the limit cycle developed in the peak-holding system is not well defined when the performance curve has a shallow maximum. The system may execute large oscillations unless the point of reversal is brought close to the peak value. This leaves the system very sensitive to noise. On the other hand, with the perturbation system the oscillations imposed have a well defined amplitude. This system is potentially less affected by noise. Chiefly this is because by slowing down the control action the estimate of the slope of the performance curve is improved. In contrast the peak-holding system is not improved by slowing down the

control action, infact the operation will deteriorate. Its sensitivity to noise can be reduced by increasing the distance below the maximum at which reversals are made. But this in turn increases the amplitude of the oscillation in the limit cycle.

The overall assessment of the two systems is as follows. The peak-holding system offers a means of making rapid progress towards the optimum point but its behaviour will be erratic unless the maximum is well defined and the noise level low. The rate of progress made by the perturbation system is basically slower, but it is possible to trade speed for more consistent performance.

While offering these advantages in principle, the perturbation system does lead to complications in the design of the equipment needed to put it into effect. In this case it was found to be possible to simplify the basic form of system and thereby overcome this difficulty.

6. DESIGN OF THE OPTIMISING SYSTEM.

Following the argument outlined in Section (5), detailed consideration was given to the design of a system using a periodic perturbation. In this section a number of modifications to the basic arrangement are developed. These modifications exploit the particular circumstances of the system under consideration.

6.1 MEASUREMENT OF THE PERFORMANCE CURVES.

The performance curves show how the controlled variable, the motor stroke, influences the efficiency as a performance measure. The motor stroke was adjusted in this case by an electro-mechanical integrator, details of which are given in Section (7.2). It was therefore convenient to take the stroke measurement from a potentiometer driven by the integrator. Similarly the efficiency measurement was obtained using an electro-mechanical servo which also provides a measurement in the form of a potentiometer rotation. Details of the efficiency measuring servo are given in Section (5) of the Appendix. In this event the voltage signals from the potentiometers were recorded on an X-Y plotter to obtain the performance curves. The stroke setting integrator was switched into a position controlled mode so that the required values of stroke could be set up.

A set of performance curves was plotted to show how the characteristics varied with load and with the input speed. An attempt was also made

to establish the effect of a change in the temperature of the hydraulic fluid.

The load torque on the transmission was controlled by setting the current in the armature of the loading generator. The current control circuit was used to do this. A test was first conducted to ensure that the armature current could be used as a reliable measure of the torque. The generator flux was set constant by running the machine with a constant generated e.m.f. of 200 volt at the controlled speed of 750 r.p.m.. A calibration curve is shown on Fig.(6.1). This plots the unbalanced voltage of the motor torque measuring bridge against the armature current. In all further tests the load is specified in terms of the armature current.

The results of these measurements, giving the performance curves, are shown on Fig.(6.2) to Fig.(6.5). The curves of Fig.(6.2) are taken with different values of load torque with the input speed held constant at 1000 r.p.m.. The hydraulic fluid in this case was at working temperature. The result of raising the input speed to 1500 r.p.m. is shown in Fig.(6.3), the other conditions remaining the same. A repetition of these tests with the hydraulic fluid cold, gave the results shown on Fig.(6.4) and Fig.(6.5). The variation in the performance curves with the fluid temperature is small in this case. This is due chiefly to the fact that the temperature rise was restricted to between 10° and 20° C. The tendency is for the point of maximum efficiency to move towards a larger stroke setting as the fluid temperature rises. This is due to the reduction of the fluid

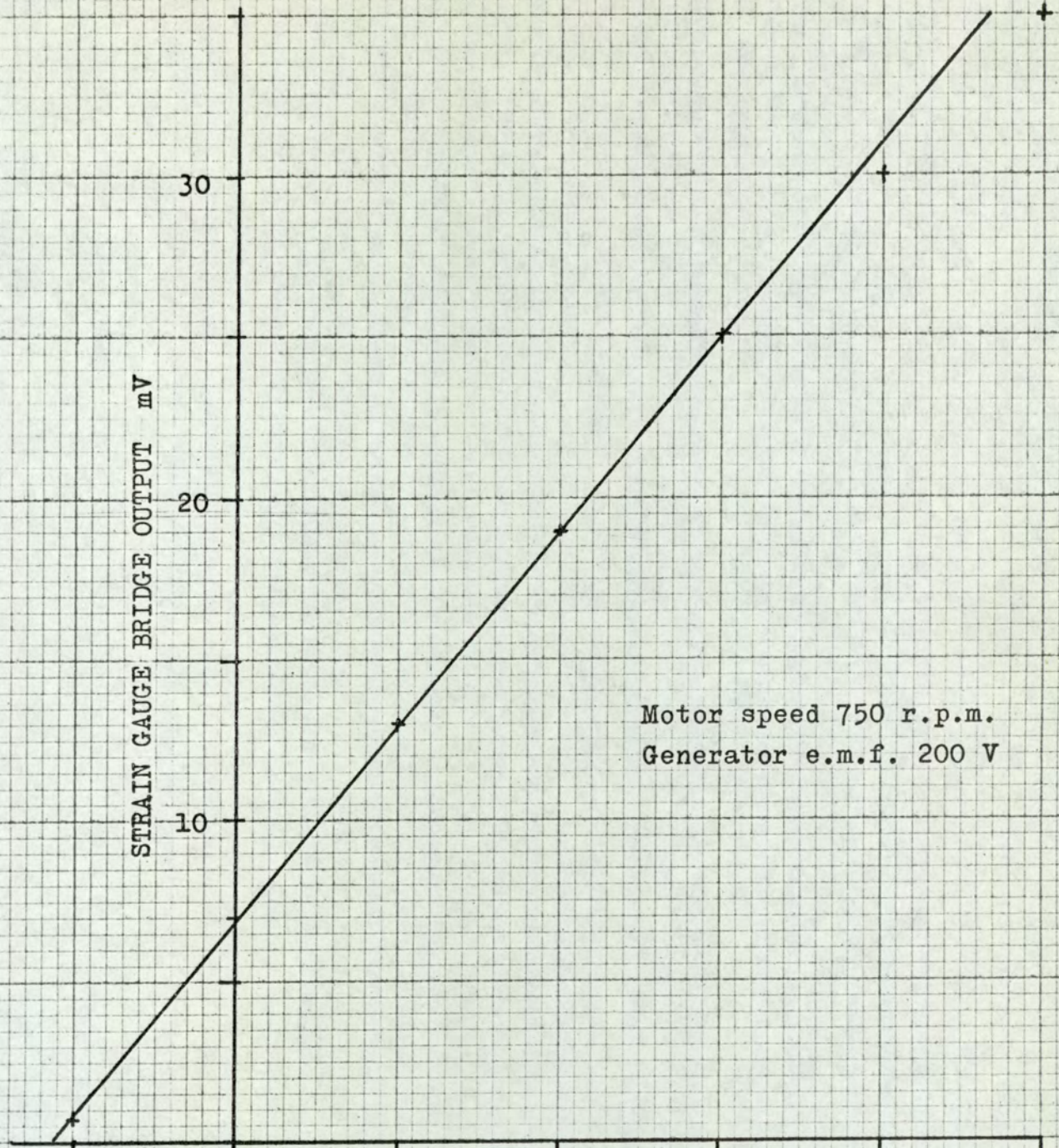

FIG.(6.1)
TORQUE CALIBRATION CURVE

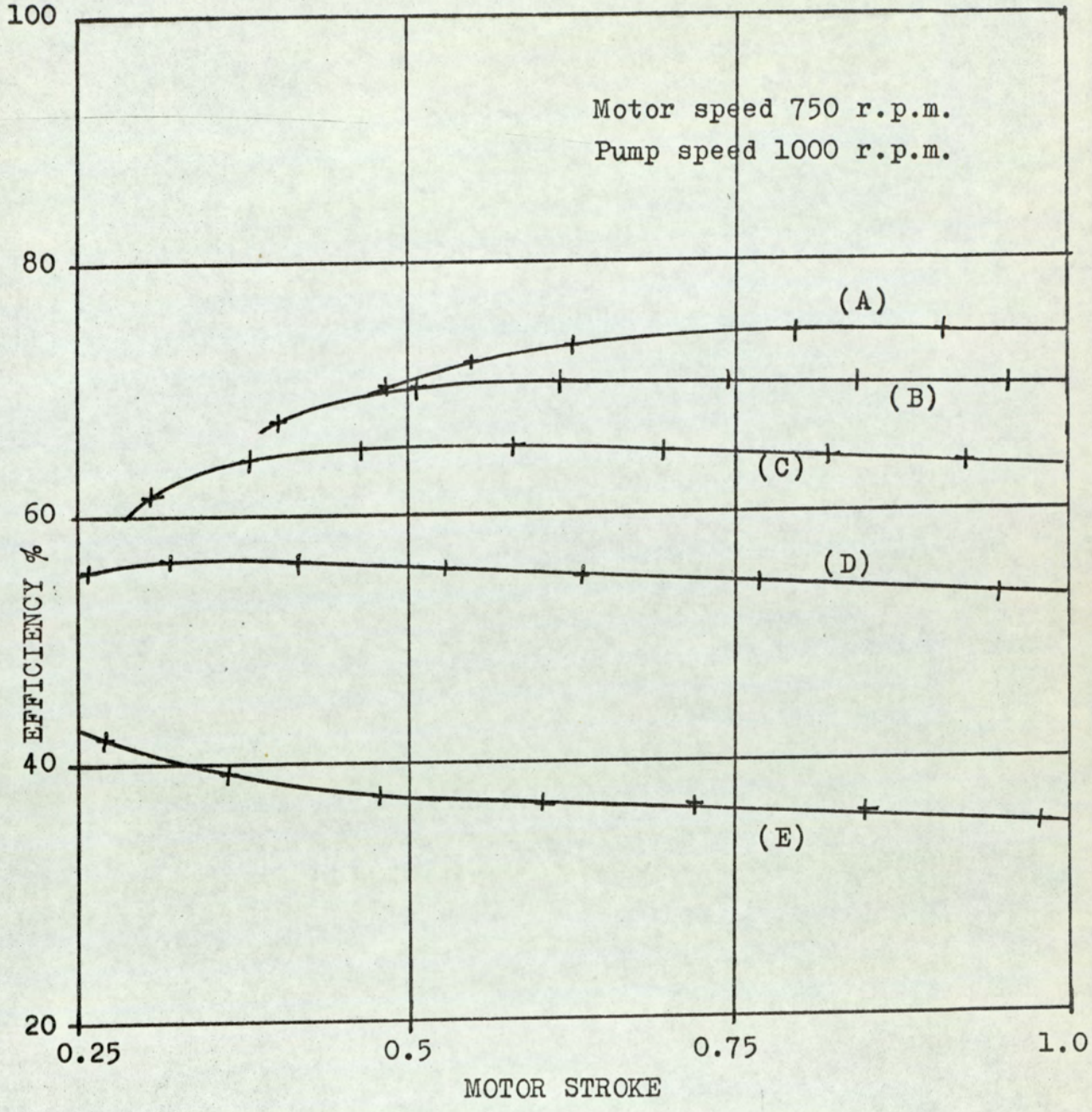

FIG.(6.2)

PERFORMANCE CURVES

Curve	(A)	load current	4 Amp
"	(B)	" "	3 "
"	(C)	" "	2 "
"	(D)	" "	1 "
"	(E)	no load	

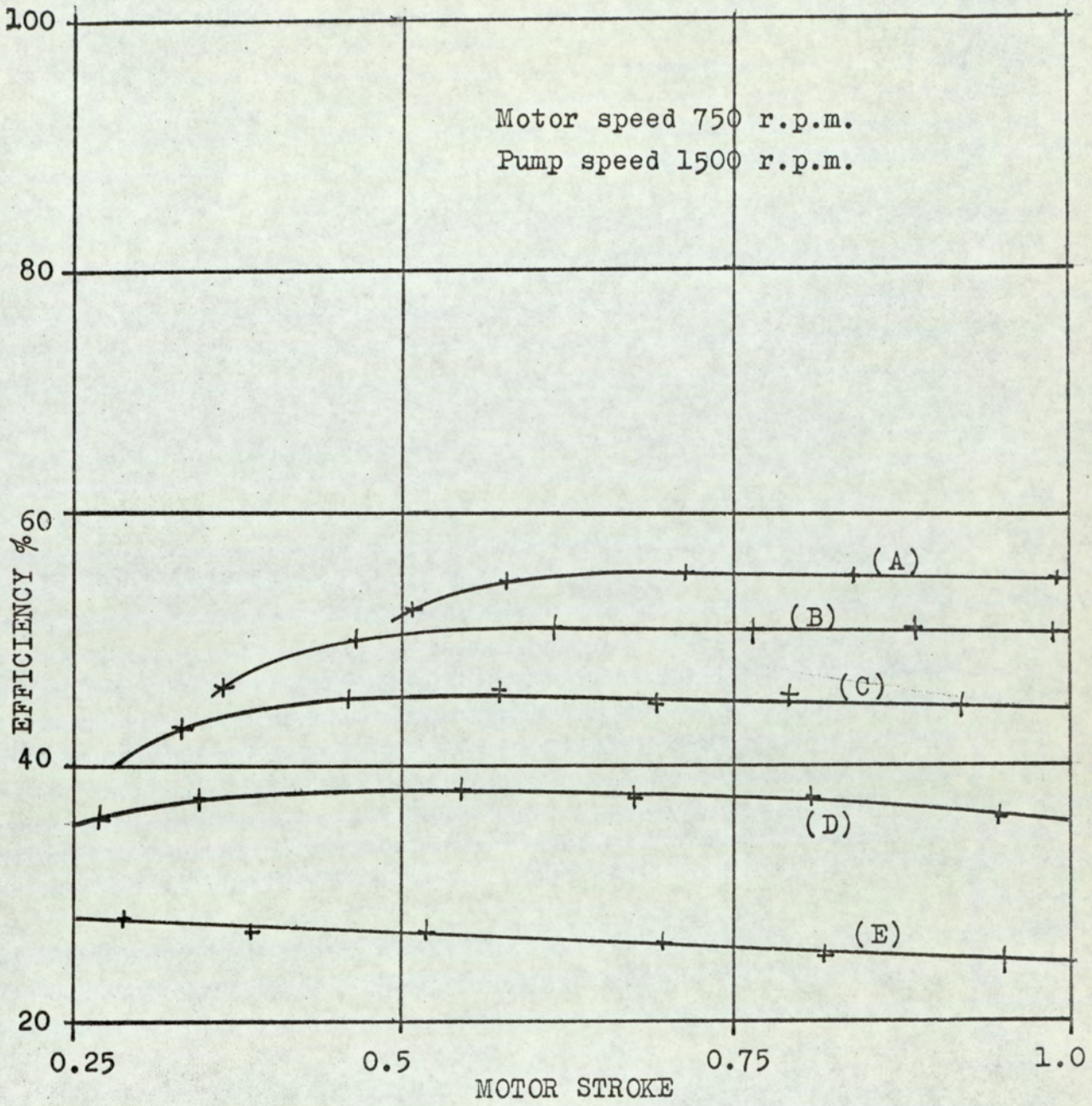

FIG.(6.3)

PERFORMANCE CURVES

Curve (A) load current 4 Amp
" (B) " " 3 "
" (C) " " 2 "
" (D) " " 1 "
" (E) no load

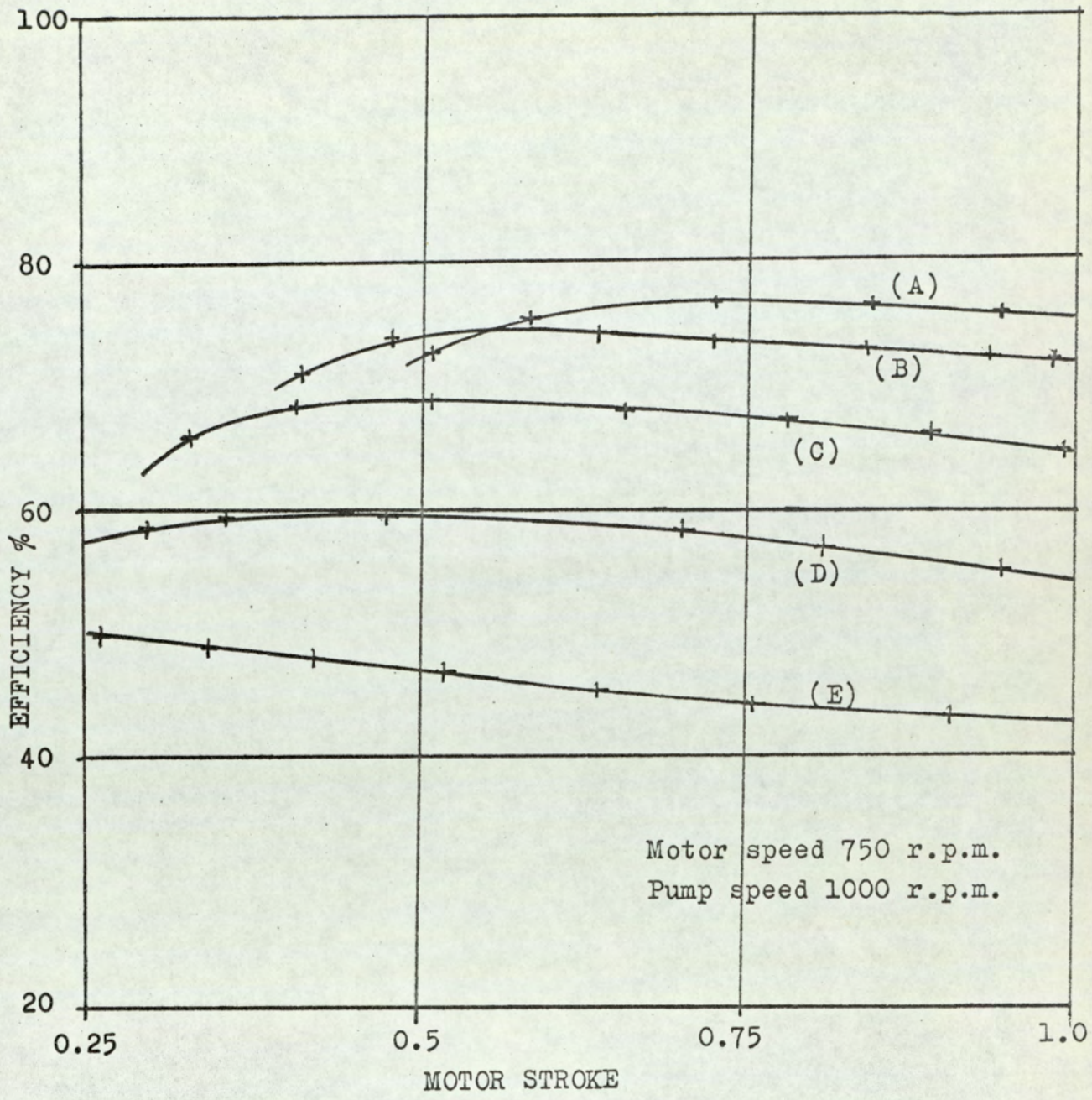

FIG.(6.4)

PERFORMANCE CURVES

Curve	(A)	load	current	4	Amp
"	(B)	"	"	3	"
"	(C)	"	"	2	"
"	(D)	"	"	1	"
"	(E)	no load			

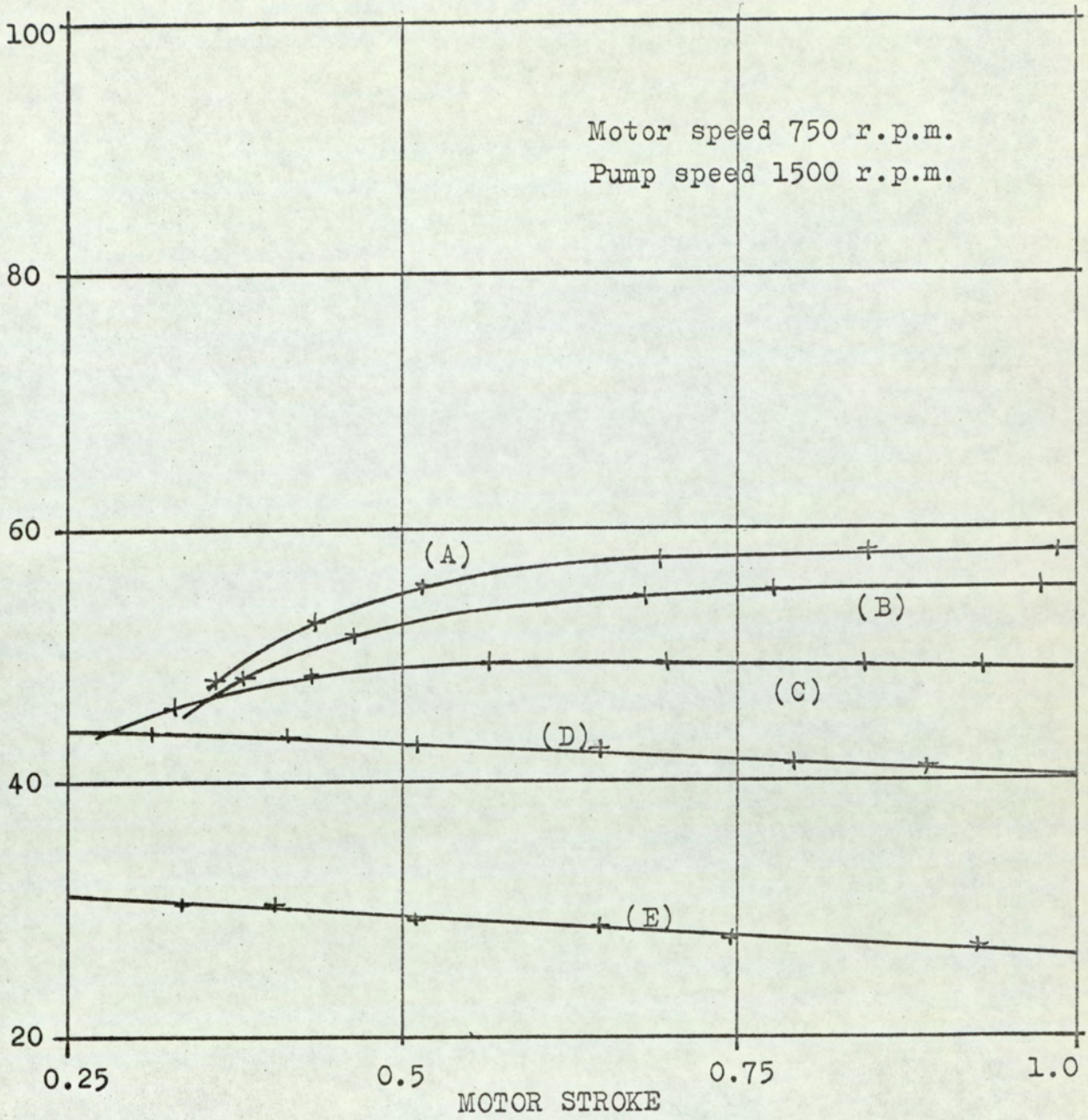

FIG.(6.5)

PERFORMANCE CURVES

Curve	(A)	load current	4	Amp
"	(B)	" "	3	"
"	(C)	" "	2	"
"	(D)	" "	1	"
"	(E)	no load		

viscosity which increases the leakage loss and reduces the loss in the pressure drop due to the flow. The level of the efficiency curves also falls as the viscosity is reduced. In other respects the efficiency varies in a manner which is consistent with the theoretical analysis of Section (3). It is notable however that while a maximum efficiency point is apparent the peak in the curves is poorly defined.

A further feature of these measurements, which is of considerable bearing on the design of the optimising system, is the noise present in the efficiency signal. The extent of this is evident from Fig.(6.6), where the efficiency measure has been recorded against time. The random fluctuations seen here appear to originate in the transmission system and may be due to aeration of the fluid. It is significant that the amplitude of the fluctuations is small. However this noise may have a considerable influence on the optimising system, particularly as the change of the efficiency over the range of motor stroke adjustment is also small. A peak-holding system would be particularly affected in this respect.

It should be noted that in this work a distinction is drawn between the measurement noise and the fluctuations in the performance measure due to the change of the operating conditions. Some authors have used the term 'measurement noise' to include all sources of fluctuation in the performance measure. This is because in some respects the effect on the optimising system is as if all the sources were combined together. In this case the term will be restricted to include only the

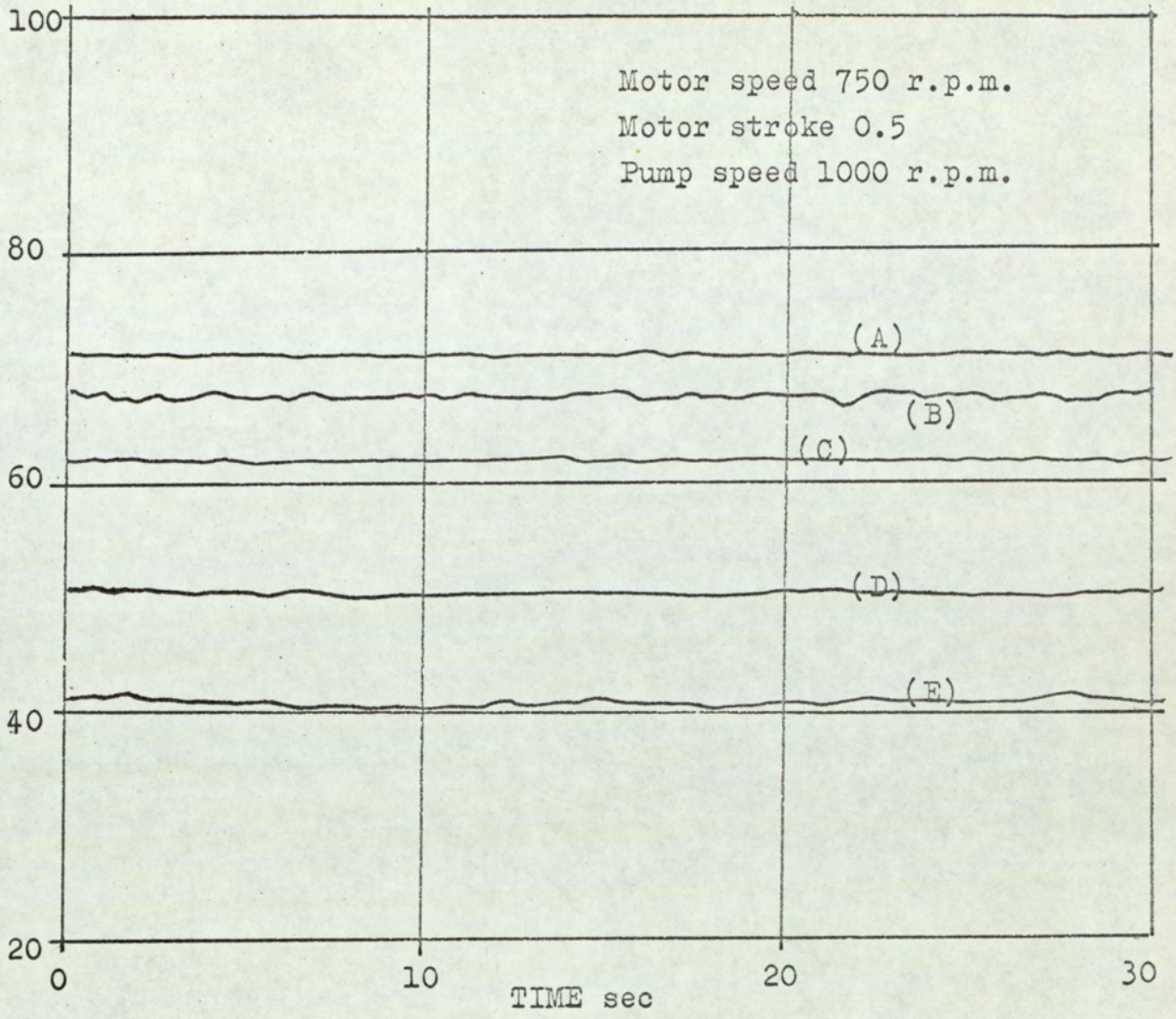

FIG.(6.6)

RECORDING OF MEASUREMENT NOISE

Curve (A) load current 4 Amp
" (B) " " 3 "
" (C) " " 2 "
" (D) " " 1 "
" (E) no load

spontaneous changes seen in Fig.(6.6). The point of distinction is then that the measurement noise is not correlated with any movement of the optimum setting of the controlled variable. On the other hand the fluctuations which accompany the changes of the operating conditions are directly correlated with the movement of the optimum position. Use is made of this in Section (6.8) where it is shown that, in view of the correlation, the design of the optimising system can be optimised.

6.2 REQUIREMENTS OF THE PERTURBATION SIGNAL.

In the general form of periodic perturbation system outlined in Section (5) a sinusoidal perturbation wave-form was envisaged. The effect of applying such changes to the motor stroke was investigated in Section (4.11.3). The objective was then to test the feedforward control system which regulates the output speed. It is clear from these results that the frequency and amplitude of the perturbation must be restricted if errors in the speed control system are to be avoided.

As far as the effect of the perturbation on the speed control system is concerned a sinusoidal wave-form is most favourable. This gives a smooth change of stroke which imposes a disturbance of minimum frequency bandwidth on the system. However it has been recognised that considerable simplifications may be made to the optimising system when a square wave-form is used. The disadvantage of the square wave form in this case is that it would develop substantial transients in the

speed control loop. For this reason step changes of motor stroke are not acceptable.

As a compromise between the two extremes it was decided to use a triangular wave-form. The advantage of this is that it can lead to a simplification of the optimising system and at the same time the discontinuity at the points of reversal is acceptably small. The wave form is generated by applying a two-state signal to the input of the control integrator. Thus a square wave perturbation is used but it is introduced before the integrator rather than following it as implied in Fig.(5.2).

The response of the efficiency measure to the triangular perturbation was investigated to determine the maximum rate of change of the motor stroke which could be used. It was apparent that if the rate of adjustment of the motor stroke was too great the efficiency measure was not the same when the stroke was increasing as when it was decreasing. The form of the figures obtained by continuously recording the efficiency against the stroke over one cycle is shown on Fig.(6.7). The three curves plotted here differ only in the rate of traverse, the time for each cycle is the same in each case. The significant feature of the figures is that the efficiency measure is higher as the stroke is decreasing i.e. the loop is traversed in an anticlockwise direction. This implies that the effect is due to an advance in the phase of the efficiency measure which is somewhat unexpected. If it had been due, for instance, to the lag in the efficiency

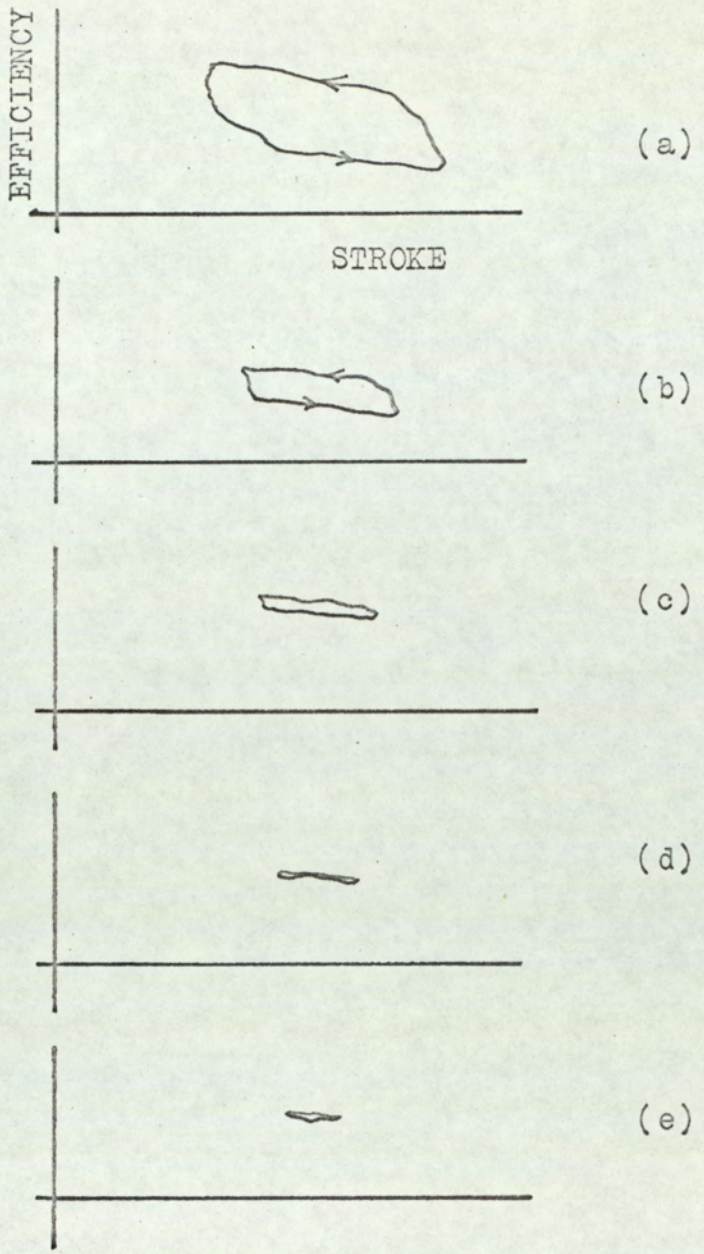

FIG.(6.7)
LOCUS RELATING EFFICIENCY TO STROKE
Perturbation frequency 0.1 Hz

measuring servo system, the loop would have been traversed in the opposite direction.

The explanation of this effect must be sought in the reaction of the transmission system. When the motor stroke is changing the speed control system makes a compensating change in the pump stroke. This is largely brought about by the feedforward control action. If the motor stroke is decreasing the lag in the feedforward system would cause the output speed to rise temporarily. The effect of the rise in speed is to increase the load torque due to the effort needed to accelerate the generator armature. The efficiency of the transmission system is considerably affected by the load torque and an increase in the load increases the efficiency. The result of decreasing the motor stroke is therefore to increase the efficiency measure and this gives rise to the effect shown on Fig.(6.7). Because of the high moment of inertia of the generator armature the change of speed required to produce the effect is small.

This effect must be taken into account in the design of the optimising system. The situation is complicated by the fact that the extent of the effect varies with the point about which the oscillation is executed. This is apparent from the results shown on Fig.(6.8) where the perturbation is applied at different operating points. The efficiency variations are more pronounced at low stroke settings. In essence this means that

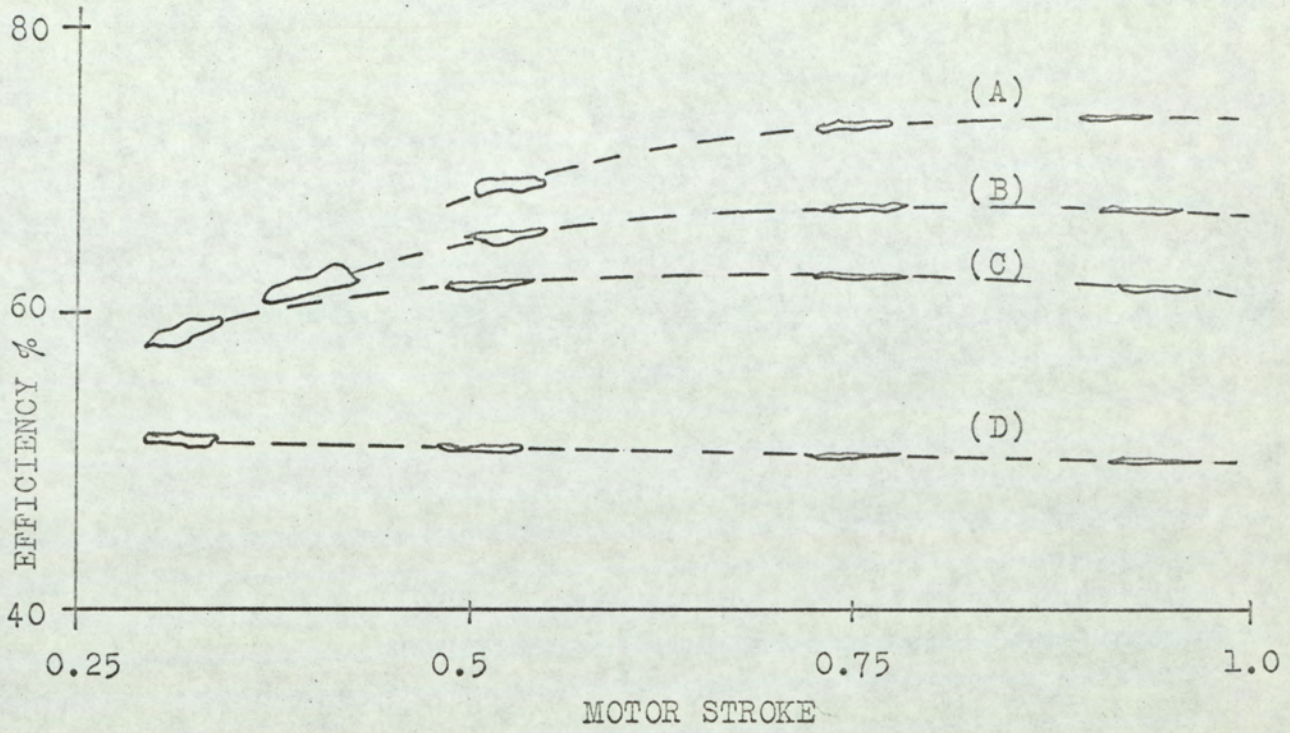

FIG.(6.8)

CHANGE OF LOCUS WITH OPERATING POINT

(A) Load 3 Amp
(B) " 2 "
(C) " 1 "
(D) " 0 "

the phase shift is a function of the stroke setting and complete phase compensation, in the optimising system, cannot be achieved over the whole operating range. The only solution in this case is to reduce the rate of traverse to a value at which the effect is unimportant. It was found that this requires that the rate of change of stroke should not exceed 1% per second. A perturbation of amplitude 2.5% would then have a period of 10 seconds.

The limiting feature in the choice of the form of perturbation is thus the performance of the speed regulating system. The limitation is imposed by the need to obtain a satisfactory efficiency measure rather than by requirements for close speed regulation. A small change of speed is sufficient to make considerable difference to the efficiency measure.

6.3 MULTIPLIER - DEMODULATOR.

The multiplier in Fig.(5.2) acts in effect as a phase sensitive demodulator. It is required to give a positive d.c. component in its output signal when the performance measure changes in phase with the perturbation. When the performance measure changes appear in antiphase with the perturbation the d.c. component must be negative.

The complexity of analogue multipliers has lead some authors to suggest using a two-state perturbation instead of a sinusoidal wave-form.[8] The multiplier may then be reduced to a switch which changes state

with the perturbation as shown in Fig.(6.9). In this case it has been decided that a two-state perturbation is not acceptable so that the simplified form is not immediately applicable. However,a development of this arrangement has been devised in order to retain the simplicity of a two-state multiplier.

In order to see how this is possible it is necessary first to recognise the role of this element as a phase sensitive demodulator, rather than as a multiplier. The demodulating action may then be obtained as shown by the wave-forms of Fig.(6.10). The perturbation wave-form is shown as (b) and results from applying the two-state signal (a) to the input of the control integrator. When the slope of the performance curve is positive, the changes of efficiency would follow as shown in (c), about a mean value Z_m. If the slope of the performance curve is negative the oscillation in Z would be in antiphase. The wave-form (c) is demodulated by first removing the mean value component. The remaining signal is then applied to two amplifiers of gain +K and -K as in Fig.(6.9). A switch selecting the output of the amplifiers is controlled by the two-state signal (d) and the resulting output wave-form becomes as shown in (e). The final wave-form has a positive mean value, corresponding to a positive slope in the performance curve. If the peak value of the stroke perturbation is Ψ_a and the slope of the performance curve is g, the mean value of wave-form (e) is given by $\frac{K g \Psi}{2}a$. When the values of Ψ_a and K are constant the mean value is proportional to the slope g and of corresponding sign.

It will now be evident that the form of demodulator

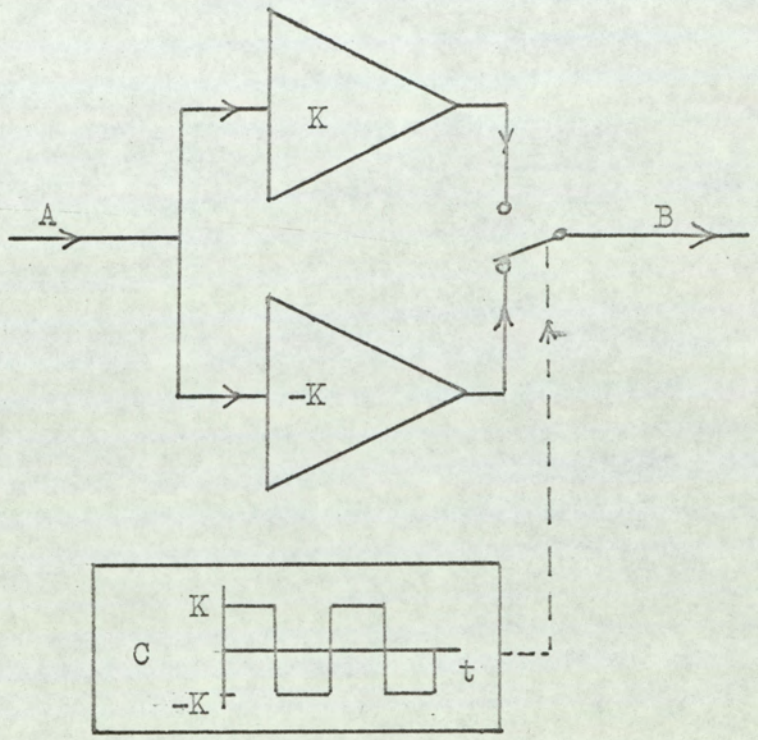

$B = A \times C$

FIG.(6.9)

SIMPLE MULTIPLIER

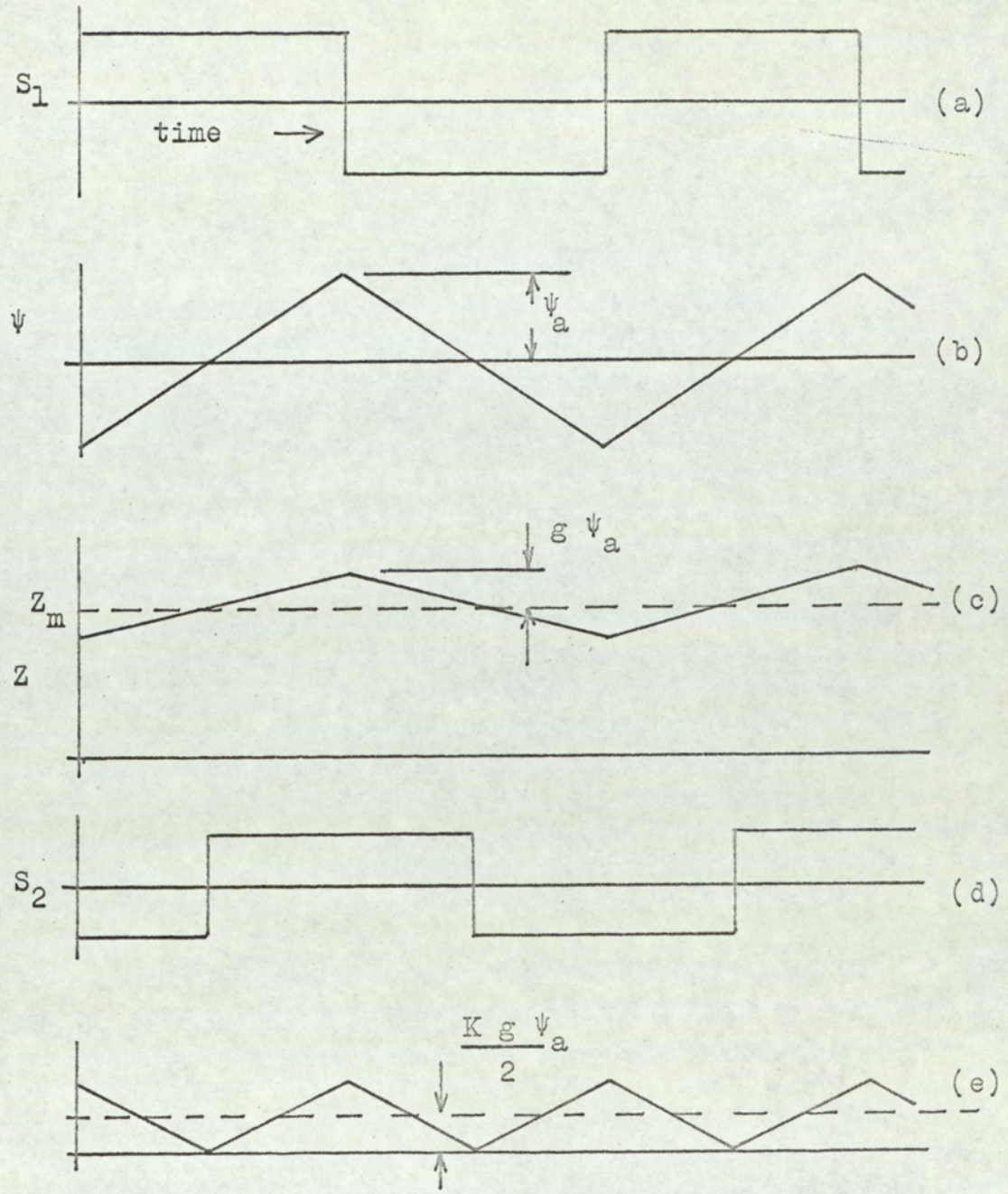

FIG.(6.10)

OPERATION OF THE DEMODULATOR

envisaged here has the same simple construction as the multiplier of Fig.(6.9). It differs in that the (c) wave-form, controlling the switch, is 90^{o} out of phase with the primary two-state signal (a). In this form the demodulator is different from what has previously been considered in the literature.

At this stage it is also as well to emphasise that the mean value of the performance signal must be removed before demodulation. If this is not done the mean value of the wave-form at the output would ideally be the same, but the harmonic content would be very much greater. Large fluctuations in this signal will adversely affect the elements which follow in the optimising control loop.

6.4 FILTERING REQUIREMENTS.

In the basic system, shown as Fig.(5.2), a band-pass filter is proposed to filter the performance signal before demodulation. This serves to remove the mean value of the signal on the low frequency side of the pass band. The attenuation on the high frequency side has the advantage of reducing the effect of measurement noise. It is proposed in this case to use a perturbation with a fundamental frequency of 0.1 Hz and there is considerable practical difficulty in designing a filter with such a low centre frequency. As the measurement noise is small in this case a high pass filter could be considered adequate but this does not present a practicable solution either. To avoid the difficulty a sampling filter has been devised.

In principle the sampling filter operates as a high-pass element and is designed to remove the mean value component of the performance signal. The arrangement is outlined in Fig.(6.11). On closure of the sampling switch the zero-order-hold retains the value of Z at the sampling instant and holds Z_o constant at this value. Subsequent changes in Z then appear at the output. The closure of the sampling switch is synchronised with the perturbation wave-form.

The instant in the cycle of the perturbation at which Z_o is set, is open to choice and we may also consider setting the value more than once in the cycle. In this we must have regard for the effect of the demodulator which follows the sampling filter. The overall requirement is then seen to be that the wave-form of variations in Z_o should contribute zero mean value at the output of the demodulator. A further factor is that when the efficiency is changing, due to a progressive change in the operating conditions, the value of Z_o should follow the mean value as rapidly as possible. Failure to track the mean value rapidly will lead to large fluctuations in the output of the demodulator.

The performance of the filter may be assessed analytically as follows. The overall transmission characteristics are studied, firstly in response to the changes in Z due to the operating conditions and secondly in transmission of the perturbation components.

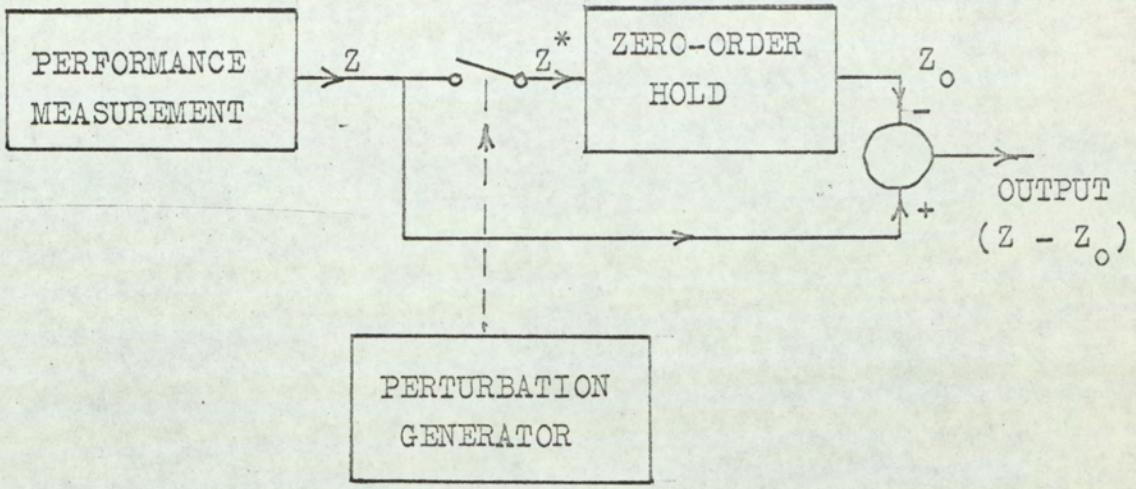

FIG.(6.11)

SAMPLING FILTER

The transfer function of the sampling filter is developed by applying the principles of analysis of sampled-data systems [15]. Taking the interval between samples to be λ in this case, we can write the transfer function of the zero-order hold as $\left(\frac{1 - \varepsilon^{-s\lambda}}{s} \right)$.

When the performance signal Z has Laplace Transform Z(s), the sampled signal Z^* has the transform,

$$Z^*(s) = \frac{1}{\lambda} \sum_{n=-\infty}^{\infty} Z(s + jn\omega_0) \quad \ldots\ldots\ldots\ldots (6.1)$$

where ω_0 is the sampling frequency $2\pi/\lambda$ rad/sec. The transform of the continuous signal Z_0 is then

$$Z_0(s) = \left(\frac{1 - \varepsilon^{-s\lambda}}{s} \right) \frac{1}{\lambda} \sum_{n=-\infty}^{\infty} Z(s + jn\omega_0) \ldots (6.2)$$

The filter output is $Z - Z_0$, designated ΔZ, and its transform becomes,

$$\Delta Z(s) = Z(s) - \left(\frac{1 - \varepsilon^{-s\lambda}}{s} \right) \frac{1}{\lambda} \sum_{n=-\infty}^{\infty} Z(s + jn\omega_0) \ldots (6.3)$$

The form of this response function can be simplified by concentrating on the frequency response. If Z is a cosine wave-form of unit amplitude we may write $\frac{1}{s \pm j\omega}$ as the transform Z(s) and then,

$$\Delta Z(s) = \frac{1}{s \pm j\omega} + \left(\frac{1 - \varepsilon^{-s\lambda}}{s} \right) \frac{1}{\lambda} \sum_{n=-\infty}^{\infty} \frac{1}{s \pm j\omega + jn\omega_0} \ldots . (6.4)$$

The wave-form of ΔZ is found by inverse transformation of this expression. Sinusoidal components are then recognised at the fundamental frequency ω, together with other components due to the modulating action of the sampler.

The fundamental component is,

$$C_o = 1 - \left(\frac{1 - \varepsilon^{-j\omega\lambda}}{j\omega\lambda} \right) \quad \ldots\ldots\ldots\ldots (6.5)$$

which varies with $\omega\lambda$ as shown in Fig.(6.12). It is to be assumed that the fluctuations in Z due to the operating conditions will be of low frequency in comparison with the sampling frequency. This implies a low value of $\omega\lambda$. The results then show that the fundamental component of the output of the filter is small and in this respect the filter acts as a high-pass filter.

The action of the sampling filter is however rather different from that of a continous high-pass filter in that modulation components are also generated. These appear at frequencies $(n\omega_o \pm \omega)$ with n taking integer values over an infinite range. Each component has a magnitude and phase given by,

$$C_n = \frac{1 - \varepsilon^{-j(n\omega_o \pm \omega)\lambda}}{j(n\omega_o \pm \omega)\lambda} \quad \ldots\ldots\ldots\ldots (6.6)$$

The modulus of this function varies with $(n\omega_o \pm \omega)\lambda$ as shown on Fig.(6.13). From this it is apparent

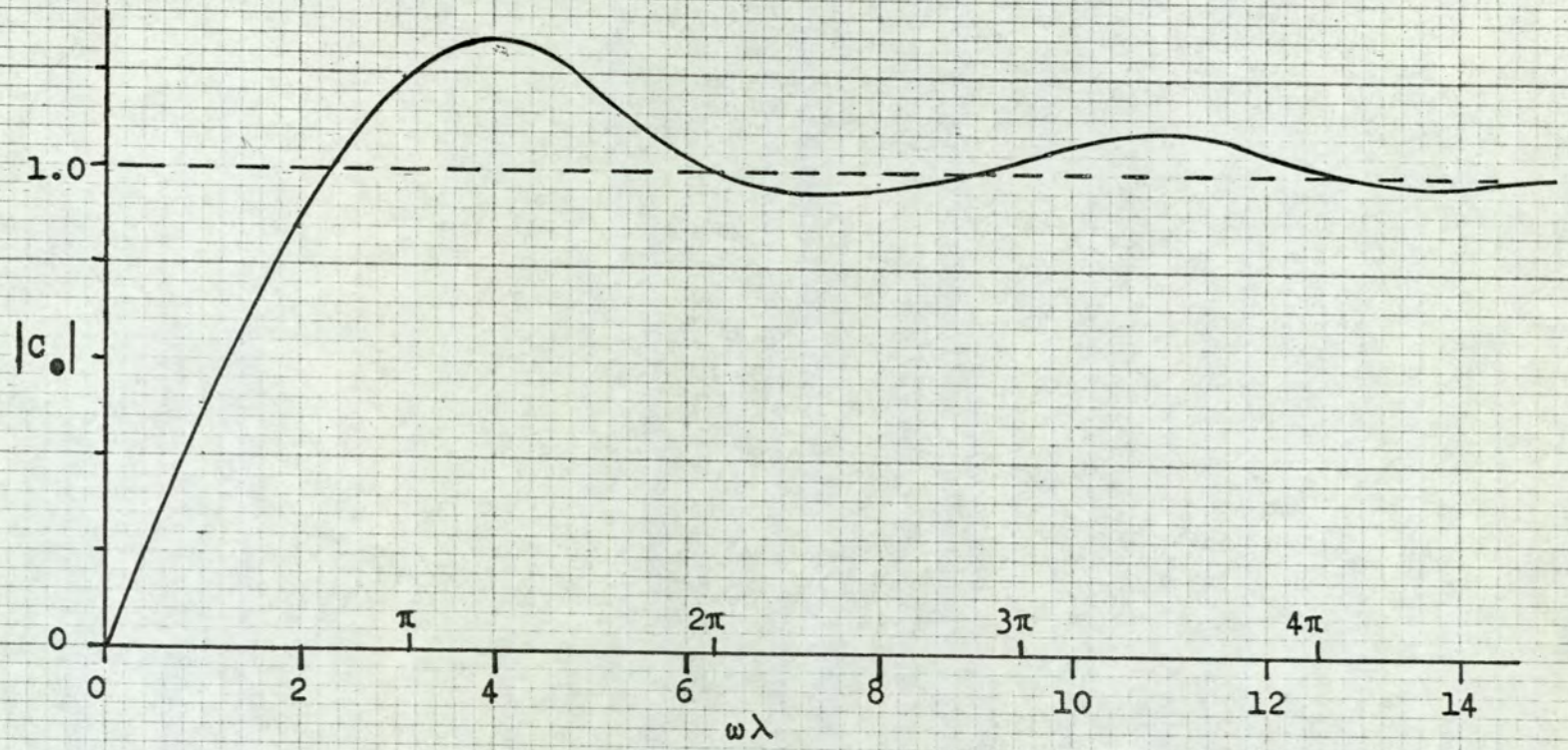

FIG.(6.12)

FUNDAMENTAL COMPONENT

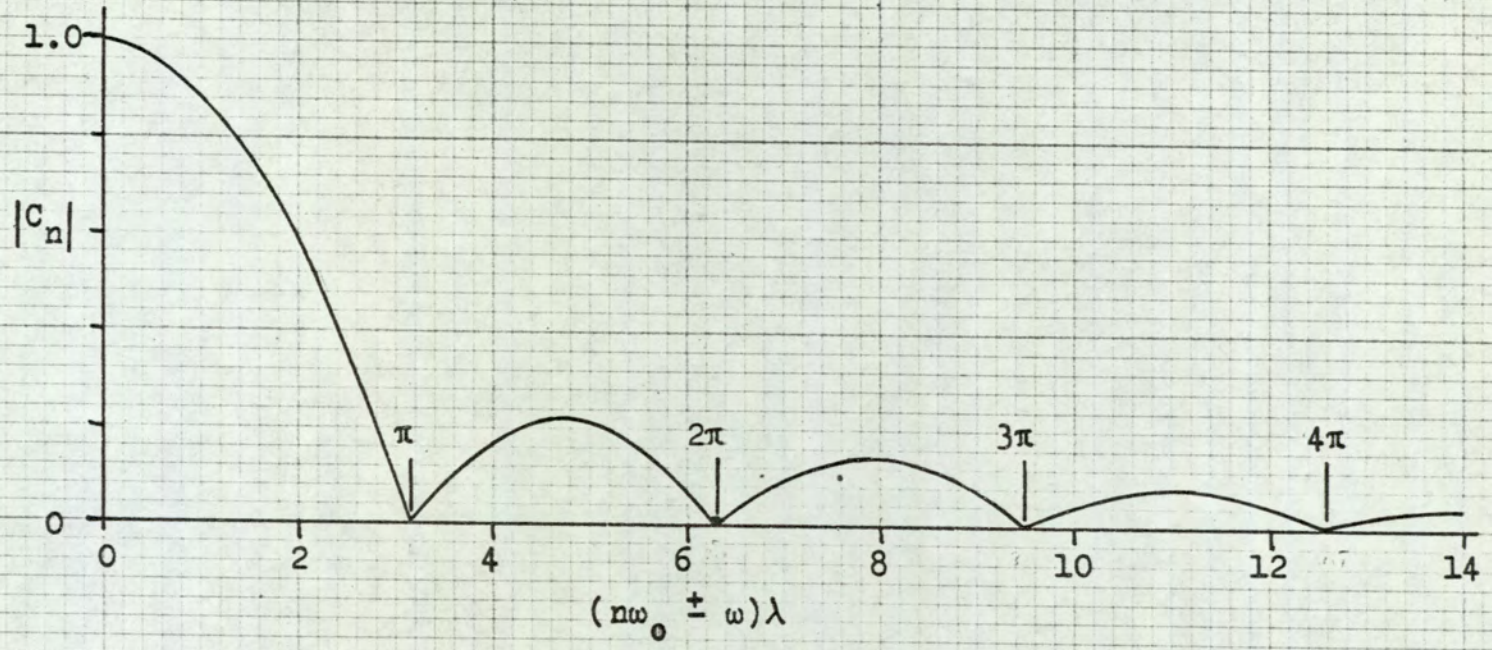

FIG.(6.13)

MODULATION COMPONENTS

that when the frequency ω is small compared with ω_o the modulation components are small in amplitude.

The overall conclusion from these results is then that ω_o should be made large compared with the highest frequency of the components of the signal Z. Provided therefore that the changes in the performance measure result from slow changes in the operating conditions, the sampling filter will effectively reject the mean value and all the other low frequency components. Measurement noise in the performance signal may well occupy a wider bandwidth than the fluctuations due to the operating conditions. The sampling filter can then be only partially successful in attenuation of the effect of measurement noise on the optimising control system.

The effect of the sampling filter on the perturbation component in the performance signal is to be assessed in terms of the requirement that this signal component should be passed without modification. When the sampling rate is set to take one sample per cycle of the perturbation, the fundamental frequency corresponds to $\omega = \omega_o$. The transmission characteristic of the filter in this case are seen on Fig.(6.12) to offer no attenuation to the signal. The modulation components are also at the zero points of Fig.(6.13), so that the fundamental component is transmitted without modification. When the perturbation wave-form is non-sinusoidal it will contain harmonics of the fundamental frequency. These will appear at frequencies

which are simple multiples of ω_0. Again it would appear that these frequency components are also transmitted faithfully. There is however a possibility of ambiguity in the mean value of the output waveform, since one harmonic component, for which n = -1, appears at zero frequency. To keep the mean value at zero requires that the sampling point be phased to coincide with the mean point on the input wave-form. In the ideal case this is half way between the points of reversal of the perturbation.

A sampling rate of one sample per cycle is the lowest rate which it is reasonable to consider. There may however be advantages in sampling at a higher rate. Certainly a higher sampling rate would enable the filter to compete with more rapid changes of the operating conditions, but the effect on the perturbation wave-form must also be taken into account. If two samples are taken in each cycle, the fundamental frequency of the perturbation wave-form is then half the sampling frequency ω_0. Reference to Fig.(6.12) and Fig.(6.13) now shows that the wave form is modulated by the sampler. It is difficult to assess the effect of this modulating action from the frequency response curves and a better impression is gained by considering directly the wave-form of the output. This wave-form is shown in Fig.(6.14) for the case when the samples are taken at the points of reversal of the perturbation. Here the wave-form (a) shows the variation in Z which leads to an output wave-form (b). This shows the modulation due to sampling. It is useful to recognise that the wave-form (b) may be

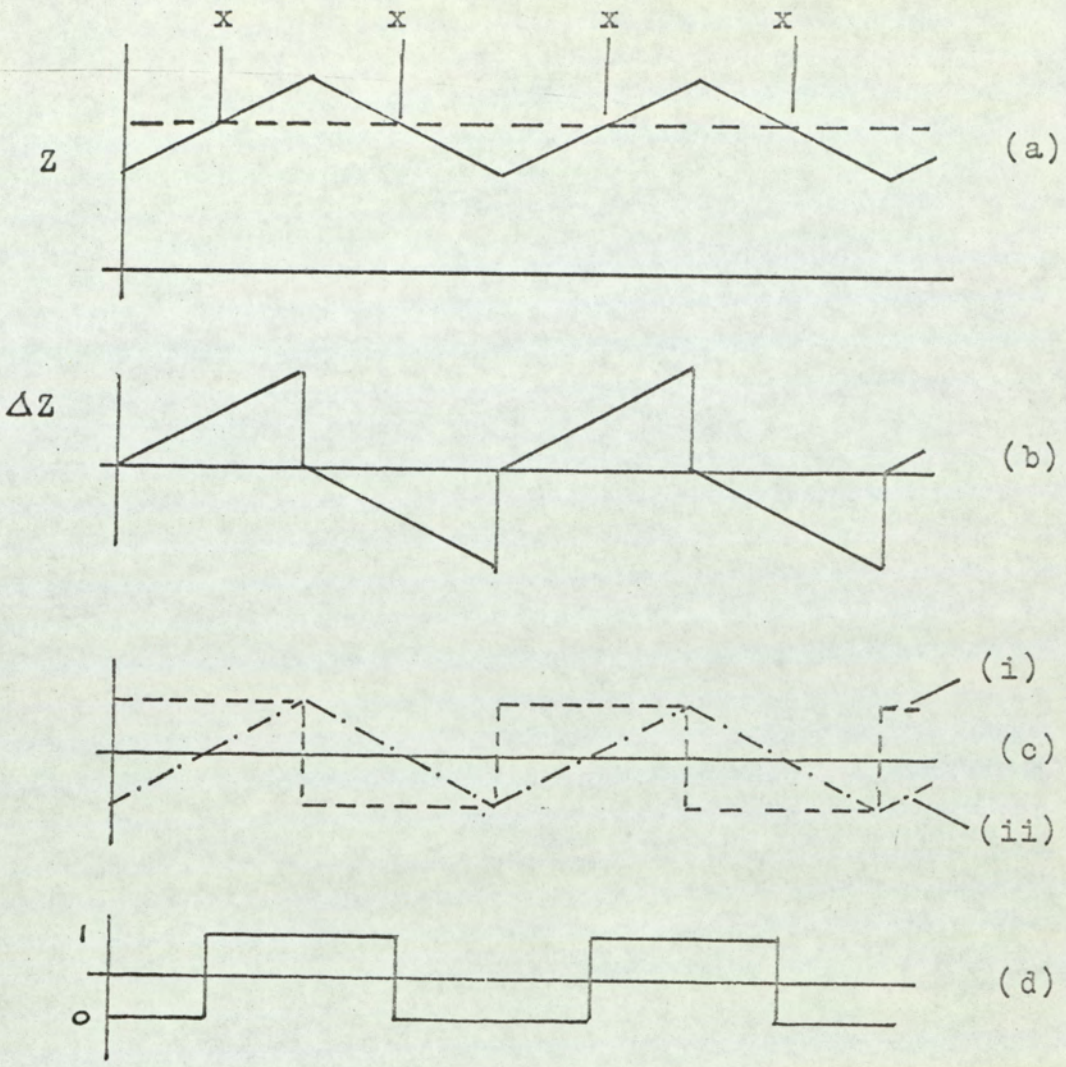

FIG.(6.14)

FILTER ACTION WITH TWO SAMPLES PER CYCLE

regarded as having two components (i) and (ii) as shown on (c). The square wave-form (i) is the result of sampling while (ii) is the true perturbation wave-form. To assess the effect of introducing the wave-form (i) the action of the demodulator must be taken into account. We require that this wave-form should not contribute to the mean value of the output of the demodulator, which should depend only on the wave-form (ii).

The action of the demodulator is to reverse the polarity of the wave-form over half the cycle. Thus in order for the wave-form (i) to give zero mean it is necessary that the switching action take place mid way through each positive and negative excursion. We therefore conclude that when two samples are taken in each cycle they must be phased to coincide with the points of reversal of the perturbation.

At first sight it would also appear that it would also be acceptable to take samples at the points x on wave-form (a). In this idealised case the wave-form (c)(i) would not appear. It must he remembered however that the wave-form (a) represents a situation in which the operating conditions are fixed and there is no measurement noise. When these effects are included it will no longer be true to expect the values at points x to be the same on successive half cycles. Any difference in these values would appear as a square wave-form component in the output (b) but in this case it would be in phase with the demodulator switch (d). There would then be a contribution to the mean value of the output of the demodulator. The conclusion

follows that the sampling switch must operate 90° out of phase with the demodulator switch when two samples are taken in each cycle. This ensures that the wave-forms produced as a result of sampling will contribute zero mean at the output of the demodulator over each separate cycle. For similar reasons it is also possible to conclude that two samples per cycle is the highest sampling frequency acceptable.

It is not wholly advantageous to use two samples per cycle. With one sample per cycle it has been shown that the perturbation wave-form is passed through the sampling filter without modification. This leads to the minimum content of harmonic and modulation components in the output of the demodulator. On the other hand the filter does not reject the low frequency variations in Z as effectively as in the case of the higher sampling frequency. In this application it has been observed that the performance curves show a much smaller variation with the controlled variable than with the operating conditions. It is important therefore to ensure that the sampling filter is as effective as possible. For this reason the sampling rate of two samples per cycle was adopted.

6.5 FURTHER CONSIDERATION OF THE OVERALL SYSTEM.

A simplified view of the action of the overall optimising system has so far been taken. The system was outlined in Fig.(5.2). The action of the multiplier has been identified with that of a demodulator. It then operates to generate a mean value component proportional to the slope of the

of the performance curve, which is used to drive the controlled variable in the direction of maximum performance.

This view is broadly adequate when the gain in the optimising loop is low. When the loop gain is high the fluctuations about the mean in the output of the multiplier will combine with the perturbation to produce substantial variations in the controlled variable. The complete wave-form of variations applied to the controlled variable may then be considerably different from what has so far been assumed.

The inclusion of a low-pass filter as shown in Fig.(5.2) is advocated in order to reduce this effect. However it does not immediately follow that this is advantageous to the operation of the complete system. In this case it was decided not to use a low-pass filter for three reasons. Firstly, because the perturbation frequency is necessarily low, the filter would place a substantial lag in the optimising control loop. Secondly the practical implementation of a filter with low cut-off frequency leads to difficulties. And thirdly the fluctuations in the output of the demodulator can contribute to the progress made towards the maximum performance. This latter feature is studied further in the following section.

6.6. PROGRESS IN ONE CYCLE.

The diagram given on Fig.(6.15) shows an outline of the optimising system, incorporating the sampling filter and the demodulator as previously described. The perturbation applied to the input of the integrator takes values $\pm$ h under the control of the timing wave-form. The period of the timing wave-form is taken as τ seconds. The demodulating switch and sampling filter are also controlled from the same wave-form. The transmission and the associated efficiency measuring system are shown as one unit. The motor stroke, acting as the controlled variable, is here designated Ψ. The efficiency Z is also influenced by the disturbance Q. This is regarded as a generalised form of disturbance representing the change of operating conditions in the transmission. It will be assumed that the lag in Z following the changes in Ψ and Q is negligable at the slow rates of change which will be imposed. As Ψ and Q change we may imagine the corresponding values of Z to define a performance surface. It will then be assumed that at a given point the slope of the surface in each direction is given by,

$$\frac{\partial Z}{\partial \Psi} = g$$

$$\frac{\partial Z}{\partial Q} = G \qquad \text{.....(6.7)}$$

We are now in a position to calculate the motion of the system as it attempts to make progress towards the maximum performance. It will be assumed that the slope of the performance surface g is constant in

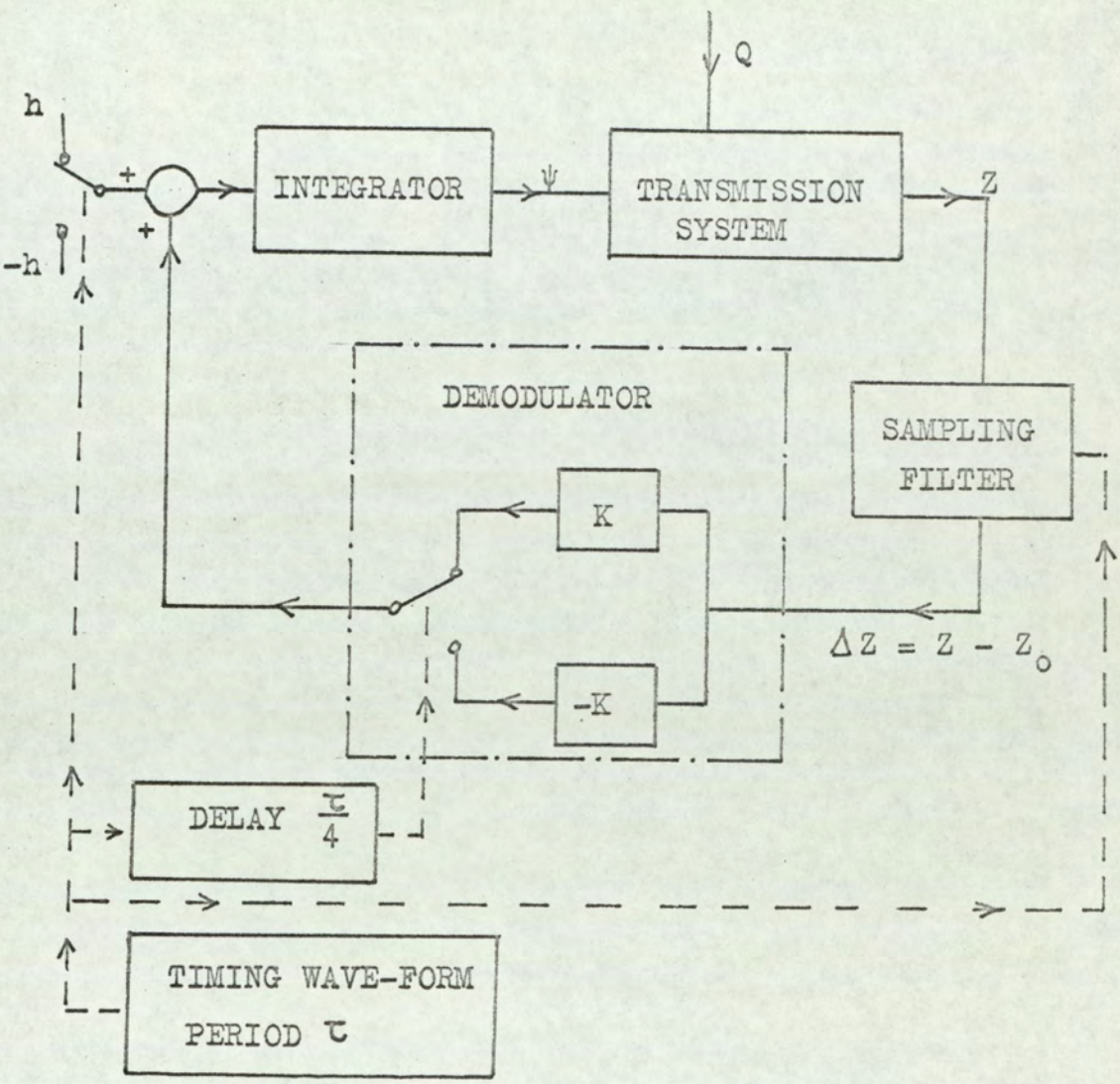

FIG.(6.15)
OUTLINE OF THE OPTIMISING SYSTEM

the operating region. In the first instance the motion will be investigated when the disturbance Q is constant.

Because the clamp in the sampling filter sets the value of Z_o instantaneously and there is no lag in the transmission system, the response in any one cycle is independent of that in the preceding cycles. The complete motion of the system is therefore apparent from the response over a single cycle.

For the purpose of analysis the diagram of Fig.(6.15) may be simplified to that of Fig.(6.16). The integrator time constant is taken as T seconds. During each cycle the system will enter one of two modes of motion under the control of the demodulating switch. Also during the cycle the perturbation signal H takes the constant values $\pm h$ in sequence.

Mode (A).

When the demodulating switch is in position a on Fig.(6.16) the system moves as indicated by the differential equation,

$$\frac{d\psi}{dt} - \frac{K g \psi}{T} = \frac{H}{T} \quad \ldots\ldots\ldots\ldots\ldots\ldots (6.8)$$

which may be solved subject to an initial value of ψ, taken as ψ_o. The solution is,

$$\psi = \frac{H}{T\alpha}(\varepsilon^{\alpha t} - 1) + \psi_o \varepsilon^{\alpha t} \quad \ldots\ldots\ldots (6.9)$$

where $\alpha = \frac{K g}{T}$ $\ldots\ldots\ldots\ldots\ldots\ldots\ldots\ldots (6.10)$

This mode is divergent when α is positive, that

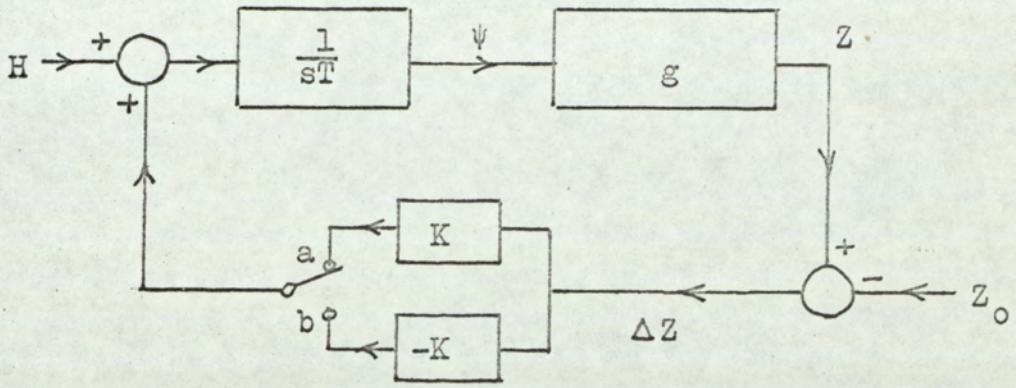

FIG.(6.16)

BLOCK DIAGRAM WITH PERTURBATION

is when g, the slope of the performance surface, is positive. With α negative the mode is stable.

Mode (B).

When the demodulating switch moves to position b on Fig.(6.16) the sign of the gain constant K is reversed. The solution of equation (6.8) then becomes,

$$\Psi = \frac{H}{T\alpha}(1 - \varepsilon^{-\alpha t}) + \Psi_0 \varepsilon^{-\alpha t} \text{.....(6.11)}$$

This mode is stable when α is positive and diverges when negative.

The response over a complete cycle may now be determined by examining the sequence in which these modes occur and giving appropriate values to H. The diagram of Fig.(6.17) has been drawn to clarify the sequence of events. In designating the modes as shown in (5) it has been assumed that g is positive. It is required to find the nett change in Ψ over the cycle designated by points (1) to (5). To do this the response equations are applied in each of the four sub-intervals as follows.

Response (1) - (2).

Because the sampling switch operates at (1) the effective initial value of Ψ is zero. The value of the perturbation H is h and the system is in Mode (B). Equation (6.11) then gives the value of Ψ at (2) as,

$$\Psi_2 = \frac{h}{T\alpha}\left(1 - \varepsilon^{-\frac{\alpha\tau}{4}} \right) \text{.....(6.12)}$$

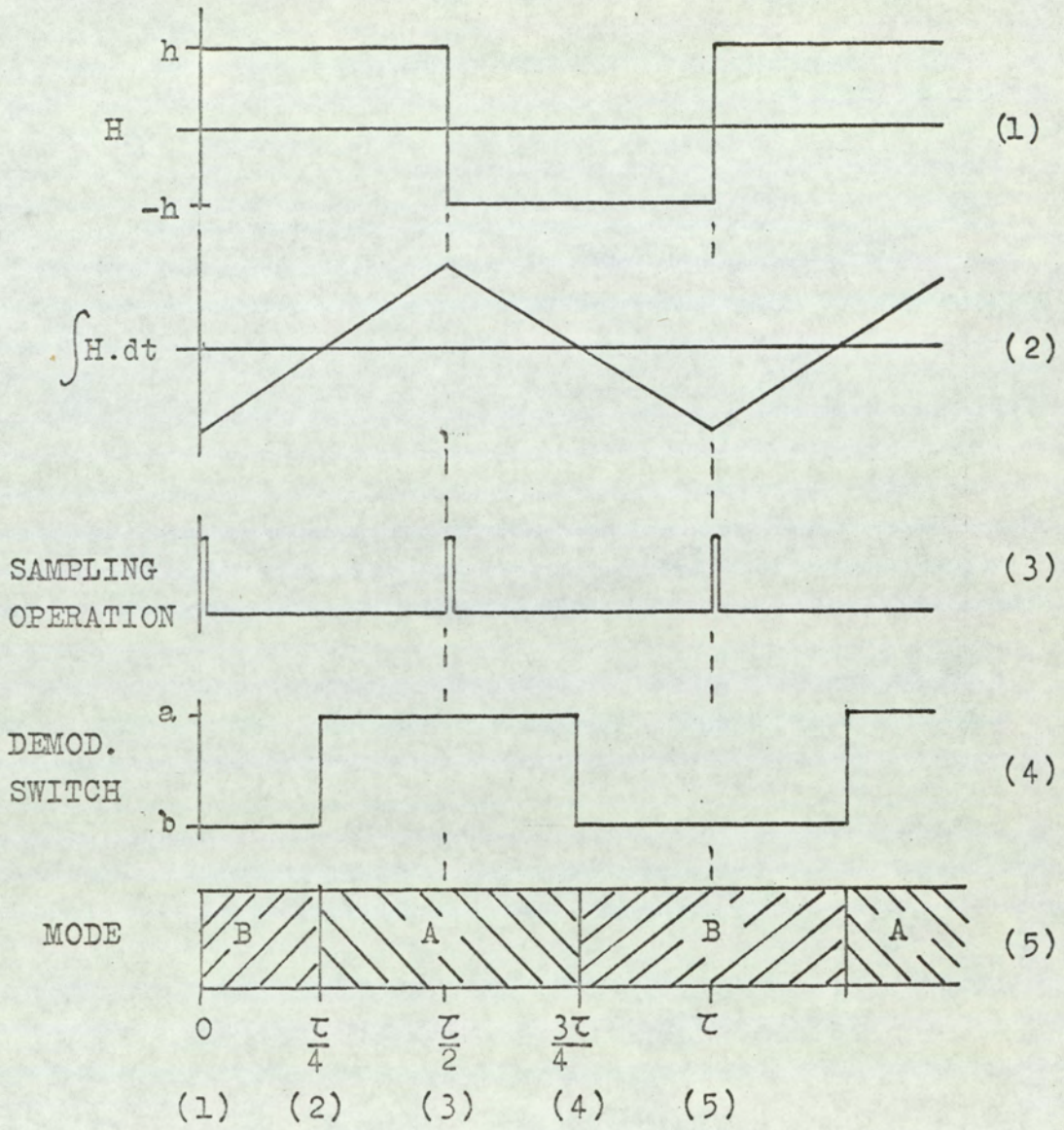

FIG.(6.17)

SEQUENCE OF OPERATIONS

Response (2) - (3).

The system is switched into Mode (A) at point (2). No change is made to the value of Z stored in the sampling filter so the value of Ψ accumulated in the first interval must be taken as an initial value Ψ_0 for this interval. The response accumulated at (3) is then given by equation (6.9) as,

$$\Psi_3 = \frac{h}{T\alpha}\left(\varepsilon^{\frac{\alpha\tau}{4}} - 1 \right) + \frac{h}{T\alpha}\left(1 - \varepsilon^{-\frac{\alpha\tau}{4}} \right) \varepsilon^{\frac{\alpha\tau}{4}} \quad \ldots(6.13)$$

which reduces to,

$$\Psi_3 = \frac{2\,h}{T\alpha}\left(\varepsilon^{\frac{\alpha\tau}{4}} - 1 \right) \quad \ldots\ldots\ldots\ldots\ldots\ldots\ldots\ldots(6.14)$$

The value Ψ_3 gives the total movement in Ψ from the starting point (1).

Response (3) - (4).

Once the sampling switch has operated at (3) the progress made in the first half of the cycle has no further influence. We therefore take the initial value of Ψ as zero. The perturbation takes the value -h and the response is given for Mode (A) from equation (6.9). The value attained at point (4) is,

$$\Psi_4 = \frac{-h}{T\alpha}\left(\varepsilon^{\frac{\alpha\tau}{4}} - 1 \right) \quad \ldots\ldots\ldots\ldots\ldots\ldots\ldots\ldots(6.15)$$

Response (4) - (5).

At point (4) the only change made to the system is to switch from Mode (A) to Mode (B). The value Ψ_4 is taken as the initial value of Ψ in equation (6.11). At point (5) we then have the response,

$$\Psi_5 = \frac{-2h}{T\alpha}\left(1 - \varepsilon^{-\frac{\alpha\tau}{4}}\right) \qquad \text{.....(6.16)}$$

The response over the complete cycle (1) - (5) may now be found by adding the progress made in the first half cycle to that in the second half i.e. $\Psi_3 + \Psi_5$. This may be simplified to the form,

$$\Psi_H = \frac{4h}{T\alpha}\left(\cosh\left(\frac{\alpha\tau}{4}\right) - 1\right) \qquad \text{.....(6.17)}$$

This equation shows the overall progress Ψ_H, representing the change in the controlled variable, in any one cycle when the perturbation H acts alone. The movement is positive when α is positive and this is realised when the slope of the performance surface is positive. The system is therefore constrained to make progress towards the maximum performance. If the slope of the performance surface is negative the progress is negative and the movement is again towards the maximum position. The amount of progress made depends on the slope g, which determines the value of α. The progress tends to zero as g tends to zero so that the maximum is approached asymptotically. The value of α also depends on the ratio $\frac{K}{T}$ which determines the loop gain of the optimising system. The higher the value of the loop gain the greater is the progress made in each cycle.

When $\frac{\alpha\tau}{4}$ is small the value of Ψ_H in equation (6.17) reduces to,

$$\Psi_H = \frac{h\, g\, K \tau^2}{8\, T^2} \qquad \ldots\ldots\ldots\ldots\ldots\ldots\ldots\ldots (6.18)$$

If we ignore the dynamical effects in the optimising loop and calculate the progress due to the mean component of the demodulator output alone, we arrive at the same result. This follows from the wave-forms of Fig.(6.10) when it is recognised that the peak value of the perturbation Ψ_a is $\frac{h\tau}{4T}$. As the loop gain is increased the value of Ψ_H given by the equation (6.17) becomes greater than that from equation (6.18). The additional progress which this represents is due to the effect of allowing the fluctuations about the mean output of the demodulator to pass to the integrator. If a low-pass filter were introduced before the integrator the progress would fall to approach that given by equation (6.18).

6.7 EFFECT OF DISTURBANCES.

If the disturbance Q is changed during the climbing motion the response obtained in the preceding section will be modified. The rate at which the disturbance may change must be slow if the optimising system is to be able to follow the changes in the position of maximum performance. It will therefore be assumed that, over any one cycle of the perturbation, the rate of change of the disturbance is constant. Also when the change of Q is small in each cycle we may take the slope of the performance surface g to be constant

over each cycle. This allows the simplification of the diagram on Fig.(6.15) which results in the diagram of Fig.(6.18). Again we may consider each cycle independently of the preceding motion and identify two modes.

Mode (A).

With the demodulating switch in position a the equation of motion is,

$$\frac{d\Psi}{dt} - \frac{K\,g\,\Psi}{T} = \frac{Q\,K\,G}{T} \quad \ldots\ldots\ldots\ldots(6.19)$$

When the value of Q changes at a constant rate, $\frac{dQ}{dt}$, the changes of Ψ follow the form,

$$\Psi = \frac{G}{g\alpha}\frac{dQ}{dt}(\varepsilon^{\alpha t} - 1 - \alpha t) + \Psi_o\,\varepsilon^{\alpha t} + Q_o\frac{G}{g}(\varepsilon^{\alpha t} - 1) \quad \ldots\ldots\ldots\ldots(6.20)$$

where again $\alpha = \frac{K\,g}{T}$ and Ψ_o and Q_o are initial values.

Mode (B)

On changing the demodulating switch to position b the sign of K is made negative. The response then becomes,

$$\Psi = \frac{-G}{g\alpha}\frac{dQ}{dt}(\varepsilon^{-\alpha t} - 1 + \alpha t) + \Psi_o\,\varepsilon^{-\alpha t} + Q_o\frac{G}{g}(\varepsilon^{-\alpha t} - 1) \quad \ldots\ldots\ldots\ldots(6.21)$$

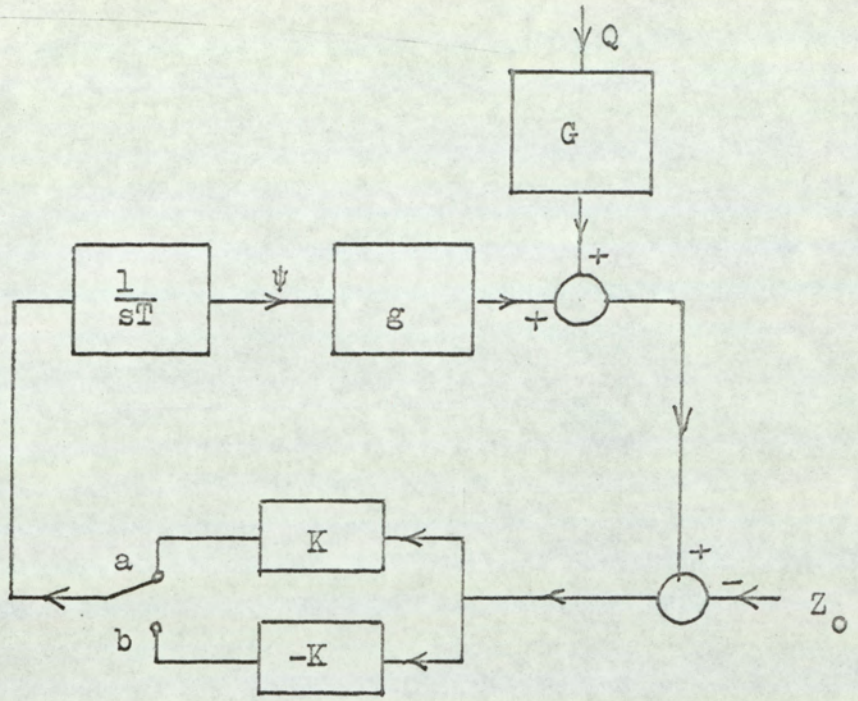

FIG.(6.18)

BLOCK DIAGRAM WITH DISTURBANCE

The change over the complete cycle (1) - (5), defined on Fig.(6.17), may now be calculated.

Response (1) - (2).

When the reference value Z_o is set in the sampling filter at point (1) the effect is to reduce the initial values Ψ_o and Q_o to zero. The system responds in Mode (B) and the movement, given by equation (6.21), takes the following value at point (2),

$$\Psi_2 = -\frac{G}{g\alpha}\frac{dQ}{dt}\left(\varepsilon^{-\frac{\alpha\tau}{4}} - 1 + \frac{\alpha\tau}{4}\right) \quad \ldots\ldots\ldots (6.22)$$

Response (2) - (3).

At point (2) the system is switched to Mode (A). The initial value of Ψ_o is Ψ_2 given by equation (6.22). Also the initial value Q_o is the change in Q over the first interval i.e. $\frac{\tau}{4}\frac{dQ}{dt}$.

The accumulated response at point (3) is then found from equation (6.20).

$$\Psi_3 = \frac{G}{g\alpha}\frac{dQ}{dt}\left[2\left(\varepsilon^{\frac{\alpha\tau}{4}} - 1\right) - \frac{\alpha\tau}{2}\right] \quad \ldots\ldots\ldots (6.23)$$

Response (3) - (4).

On resetting the value of Z_o at point (3) the system continues in Mode (A) with zero initial conditions. The response at (4) is then,

$$\Psi_4 = \frac{G}{g\alpha}\frac{dQ}{dt}\left(\varepsilon^{\frac{\alpha\tau}{4}} - 1 - \frac{\alpha\tau}{4}\right) \quad \ldots\ldots\ldots\ldots\ldots\ldots (6.24)$$

Response (4) - (5).

At point (4) the system enters Mode (B) and continues with the initial conditions taken over from the preceding interval. The response at (5) is given by equation (6.20).

$$\Psi_5 = \frac{G}{g\alpha}\frac{dQ}{dt}\left[2\left(1 - \varepsilon^{-\frac{\alpha\tau}{4}}\right) - \frac{\alpha\tau}{2}\right] \ldots\ldots (6.25)$$

The total change in Ψ over the complete cycle is obtained by adding Ψ_3 and Ψ_5,

$$\Psi_Q = \frac{G\tau}{g}\frac{dQ}{dt}\left[\frac{4}{\alpha\tau}\sinh\left(\frac{\alpha\tau}{4}\right) - 1\right] \quad \ldots\ldots\ldots (6.26)$$

This value tends to zero as the constant α is made small by reducing the gain $\frac{K}{T}$. The limiting value is also zero when the slope of the performance surface, g, is taken to zero. The direction of the change Ψ_Q is such as to assist the hill-climbing action when $\frac{dQ}{dt}$ is positive and to oppose it when negative.

6.8 OPTIMUM GAIN SETTING.

The progress made in climbing a constant slope segment of the performance surface was calculated in Section (6.6). It was observed that the advance in each cycle was made larger by increasing the gain constant $\frac{K}{T}$. However the results of Section (6.7) show that this also has the effect of increasing the response to the disturbance. By looking carefully into the balance of these two effects it is possible to show that an optimum choice of $\frac{K}{T}$ can be made.

The form of the disturbance Q has not previously been defined precisely. It will now be identified as a composite parameter determining the operating conditions for the transmission system. The factors which together settle the operating conditions are the load torque, the speed of the prime mover and the temperature of the hydraulic fluid. Any change in one or more of these factors will disturb the optimising system. The disturbance will have the effect of changing the efficiency value for a given setting of the motor stroke and will also alter the position of the point of maximum efficiency. Thus the changes of the performance measure due to this form of disturbance are correlated with the movement of the optimum point. The following analysis makes use of this correlation to establish the optimum value of $\frac{K}{T}$.

The overall requirement of the optimising system is that it should hold the performance measure as close to its maximum value as possible in the changing situation. In assessing the ability of the system to do this, three factors must be taken into consideration,

(1) Progress towards the optimum setting due to the perturbation.
(2) Effect of the disturbance on the progress towards the optimum setting.
(3) Progressive movement of the optimum setting.

The first of these factors has been analysed in Section (6.6) where the progress made in one cycle was designated Ψ_H. The second factor was studied in

Section (6.7) and the change of motor stroke in one cycle was defined as Ψ_Q. As far as the third factor is concerned we will assume that the optimum stroke setting, Ψ_o , changes linearly with the disturbance. We can then define,

$$\frac{d\Psi_o}{dQ} = U \quad \ldots\ldots\ldots\ldots\ldots\ldots (6.27)$$

Now, if the rate of change of the disturbance is constant, we can say the the nett change in the stroke relative to the optimum setting is,in each cycle,

$$\Psi_Q + U \frac{dQ}{dt}\tau - \Psi_H = \Delta\Psi \quad \ldots\ldots\ldots\ldots (6.28)$$

To avoid possible confusion in the sign of each term in this expression it will be interpreted as if the modulus of each term has been taken, i.e. positive values will be assigned. That Ψ_Q is of opposite sign to Ψ_H ensures consideration of the condition of least progress per cycle in equation (6.28).

The effect of the disturbance in Ψ_Q is proportional to $\frac{dQ}{dt}$ and,at some value of $\frac{dQ}{dt}$,it will then be possible to identify that no nett progress is made towards the optimum when $\Delta\Psi = 0$.

We have an expression for Ψ_H in equation (6.17) which may be written,

$$\Psi_H = \frac{h\tau}{T} F_1 \quad \ldots\ldots\ldots\ldots\ldots (6.29)$$

where,

$$F_1 = \frac{4}{\alpha\tau}\left[\cosh\left(\frac{\alpha\tau}{4}\right) - 1\right] \quad \text{.....(6.30)}$$

Also we get Ψ_Q from equation (6.26) and can write this as,

$$\Psi_Q = \frac{G\tau}{g}\frac{dQ}{dt}F_2 \quad \text{.....(6.31)}$$

where,

$$F_2 = \frac{4}{\alpha\tau}\sinh\left(\frac{\alpha\tau}{4}\right) - 1 \quad \text{.....(6.32)}$$

On substituting into equation (6.28) and setting $\Delta\Psi = 0$ we can solve for $\frac{dQ}{dt}$ and get,

$$\frac{dQ}{dt} = \frac{\frac{h}{T}F_1}{U + \frac{G}{g}F_2} \quad \text{.....(6.33)}$$

This value of $\frac{dQ}{dt}$ represents the rate of change of disturbance at which no nett progress is made by the optimising system in tracking a moving optimum point. If the rate of change is greater than this value the system will retreat from the optimum point. The system will be at its best in this respect when the value of $\frac{dQ}{dt}$ given by equation (6.33) is a maximum and we now consider the choice of parameters to achieve this.

The factor $\frac{h}{T}$ is the rate of movement of the motor stroke due to the perturbation. This should be as large as possible to maximise $\frac{dQ}{dt}$. The performance of the speed control system on the transmission has been shown to be the limitation on this choice. The paramaters U, G, and g are defined by the performance curves of the system and are not open to adjustment. The factors F_1 and F_2 are both

functions of $\propto\tau$. In this the choice of τ, the period of the perturbation, is determined by the amplitude of the stroke perturbation and consideration of the action of the sampling filter. It remains to adjust $\propto$ i.e. $\frac{K}{T}g$. Again we have no control over g, the slope of the performance curve, so that $\frac{K}{T}$ becomes the design parameter.

The value of $\frac{K}{T}$ which maximises equation (6.33) depends on the values of U, G and g. The data necessary to obtain typical values are contained in the performance curves of Fig.(6.2). From these results curves of efficiency against load current have been drawn, as shown on Fig.(6.19), for constant values of motor stroke. Reference to the defining equations (6.7) shows that the slope of these curves is the parameter G. In this case the disturbance variable is identified with the load current, the input speed and the fluid temperature being constant. The slope value taken from the curves is an average value for which G = 9.4. A curve giving the optimum motor stroke as a function of the load current is also derived from Fig.(6.2) and appears as shown on Fig.(6.20). The slope of this curve gives the value of U as defined in equation (6.27). The value U = 0.25 is an appropriate choice. The remaining parameter g is the slope of the performance curves of Fig.(6.2) which varies, approaching zero as the maximum is reached. A typical figure for g on the steep part of the curves is 8% per unit stroke, but the value varies substantially with the stroke setting and the load.

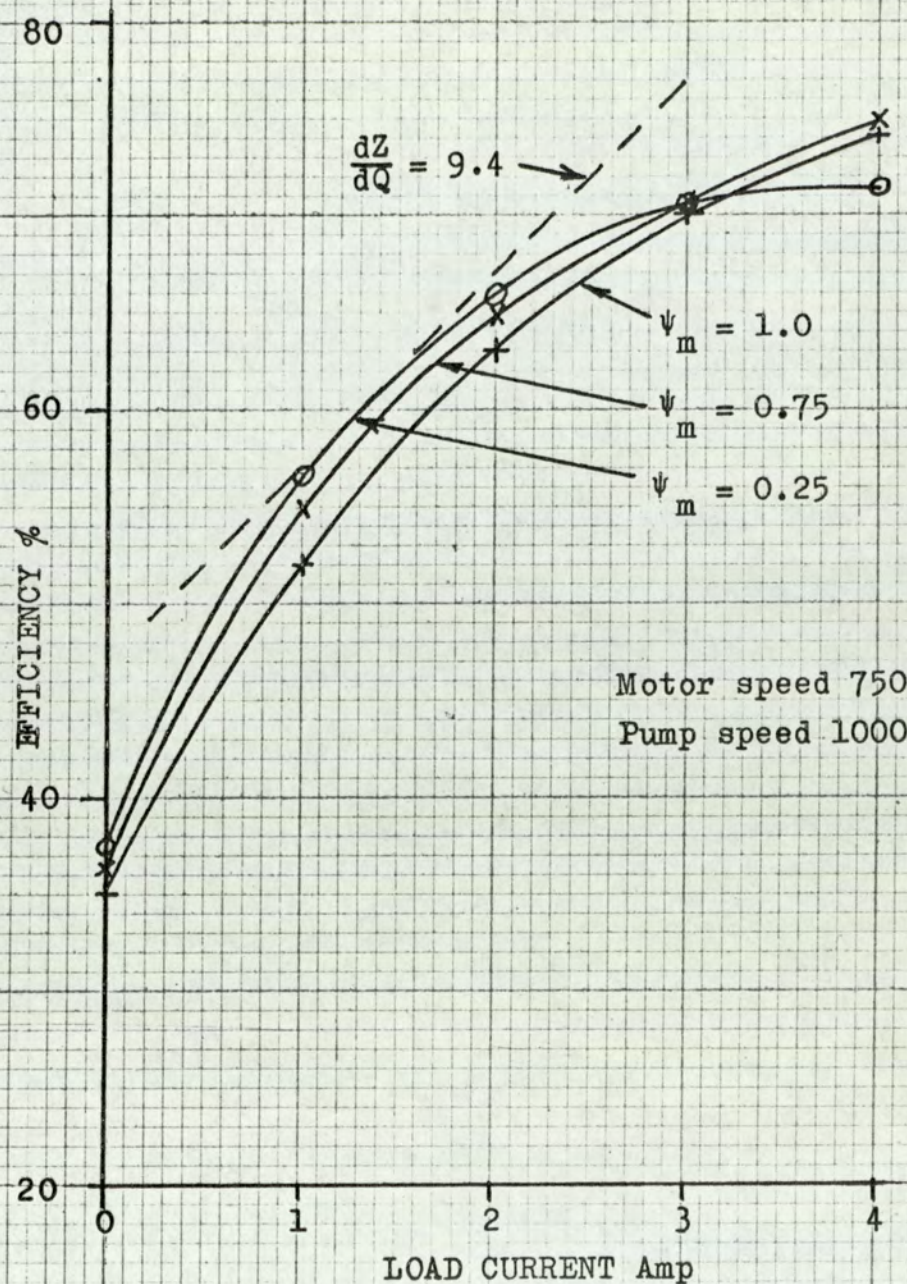

FIG.(6.19)
EFFICIENCY VARIATION AT CONSTANT STROKE

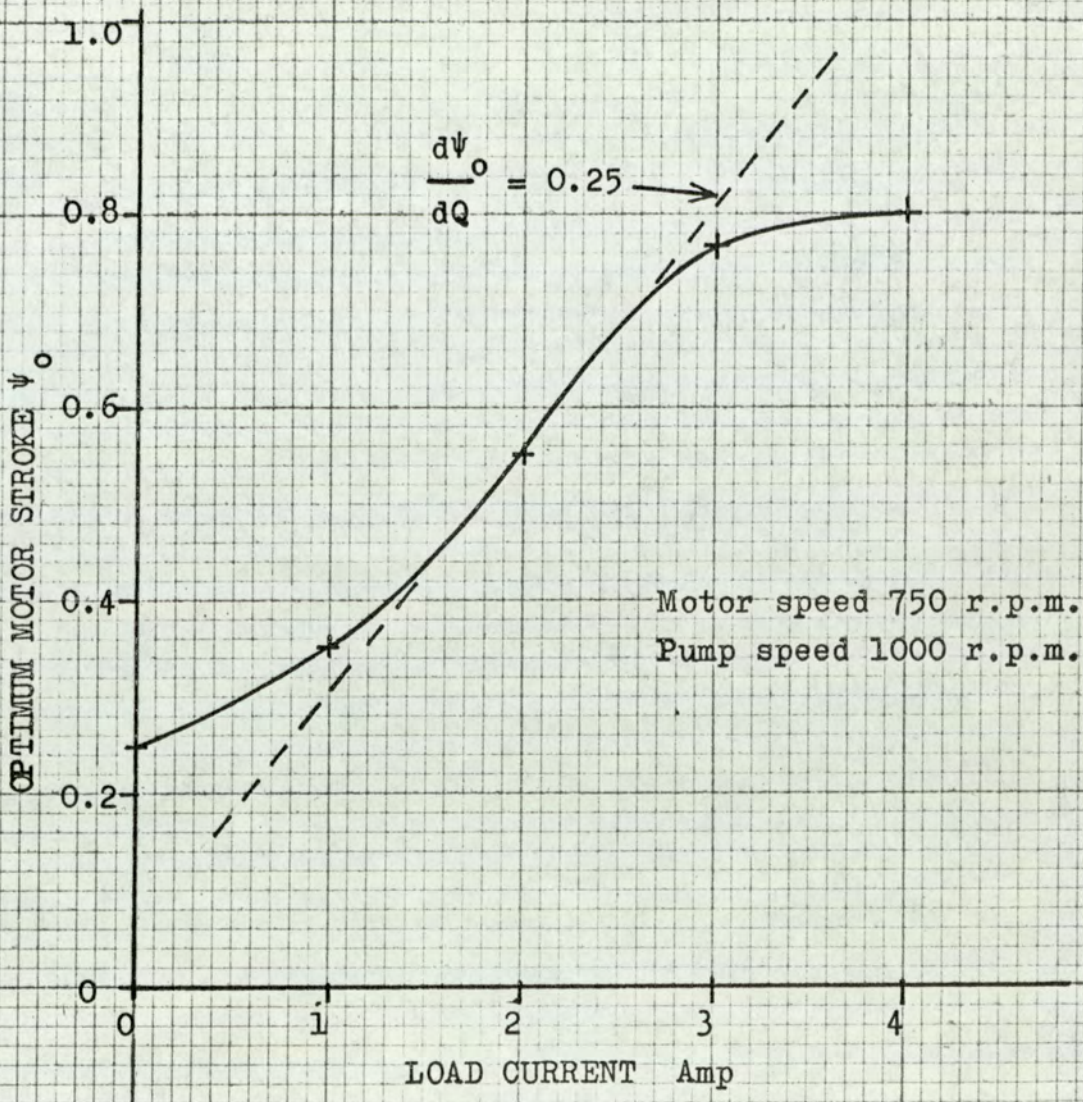

FIG.(6.20)
VARIATION OF OPTIMUM STROKE
WITH LOAD

The result of evaluating equation (6.33) as a function of $\frac{\alpha\tau}{4}$ is shown on Fig.(6.21) for several values of g. As expected the curves exhibit a maximum, the position of which varies with g. The way in which the maximum position changes is observed more clearly by plotting as shown on Fig.(6.22). To find an appropriate value of $\frac{K}{T}$ we observe that the slope of a line on Fig.(6.22) is,

$$\frac{\alpha\tau}{4\,g} = \frac{K}{T}\frac{\tau}{4} \qquad \ldots\ldots\ldots\ldots\ldots\ldots\ldots\ldots(6.34)$$

A straight line approximation is therefore constructed on Fig.(6.22). The line is drawn through the origin because α must be zero when g is zero. The slope of this line is 0.2. When the period of the perturbation τ is 10 sec. we then get $\frac{K}{T} = 0.08$.

This analysis has been based on the choice of the optimum value of the gain factor $\frac{K}{T}$, to enable the system to track effectively the changes in the position of maximum efficeiency. It has been assumed that the changes are due to variations in the load on the transmission. The efficiency also changes with the input speed and the temperature of the hydraulic fluid. It has not been possible to assess reliably the effect of changes in the fluid temperature but the effect of changing the input speed can be observed. For instance the performance curves of Fig.(6.2) are taken with an input speed of 1000 r.p.m. and the effect of raising the speed to 1500 r.p.m. can be seen on moving to Fig.(6.3). The general effect of increasing the input speed is to reduce the efficiency at any given stroke setting. The effect

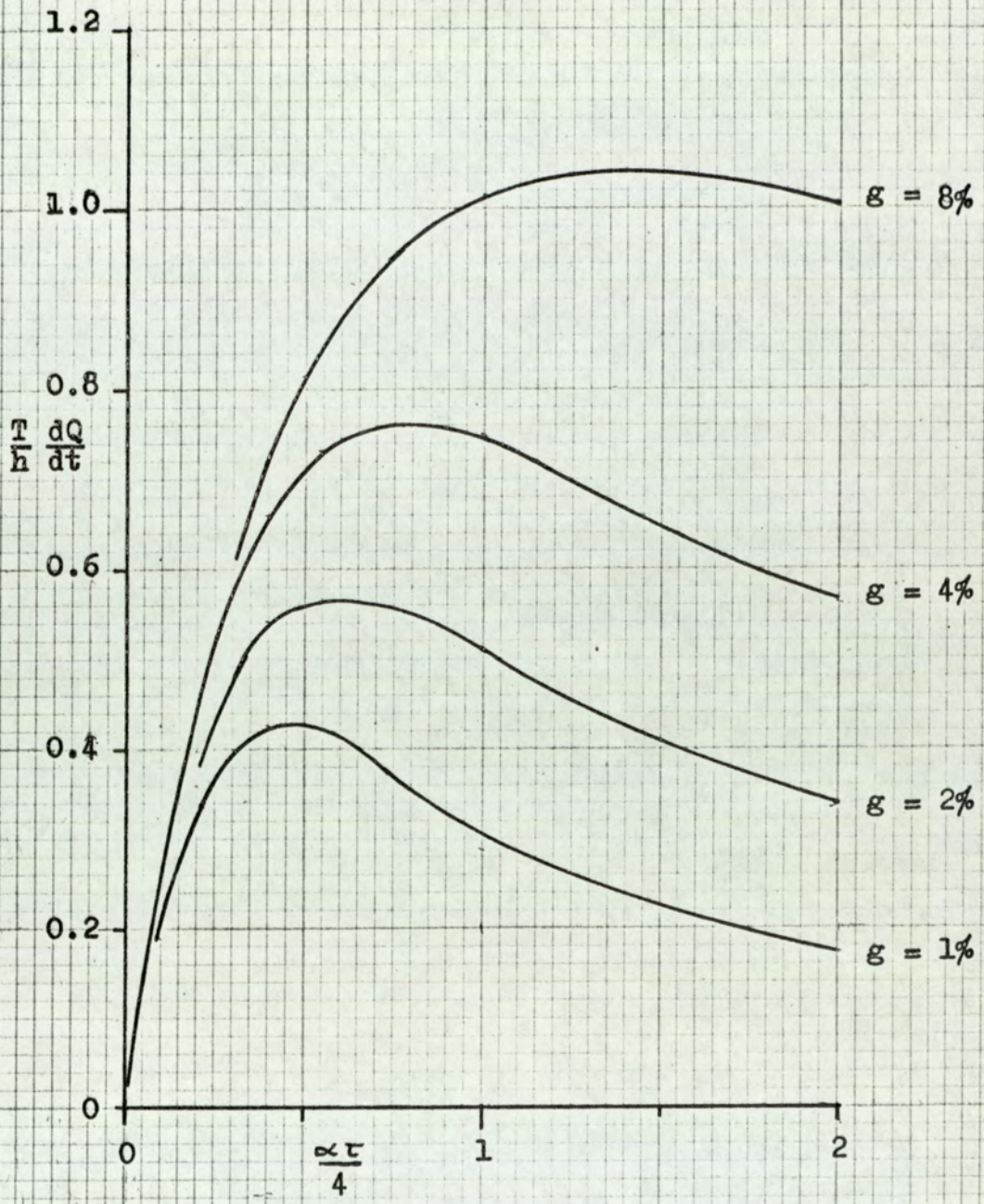

FIG.(6.21)
SOLUTION OF EQUATION (6.33)

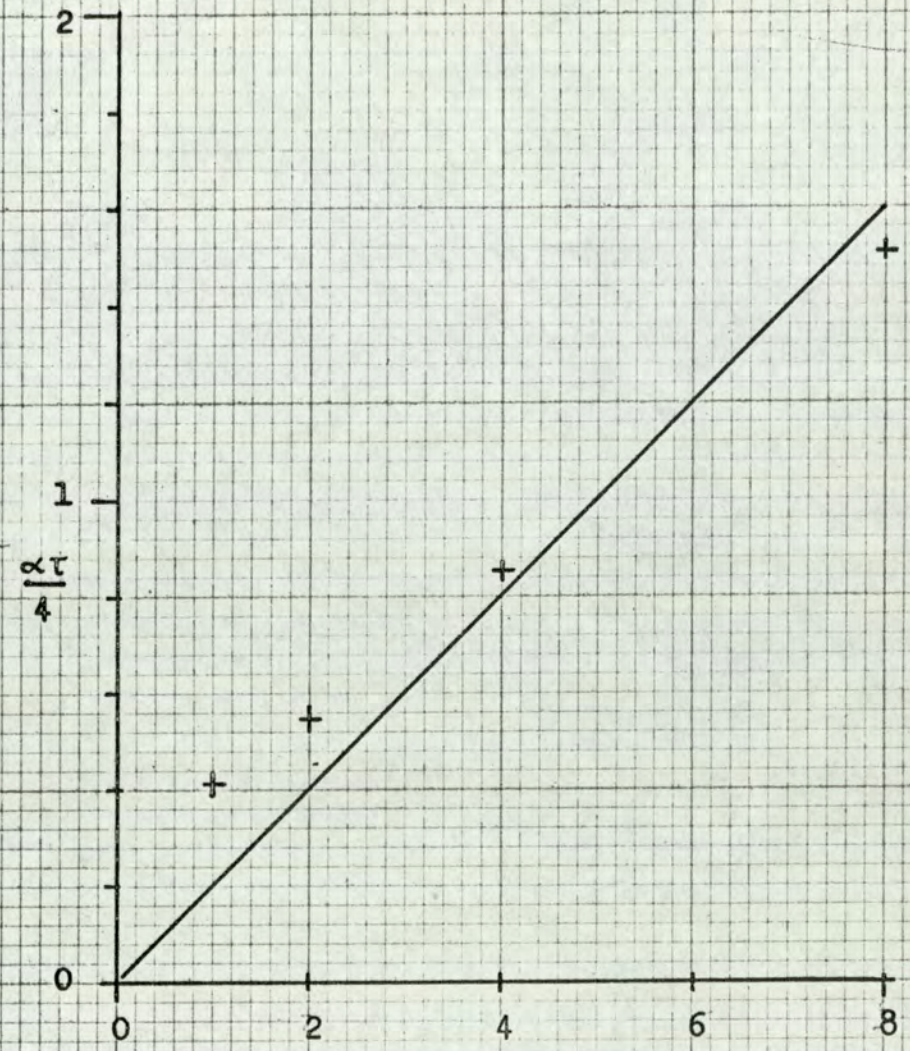

FIG.(6.22)

OPTIMUM VALUE OF $\frac{\alpha\tau}{4}$

on the position of maximum efficiency is slight with a tendency to move towards a lower stroke setting.

To analyse this case the disturbance Q is identified with the input speed change. The value of U is then small because the maximum position changes only slightly. In equation (6.33) the effect of reducing U is to move the point of maximum $\frac{dQ}{dt}$ to a lower value of $\frac{\alpha\tau}{4}$. This would lead in turn to a lower value of $\frac{K}{T}$. When both the input speed and the load are changing together it would be necessary to arrive at a compromise in the choice of the gain setting. In this case the further study was restricted to the condition of load variation and the system was set up to give the optimum gain for this case.

6.9 THEORETICAL PERFORMANCE.

With the value of the gain factor $\frac{K}{T}$ established in the preceding section we can assess the performance which the system is likely to exhibit.

Firstly it has been shown that the system will make greater progress towards the maximum point when the load is increasing than when it is decreasing. In neither case, however, is there any change in the controlled variable once the slope of the performance curve has become zero, i.e. at the maximum point. As the maximum point changes due to the load change the system will fall behind. When the load is decreasing the lag will be greater than when the load is increasing. In a progressive change of load the system will eventually lag to a point where the slope of the performance curve is sufficient for the progress

to equal the rate of movement of the maximum point. This is the situation for which the optimum choice of $\frac{K}{T}$ has been made, taking the worst condition of decreasing load. We can therefore use the results of Section (6.8) to decide what rate of change of load the system can tolerate.

With the value of $\frac{K}{T}$ set to give the straight line approximation on Fig.(6.22), the value of $\frac{T}{h}\frac{dQ}{dt}$ which satisfies equation (6.33) is as shown on Fig.(6.23). Typically from this curve we see that when g is 8%, $\frac{T}{h}\frac{dQ}{dt}$ is 1.0 . The value of $\frac{h}{T}$ is the rate of movement of the motor stroke due to the perturbation. This has been set to 0.011 s^{-1}. If therefore the rate of change of load is maintained at 0.011 amp per second the system will lag to a point where the slope of the performance curve is 8%. This value of slope is about the maximum seen on the performance curves so that the system must depart considerably from the maximum point. It should be noted that the rate of change of load which this represents is as low as 13% of full load per minute.

A second feature of the performance is the wave-form of changes in the motor stroke. This wave-form is the result of the superposition of the perturbation wave-form and the fluctuations in the output of the demodulator. The analysis of Section (6.6) has shown how

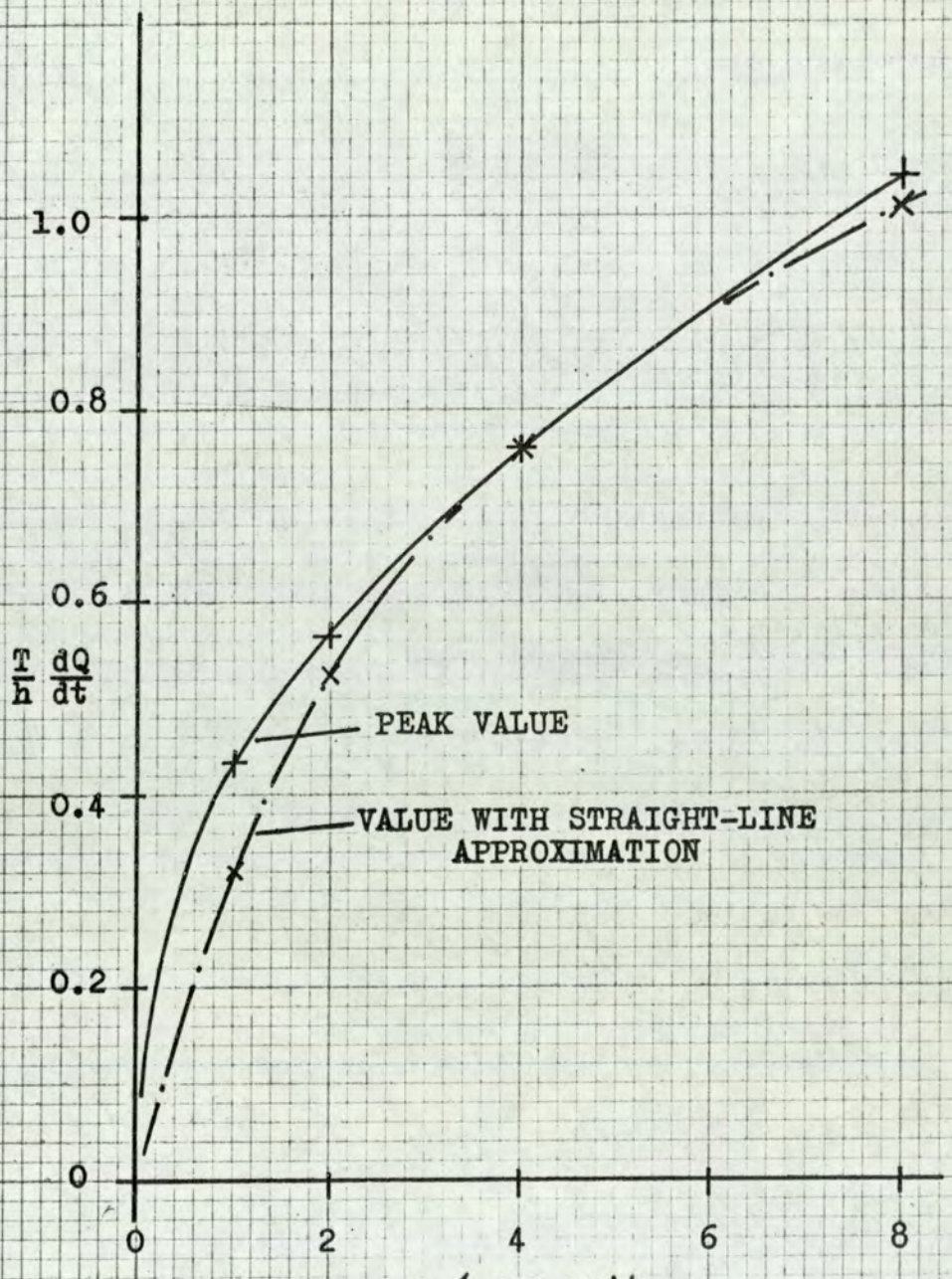

FIG.(6.23)
LIMITING VALUE OF $\frac{T}{h}\frac{dQ}{dt}$

changes of stroke may be evaluated over one cycle, when the operating conditions are fixed. Taking the slope of the performance curve g as 4% and the value of $\frac{K}{T}$ as calculated in Section (6.8), we get $\frac{\alpha\tau}{4}$ as 0.8 . This leads to the wave-form shown on Fig.(6.24). Here the ordinates are expressed in ratio to the maximum excursion of the stroke under the influence of the perturbation alone. It is then clear that the progress made at the end of the cycle is comparable with the excursion due to the perturbation. This measure of progress is comparatively large. The extent of the progress will vary with the slope of the performance curve as shown by equation (6.17). Over the range of values expected the progress is approximately proportional to the slope g.

6.10 CONSTRAINTS.

The range over which the motor stroke may be adjusted is limited. It is desirable to limit the minimum setting to about 0.25 as the dynamical performance of the transmission deteriorates considerably below this value. The maximum stroke setting is limited in two respects. There is clearly an absolute limit set by the design of the motor but the need to maintain control of the output speed may prevent this limit being reached. This latter restriction comes into effect when the motor speed is higher than the pump speed. In which case the motor stroke must always be less than the pump stroke. The limit of the motor stroke is then

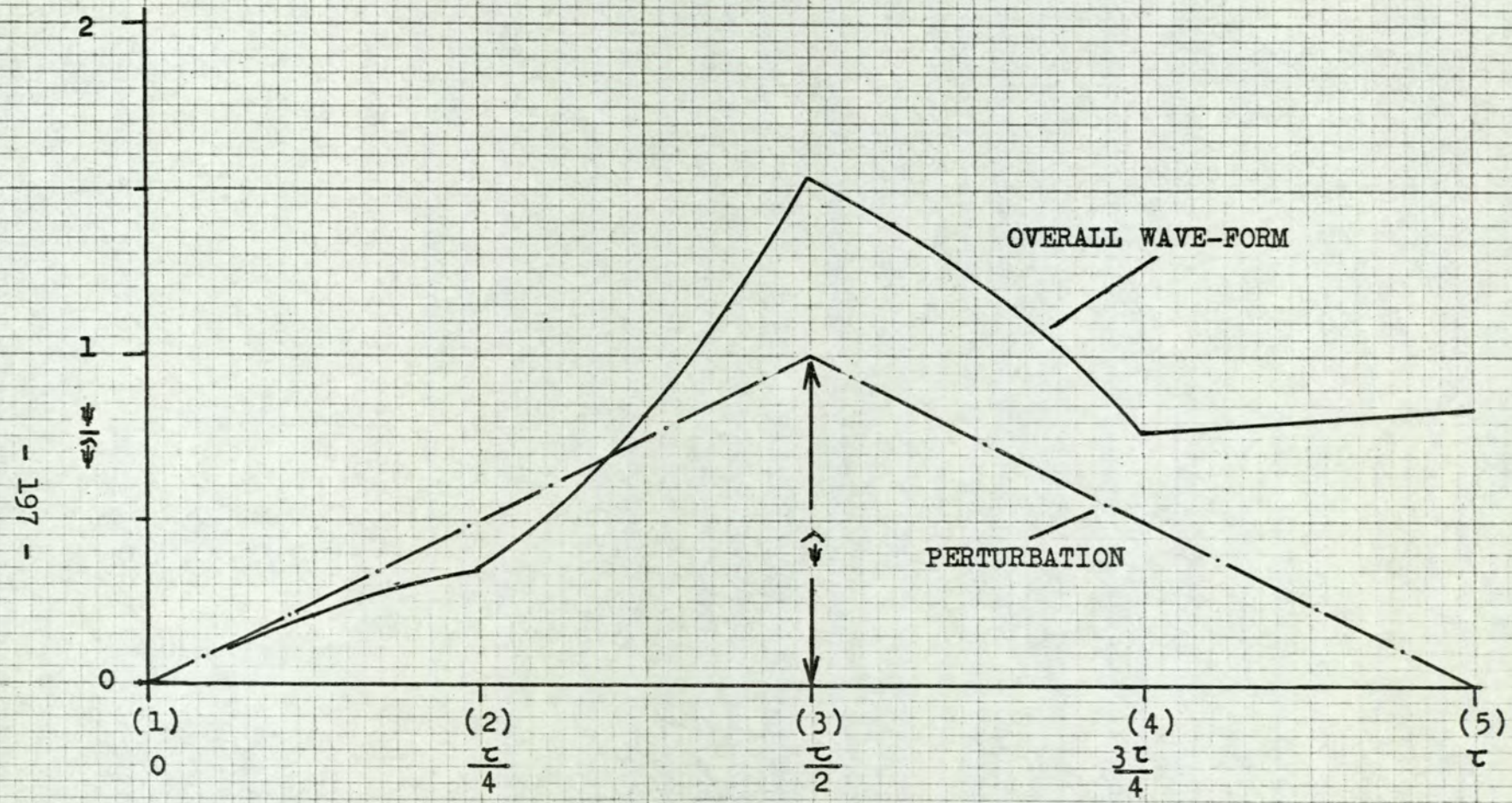

FIG.(6.24)

TYPICAL WAVE-FORM OF STROKE ADJUSTMENT

reached when the pump is set to maximum stroke.

To prevent the optimising system driving the motor stroke beyond these limits it is necessary to override the control action. In this case a limit switch circuit was designed to switch off the input to the integrator when the limit is reached. The connection is restored when the perturbation changes direction, causing the system to move away from the limit.

6.11 CHOICE OF PERTURBATION PERIOD.

The rate of movement of the motor stroke is limited by the dynamical response of the speed control system on the transmission. This means that the period and the amplitude of the perturbation are related i.e. if the amplitude is increased the period must be extended proportionately. Consideration of the operation of the sampling filter has lead to the conclusion that, for best performance, the sampling period should be as short as possible. The sampling period is half the perturbation period, so there is a need to keep the amplitude as small as possible. A small amplitude of perturbation is also of advantage in view of the action of the limit circuit in applying the constraints. The extent to which the mean stroke setting can approach the limit is determined by the perturbation amplitude, as the limit circuit will operate on the peak of the wave-form.

However, too great a reduction of the amplitude can have an adverse effect. In Section (6.8) it was shown that for optimum performance of the optimising

system, the loop gain should be set to make $\frac{K\tau}{T}$ equal to 0.8 . As the period τ is made shorter the gain factor $\frac{K}{T}$ then becomes larger. In effect as the amplitude of the perturbation is made smaller the loop gain must be increased to maintain the optimum performance. The limit to the loop gain is set by the measurement noise. When the gain is high the noise will produce large fluctuations in the motor stroke, since it is amplified by the gain factor $\frac{K}{T}$.

To assess these conflicting requirements analytically would require a detailed knowledge of the statistical characteristics of the measurement noise. In this case a qualitative assessment was made leading to a choice of 10 seconds for the perturbation period and an amplitude of 2.5% in the stroke movement.

7 IMPLEMENTATION OF THE OPTIMISING SYSTEM.

The considerations outlined in Section (6) have established the general principles on which the design of the optimising system should be based. In this section the further developments are discussed, leading to the design of the equipment.

7.1 GENERAL SYSTEM ARRANGEMENT.

A block diagram of the system is shown on Fig.(7.1). The operation may be understood by reference to Fig.(7.2) which shows the wave-forms generated. The timing wave-form S_o is of twice the frequency required in the perturbation. A bistable multivibrator B_1 is arranged to trigger on the positive excursion of the timing wave-form. The state of this bistable is shown by the wave-form S_1. The output of the bistable is used to operate a relay RL1, with change-over contacts. These contacts select the two-state input to the integrator and thereby generate the perturbation. As the integrator is an a.c. servo-system with 50 Hz carrier, the signals ϕ_1 and ϕ_2 are equal in amplitude and of opposite phase.

In the lower part of the block diagram the efficiency Z is introduced as a performance measure. It is converted into a d.c. voltage signal by means of a potential divider. This is a rotary potentiomater which is driven by

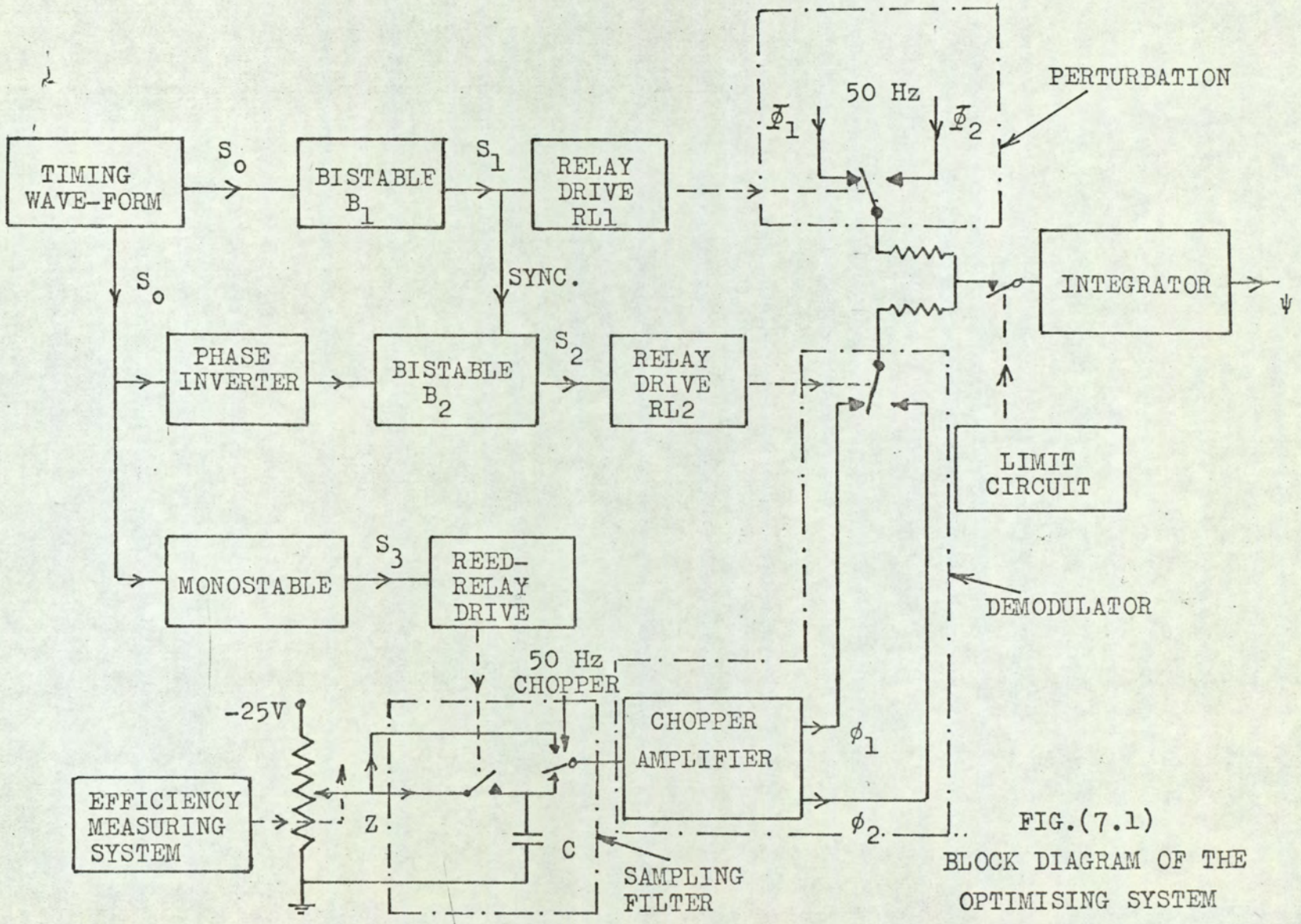

FIG.(7.1)
BLOCK DIAGRAM OF THE OPTIMISING SYSTEM

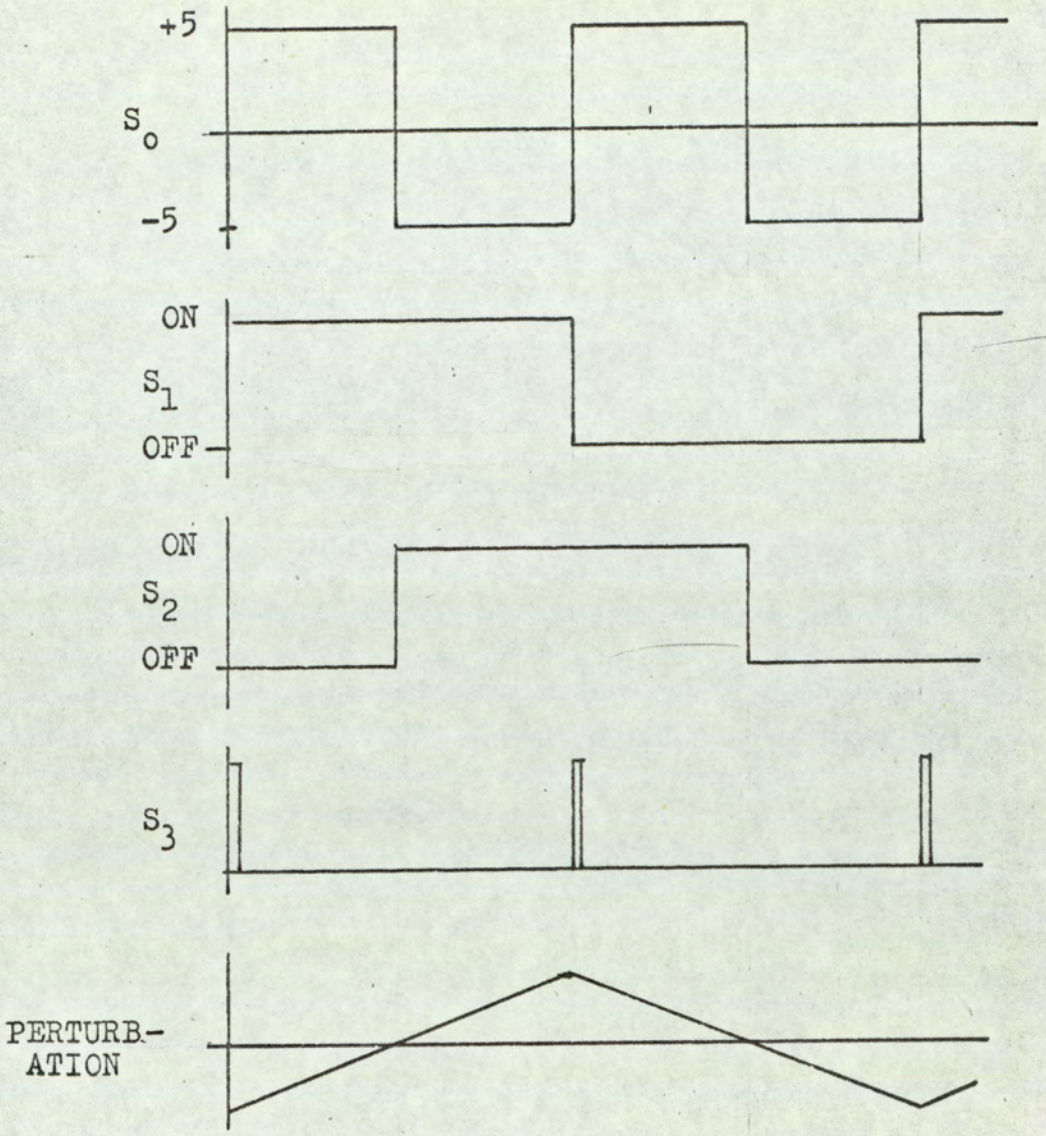

FIG.(7.2)
SEQUENCE OF WAVE-FORMS

the efficiency measuring system (See Section (5) of the Appendix). The efficiency signal is sampled in the sampling filter. A reed switch is closed for a short period to allow the storage capacitor C to charge to the wiper potential. This capacitor operates as a zero-order hold.

Following the sampling operation it is necessary to generate a signal proportional to ΔZ, the difference between the stored value Z_o and the current value of Z. This signal is then applied to the integrator, through the demodulator. It is necessary to modulate the ΔZ signal at 50 Hz, since the integrator is to operate with a 50 Hz carrier signal. This is conveniently done with a chopper relay as shown. In the demodulator the chopper amplifier provides two output signals of equal amplitude but of opposite phase. These signals are switched to the integrator alternately by the demodulating switch.

Control of the demodulating switch must be such that it changes state precisely half way between the points of reversal of the perturbation. To achieve this a second bistable multivibrator B_2 is triggered in step with the negative excursions of the timing wave-form. Its state is shown by the signal S_2. Synchronisation of the two bistable circuits B_1 and B_2 is essential. When first switched on the circuits may take up either state at random. Sometimes the state signal S_2 would then appear shifted in phase by half a cycle

with respect to S_2. This would cause the optimising system to move down the performance curve, rather than up it. To avoid this a synchronising pulse is transferred from bistable B_1 to ensure that S_2 is always off when S_1 makes the excursion from off to on.

The sampling switch is arranged to operate twice in each cycle at the points of reversal of the perturbation wave-form. A mono-stable multivibrator controls the sampling duration, and is triggered directly from the positive excursions of the timing wave-form, as shown by the signal S_3.

Constraints limiting the range of movement to the motor stroke are operated by a limit circuit. This breaks the connection to the integrator when the limit is reached.

The particular features of this system which are important design considerations are as follows. The use of a timing wave-form of twice the required perturbation frequency simplifies the design. This also ensures that the phase relationship between the switches controlling the perturbation and the demodulator is precisely maintained. Another feature is the choice of a 50 Hz a.c. carrier system for the integrator and this has two advantages. Firstly it is possible to construct an integrator with very low drift, since d.c. drift in the amplifiers is not then important. Secondly the drift problem is also reduced in the amplification of the signal from the sampling filter. Drift at this point in the system is not of such fundamental importance as drift in the integrator.

If the integrator tends to drift, by moving progressively further in one direction of the perturbation than the other, the system must compensate by moving off the position of maximum efficiency. Drift in the integrator must therefore be avoided as a fundamental requirement. On the other hand a similar drift in the amplifiers of the demodulator is not so important, provided that it affects both the direct and phase inverted signals equally. This is because the drift appears before the demodulating switch. Its effect would be to add a further square wave-form to the input of the integrator, 90° out of phase with the two-state signal giving the perturbation. This only adds unnecessarily to the fluctuations in the controlled variable and does not affect the hill-climbing action. A drift affecting one channel of the demodulator is important however, and has similar effect to the drift in the integrator. It is therefore necessary to ensure that any drift affects both channels equally and this requirement could present a major problem as the changes in the efficiency are small and hence the gain must be large. It is doubtful whether the requirements for low drift could be met without moving to an a.c. carrier system.

In the following sections the detailed arrangements of the various sub-units of this general system are described.

7.2 DETAIL OF THE INTEGRATOR.

The arrangement of the integrator system is shown in Fig.(7.3). A 50 Hz, two phase servo-motor M is controlled through a high gain a.c. amplifier A. The amplifier is of similar form to that described in Section (5.4) of the Appendix but with one fewer stages of amplification. The motor is directly coupled to an a.c. tachometer-generator G, which provides the speed feedback signal. The motor is also geared down to drive four rotary potentiometers as the output elements. The system may be operated in either of two modes.

Position Controlled Mode.

In this mode a position control loop is set up by using one of the potentiometers on the output shaft. The tachometer signal is introduced to stabilise the system. In this way the output shaft is made to follow the movement of the position reference potentiometer.

This arrangement was used when it was required to set a prescribed value of the motor stroke in the static tests. An external input point is included so that a sinusoidal oscillation could be introduced for frequency response testing.

Integrating Mode.

In this case the input to the amplifier is switched to select the combined perturbation and optimising control signals. This input signal is balanced against the output of the tachometer-generator. There is no problem of instability and the feedback signal is made as

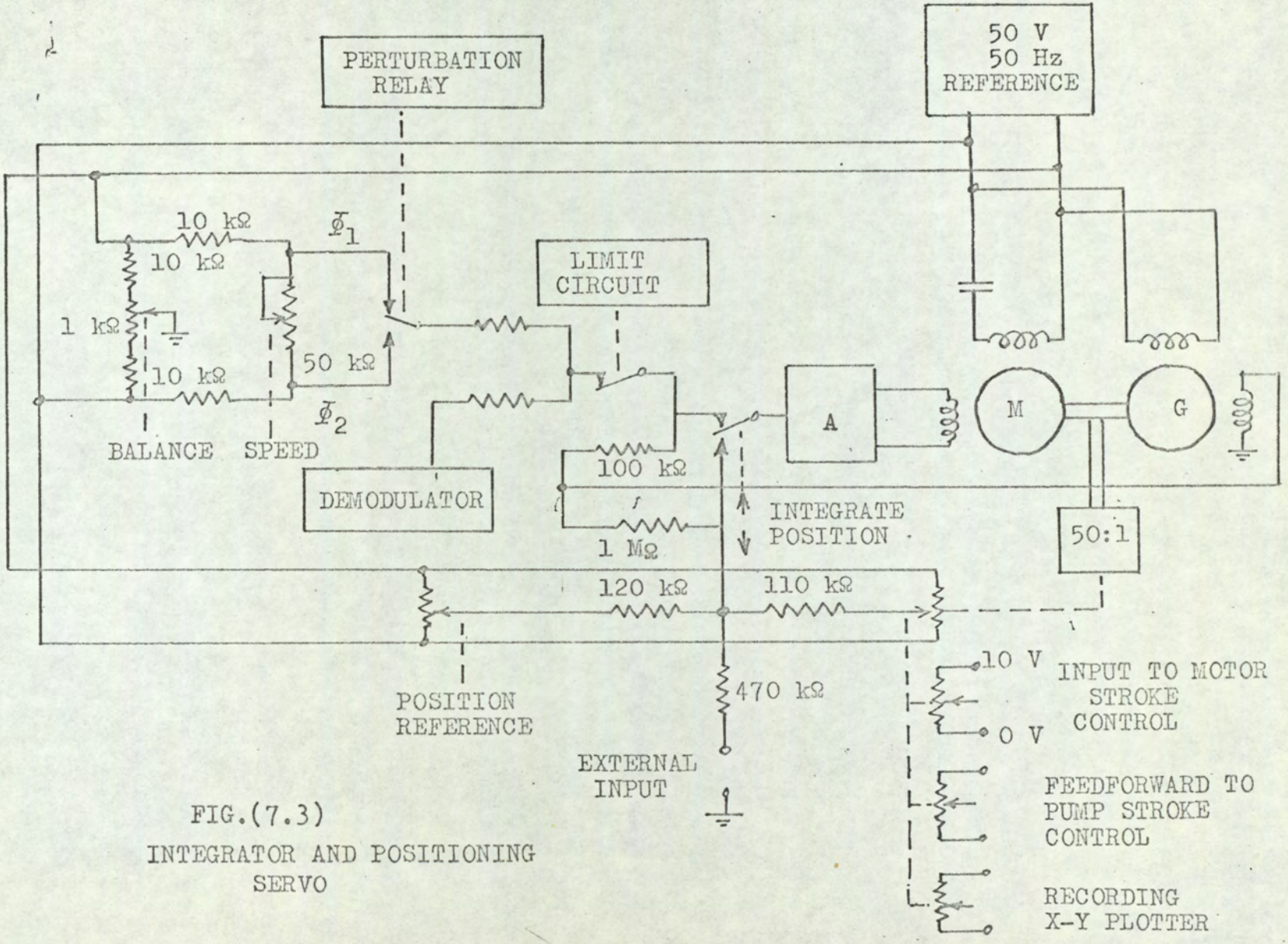

FIG.(7.3)

INTEGRATOR AND POSITIONING SERVO

large as the loading limit on the generator will allow. This ensures low drift and linearity in the response. A fine balancing adjustment is provided in the perturbation source to allow the signals ϕ_1 and ϕ_2 to be set for perfect symmetry. This ensures that the mean position of the integrator does not change when the perturbation is applied.

The limit circuit operates a switch as shown. The action is to open the input circuit, leaving the tachometer feedback signal connected. This has the effect of producing a rapid deceleration of the integrator motor due to the feedback action.

7.3 LIMIT CIRCUIT.

It is required to limit the range of motor stroke adjustment as a constraint on the optimising system. The minimum stroke limit is taken as 0.25, while the maximum limit is reached when either the motor stroke or the pump stroke reaches its maximum value. Micro-switches were set up to detect the limiting conditions. Two were set to be operated by the output shaft of the integrator, one at the full stroke position and the other at 0.25 stroke. The full stroke setting on the pump was detected by a micro-switch operated by the stroke setting servo-piston.

Following from the analysis of the response to the perturbation is Section (6.6), we can say that the

system can only move towards a limit when the perturbation is directed towards the limit. This however neglects the effect of noise in the performance signal.

A simple form of limit circuit is shown in Fig.(7.4). A change-over contact, on the relay controlling the perturbation, is used in conjunction with the normally closed contacts of the micro-switches. The operation is then as follows. When the perturbation is switched to cause a movement towards the maximum stroke position, the circuit is completed through the maximum stroke switches on the pump and motor. If either switch is opened the integrator will stop. With the perturbation switched to give a movement towards the minimum stroke limit, the minimum stroke switch completes the circuit. It should be noted that the maximum stroke switches cannot normally be open at the same time as the minimum stroke switch. The complete cycle of operations on reaching a limit is then as follows. When the perturbation is moving the system towards maximum stroke the maximum stroke switches will operate to stop the integrator when the limit is reached. Once stopped the switches will remain open and the system will retain this state until the perturbation is switched into the reverse direction. The change-over switch then moves to allow the integrator to be activated through the minimum stroke switch. The system should then move away from the limit.

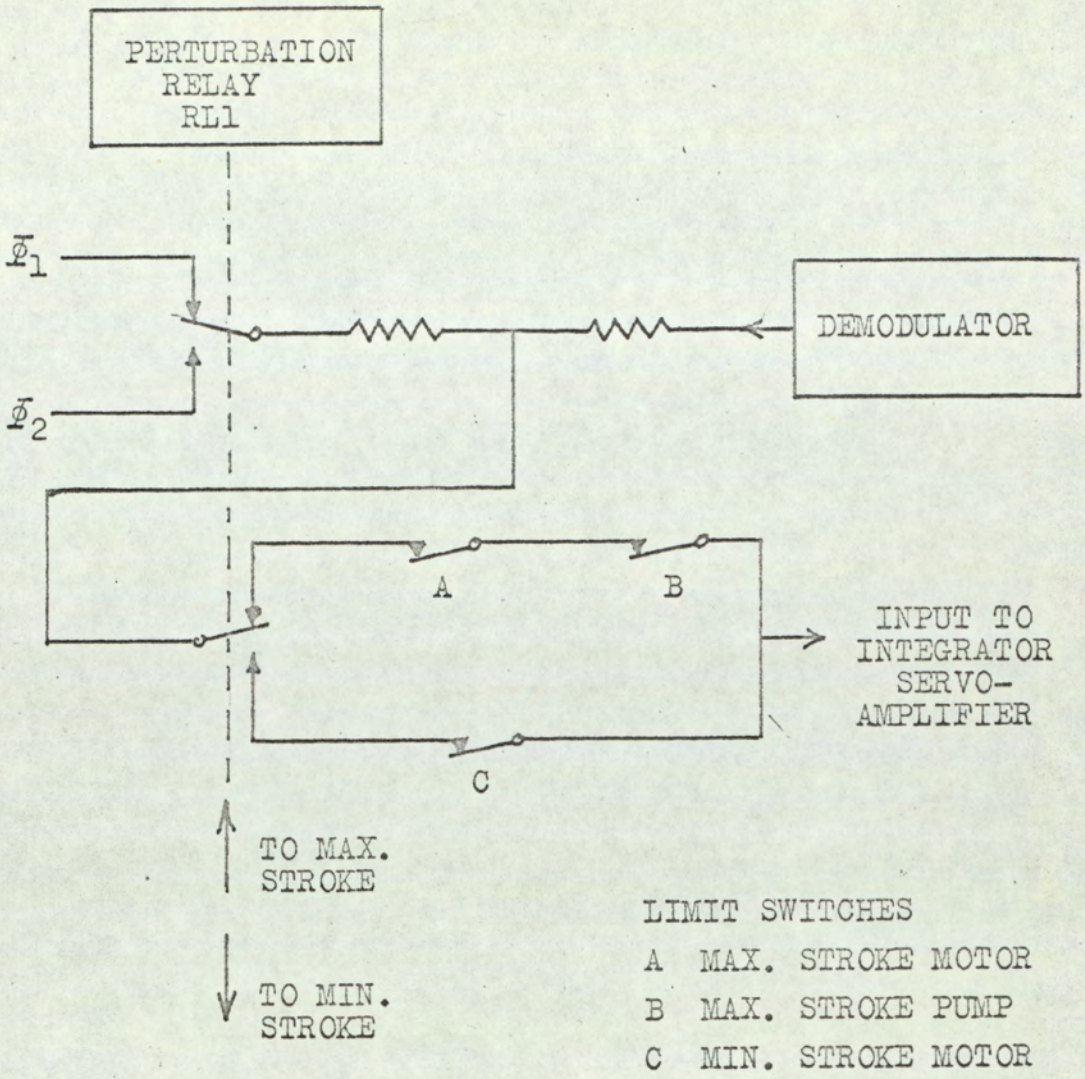

FIG.(7.4)

LIMIT SWITCH CIRCUIT

This simple form of limit circuit can be defeated by noise in the performance signal. The noise may be due either to the disturbance applied to the transmission system, or to measurement noise. If the total effect of the noise were large enough to overcome the perturbation, the system may continue to move past the limit in the opposite direction to the perturbation. However the limit circuit will ensure that the perturbation cannot reinforce this movement and eventually the system must move away from the limit. To make a limit circuit capable of preventing any movement beyond a limit requires an unreasonable increase in the complexity and this simple form of circuit was adopted in this case.

A further consideration is the reliability of the circuit. It is a feature of the circuit described that it will fail safely to the most commonly expected switch fault. It arises when switches are used to transmit small signals that the switches may fail to make contact due to small surface defects. A fault of this type will leave the system able to move in one direction only and it will continue until stopped by the limit switch. The alternative form of circuit using normally open contacts would fail allowing the system to continue beyond the limit.

The results of a test on the limit circuit is shown in Fig.(7.5). The system was operated with the perturbation alone applied to the integrator. On starting the sequence at (a) the perturbation drove the stroke to the maximum limit at (b). The movement would normally have continued to (c) but

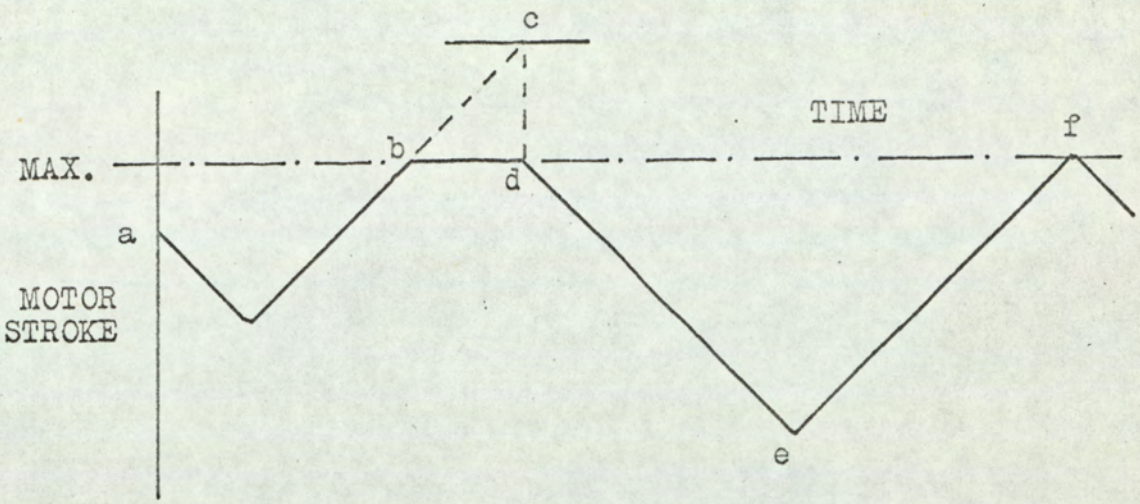

FIG.(7.5)

OPERATION OF THE LIMIT CIRCUIT

the limit circuit operates to stop the integrator at (b). The change-over of the perturbation relay at (d) re-connects the integrator and the system moves away from the limit. This movement carries the stroke away from the limit by an amount equal to the normal traverse of the perturbation. The return movement therefore brings the stroke up to the limit at (f). In the absence of any control action from the optimising loop, the limit circuit places the mean motor stroke at a distance equal to the amplitude of the perturbation from the limit. Thus the amplitude of the perturbation determines the extent to which the limit may be approached.

7.4 MULIIVIBRATOR CIRCUITS.

Two basic types of multivibrator circuit are required to implement the arrangement of Fig.(7.1). The two bistable circuits B_1 and B_2 are basically the same and there is one monostable circuit. It was convenient to design special purpose circuits for these rather than to use standard logic elements.

Bistable Circuit.

The circuit designed for this purpose is shown in Fig.(7.6). It is intended to trigger with a positive going 10 Volt step applied to any of the input points A, B and C. Triggering at A and C will drive T_1 into the "on" state while the action at B is to bring T_2 "on". In bistable B_1 the requirement is to divide the timing wave-form frequency by two and this

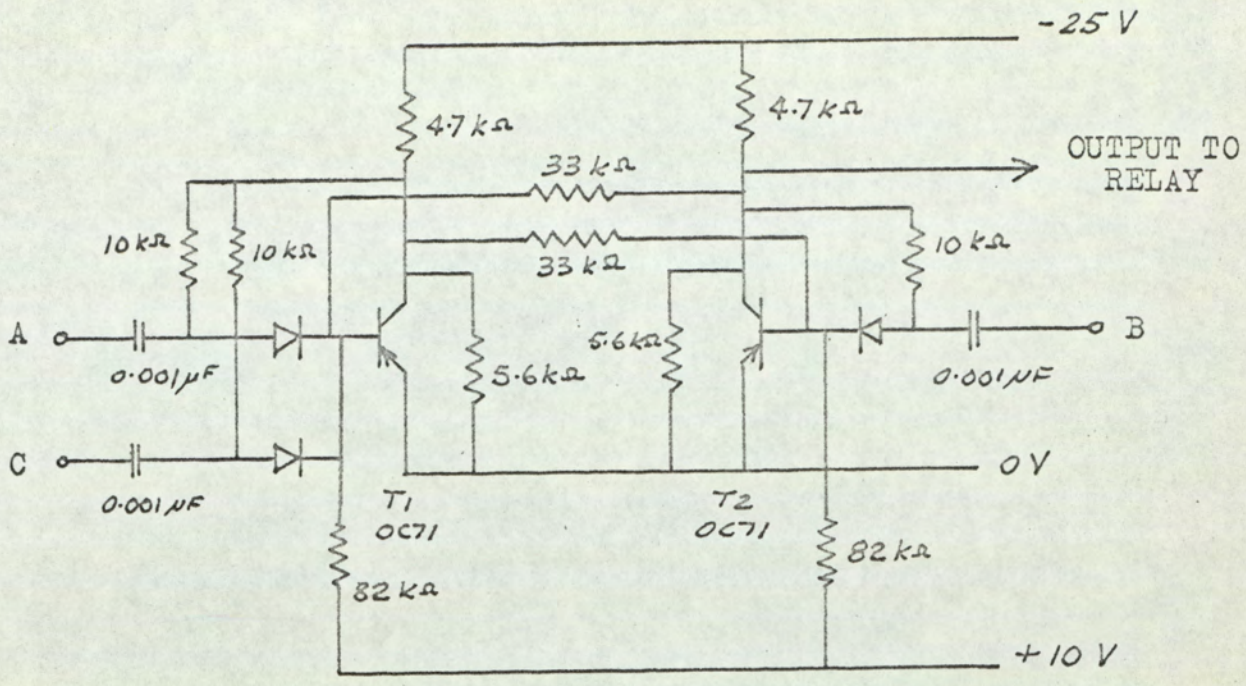

FIG.(7.6)

BISTABLE CIRCUIT

is achieved by applying the timing wave-form to A and B together. The bistable B_2 also receives the timing wave-form at A and B, but in addition the output of B_1 is connected to C to provide the synchronising action.

Monostable Circuit.

The circuit is shown in Fig.(7.7). A positive-going 10 Volt step applied to the trigger input causes the transistor T_2 to turn "on" for 10 ms, before recovering to the normally "off" state.

Subsidiary Circuits.

Three subsidiary circuits are required as shown on Fig.(7.8).

7.5 CHOPPER AMPLIFIER.

Considerable care is required in the design of this amplifier in conjunction with the storage capacitor. The amplifier is required to produce two output signals of precisely the same amplitude but of opposite phase. The amplitude must be proportional to the difference between the voltage held on the storage capacitor and the varying voltage value representing the efficiency. The feature which requires particular attention is the need to retain the voltage held on the storage capacitor over a long period. The storage capacitor must charge completely during the sampling interval of 10 ms and then hold the charge over a further 5 seconds. To give rapid recovery during the sampling interval we require a small value of capacitance, but a large

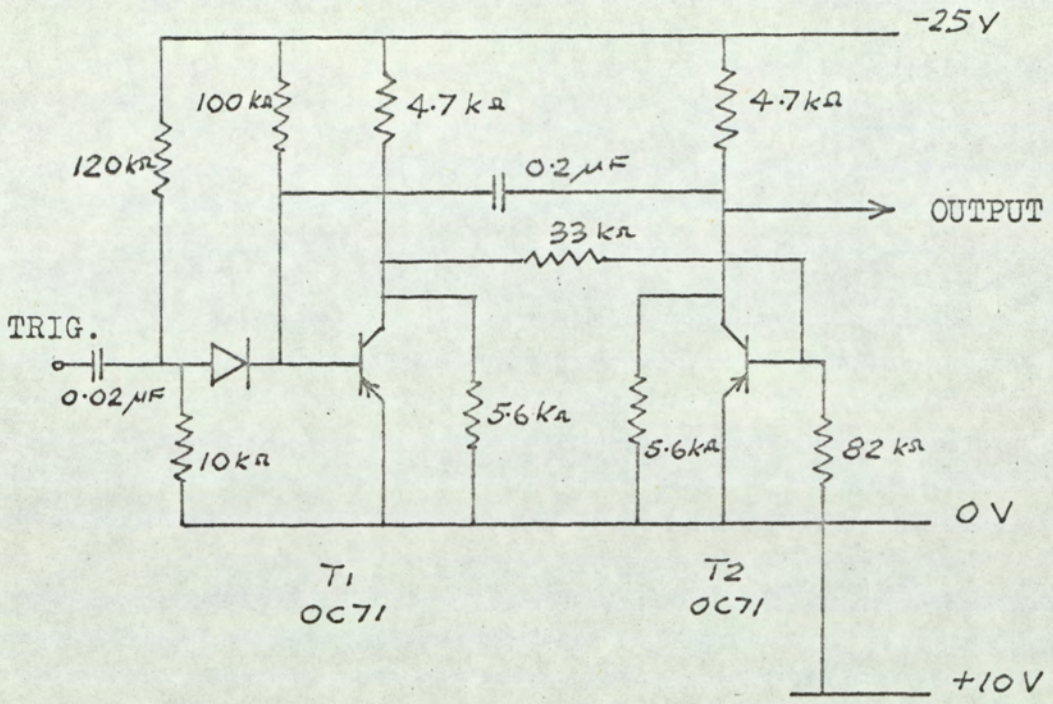

FIG.(7.7)

MONOSTABLE CIRCUIT

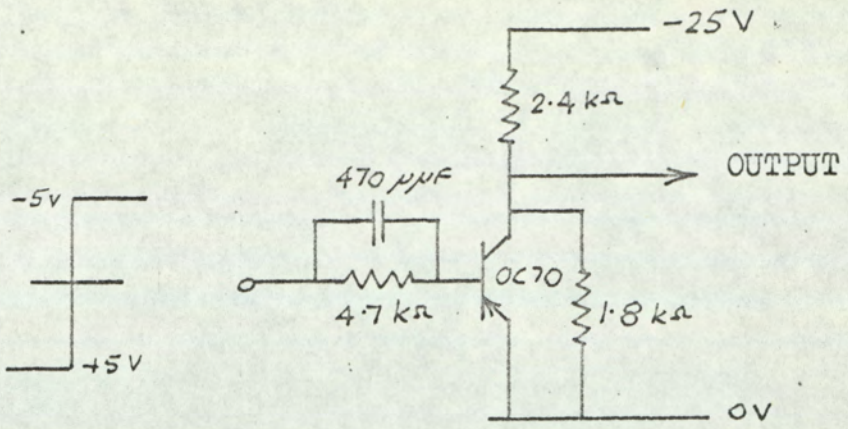

(a) PHASE INVERTER

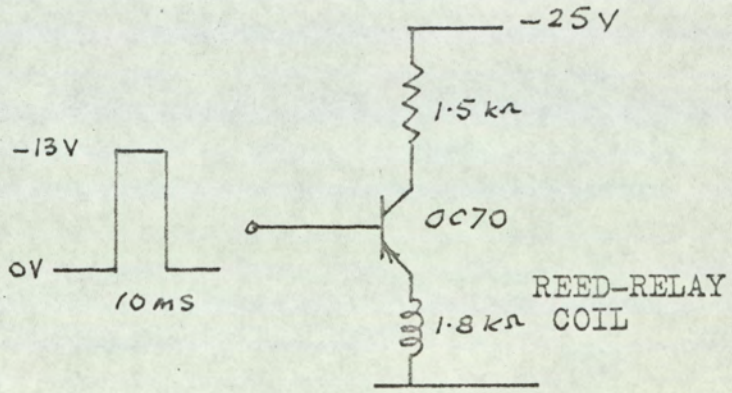

(b) REED-RELAY DRIVE

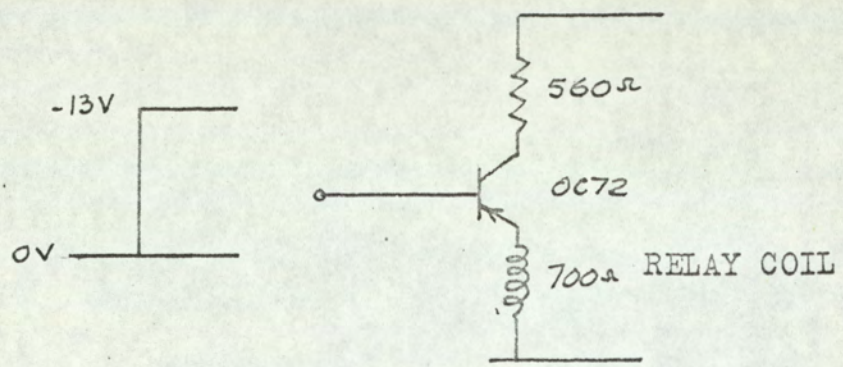

(c) RELAY DRIVE

FIG.(7.8)
SUBSIDIARY CIRCUITS

value is of advantage in maintaining the stored voltage. A satisfactory compromise can only be achieved by ensuring that the charge lost by the capacitor during the 5 second holding period is reduced to a minimum. This requires that the input current taken by the chopper amplifier must be very low.

The effect of the input current of the chopper amplifier is to cause a progressive change in the voltage held on the storage capacitor. This will cause a corresponding increase in the amplitude of the signals ϕ_1 and ϕ_2. It is important to note that both signals are affected in the same way and that the drift appears before the demodulating switch. The change-over action of the demodulating switch will cause a reverse of the phase of the signal applied to the integrator, half way through the holding period. If the drift continues at constant rate over the complete perturbation cycle the effect on the output of the integrator will average to zero. This drift cannot therefore produce a shift from the optimum setting of the motor stroke. But there will be large fluctuations in the stroke setting. This will place an undesirable demand on the speed control system of the transmission.

To avoid this it was decided to design to hold the stored voltage within 0.1% over the 5 second period. The allowable current drain due to the chopper amplifier may then be estimated. We note that the storage capacitor is connected to the amplifier through the chopper switch for half the holding period. With a storage capacitor of 1 μF holding

20 Volt this requires that the input current be less than 8×10^{-9} Amp. .

With this in mind the arrangement of Fig.(7.9) was adopted. It is necessary to adjust the operating point of the valves to reduce the grid current to a minimum. The input circuit is d.c. coupled as this ensures a minimum loss of charge from the storage capacitor. The d.c. level of the grids can then vary by 25 Volt but in this circuit the change in the operating point of the valves is slight, and the minimum grid current setting is maintained. Equality in the amplitudes of the output signals ϕ_1 and ϕ_2 is ensured by the symmetry of the circuit. A further important consideration in the design of the amplifier is the need for linearity. When the operating conditions in the transmission are changing there may be a large change in the efficiency value over the holding period. The system can only operate correctly if this change is amplified linearly. There is also the possibility of a fluctuation in the measures efficiency value due to measurement noise. The overall requirement is that linearity must be maintained up to the largest change in the efficiency signal which may appear during the holding period. To estimate this change we proceed as follows.

It was shown in Section (6.9) that the maximum rate of change of load which the system can tolerate will be of the order of 0.011 Amp per second. The change of efficiency which this would produce during the holding period is given by $G \frac{dQ}{dt} \frac{\tau}{2}$. With τ = 10 s

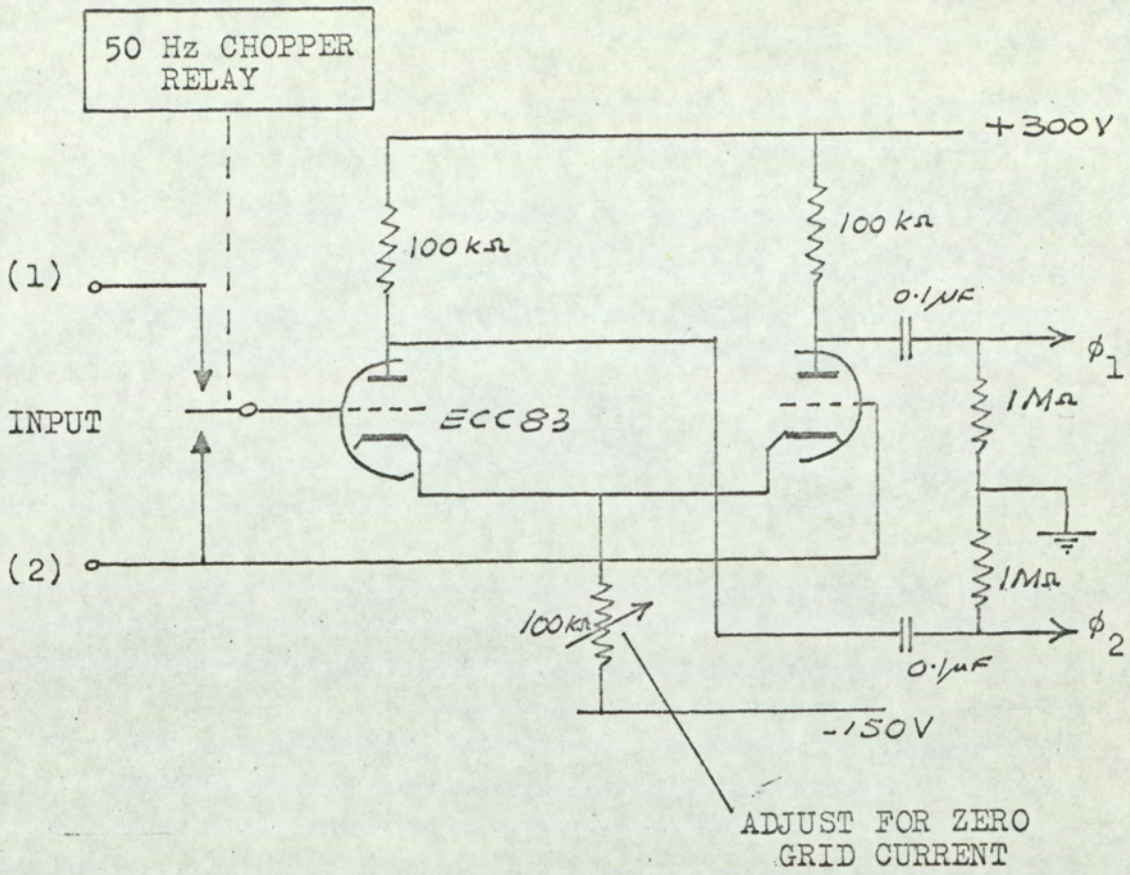

FIG.(7.9)

CHOPPER AMPLIFIER

and G = 9.5 % per Amp we get a change of 0.5 %. The wave-form of stroke changes due to the control action was also evaluated in Section (6.9) and is shown on Fig.(6.24). The maximum change of stroke over the interval between sampling instants is of the order of three times the amplitude of the perturbation. When the amplitude is 2.5% and the slope of the performance curve is 4% we calculate the change of efficiency to be 0.3%. Allowance must also be made for the measurement noise and this would suggest that the total linear range of 2% efficiency change would be adequate. This is not difficult to achieve with the circuit used and the linear range available was found to be in excess of 20%. Infact the linear range of the integrator is the limiting feature and it was found that the overall system was linear up to at least 7% change of efficiency, which is adequate in this case.

It is necessary to recognise that the output signals derived from the amplifier are of approximately square wave-form. In passing this wave-form on to the integrator it is possible that the harmonic components would adversely affect the integrator. The response of the integrator is not significantly affected in this case and additional filtering was considered unnecessary. The integrator responds linearly to the fundamental component of the input and the gain of the chopper amplifier is therefore assessed in terms of the fundamental component of its output wave-form.

The phase of the fundamental component should coincide with that of the signal from the tachometer generator of the integrator. There is a lag in the chopper relay which gives the amplified signal carrier about 10^{o} phase shift and this is small enough to be of no effect.

7.6 GAIN SETTING FOR THE CONTROL LOOP

The analysis of Section (6.8) has fixed the required value of the gain factor $\frac{K}{T}$ as 0.08 . This figure represents the combined gain of the chopper amplifier and the integrator. It defines the rate of change of the motor stroke for 1% change of efficiency. The section of the control loop which is to provide this gain factor is indicated on Fig.(7.10). Regarding the gain of the chopper amplifier as fixed, it is necessary to allocate a value to the summing resistor R.

The gain of the integrator may be defined in terms of the current input required at the summing junction to give unit output speed in the stroke movement. This was found to be 4.55×10^{3} $(\text{Amp sec})^{-1}$. If A is the gain of the chopper amplifier, giving the ratio of r.m.s. voltage output at 50 Hz to the percentage change of efficiency, the overall gain becomes,

$$\frac{\dot{\psi}}{\Delta Z} = 4.55 \times 10^{3} \frac{A}{R} \qquad \text{.....(7.1)}$$

This must be set to the required value of $\frac{K}{T}$. The gain A was found to be 1.8 Volt and this leads to the value 100 kΩ as the nominal value of R.

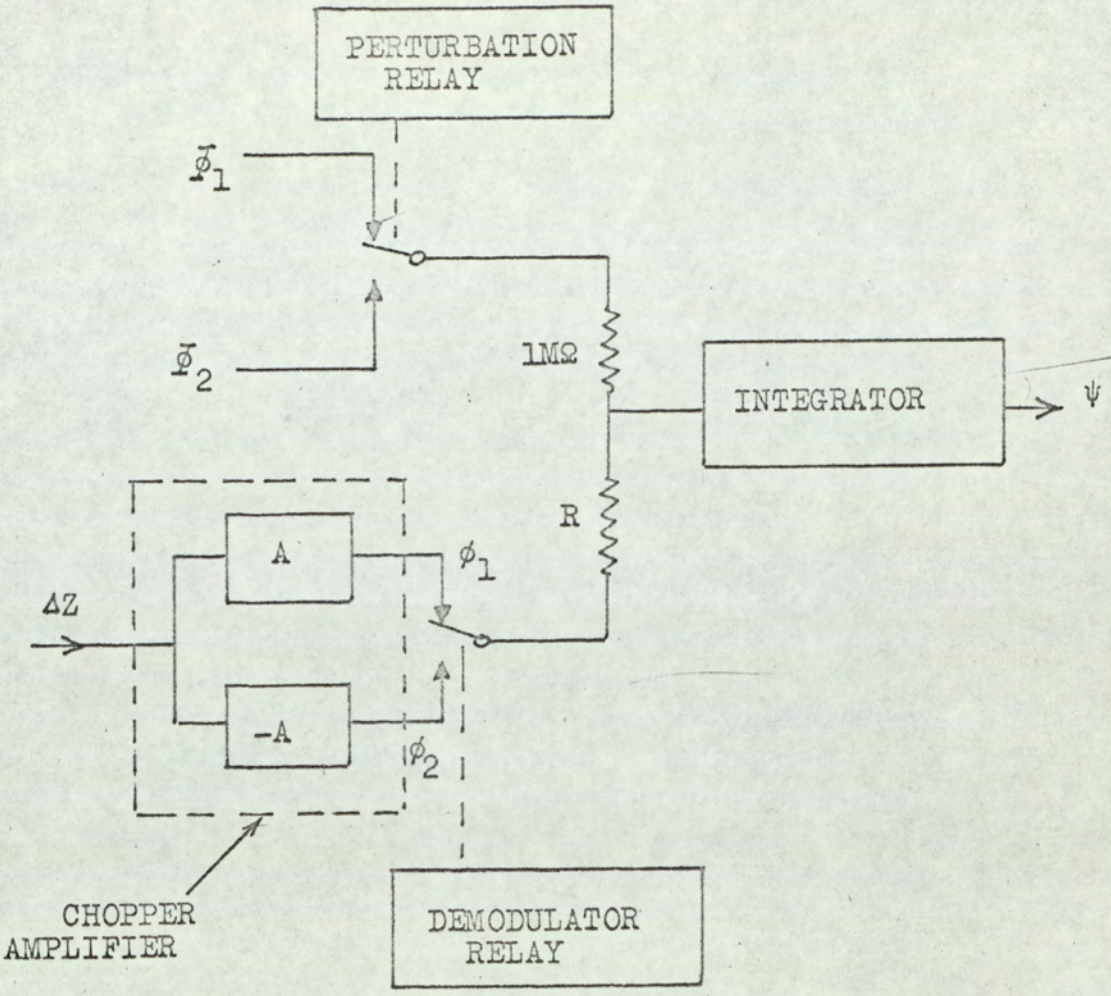

FIG.(7.10)

SUMMATION OF PERTURBATION AND OPTIMISING SIGNALS

7.7 SETTING UP PROCEDURE.

To ensure that the optimising action will carry the system towards the maximum efficiency, it is necessary to set the correct phase relationship between the demodulating switch and the perturbation switch. There is a possibility of 180° phase error in this setting and the effect of this would be to make the system move towards the minimum efficiency. The phase setting is achieved by the appropriate wiring of the relay contacts. A test was devised to check this as follows.

The system is operated without the transmission running, the efficiency measuring system is then inoperative. When the optimising loop is connected the motor stroke movements follow the perturbation. If then a manual change is made in the efficiency signal this alters the pattern of stroke movements. The effect of increasing the efficiency signal should be to reinforce the movement produced by the perturbation. When the perturbation has increased the stroke above the mean position an increase in the efficiency signal must move the mean position in the direction of increased stroke.

With the system operating in this way it is also possible to test the action of the chopper amplifier and storage circuit. In this test confirmation was obtained that the correct gain setting had been achieved and that drift had been adequately reduced.

7.8 OPERATING CHARACTERISTICS OF THE SYSTEM.

Two sets of tests were conducted to provide an assessment of the operating characteristics of the system. One test sequence was made with fixed operating conditions in the transmission, i.e. with the load torque and the input speed fixed. The other tests were implemented with the load changing.

7.8.1 FIXED OPERATING CONDITIONS.

It was required to observe how the system moved in reaching the maximum point on a stationary performance curve. To do this the motor stroke was set initially away from the maximum efficiency point, the optimising loop was then closed and the resulting motion recorded.

As a basis of comparison the stroke movements were first recorded with the perturbation acting alone, that is with the optimising loop open. The result is shown on Fig.(7.11).

A series of tests were made with different values of load. With the load current set to zero, the stroke movement from an initial setting at maximum stroke is shown on Fig.(7.12). A second test under the same conditions gave the result shown on Fig.(7.13). In each case there is an overall movement towards a lower stroke setting, as the point of maximum efficiency is close to the minimum stroke position. Although the trend is the same in the two records there are differences in detail, due to the effect of the measurement noise. This random variation, combined

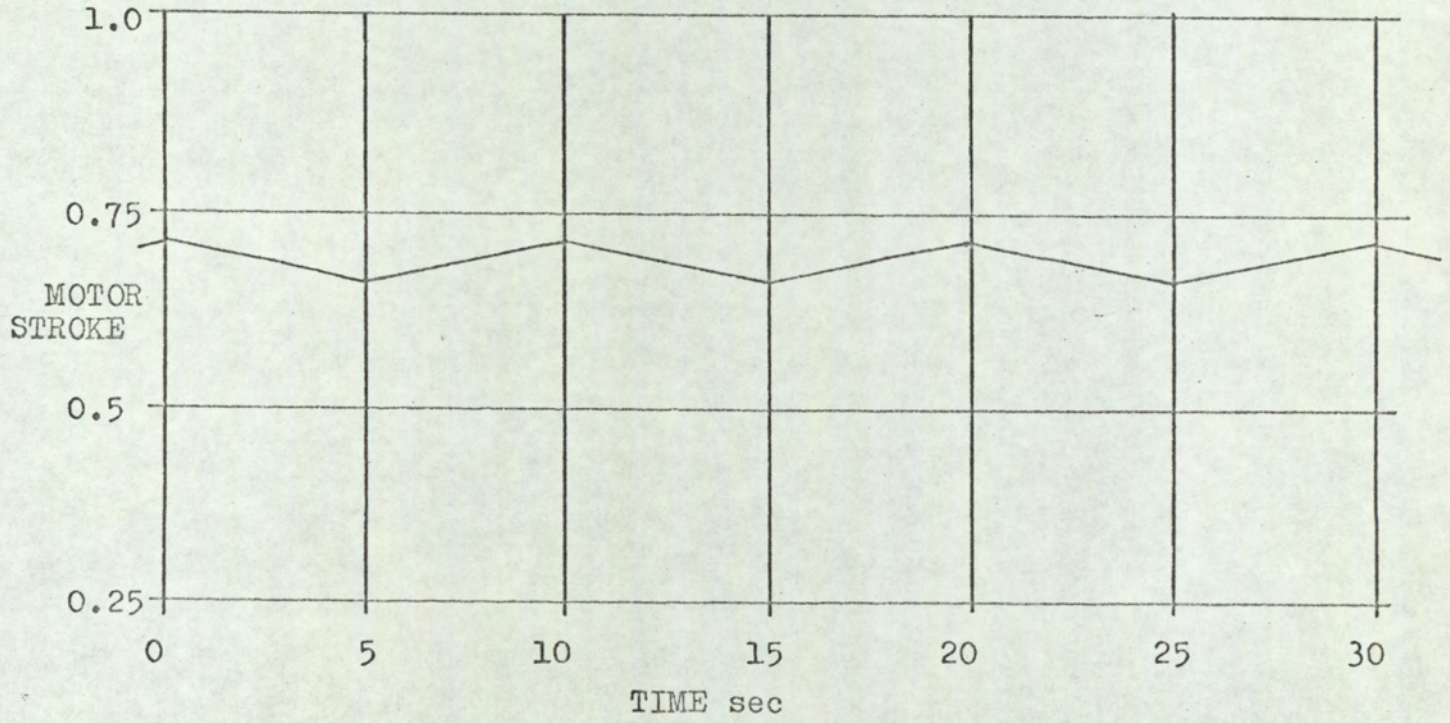

FIG.(7.11)

PERTURBATION WAVE-FORM

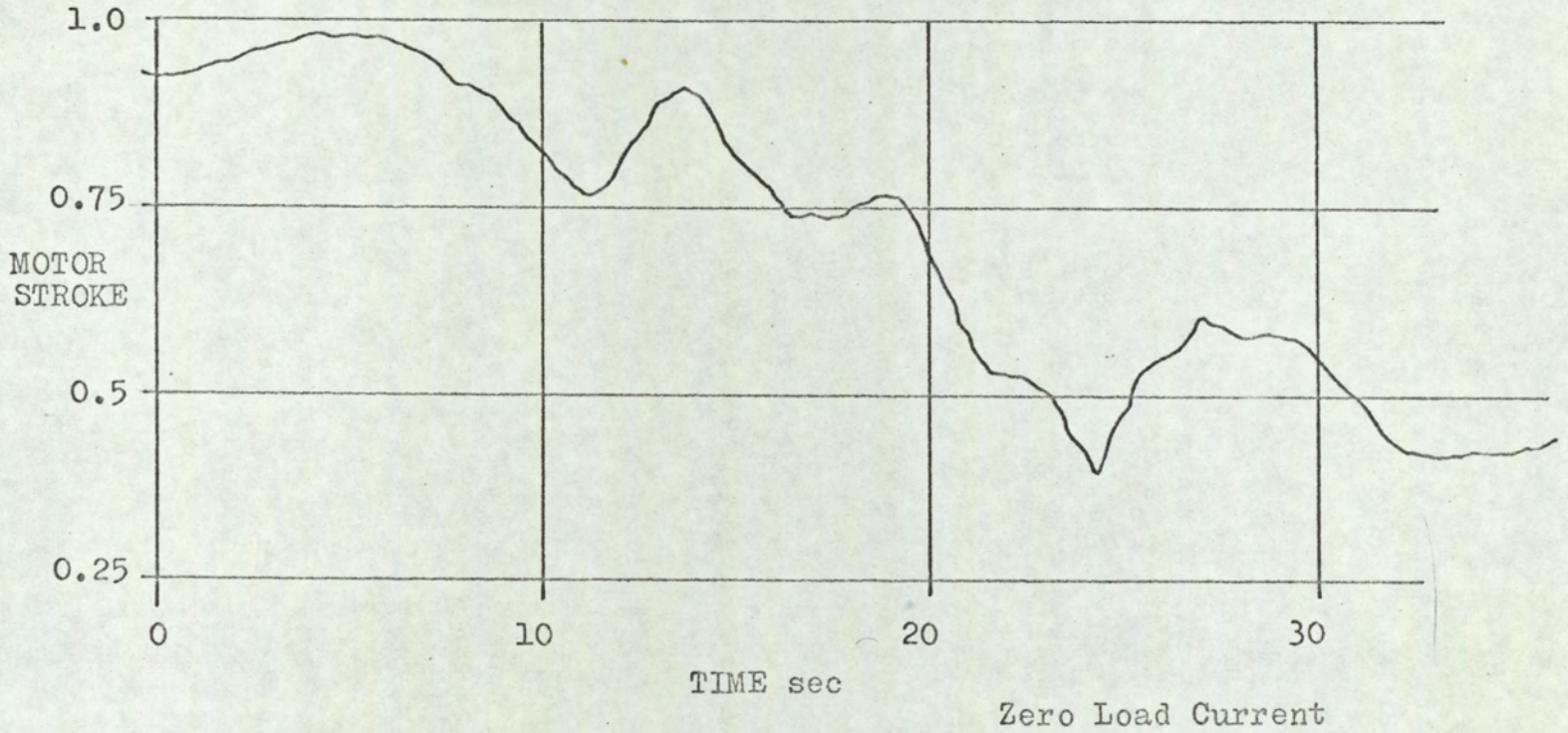

FIG.(7.12)
OPTIMISING TRANSIENT

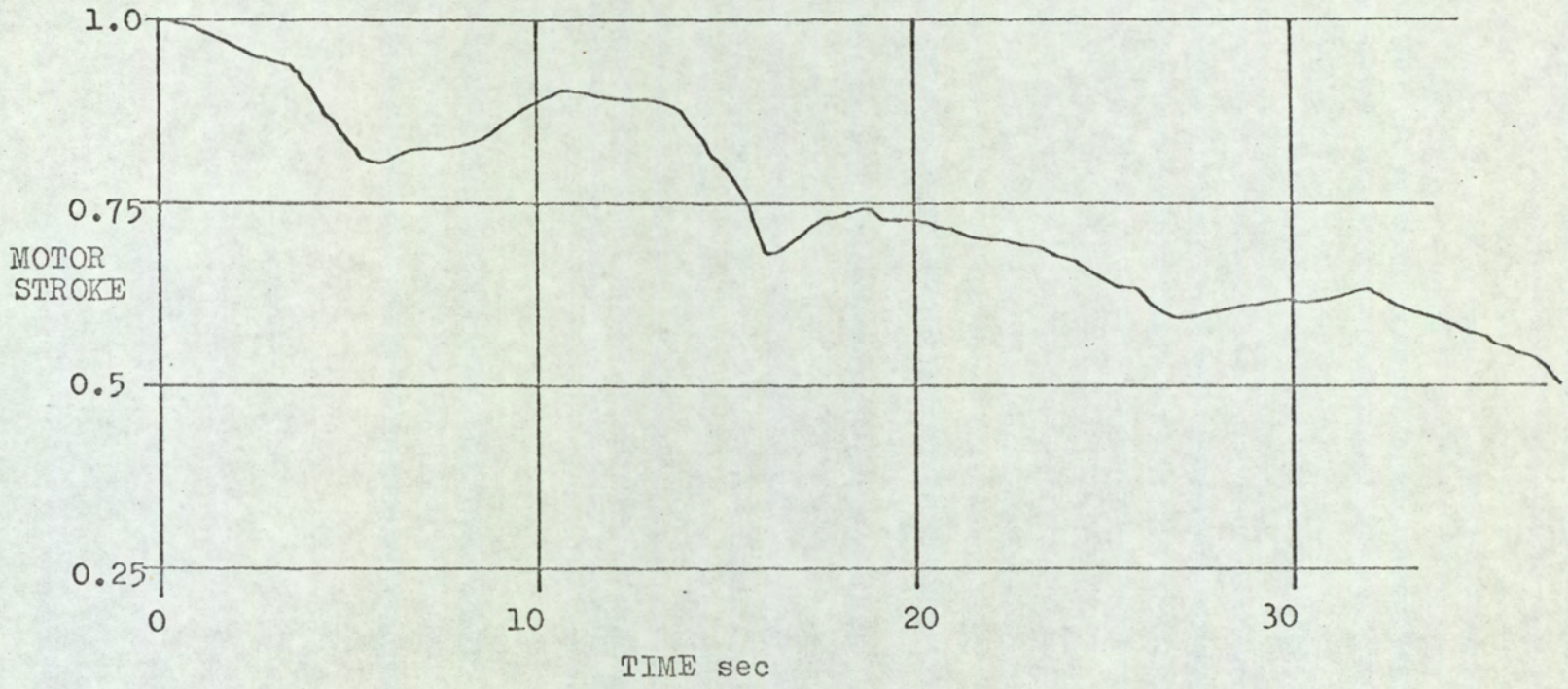

Zero Load Current

FIG.(7.13)
OPTIMISING TRANSIENT

with uncertainty about the slope of the performance curve, makes it impossible to establish a quantitative comparison with a theoretical response. It is significant, however, that the progress made towards the optimum position covers two thirds of the range of adjustment in four cycles of the perturbation. This represents a substantial amount of progress per cycle and is the result of the high gain setting in the optimising loop. Against the time scale the rate of progress is slow, due to the low perturbation frequency.

The result shown on Fig.(7.14) was obtained with the load again set to zero current, but the initial stroke setting was at the minimum value. The system is constrained by the limit circuit and continues close to the initial setting as this is the maximum efficiency point.

When the load current had been increased to 1 Amp, the same sequence of tests gave the results shown on Fig.(7.15) to Fig.(7.17). The maximum efficiency was then at about the half stroke position. The differences in Fig.(7.15) and Fig.(7.16) again indicate the extent of the effect of measurement noise. It is useful to compare Fig.(7.13) with Fig.(7.15). The difference in the rate of progress is evident, the progress being greater in Fig.(7.13) due to the higher slope of the performance curve in that case. In Fig. (7.17) the system is able

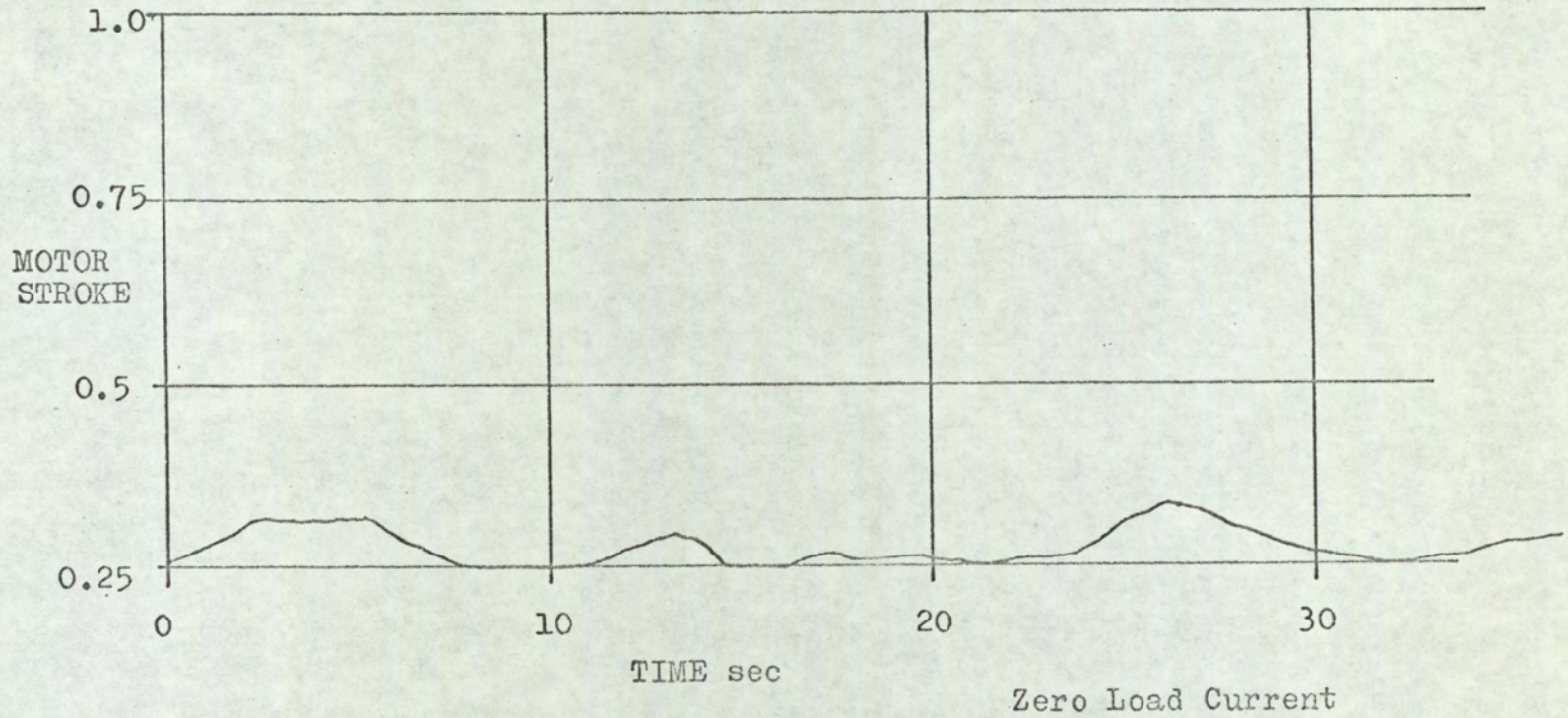

FIG.(7.14)
OPTIMISING TRANSIENT

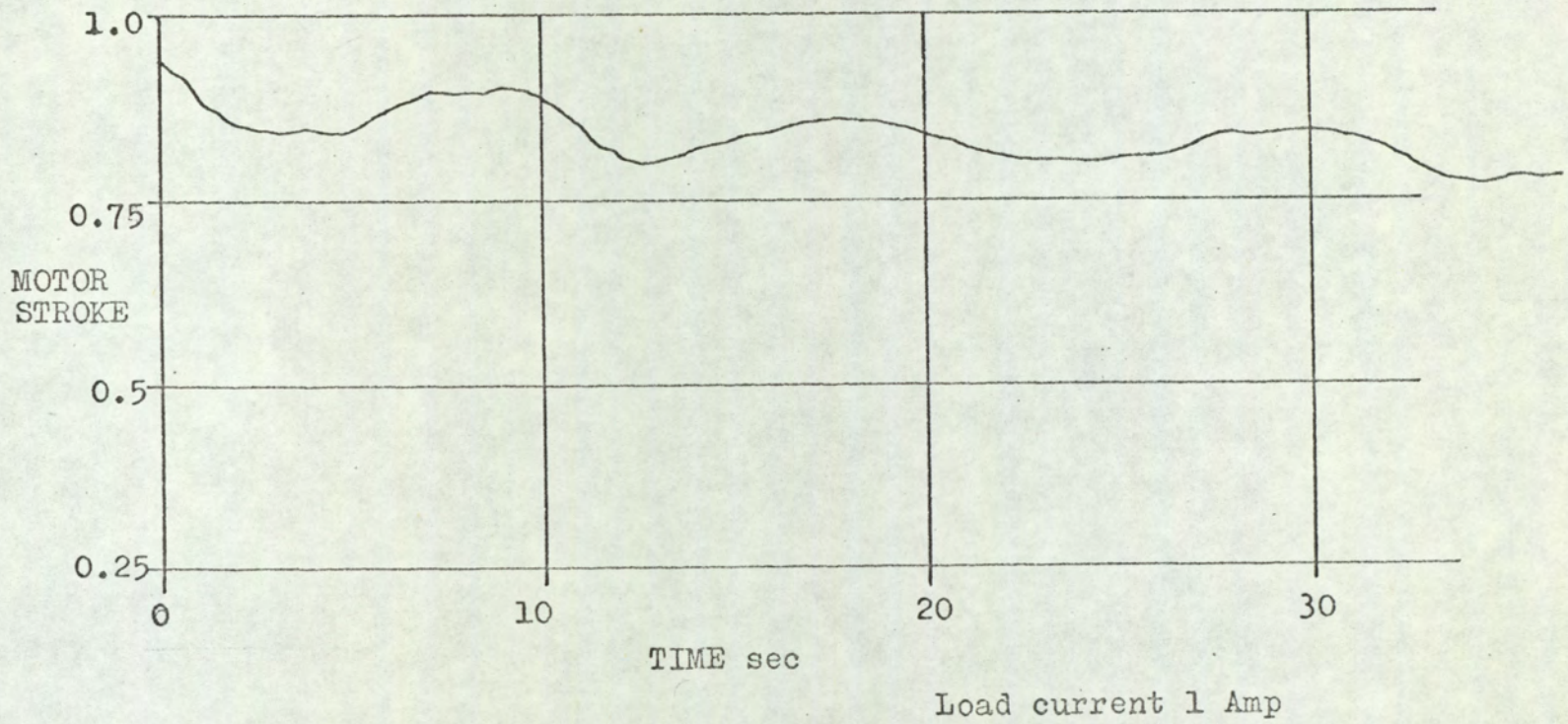

FIG.(7.15)
OPTIMISING TRANSIENT

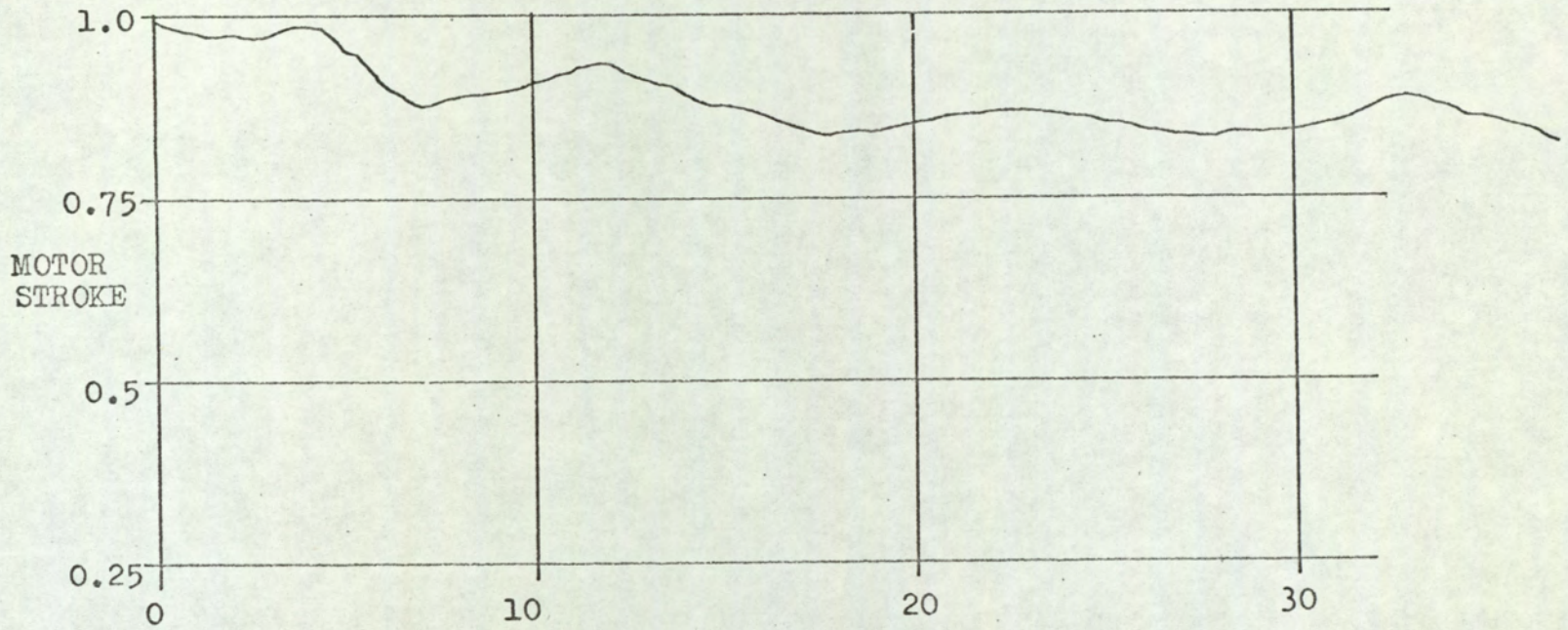

Load current 1 Amp

FIG.(7.16)

OPTIMISING TRANSIENT

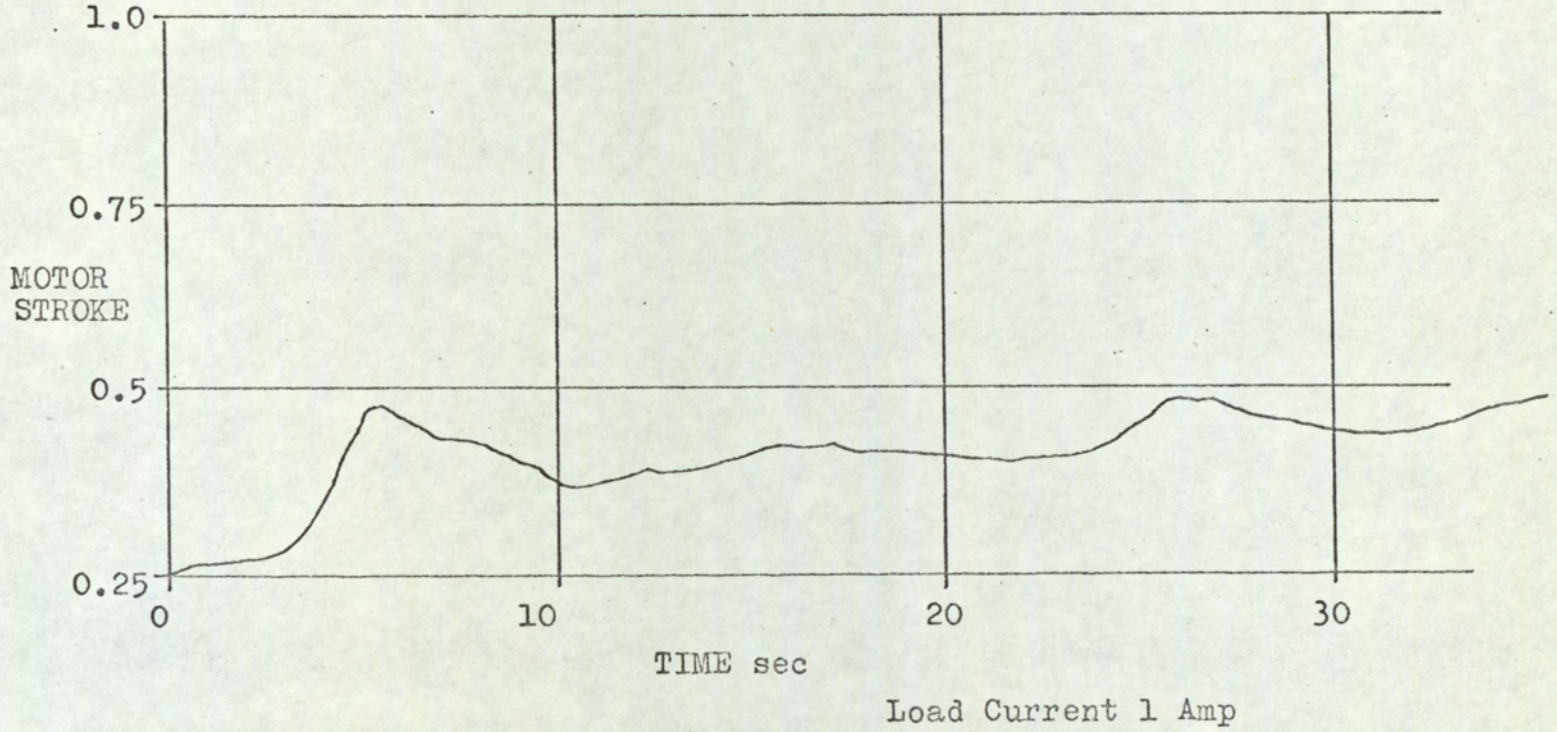

FIG.(7.17)
OPTIMISING TRANSIENT

to move away from the initial setting at the minimum stroke position after an operation of the limit circuit.

A further increase in the load current to 2 Amp gave rise to the results shown in Fig.(7.18) and Fig.(7.19). The maximum efficiency was then near to the maximum stroke position. In Fig.(7.19) the system was started at the minimum stroke and moved rapidly away in the first cycle. This is due to the high slope of the performance curve at that point. In Fig.(7.18) the system acquired the maximum point and continued to oscillate following the perturbation with little control action.

Together these results indicate that the system operated in the manner expected as far as the general trend of movement is concerned. The measurement noise has significant effect in the detailed form of the response but the operation of the system is otherwise acceptable.

7.8.2 VARYING LOAD CONDITIONS.

The effect of progressively changing the operating conditions has been studied theoretically in Section (6.7). The conclusions reached showed that if the change of operating conditions was in a direction which increased the efficiency, there would be a movement assisting the normal hill-climbing action. Conversely when the efficiency was decreasing the hill-climbing action would be retarded.

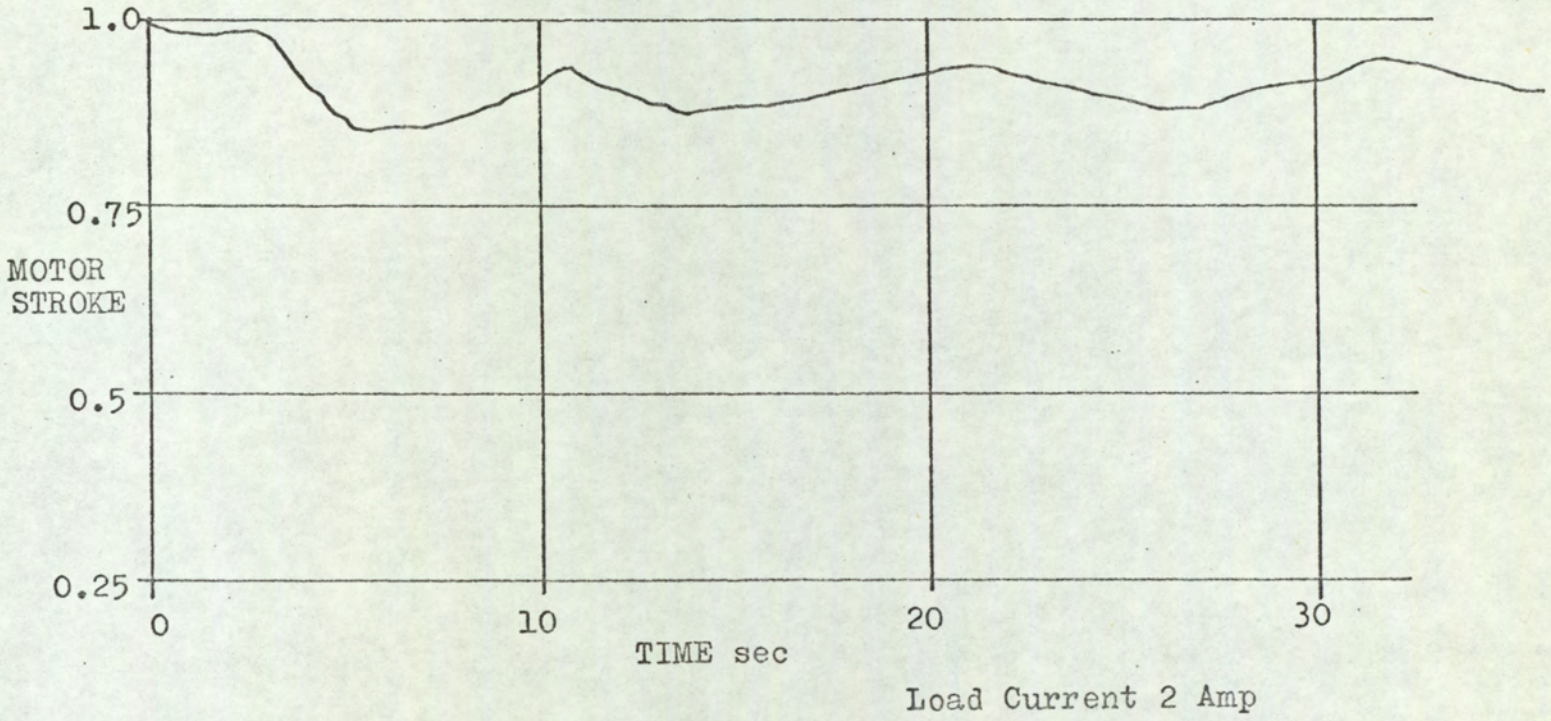

FIG.(7.18)
OPTIMISING TRANSIENT

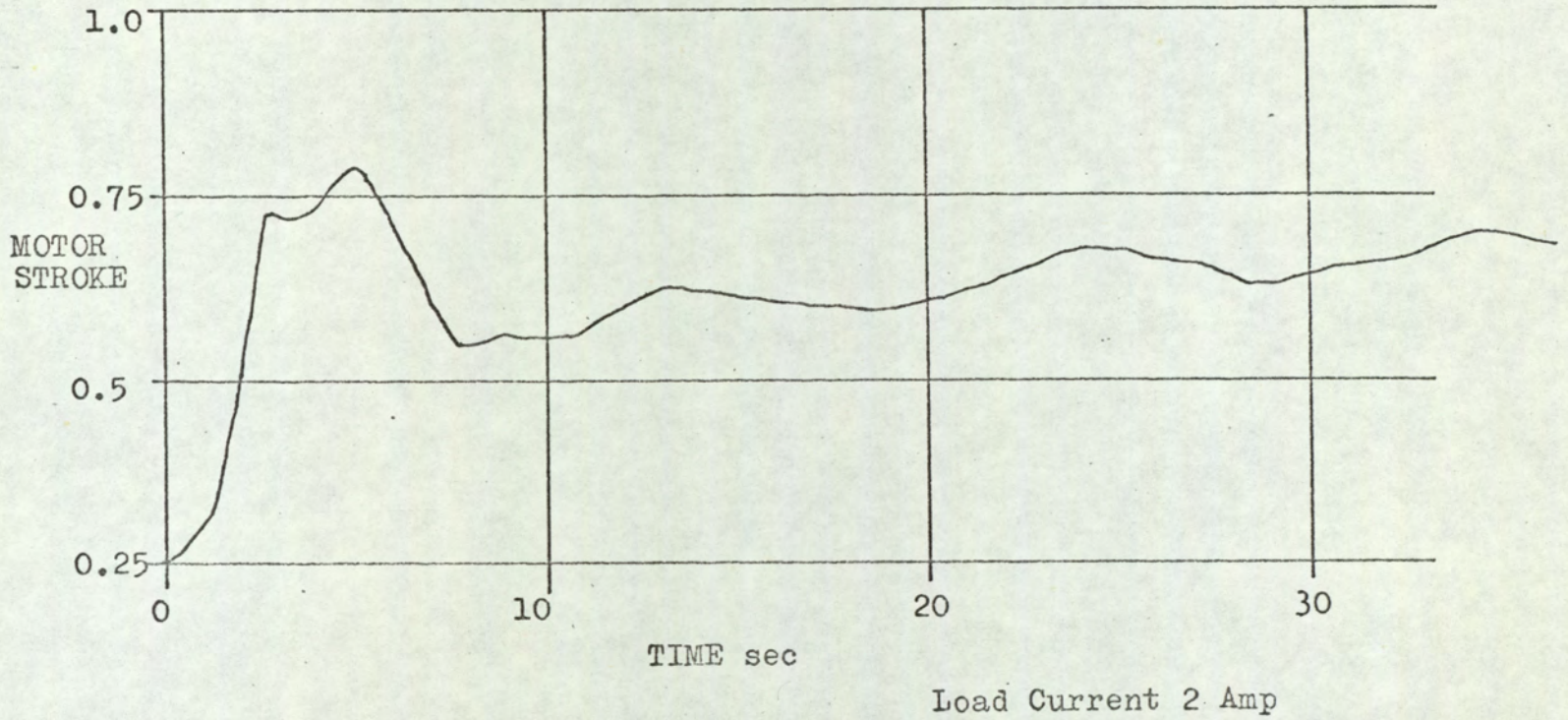

FIG.(7.19)
OPTIMISING TRANSIENT

To test this theoretical result it was arranged to change the load current at constant rate. To do this a ramp function change of voltage from a wave-form generator* was applied to the external input of the current control system. The current control system is described in Section (2.2) of the Appendix and this provides an accurate control of the load current.

The detailed effect of changing the operating conditions at constant rate was analysed in Section (6.7). In the particular case when it is the load current which is changing, it was calculated in Section (6.9) that a rate of change of 0.011 Amp per second would be about the maximum which the system could tolerate. The system was therefore subjected to rates of change of load up to 1 Amp per minute.

A typical recording of the movement is shown on Fig.(7.20) for the case when the load current was increasing. The system starts at the minimum stroke setting which corresponds to the maximum efficiency point at zero load current. The performance curves have revealed that the point of maximum efficiency moves towards the maximum stroke position as the load is increased. The system is seen to follow this movement with a small lag.

When the load current was decreasing the response was as shown on Fig.(7.21). The system started in

* Servomex Ltd., Wave-form generator Type LF 51.

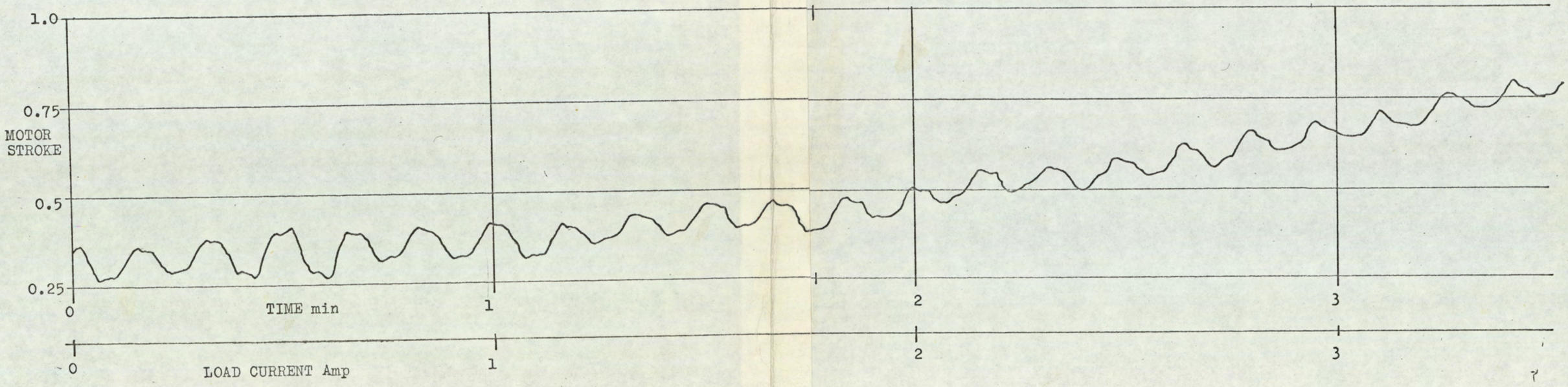

FIG.(7.20)
OPERATION WITH INCREASING LOAD

FIG.(7.20)
OPERATION WITH INCREASING LOAD

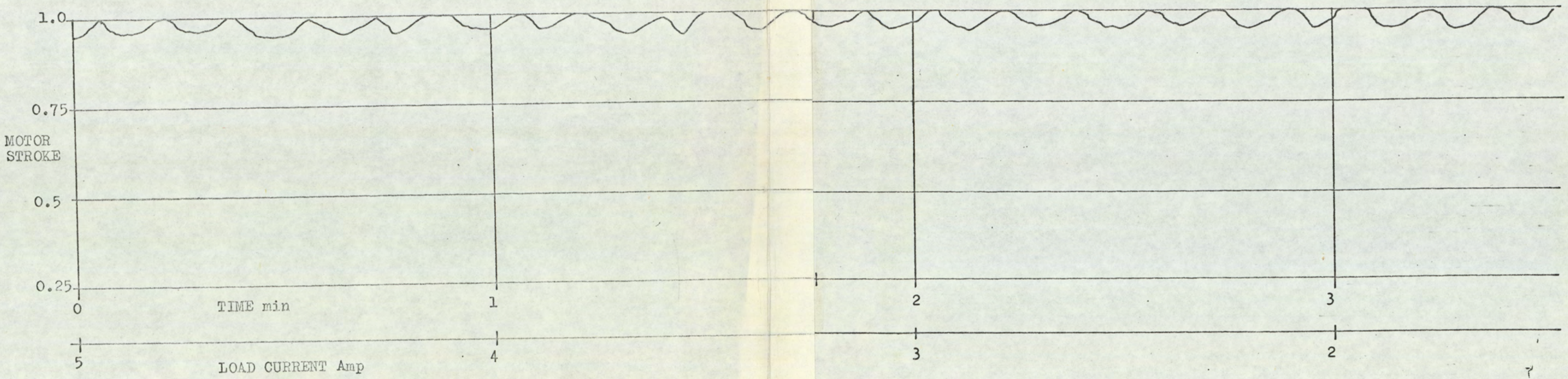

FIG.(7.21)
OPERATION WITH DECREASING LOAD

FIG.(7.21)
OPERATION WITH DECREASING LOAD

the maximum stroke position as this is the optimum setting at high load. By the time the load current has been reduced to 1 Amp the optimum setting is at about half stroke, but the system continued to oscillate against the maximum stroke limit. The effect of the reducing load was sufficient to prevent any progress being made to follow the movement of the optimum point.

The results presented in these two conditions were obtained with a high rate of change of load current. This exaggerates the effects sufficiently to make them obvious. At lower rates of change the system was better able to track the movement against the retardation due to the decreasing load. When the load was increasing the system continued to follow the optimum position with a slight lag and there were no marked changes in performance. It is clear that the main limitations of the system are seen when the load is decreasing. For there to be any progress in following the optimum position the rate of change of load current must be as low as 0.2 Amp per minute.

The overall impression is that the results confirm what has been expected from the analysis. They also emphasise that the system is only able to compete with slow changes in the operating conditions.

8. REVIEW OF THE SYSTEM PERFORMANCE.

The performance of the optimising system is primarily to be assessed in terms of its ability to follow the continuous movement of the optimum point. Indeed it is only when the optimum point is continually changing that there is a need to consider using such a system. In following the movement it is clearly a requirement that the controlled variable be held as close as possible to the optimum point. But this cannot be achieved without a compromise. The need for compromise stems from the fact that the changes in the operating conditions, which move the optimum point, also cause variations in the performance measure. The optimising system must discriminate between these variations and the changes in the performance measure produced by the controlled variable. A lackof discrimination produces errors in the estimate of the slope of the performance curve on which the control action depends. Discrimination can be improved by slowing down the rate of movement towards the optimum point. This allows a longer time for the correlation,between the changes in the controlled variable and the performance measure, to be established. The need to improve the discrimination thus conflicts with the requirement to follow the optimum point rapidly. In this case the result of the compromise is that the system is only able to compete with slow changes in the operating conditions.

The characteristics of the transmission system used in this work proved to be unfavourable to the optimising system. The most significant feature was the shape of the performance surface. This performance

surface is regarded as displaying the performance measure as a function of two variables. One co-ordinate is the controlled variable and the other is the disturbance in the operating conditions. In this case the controlled variable was the motor stroke and the operating conditions were changed by varying the load on the transmission. The slope of the performance surface along each co-ordinate is the significant feature. These values indicate the relative sensitivity of the performance measure to local changes in the operating conditions and the controlled variable. In this case the change of efficiency, as the performance measure, with the motor stroke was small compared with the change produced by the load. That is to say the slope of the performance surface in the direction of the disturbance is much greater than in the direction of the controlled variable. This means that ultimately the optimising system can only compete with slow changes of the operating conditions.

A second factor contributing to the slow response is the need to use a low perturbation frequency. The frequency is limited by the need to avoid errors in the efficiency measure, due to dynamical effects in the transmission. An increase in the perturbation frequency is, for the most part, advantageous. The rate of progress made by the optimising system would increase, as also would the maximum rate of change of the operating conditions which the system could accept. To realise these advantages however, the loop gain would have to be increased to retain the optimum setting. This would exaggerate the effect of the measurement noise.

It appears therefore that the form of the performance surface and the measurement noise together set the limitations to what can be achieved by the optimising system.

In the analysis of the system it has been shown in general terms that an optimum value exists for the gain in the optimising control loop. The optimum is seen when the need for a rapid hill-climbing action is balanced against the sensitivity to the disturbance. The optimum value has been chosen to allow the system to compete with the maximum rate of disturbance of the operating conditions. In this case the value of the loop gain required is high and consequently the progress made towards the optimum point in each cycle is large. Typically it may be as large as twice the perturbation amplitude in one cycle. Even so the rate of change of load on the transmission must be slow. A rate of change as low as 5% of full-load in one minute may have sufficient effect to cancel any progress made by the optimising system.

The extent to which the efficiency may be increased by the optimising system is an important consideration. In this case the efficiency may be raised by about 5% by reducing the stroke from the maximum position. The fact that at low load the efficiency may be as low as 25% is significant,as this change then represents a saving of 20% in the output power. It is not always to be expected that the improvement will be as small as this. A greater improvement would be shown when the fluid flow contributes a higher proportion of the loss in relation to that due to

the pressure. The effect of the motor stroke adjustment, in reducing the flow, would be to show a greater change in the losses. This condition will exist when the length of pipework between the pump and motor is large and when the output speed is high. In this case the pipework was short and the output speed low, so that the system approached the worst case in this respect.

The possible improvement in the efficiency must also be considered in relation to the level of power involved. The economic value of the optimising system is to be judged in terms of the value of the energy saved. For reasons of convenience the transmission system used in the tests was a small one, and it would be difficult to see a justification for using an optimising system on such a small unit. It may well be however, that an economic situation would exist with much larger units.

The dynamical properties of the transmission system have been shown to restrict the perturbation frequency. The particular hydraulic system used in the tests was slow in dynamical response. This was due to three factors,

(a) The fluid circuit was made up of flexible hose which contributes a large compliance.
(b) The transmission controlled a load of high moment of inertia.
(c) The response of the stroke setting mechanism was slow.

The use of the feedforward control system developed in this case gives a considerable improvement on what could be achieved by regulating the output speed with feedback control alone. Even so the adjustment of

the motor stroke initiates transient speed changes. These changes of speed result in significant changes of the load torque, due to the high moment of inertia of the load. The dominant effect is then a change of the efficiency following from the change of torque. The choice of a ramp-function for the perturbation wave-form, rather than a square wave-form, reduces this effect significantly. But there is still a need to restrict the rate of stroke movement so that the efficiency will follow the stroke changes. For there to be any improvement in this limitation it would be necessary to re-design the transmission system having regard for the three factors listed above.

Measurement noise has been identified as a significant feature affecting the optimising system. This has been taken to mean the changes of the performance measure due to causes other than the operating conditions and the controlled variable. In this case the noise contributed in this sense was small. Such noise as existed was probably due to causes like the finite resolution of the potentiometer pick-off elements and aeration of the hydraulic fluid. In the test system the random fluctuations of measurement noise made a theoretical analysis impossible. The operation of the system was otherwise satisfactory, but it would be improved if the noise level could be reduced.

9. CONCLUSION.

The form of optimising system chosen for the application considered here was one using a periodic perturbation of the controlled variable. In the design of the system it was necessary to devise a number of refinements to the basic form of system previously described in the literature. A triangular wave-form was used for the perturbation. This combines the features that it is simple to generate and does not impose too great a disturbance on the controlled plant. It is also possible to incorporate quite simply the constraints on the movement of the controlled variable. The need to filter the performance measure, chiefly to remove the mean component, has been met by developing a special form of filter. This filter operates by sampling the input signal and has the advantage that it will operate with a low cut-off frequency. The need for this arises when the perturbation frequency is low so that the continuous form of high-pass filter has complications. The process of demodulating the performance signal is required to generate the movement towards the optimum point. It has been possible to use a simple form of demodulator, involving only a biphase amplifier and a change-over switch. With these refinements the system has been reduced to one which could be manufactured comparatively cheaply but it is only adequate for the conditions where measurement noise in the performance signal is small.

The theoretical analysis of the system has been developed to take advantage of the simplifications which this new form of system introduces. The rate

/of progress

made by the system in climbing the performance surface has been calculated. In addition the effects of continuously changing operating conditions was studied. The point of view adopted was that of the need to maximise the rate of progress towards the moving optimum point. A compromise is necessary in this situation. The need for rapid progress towards the optimum point due to the perturbation is set against the retarding action of the changing operating conditions. An optimum setting of the gain in the optimising control loop was then shown to exist. This analysis does not take quantitative account of the measurement noise and the conclusion reached is only valid when the noise level is low.

An optimising system designed on these principles has been applied to maximise the efficiency of a hydraulic transmission. This has allowed the design requirements to be interpreted in detail and in a numberof cases the requirements could only be met by a careful choice of equipment. Two subsidiary problems required solution. One was the control of the output speed of the transmission. A system involving a combination of feedback and feedforward signals was developed for this purpose. The introduction of the feedforward signals was shown to offer marked advantages over what could be achieved with feedback alone. The other problem concerned the need to obtain a continuous measurement of the efficiency. This was done by using a self-balancing bridge system which represents a novel form of measuring technique.

The overall performance of the optimising system has been shown to have considerable practical limitations. In particular the rate of change of the operating conditions must be slow. This is to some extent an inherent limitation of the optimising system but some features of the transmission system used in the tests were not advantageous to this form of control. In this respect the results give a pessimistic view of what may be achieved by optimising control in more favourable circumstances.

The further development of this research could persue the following lines. Firstly the design of the transmission system could be improved. A significant improvement would be obtained by replacing the electro-hydraulic control valves with ones giving a faster response. The feedforward control system used to regulate the output speed is capable of better performance. This could be achieved by dynamical compensation of the feedforward action.

The sources of measurement noise have not been identified conclusively and further study could lead to a reduction of the noise present. The design of the optimising system has relied on the low level of noise and a quantitative assessment of its effect has not been made. Further insight might show how a quantitative account of the noise could be introduced in the design.

The performance of the optimising system in following changes due to load variations has been studied. It would also be valuable to observe the performance in response to changes of the input speed.

10. ACKNOWLEDGEMENTS.

This work has been conducted with the support of the Research Centre of Joseph Lucas Ltd.. The advice of Mr. A.C. Sutherland and Mr. S.A. Beesley of that organisation in forming the overall concept of the project is acknowledged with appreciation.

The hydraulic machines were provided and modified by Lucas Industrial Equipment Ltd.. The detail of the modification was designed by Mr. R. Cope who also advised on the construction of the hydraulic system.

The advice of Dr. D.H. Sansome of the University of Aston on the design of the torque measuring equipment has been acknowledged in a footnote to the appropriate section.

The interest and encouragement of Prof. E. May, Prof. J.E. Flood and Prof. W.K. Roots of the University of Aston, as supervisors at various times, has been received with gratitude.

11. REFERENCES.

(1) EVELEIGH V.W.
"Adaptive Control Systems"
Electro-Technology 1963 April p.79

(2) BLACKMAN P.F.
"An Exposition of Adaptive Control - Extremum Seeking Regulators"
ed. WESTCOTT J.H. 1962 p.36
(Pergamon Press, New York)

(3) GRENSTED P.E.W. and JACOBS O.L.R.
"Automatic Optimisation"
Trans. Soc. Instrum. Technol. 1961 Sep. Vol.13 p.203

(4) WILL P.M.
"Review of the Literature of Adaptive Control"
Trans. Soc. Instrum. Technol. 1963 Jun. Vol.15 p.161

(5) EVELEIGH V.W.
"General Stability Analysis of Sinusoidal Perturbation Extrema Searching Adaptive Systems"
IFAC Congress (Basle) 1963 407/1
(Butterworth, London)

(6) JELONEK Z.J., GARDINER A.B. and REASIDE D.
"A Theoretical Comparison of Three Types of Self-optimising System"
Proc. I. Mech. E. 1965 Vol.179 No.3H(x) p.100
(Automatic Control, Nottingham 1965)

(7) ROBERTS J.D.
"On the Design of Optimal Extremal Regulators"
Proc. I. Mech. E. 1965 Vol.179 No.3H(x) p.93
(Automatic Control, Nottingham 1965)

(8) DOUCE J.L. and BOND A.D.
"The Development and Performance of a Self-optimising System"
Proc.I.E.E. 1963 Mar. Vol.110 No.3 p.619

(9) NG K.C., MURTHY K.K., STOCKWELL D.H. and MORRIS K.R.
"Recent Advances in Hill-climbing Technique"
Second UKAC Control Convention
Advances in Computer Control
I.E.E. Publication No.29 1967 Apr. C15

(10) TSIEN H.S. and SERDENGECT S.
"Analysis of Peak-holding Optimalising Control"
J. Aero. Sci. 1955 Aug.

(11) MOROSANOV I.S.
"Methods of Extremum Control"
Automation and Remote Control 1957 Vol.18 p.1077

(12) PERRET R. and ROUXEL R.
"Principles and Application of an Extremal Computer"
IFAC Congress (Basle) 1963
(Butterworth, London)

(13) MORAN F., BERGER C.S., XIROKASTAS D.
"Development and Application of Self-optimising Control to Coal-fired Steam-generating Plant"
Proc.I.E.E. 1968 Vol.115 No.2 p.30

(14) SMITH P.E.
"Dynamic Representation of a Hydraulic Constant-speed Drive"
Trans.A.I.E.E. 1958 Vol.77 pt.II p.28

(15) RAGAZZINI J.R. and FRANKLIN G.F.
"Sampled Data Control Systems"
(McGraw Hill, New York) 1958 Section 3.3 p.34

(16) D'AZZO J.J. and HOUPIS C.H.
"Feedback Control System Analysis and Synthesis"
(McGraw Hill, New York) 1960 Ch.18 p.427

(17) Ibid. Ch.10 p.255

(18) KOENIG H.E. and BLACKWELL W.A.
"Electro-Mechanical System Theory"
(McGraw Hill, New York) 1961 Ch.9 p.233

(19) Reference (16) Ch.6 p.113

(20) Reference (16) Ch.13 p.318

APPENDIX

The Appendix covers the essential details of the circuits used in implementing the test rig. This has required the control of the input speed to the pump and the load applied to the motor. The load was controlled by setting the armature current in the loading generator. Details of the hydraulic system are also given and the circuits used in the overall speed control system. Finally the arrangement for obtaining a continuous measurement of the efficiency is described.

1. ELECTRICAL DRIVE ARRANGEMENTS

The specifications of the motor required to drive the pump and the generator used to load the hydraulic motor are subject to the following considerations.

1.1 LOADING GENERATOR.

The generator must be capable of absorbing the power output of the hydraulic motor over a range of speeds. The range of operating conditions likely to be involved was assessed in Section (3) and the line A-B drawn on Fig.(3.6) indicates the maximum torque likely to be demanded at any speed. We note that the maximum torque is called for at the maximum speed, so that the maximum power rating of the generator is 8 h.p. at 2000 r.p.m..

It was decided to run the generator at a constant armature supply voltage of 200 Volt and regulate the field to compensate for speed changes. This means that the maximum torque is demanded when the field is weakest and some de-rating of the machine is necessary to provide a reasonable

speed range. A low speed limit of 750 r.p.m. was chosen to give a speed range of 2.67:1, the maximum range acceptable with a standard machine. The specification of the loading generator then becomes:-

Generator d.c. - 200 Volt
30 Amp
750 - 2000 r.p.m.

In order to control the load torque it was decided to use a booster-generator in the armature circuit, with feedback control setting the armature current. This has the advantage of requiring the control of lower power by the field excitation amplifier than would be the case if the main generator field were controlled. This booster-generator must be capable of driving the full-load armature current against the resistance of the armature circuit. It was estimated that 40 Volt would be sufficient to do this. The specification of the booster-generator then becomes:-

Booster-generator No.1 - 40 Volt
30 Amp
1500 r.p.m.

Fitted with two field windings for push-pull operation from a 24 Volt supply, each field winding to be capable of giving full output.

1.2 DRIVE MOTOR.

The limitations on the drive motor arise from the requirements of the electrical machine rather than the pump. The limiting feature of the pump is the maximum speed limit of 3000 r.p.m., but as the maximum speed rating of standard d.c. motors is 2000 r.p.m. and this lower figure was taken as the operating maximum. To achieve a wide speed range it was decided to vary

both the armature voltage and the field current of the motor. The control of the armature voltage was obtained by using a booster-generator in series with the armature. It was also convenient to use this booster-generator as part of a speed control loop regulating the motor speed. This has the advantage of requiring the control of lower power by the field excitation amplifier than would be necessary to regulate the motor field. Also the lower time constant of the booster-generator field makes the response more rapid.

With a fixed armature circuit supply voltage of 200 Volt and ± 100 Volt from the booster-generator the motor speed range is 3:1. This range may be extended by an adjustment of the motor field to give a range of 4:1. The speed range is then from 500 to 2000 r.p.m.. The power requirements are obtained from the pump characteristics given on Fig.(3.5). The demand is for 10 h.p. at 2000 r.p.m. so that the motor specificatinn becomes:-

Motor d.c. - 300 Volt
1500 - 2000 r.p.m.
10 h.p.

The booster-generator has the specification:-

Booster-generator No.2 - 100 Volt
30 Amp
1500 r.p.m.

Fitted with two field windings for push-pull operation fron a 24 Volt supply.

With armature control it is necessary to check the maximum armature current overload i.e. when the booster-generator circulates a current limited only by the circuit resistance. This turns out to be 80 Amp

which is an acceptable short term overload, so that there is no need to include extra resistance in the armature circuit to limit the current.

2. CONTROL OF THE ELECTRICAL MACHINES.

The general arrangement of the control circuit of the electrical machines is as shown on Fig.(A2.1). The motor and generator armatures are connected to the same 200 Volt supply, so that the load on this supply is only that necessary to meet the losses in the system and start the motor.

It was necessary to design two field excitation amplifiers. One controlling booster-generator No.1 in the generator circuit required an output rating of 1.5 Amp at 24 Volt. The other for booster-generator No.2 rated at 3 Amp. The circuit diagram of the amplifiers is given on Fig.(A2.2) where the output transistors are changed to OC29 when the lower current rating is required. The linear range of the amplifier is $\pm$ 150 mV at the input point.

2.1 CHARACTERISTICS OF THE SPEED CONTROL SYSTEM.

The detail of the speed control circuit for the motor is shown on Fig.(A2.3). The loop gain is such that full output from the booster-generator is obtained for a drop of 60 r.p.m. in speed. The closed loop transfer characteristic from the external input point is as shown on Fig.(A2.4), which indicates acceptable linearity over a 3:1 speed range. The dynamical response is limited by the armature inertia and saturation of the booster-generator. The frequency response relating

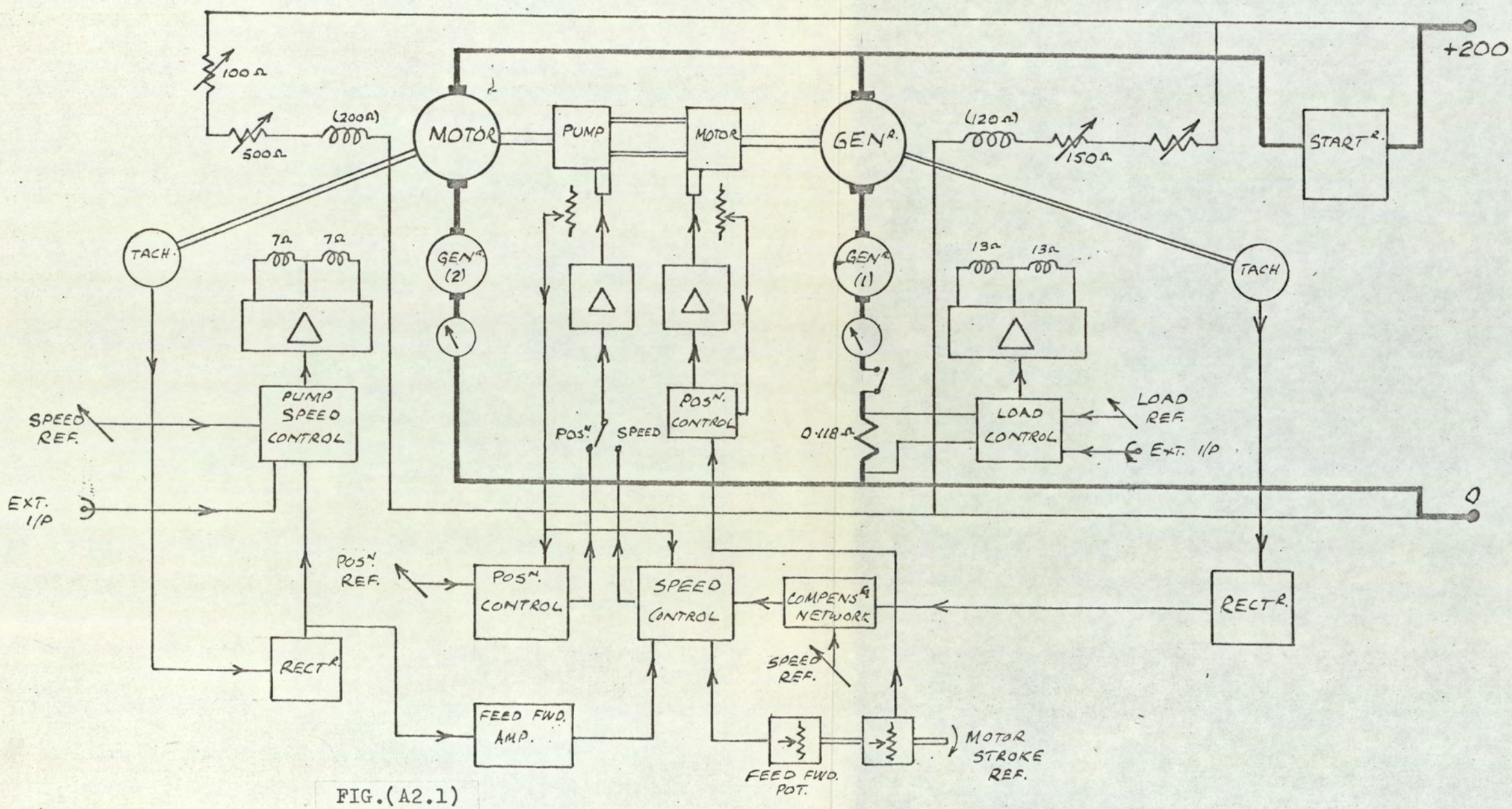

FIG.(A2.1)

GENERAL ARRANGEMENT OF CONTROL CIRCUIT

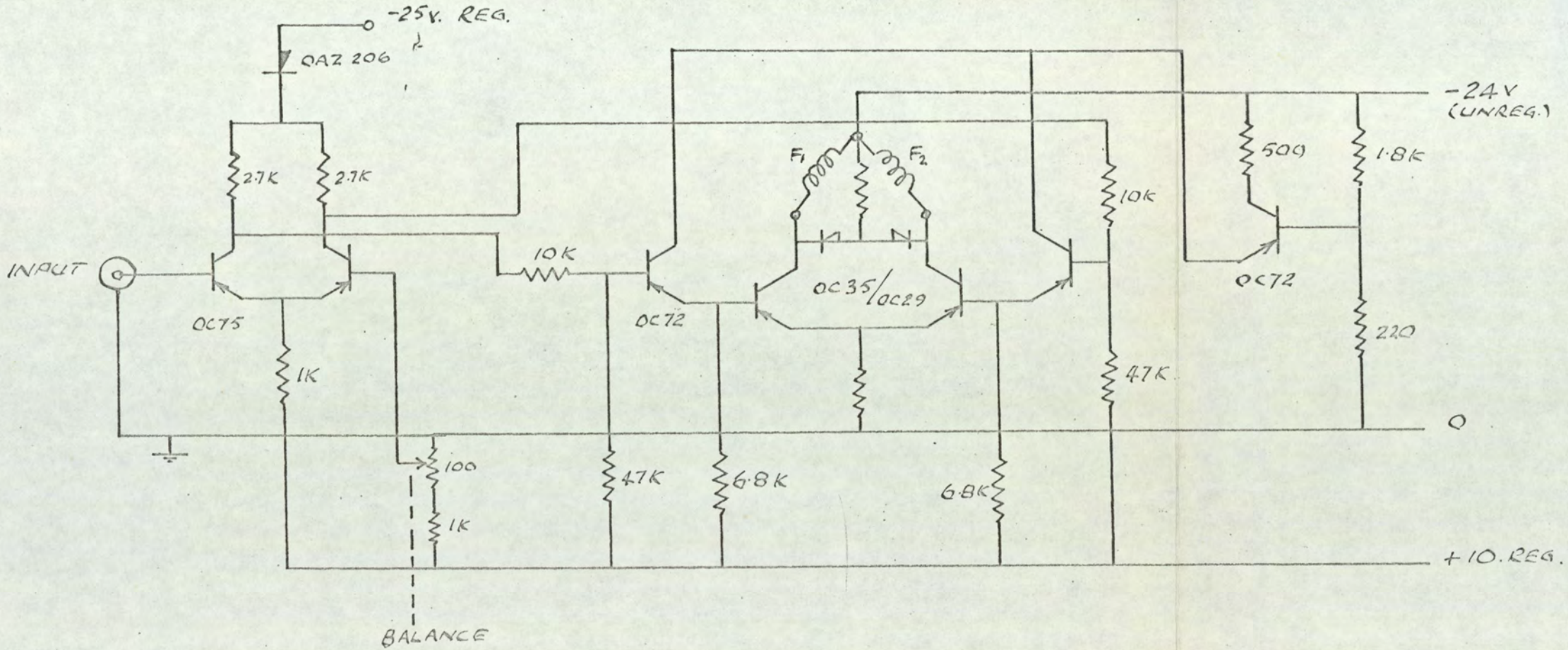

FIG.(A2.2)

GENERATOR FIELD CONTROL

AMPLIFIER

- 257 -

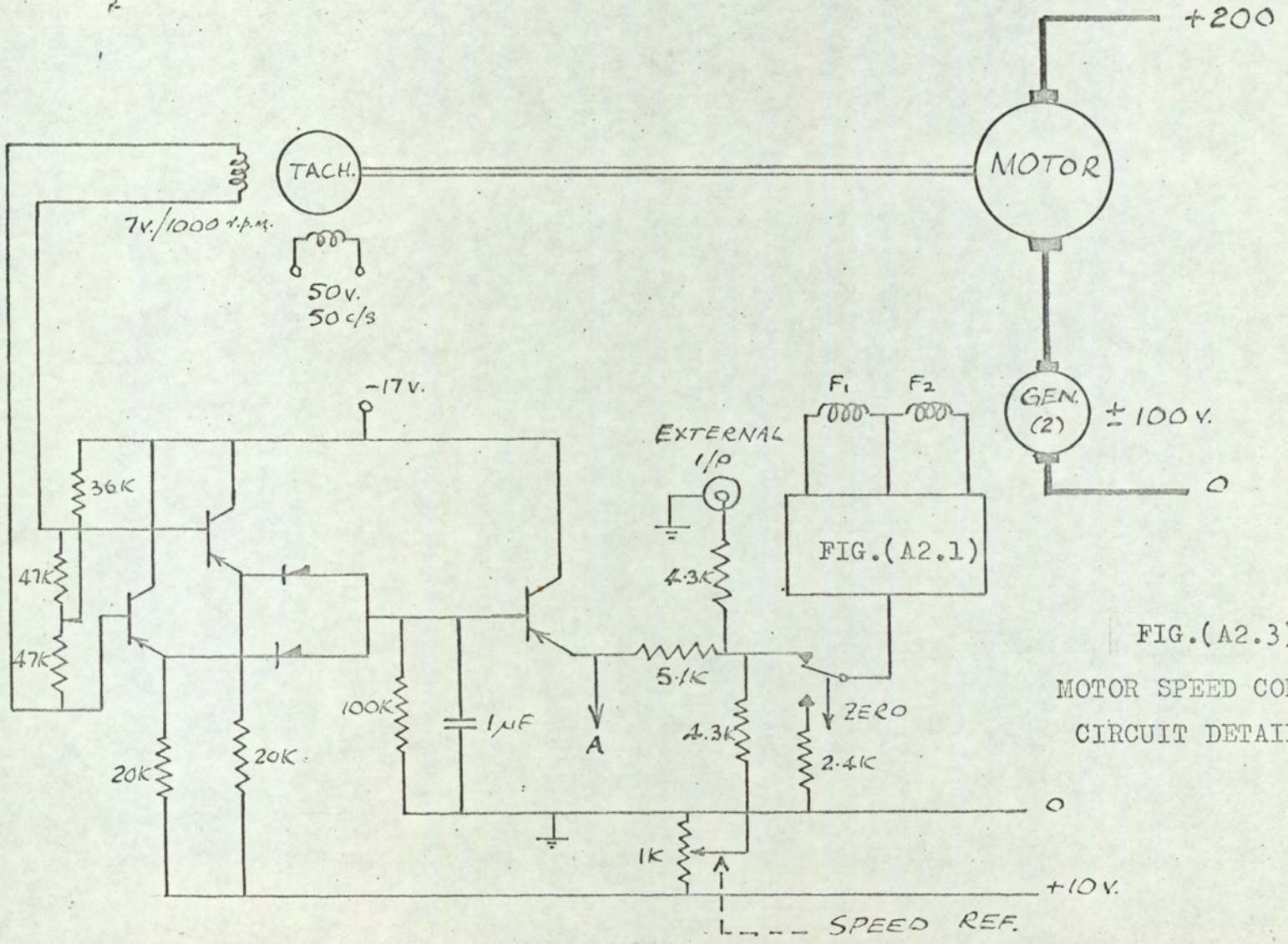

FIG.(A2.3)

MOTOR SPEED CONTROL CIRCUIT DETAIL

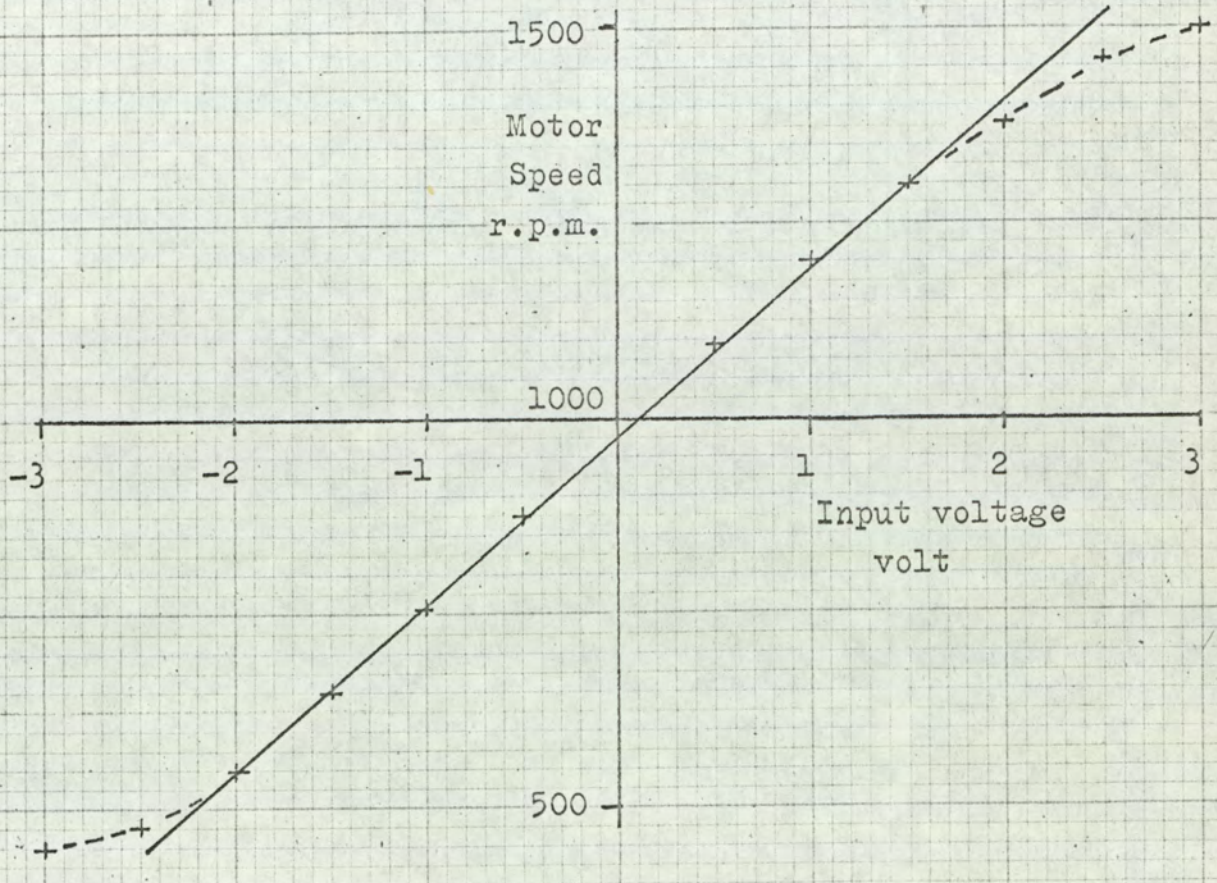

FIG.(A2.4)

MOTOR SPEED CONTROL SYSTEM

STEADY STATE CONTROL CHARACTERISTIC

the motor speed to the input to the control loop is shown on Fig.(A2.5), for an input amplitude of 2 Volt. The bandwidth of the response is 0.5 Hz. A step function input indicated that the maximum acceleration available is approximately 800 r.p.m./sec. The system is stable so that the addition of a compensating network is not required,also saturation prevents any improvement in the speed of response by this means.

2.2 GENERATOR CURRENT CONTROL SYSTEM.

The detail of the armature current control system for the generator is given on Fig.(A2.6). The loop gain is such that the amplifier saturates with 2 Amp error in the armature current i.e. a 40 Volt change of the generator e.m.f. will produce only 2 Amp change of current. The steady state transfer characteristic relating the armature current to the external input voltage is shown on Fig.(A2.7). It is noted that there is acceptable linearity over the required range of $\pm$ 30 Amp.

The dynamical response is limited by the field time constant of the booster-generator. A frequency response test with an input amplitude of 0.75 Volt gave the results shown on Fig.(A2.8); the bandwidth is 2 Hz. A step response test showed that the maximum rate of rise of the armature current was 45 Amp/sec. The system is stable without compensation and saturation limits the speed of response to the maximum available with the circuit used.

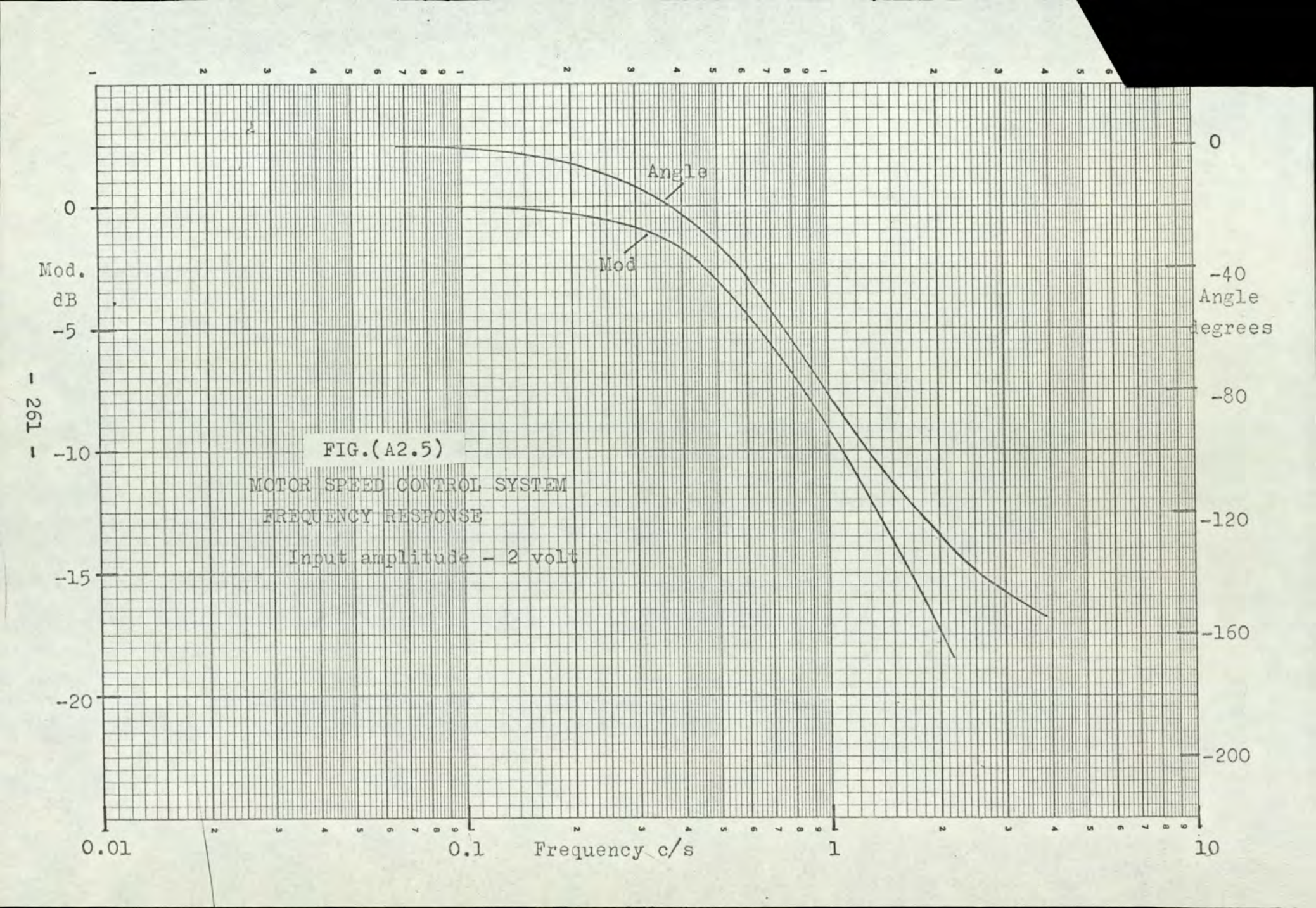

FIG.(A2.5)

MOTOR SPEED CONTROL SYSTEM
FREQUENCY RESPONSE

Input amplitude - 2 volt

FIG.(A2.6)
GENERATOR CURRENT CONTROL
CIRCUIT DETAIL

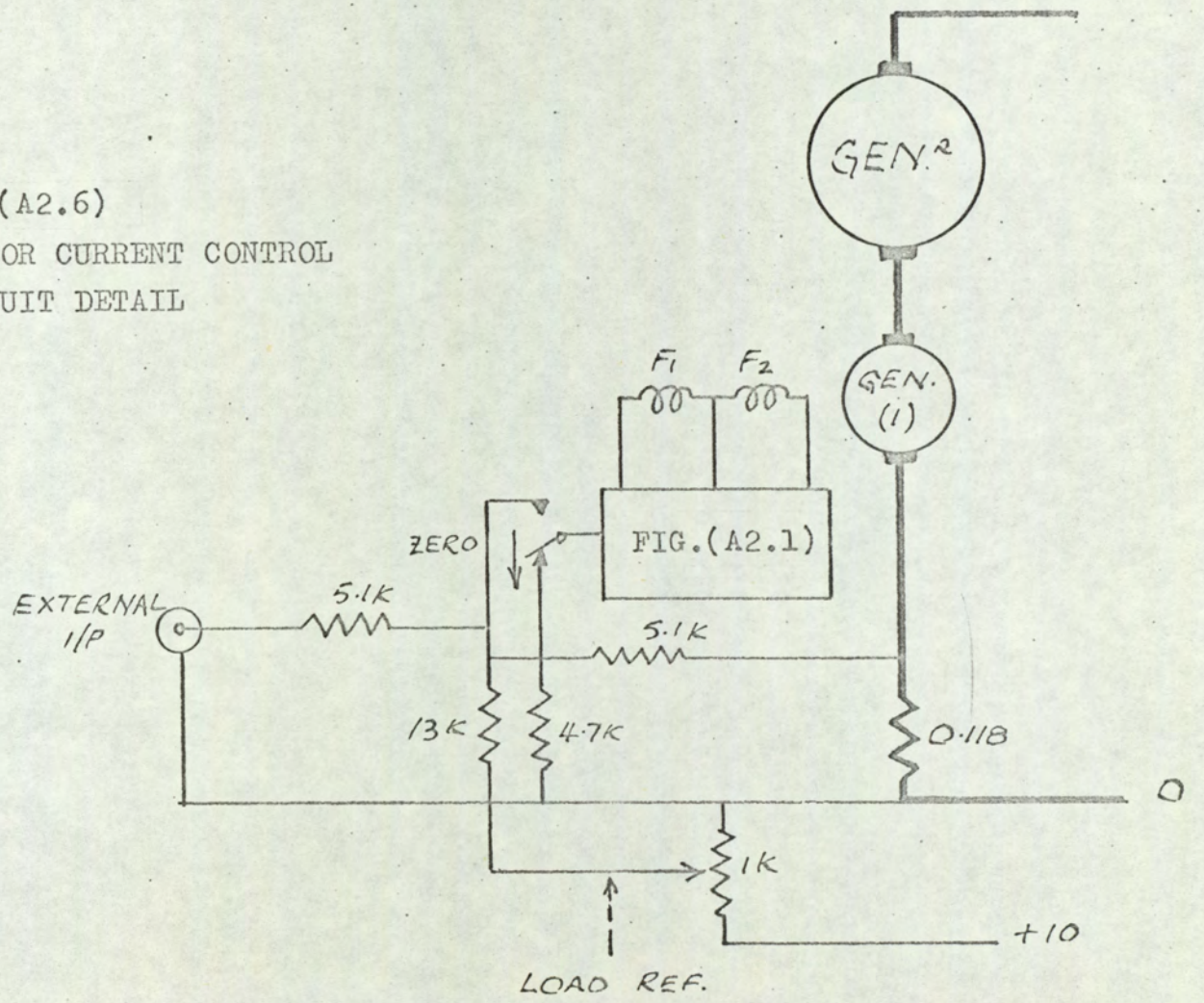

FIG.(A2.7)

GENERATOR CURRENT CONTROL

STEADY STATE CONTROL CHARACTERISTIC

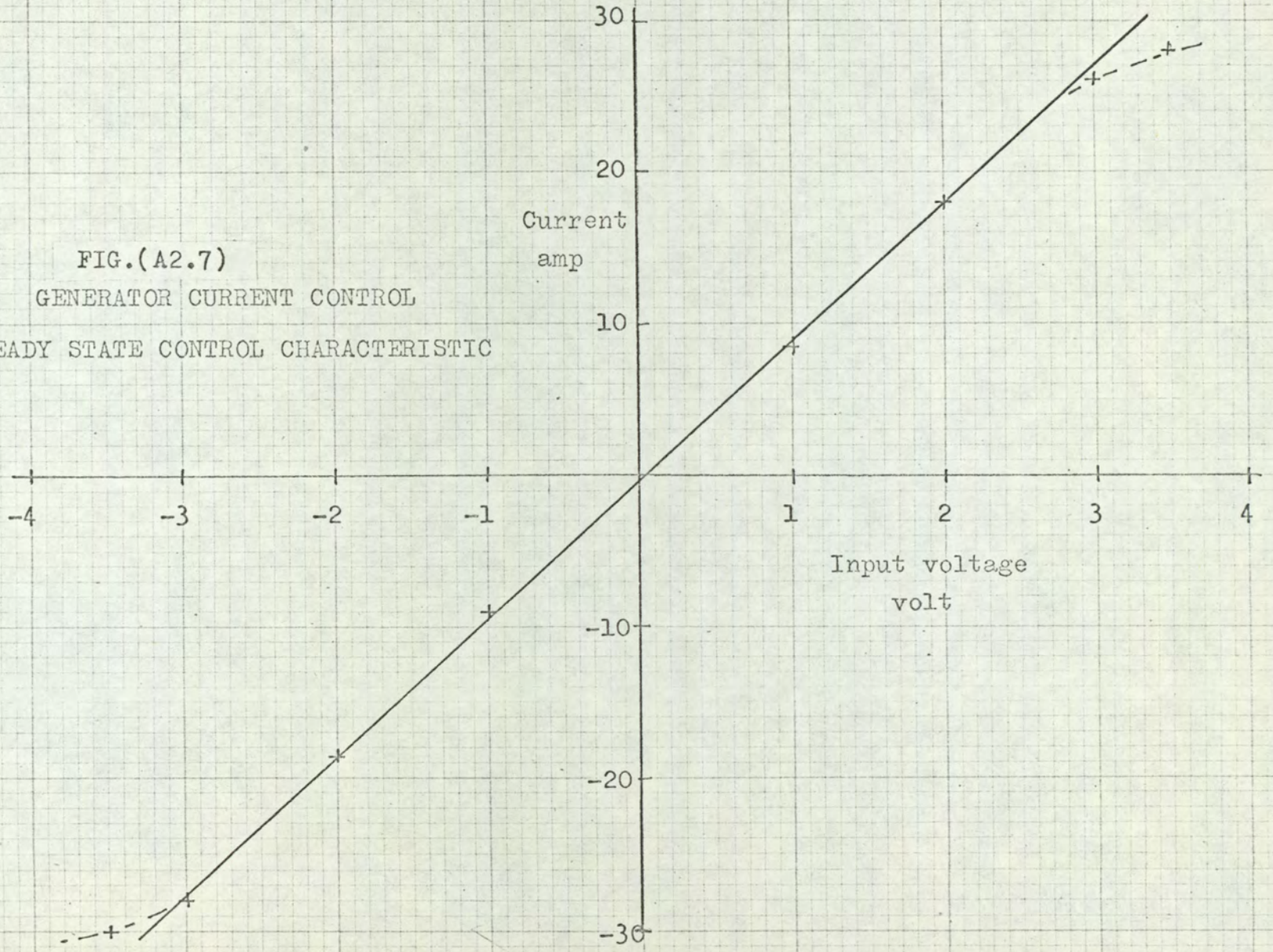

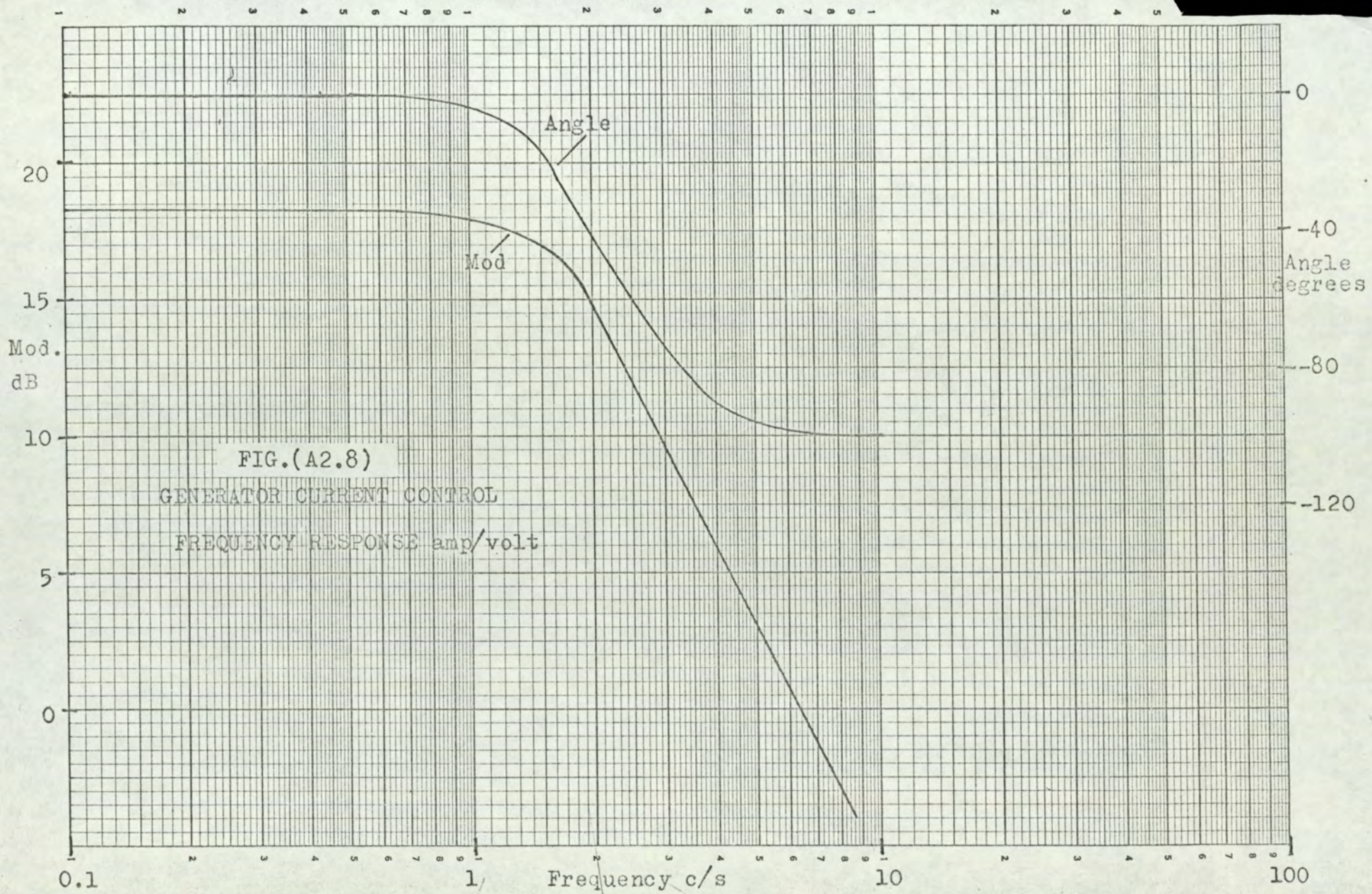

FIG.(A2.8)

GENERATOR CURRENT CONTROL

FREQUENCY RESPONSE amp/volt

3 HYDRAULIC SYSTEM.

3.1 MACHINES

The machines used in the test rig were Type IP 125 units* with a special modification incorporated in the cam plate control mechanism. The modification was necessary to allow a measurement of the position of the servo piston to be made. It consisted of a sleeve locking the pilot piston to the servo piston so that the manual servo rod registered the position of the servo piston. Control of the servo piston was obtained by using a solenoid operated ball-valve Type CSS3*.

3.2 HYDRAULIC CIRCUIT.

An outline of the hydraulic circuit is shown on Fig.(A3.1). The main circuit and the motor body are primed at 15 p.s.i. and a system of non-return valves directs fluid to the low pressure side of the circuit to make up the leakage flow. A high pressure relief valve is included with the non-return valves so that the system may operate in either direction of flow.

It is required that the torque measured on the pump and motor body mountings should be the same as the shaft torque. To avoid torque on the mounting due to unbalanced fluid flow, the main circuit is made up of two parallel paths. The full significance of this is explained in

* Manufactured by Lucas Industrial Equipment Ltd.

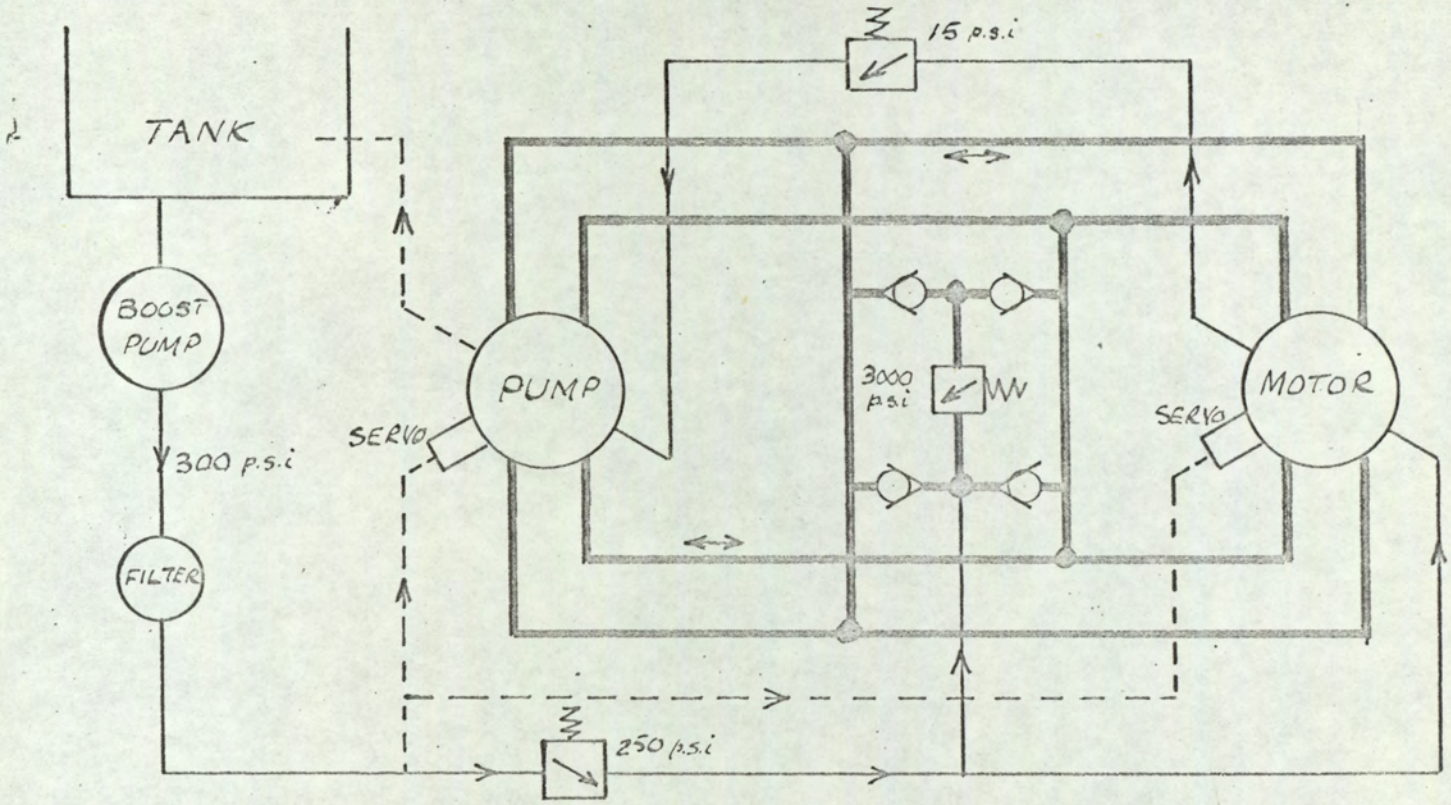

FIG.(A3.1)

HYDRAULIC CIRCUIT

Section (5) of the Appendix.

The supply to the rig at approximately 300 p.s.i. provides the pressure line to the servo-piston control circuits.

3.3 STROKE CONTROL ARRANGEMENTS.

Control of the stroke of the pump and motor is obtained by regulating the position of the servo-piston using a solenoid operated ball valve. This arrangement was described in some detail in Section (4.3). In order to link the stroke control mechanism to the main control circuits it was necessary to design an amplifier to energise the solenoid of each ball valve. The circuit diagram of the amplifier is given on Fig.(A3.2). The current in the solenoid varies between 160 mA and 360 mA to control the servo-piston, the lower value causing a movement towards zero stroke. A fixed stroke setting is maintained when the current is approximately half way between these limits. It is difficult to measure the relationship between the current and the speed of travel of the servo-piston, as there is some hysteresis present. The maximum rate of travel is set up with an input of ± 2 μA either side of balance condition. The input resistance of the amplifier is low, of the order of 1 kΩ.

To hold a fixed stroke setting it is necessary to use a position control system. A linear potentiometer was connected to the manual servo-rod, and hence to the servo-piston, to give a position feedback signal. The circuit detail of the position control system setting the motor stroke is given on

FIG.(A3.2)

CAM PLATE CONTROL AMPLIFIER

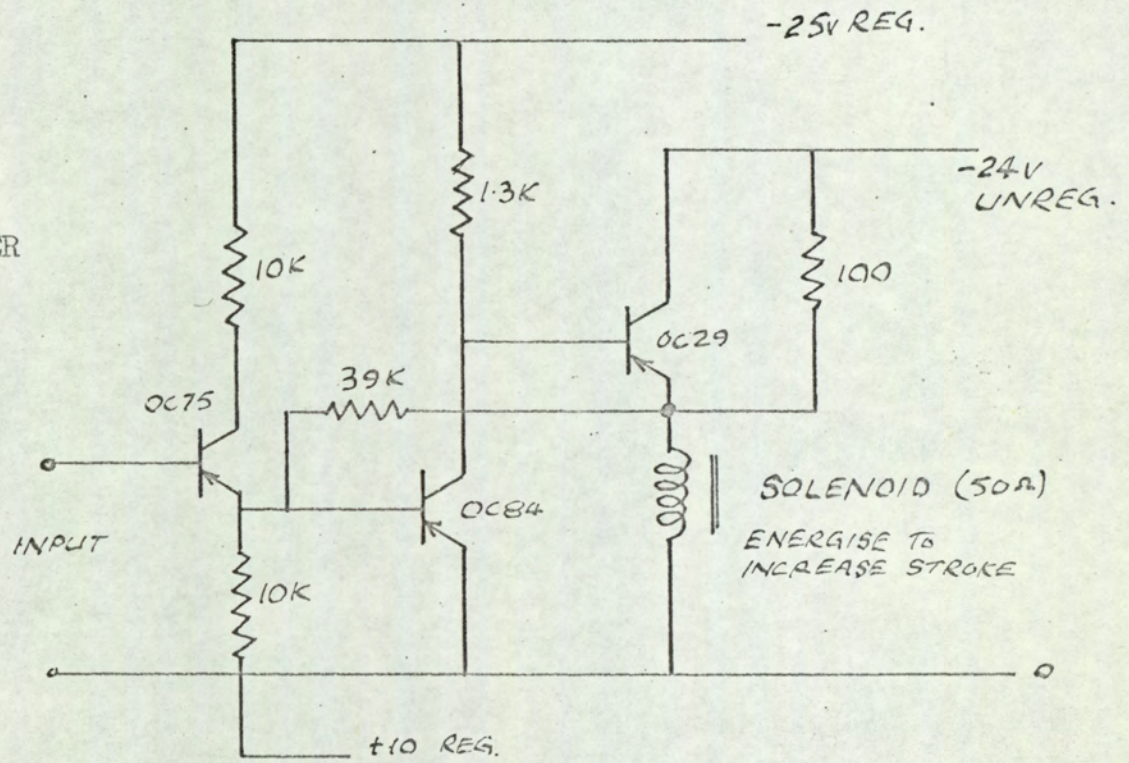

Fig.(A3.3), where the facility is included for switching to maximum stroke for starting. The stroke setting is controlled from the movement of the reference potentiometer. This is also ganged to a second potentiometer which is then used to give the feedforward signal for the pump stroke control system (See Section 4.7). To obtain an indication of the stroke setting on the control panel of the test rig, a moving-coil instrument with 100 μA movement was connected to measure the voltage at point A in the circuit.

The travel of the pick-off potentiometer was approximately half an inch and the control loop gain then gave the maximum rate of movement of the servo-piston with a position error of approximately 0.001 inch. The setting accuracy was therefore high and limited primarily by the linearity of the potentiometer (nominally 0.1%) and drift in the amplifier. The overall accuracy of the stroke setting was expected to be better than 0.5%.

The circuit detail of the position control loop regulating the pump stroke is different from that of the motor and is shown on Fig.(A3.4). There is a facility for switching to zero stroke when starting the rig. The diagram also includes the details of the circuit of the speed control system from the output tachometer. The speed-position control switch changes the control of the pump stroke from the overall speed control system to an isolated position control system.

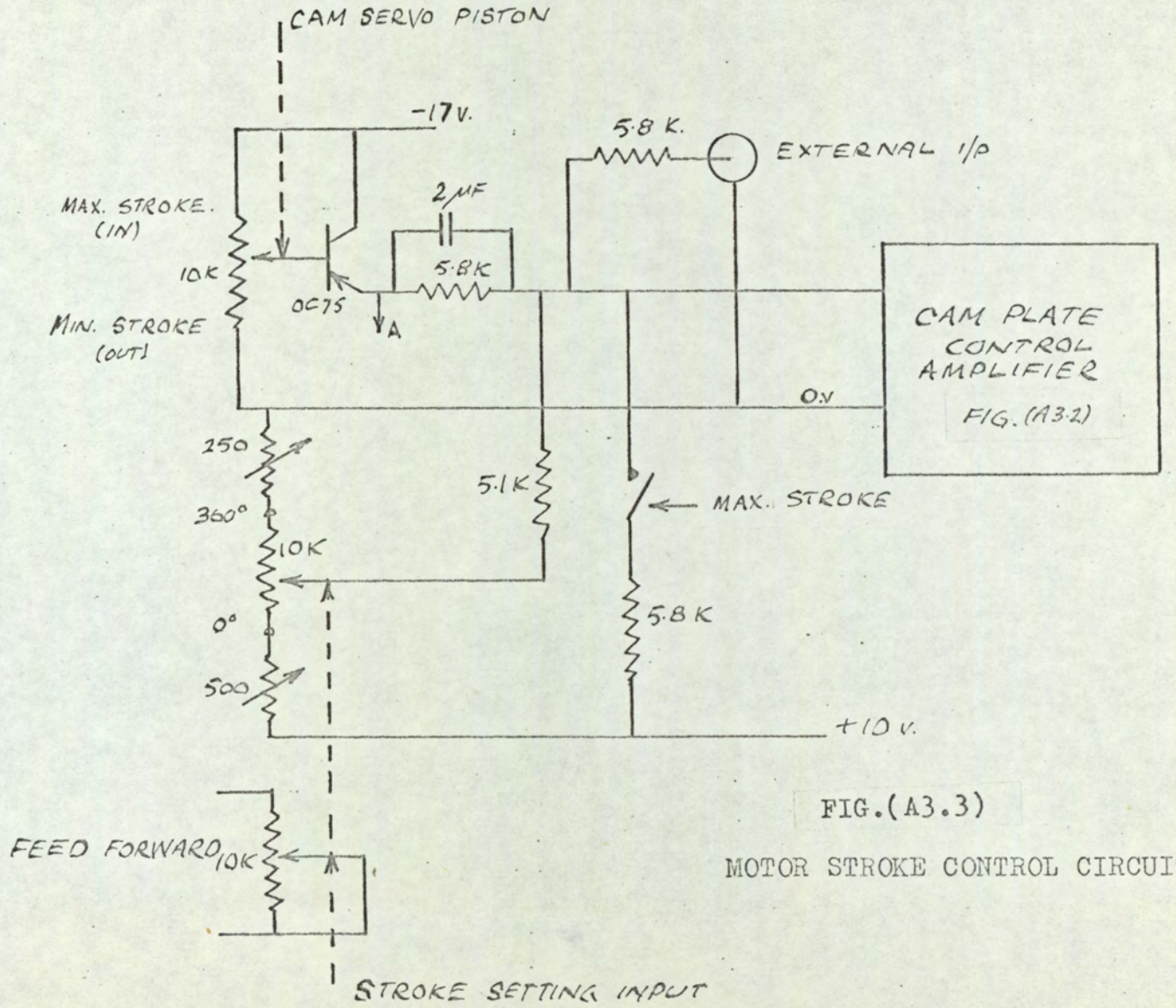

FIG.(A3.3)

MOTOR STROKE CONTROL CIRCUIT

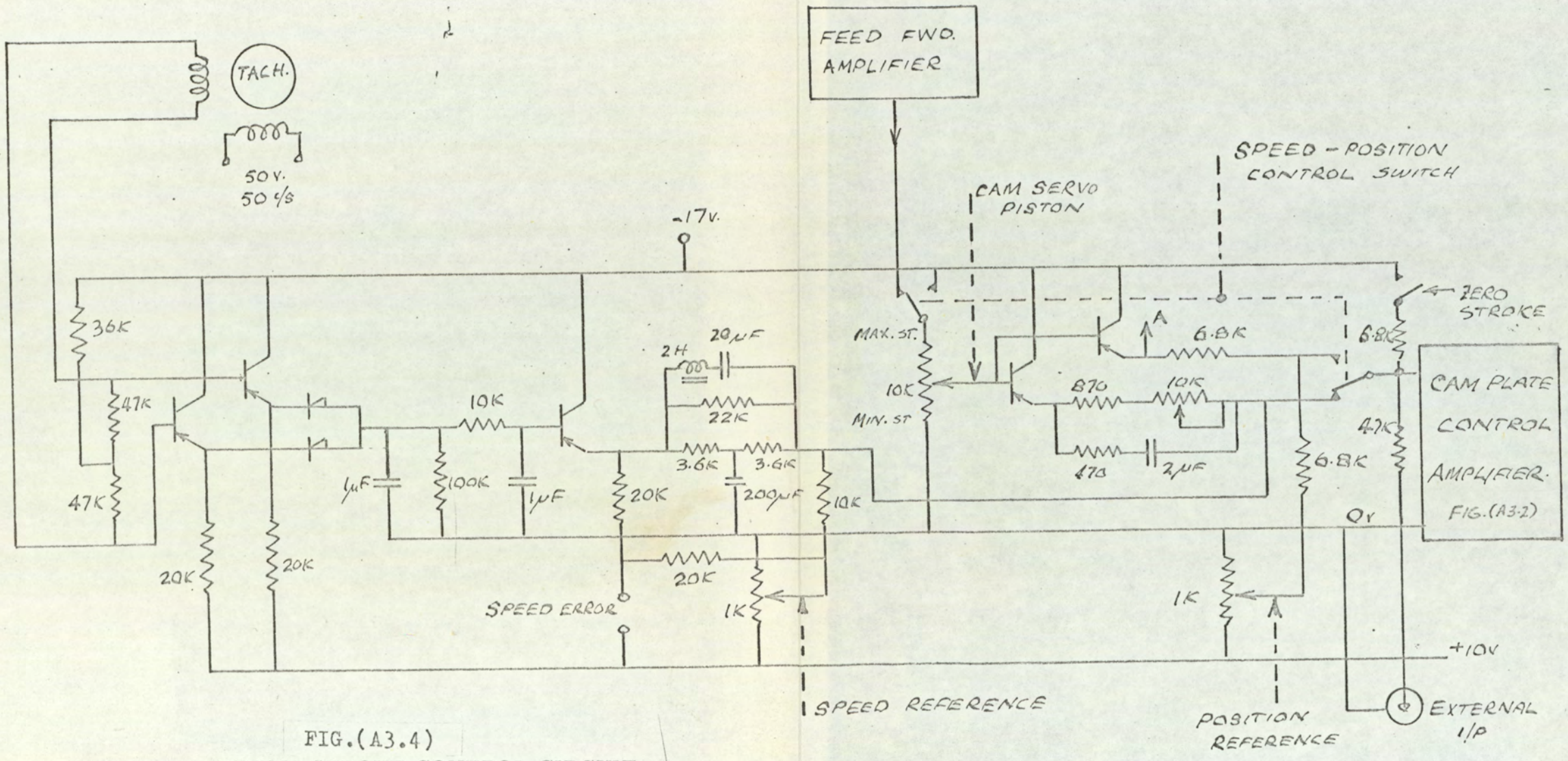

FIG.(A3.4)
PUMP STROKE CONTROL CIRCUIT

4. FEEDFORWARD AMPLIFIER.

To implement the requirements of the feedforward system it was necessary to generate a signal of the form shown on Fig.(4.23). The circuit given on Fig.(A4.1) was designed to do this. The input signal, proportional to the pump speed, was derived from point A in the drive motor speed control circuit of Fig.(A2.3). Additional smoothing of the rectified tachometer signal is incorporated at the input. The set-zero and gain controls were used to set up the required form of transfer characteristic.

5. MEASUREMENT OF EFFICIENCY.

It was required to obtain a continuous measurement of the efficiency of the transmission system. This means that the measuring system must operate automatically and, as far as is known, this form of measurement has not previously been attempted.

The measurement involves taking the ratio of output power to input power. The power in each case was obtained from separate measurements of torque and speed. Torque measurements are difficult to obtain accurately, but with careful design the strain gauge system adopted gave satisfactory results. The choice of strain gauges was dictated in this case by the need to perform the efficiency computation. It was convenient to do this by means of a servo-balanced bridge circuit.

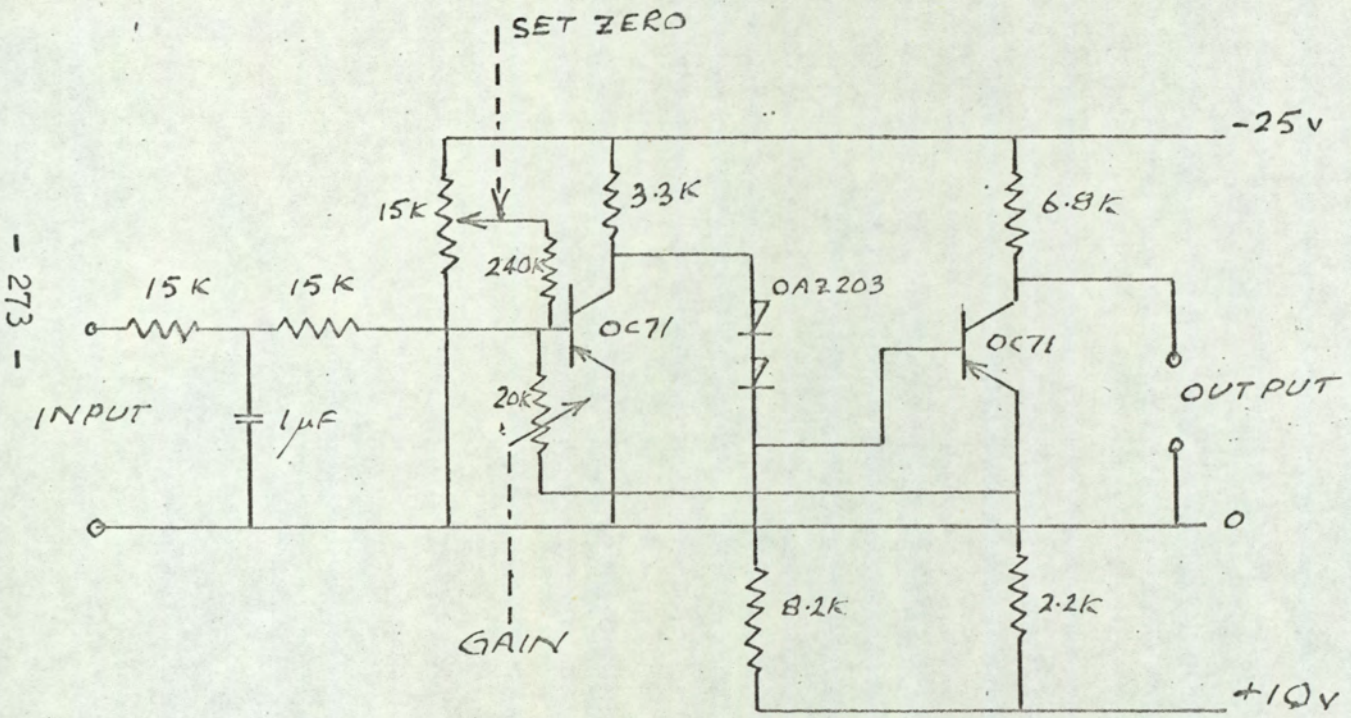

FIG.(A4.1)

FEEDFORWARD AMPLIFIER

An alternative system was considered, based on measurements of the electrical power in the armature of the drive motor and of the loading generator. This was finally discarded due to the difficulty of making accurate allowance for the losses in the electrical machines. The strain gauge system was also preferred because the measurement is made directly on the hydraulic machines and is therefore independent of the form of prime mover and load.

The need to work with small signals from the strain gauge bridges gave rise to a decision to employ a 50 Hz carrier system. This avoids the difficulty of drift in d.c. amplifiers. The carrier was introduced by using a.c. tachometer-generators to measure the speed values. This has the further advantage of removing the problem of commutator ripple present in d.c. tachometer-generators.

5.1 TORQUE MEASUREMENT.

There is difficulty in making measurements on the rotating drive shafts of the machines, due chiefly to the need to employ slip rings to transfer small signals. To avoid this it was decided to measure the torque on the bodies of the pump and motor, by mounting each on a torque-tube. In order that the torque measured in this way should be the same as the shaft torque it is necessary to eliminate two sources of error, (a) unbalanced fluid flow and (b) bending loads.

(a) Unbalanced fluid flow.

If the flow of fluid from the machine is taken from a point off the central axis,

there will be a torque on the body resulting from the difference in pressure between the inlet and outlet ports. To avoid this two inlet and outlet connections were used, these being symmetrically placed about the axis of the machine. The detail of the machine construction is shown on Fig.(A5.1) and this, together with the hydraulic circuit given on Fig.(A3.1), makes the point clear.

(b) Bending loads.

There is a bending load due to the dead weight of the machine and, in as much as this is constant, it could be eliminated in the electrical balancing of the strain gauge bridge. Varying bending loads may also be present due to mechanical unbalance of the rotating parts and these cannot be so eliminated.

Both the effects may be eliminated by an appropriate arrangement of strain gauges. A system of eight gauges was used, these being placed round the circumference of the torque-tube as shown on Fig.(A5.2)(a). When connected in the bridge circuit as shown in Fig.(A5.2)(b), the bending strain will not unbalance the bridge.

The choice of material for the torque-tube required special consideration. Because the tube was necessarily of large diameter to accommodate the gauges and the torque was small, it was not possible to use steel. The shell thickness required in steel is then unreasonably

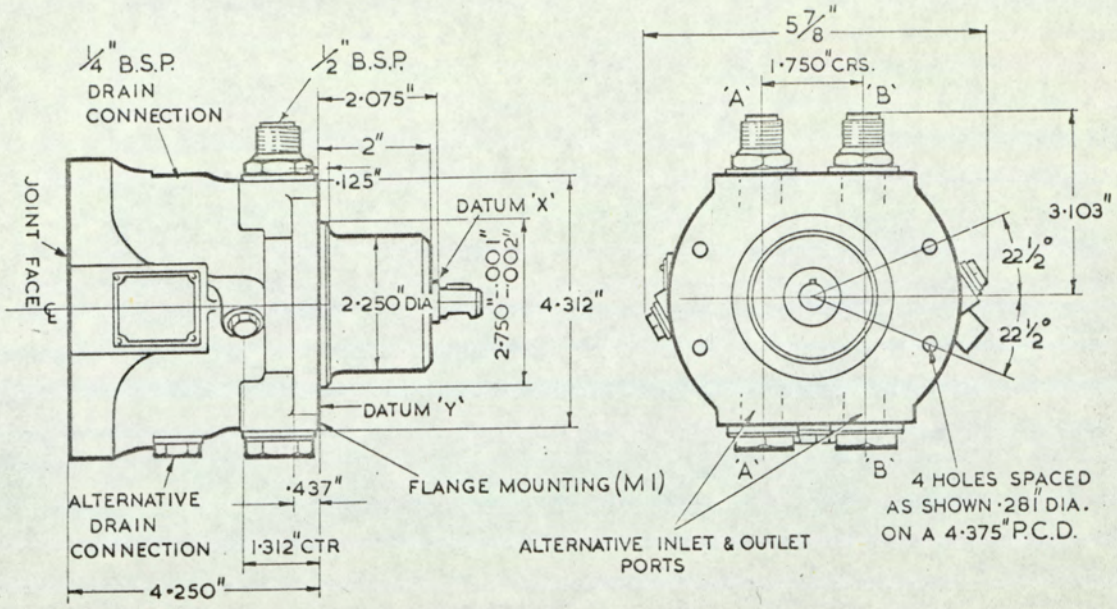

Inlet ports 'A'
Outlet ports 'B'

FIG.(A5.1)

DETAIL OF PUMP AND MOTOR

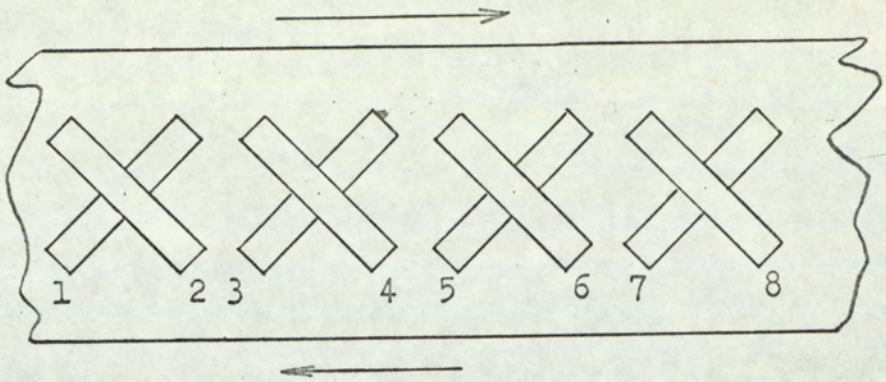

SHEAR STRESS

Gauges (1),(3),(5),(7) in tension
(2),(4),(6),(8) in compression

(a)

DEVELOPED VIEW OF CIRCUMFERENCE

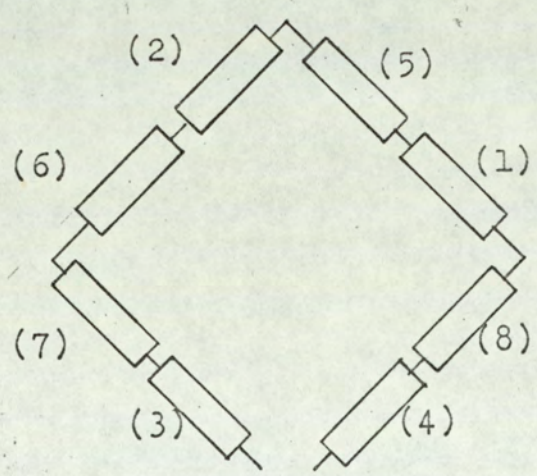

(b)

BRIDGE CIRCUIT

FIG.(A5.2)

ARRANGEMENT OF STRAIN GAUGES

small. A material of high elasticity is required and the most suitable combination of properties is found in the thermo-setting polymer "Araldite"*. The form of torque-tube used is shown in Fig.(A5.3). Two of these tubes were constructed by machining a cast cylinder of the material and efforts were made to ensure that as far as possible the two were identical.

5.2 MECHANICAL DESIGN OF THE TORQUE-TUBE.*

It can be shown that for a cylindrical tube under torsional load the strain ε is given by,

$$\varepsilon = \frac{16\,T}{\pi\,G}\left(\frac{D}{D^4 - d^4}\right) \qquad \text{.....(A5.1)}$$

where T is the torque, G is the shear modulus, D is the outer diameter and d the inner diameter. The shear modulus of "Araldite" is 3.2×10^5 lb/in^2. It is required to find the diameters D and d. Taking the maximum torque of 24 lb ft and the strain limit of 0.1% at this load, a trial and error solution gives $D = 2"$ and $d = 1.6"$.

As the tube was also to carry the dead weight of the machine it is necessary to check that the tube will be strong enough to support the torsion and bending loads together. The maximum stress due to bending is

* The advice of Dr. D.H. Sansome of the Department of Mechanical Engineering, The University of Aston, on this point is acknowledged with gratitude.

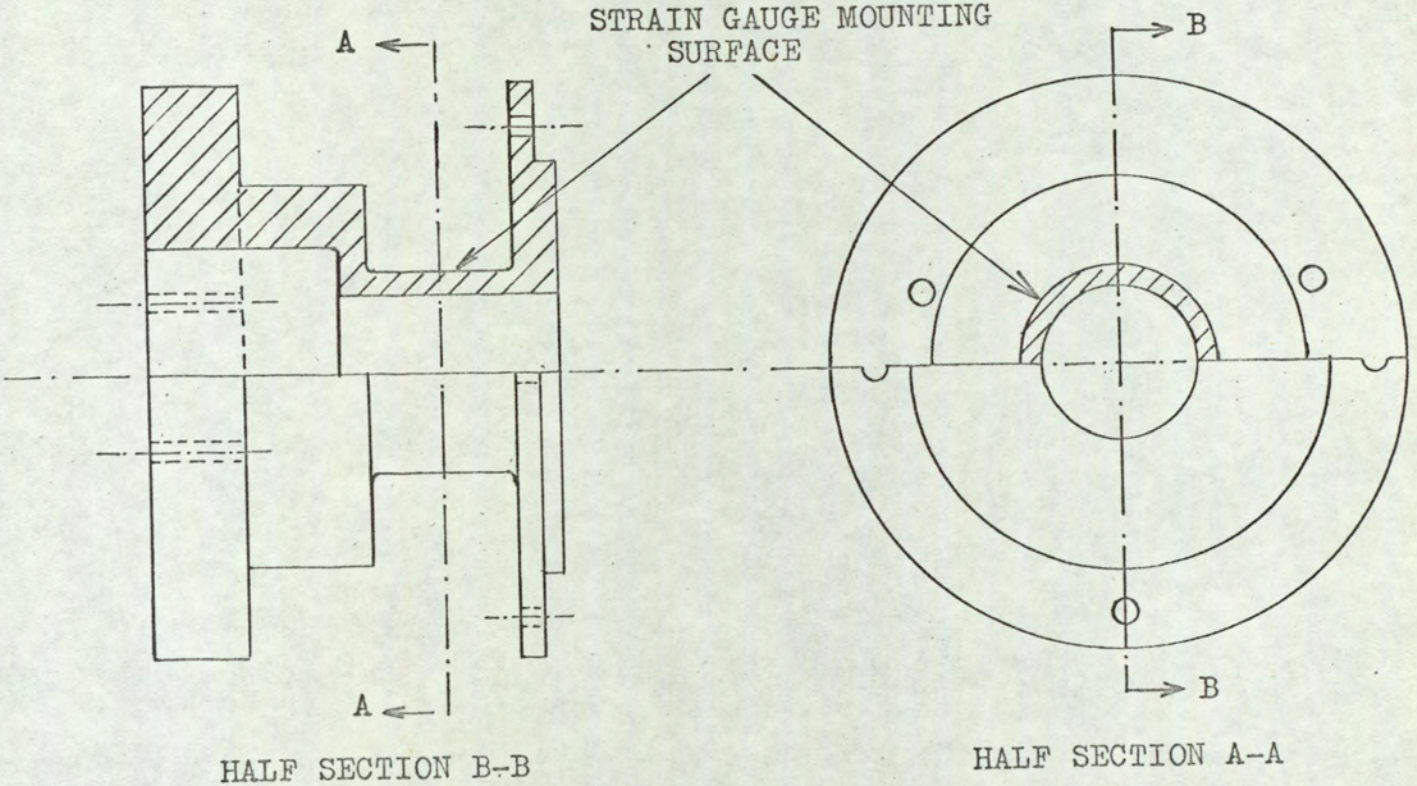

FIG.(A5.3)

DETAIL OF TORQUE TUBE

SCALE:- Half Full Size

given by,

$$S_b = \frac{32\ M\ D}{\pi(D^4 - d^4)} \quad \text{.....(A5.2)}$$

where M is the bending moment applied. The machine weighs 20 lb and the centre of gravity is 6" from the remote end of the torque-tube so we get a bending stress of 260 lb/in^2. The stress due to torsion has been fixed by designing for 0.1% strain and the shear stress is given by,

$$S_t = \varepsilon\ G \quad \text{.....(A5.3)}$$

The resolution of these stresses gives the maximum combined stress S_m,

$$S_m = \frac{S_b}{2} + \frac{1}{2}\sqrt{S_b^{\,2} + 4\ S_t^{\,2}} \quad \text{.....(A5.4)}$$

With the figures obtained above we get a maximum stress of 480 lb/in^2. This is to be compared with a yield point of 9 x 10^3 lb/in^2 for the material. The factor of safety in this case is 19.

5.3 ELECTRICAL DESIGN.

The resistance value of the strain gauges is open to choice. This is subject to the need for high sensitivity in the bridge circuits. It can be shown that the output voltage of the bridge on open circuit, V_o is given by,

$$V_o = V_i\ k\ \varepsilon \quad \text{.....(A5.5)}$$

where V_i is the supply voltage across the bridge,

k is the strain gauge constant and ε is the strain. In order to maximise V_o the gauge constant, the supply voltage and the strain should all be as large as possible. The gauge constant is fixed by the type of gauge. It was decided to use metal foil gauges rather than semiconductor gauges. The metal foil gauges have a lower gauge constant but are the more stable under changes of temperature. The strain is fixed by the mechanical design of the torque-tube and a maximum value of 0.1% has been taken to be consistent with reliable operation. The bridge supply voltage is limited by the power dissipation in the gauges. If the total power dissipated in the eight gauges is P_g and the resistance of each gauge is R_g, the supply voltage is given by,

$$V_i = \sqrt{2 R_g P_g} \quad \text{.....(A5.6)}$$

This shows that gauges of high resistance are to be preferred. Gauges of nominally 2.5 kΩ resistance were used. The maximum power dissipation must be restricted in this case by consideration of the fact that the material on which they are to be mounted is a poor conductor of heat and can also be radically affected by high temperatures. A maximum dissipation of 4 Watt was taken and this leads to a supply voltage of 140 Volt. This would only be used for short term operation and a continuous dissipation of 2 Watt was selected as the basis for further design calculations.

On giving the gauge constant a value of 2, equation (A5.5) may be evaluated to give the maximum output voltage of

280 mV at the maximum power dissipation, and 200 mV at the contiuous rating.

5.4 EFFICIENCY COMPUTATION.

To obtain the efficiency the ratio of the products of torque and speed at the output and input must be computed. This can conveniently be done using the arrangement shown in Fig.(A5.4) which is a servo-balanced bridge system. The pump bridge is supplied with a voltage proportional to the pump speed, so that the open circuit voltage output is proportional to the input power to the pump. Similarly a signal proportional to the output power of the motor is obtained from the motor bridge. To obtain the power ratio, and hence the efficiency, the two bridges are connected in a further bridge which is driven into balance by a servo-motor.

A number of balancing adjustments are included in the circuit of Fig.(A5.4). The potentiometers RV1 and RV2 are fitted to allow an initial resistance balance to be obtained in each bridge when unstrained. It is also necessary to balance the stray capacitance and trimmers C1 and C2 are provided for this purpose. Careful attention to the wiring of the circuit is necessary with a view to keeping the stray capacitance as near to a balanced distribution as possible.

It is intended that the position taken up by the servo-driven potentiometer should indicate the value of the efficiency. The precise relationship is identified in the following analysis. The necessary parameters of

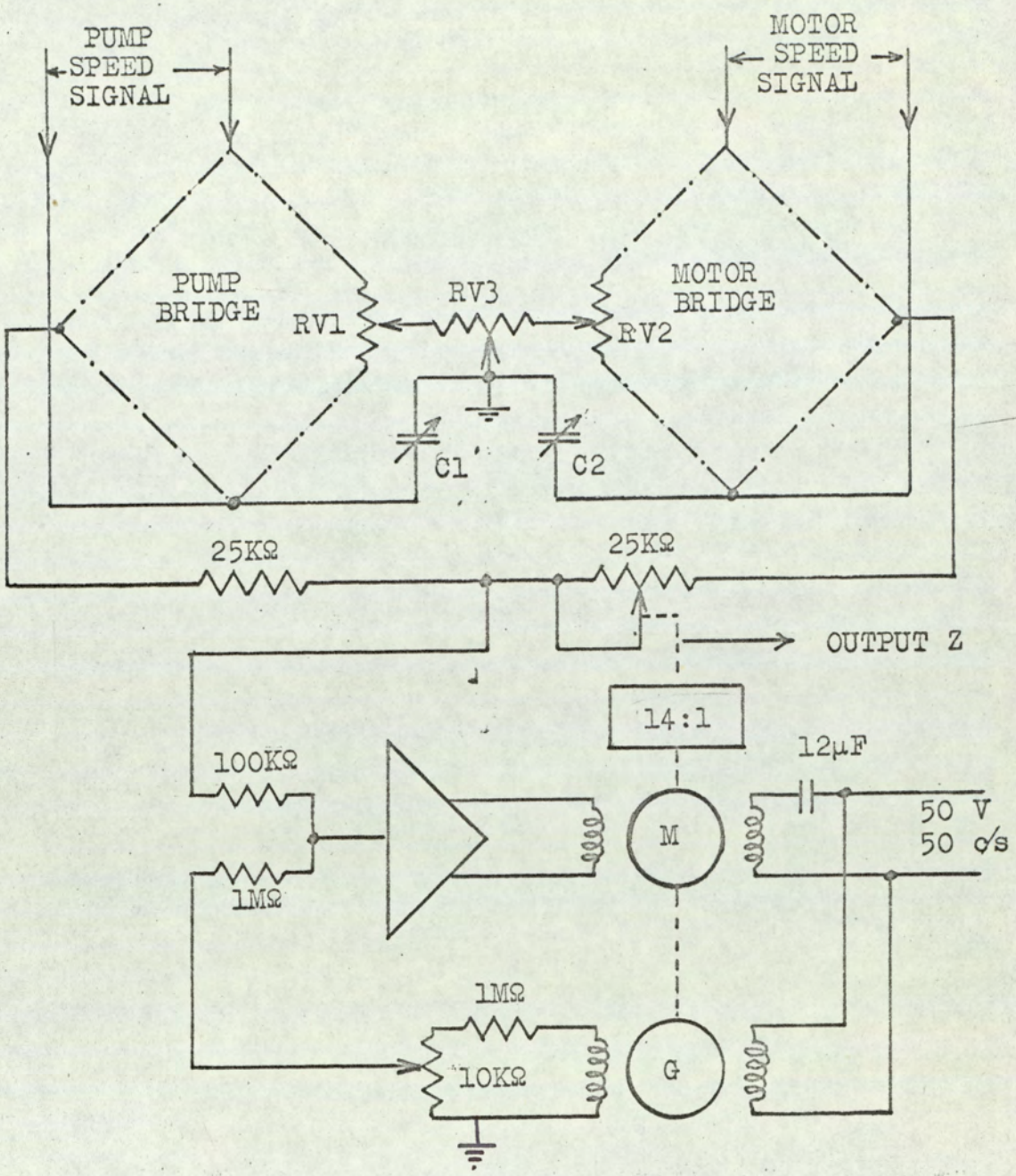

FIG.(A5.4)

EFFICIENCY MEASURING SYSTEM

the circuit are given in Fig.(A5.5), where r_p and r_m represent the source resistance of the pump and motor bridges. The voltage sources E_p and E_m are the open-circuit output voltages of the bridges, which are proportional to the power values. The fractional movement of the balance potentiometer is shown as a. The unbalanced voltage e which is applied to the servo-amplifier is given by,

$$e = \frac{E_p(r_m + a R_m) - E_m(r_p + R_p)}{R_p + a R_m + r_p + r_m} \quad \ldots\ldots(A5.7)$$

At balance e is zero and

$$\frac{E_m}{E_p} = \frac{r_m + a R_m}{r_p + R_p} \quad \ldots\ldots\ldots\ldots\ldots\ldots(A5.8)$$

This ratio is the required efficiency value Z which can be written,

$$Z = a\left(\frac{R_m}{r_p + R_p}\right) + \frac{r_m}{r_p + R_p} \quad \ldots\ldots\ldots(A5.9)$$

This shows that a straight line relationship exists between Z and a. The correspondence between Z and a cannot be very close as long as r_p and r_m remain finite but it is as well to make the relationship as close as possible. For instance it is desirable that a = 1 when Z = 100% . To give this we must have $r_p + R_p = r_m + R_m$. A potentiometer RV3 is incorporated in the circuit of Fig.(A5.4) to allow this setting to be achieved by a differential adjustment of r_m and r_p. The minimum value of efficiency which can be registered is set when a is zero. We then have,

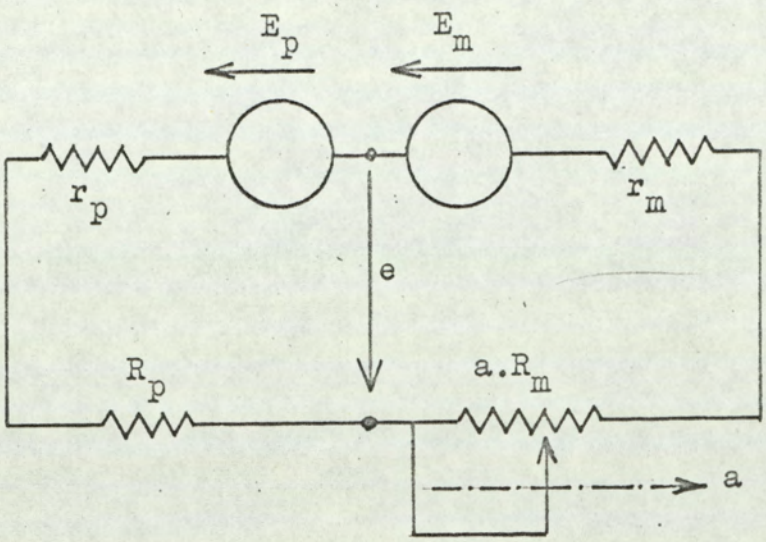

FIG.(A5.5)

SERVO-BRIDGE CIRCUIT

$$Z = \frac{r_m}{r_p + R_p} \quad \text{.....(A5.10)}$$

To make this small enough to allow an adequate range of measurement requires a high value of R_p. In this case R_p was set to 25 kΩ so that, with r_m and r_p nominally 5 kΩ the minimum indicated efficiency becomes 16.7%. A Wheatstone Bridge was used to set equality between r_p and r_m, giving at the same time an accurate value for use in the calculation. A calibration graph can then be drawn relating the efficiency to the angle of rotation of the balancing potentiometer. This is given on Fig.(A5.6).

5.5 SERVO-BALANCING SYSTEM.

This system is required to respond to the unbalanced voltage e of Fig.(A5.5), causing the servo-motor to drive the balancing potentiometer to the position where e is zero. The arrangement is shown in detail on Fig.(A5.4).

The loop gain of the servo changes with the value of the efficiency and with the power transmitted. These changes are evident in the gain of the servo-bridge circuit of Fig.(A5.5). The gain is obtained by differentiation of equation (A5.7) as,

$$G = \frac{de}{da} = \frac{E_p R_m}{R_p + a R_m + r_p + r_m} \quad \text{.....(A5.11)}$$

for small changes about the balance position. Here the gain G varies with E_p and a.

The minimum gain occurs at a = 1 when,

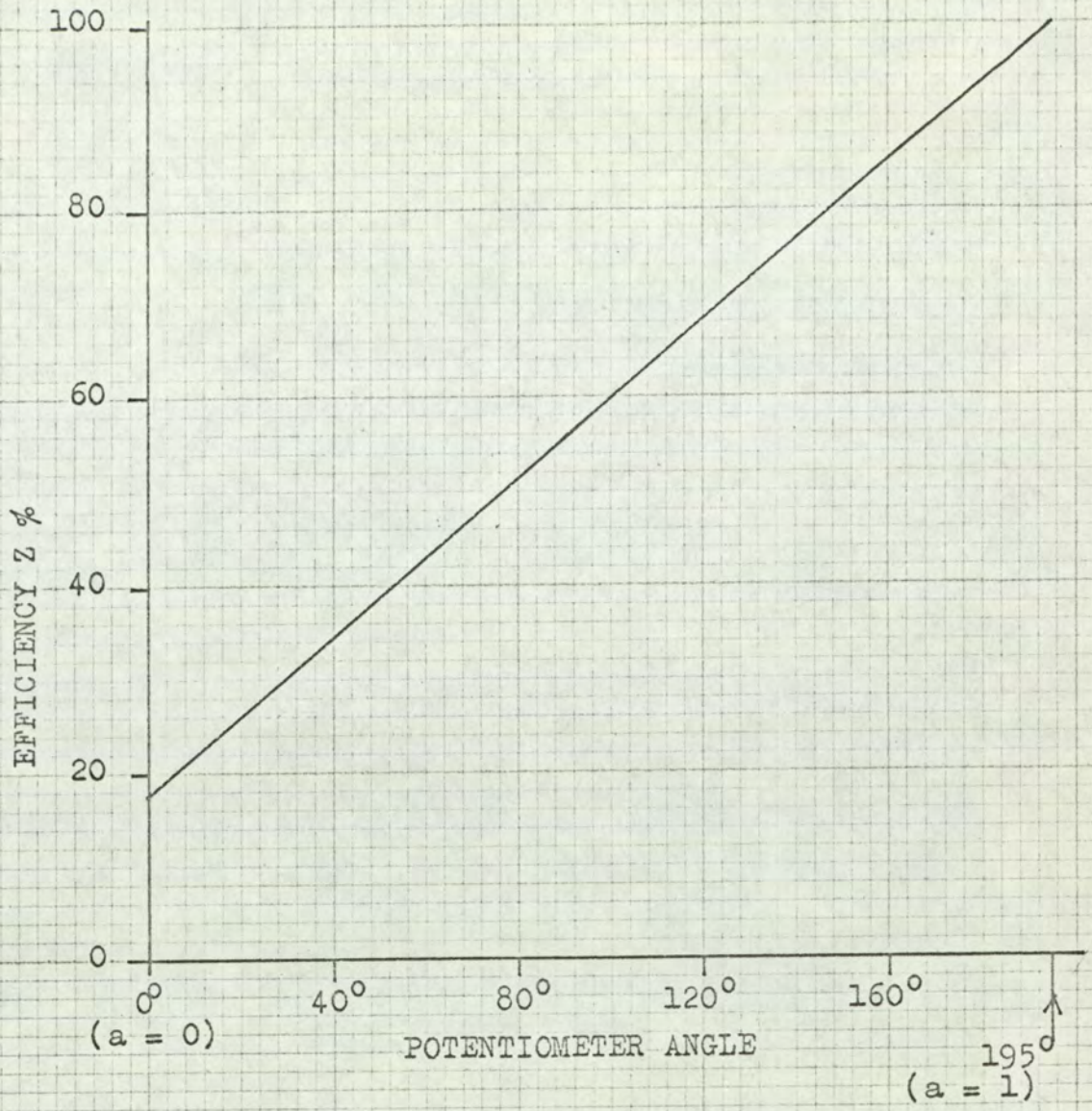

$$Z = \frac{a\,R_m}{R_p + r_p} + \frac{r_m}{R_p + r_p}$$

$R_m = 25.75\ k\Omega \quad r_m = 5.52\ k\Omega \quad R_p + r_p = 31.2\ k\Omega$

FIG.(A5.6)
CALIBRATION GRAPH

$$G_{min} = \frac{E_p R_m}{R_p + r_p + R_m + r_m} \quad \text{.....(A5.12)}$$

With the nominal values of resistances this gives,

$$G_{min} = \frac{5}{12} E_p \quad \text{.....(A5.13)}$$

The maximum gain appears at a = 0,

$$G_{max} = \frac{E_p R_m}{R_p + r_p + r_m} \quad \text{.....(A5.14)}$$

$$\text{i.e. } G_{max} = \frac{5}{7} E_p \quad \text{.....(A5.15)}$$

It can be seen that the variation of gain with a is not large by comparison with that due to E_p. Since E_p is proportional to the power input to the pump it may vary as much as 10:1 . This change of gain will affect both the setting accuracy and the dynamical performance of the system.

The setting accuracy is determined by the sensitivity with which a balance can be resolved. This is largely dependent on the sticking friction which the servo-motor must overcome before a movement can take place. The unbalanced voltage required in the bridge, in order to produce sufficient torque to overcome the friction, determines the zone of uncertainty about the balance position. To make this zone acceptably small requires an appropriate choice of gain in the servo-amplifier.

The zone of uncertainty required is taken as $\pm 1\%$ efficiency at minimum gain. It is assumed that the minimum value of the input power will be one tenth of full-load power. The bridge circuit was designed in Section (A5.3) to give an output of 280 mV at maximum power, so that the present design calculation will be based on 28 mV. The value of the minimum gain is given by equation (A5.13) and takes the value 1.17×10^{-2} Volt. Hence a balance error of 1% will give an unbalanced voltage of 117 μV. The gain of the servo-amplifier must therefore be such that the servo-motor moves freely with this level of input signal.

An amplifier designed for this purpose followed the circuit diagram shown on Fig.(A5.7). Particular attention has been given to obtaining the high gain required with freedom from 50 Hz noise. With this amplifier the sticking level of the servo-motor was 50 μV at the input and full output was obtained with 200 μV. The internal noise was equivalent to 4 μV at the input. This performance leads to the expectation that the zone of uncertainty will be 0.5% under the worst conditions.

The need to work with such low input signals in this amplifier justified the choice of an a.c. carrier system. It would be very difficult to achieve this performance with d.c. amplification. It is also evident that precise balancing of the strain gauge bridges is required to keep the residual unbalanced voltage of each to a low value.

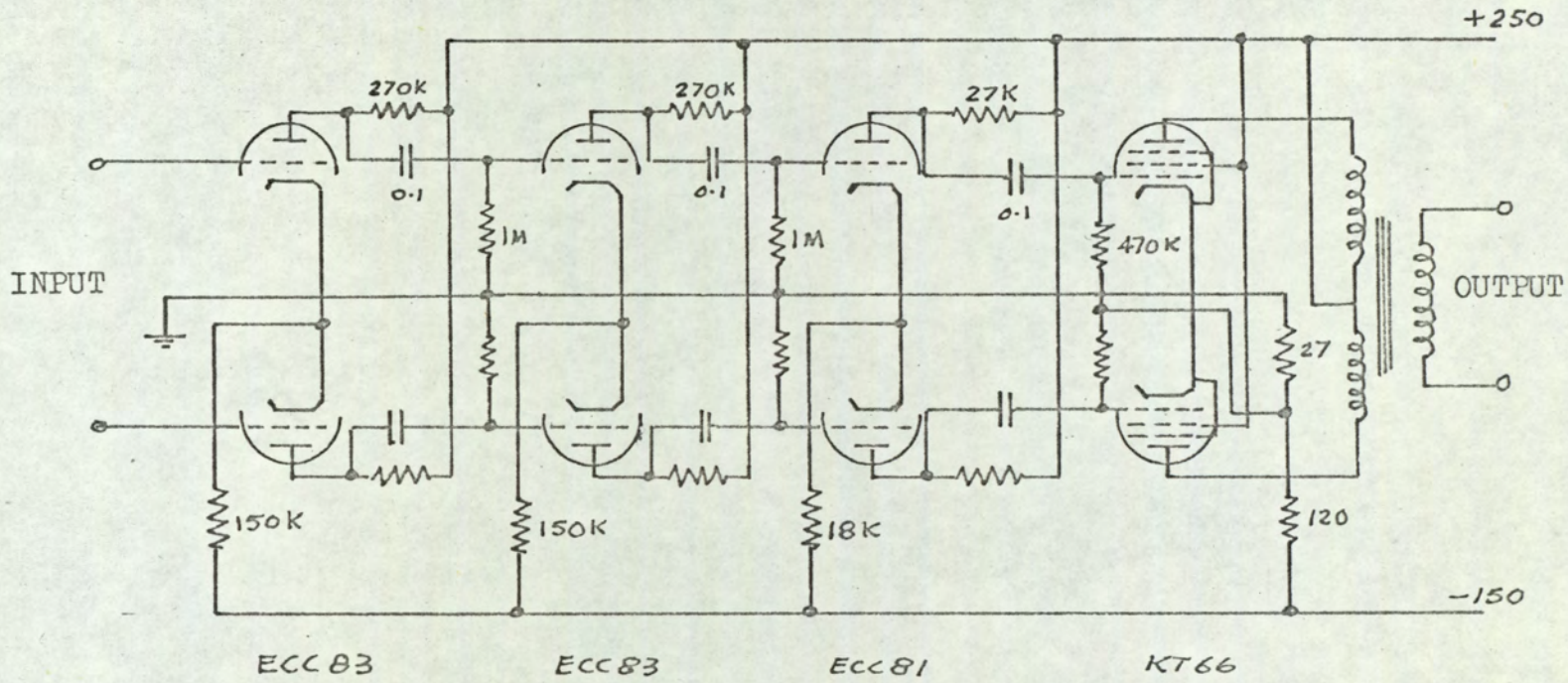

FIG.(A5.7)

50 c/s SERVO AMPLIFIER

The variation of the loop gain of the system also changes the dynamical performance of the servo. Instability is possible at the high gain condition and tachometer feedback is included to prevent oscillation at this extreme. It is unwise to use more than the minimum of tachometer signal however, since the speed of response is considerably affected when the loop gain is low. For instance, if the tachometer voltage at the input to the servo-amplifier is 1 mV at the maximum speed, the balance error would have to be 10% at the minimum gain before full speed is realised. This is about five times the error required for full speed in the absence of the tachometer signal. In practice it was necessary to set the tachometer signal to about twice this value.

The speed of response can be increased by reducing the gear ratio between the servo-motor and the balancing potentiometer. A limitation to this is set by the requirement for a low sticking level since a considerable proportion of the sticking friction is due to the potentiometer. An effective ratio of 14:1 was used as the minimum consistent with the required zone of uncertainty. With this ratio the balance potentiometer was completely traversed in 0.5 sec at full speed. At low gain the settling time for a large error correction was about 2 sec.

The performance achieved in this way was considered adequate in resolution and speed of response to meet the requirements of the optimising system.

5.6 SPEED SIGNAL AMPLIFIERS.

The strain gauge bridges were designed in Section (A5.3) to operate with a maximum supply voltage of 140 Volt. It is required that this voltage be varied in proportion to the pump or motor speed so that the bridge output will be proportional to power. The output from a standard 2", 50 Hz a.c. tachometer-generator is approximately 7 Volt per 1000 r.p.m., so that amplification is needed in the supply to the bridges.

An amplifier for this purpose requires chiefly a reliably maintained gain, low distortion, small phase shift and high input resistance. The input resistance is limited by the requirement that the maximum load placed on the tachometer-generator should correspond to not less than 100 kΩ resistance. The gain required is approximately 10.

The form of amplifier designed for this purpose is shown in Fig.(A5.8). The gain is precisely defined by the turns ratio of the output transformer secondary windings, two of which form the feedback circuit. The input circuit is balanced because it is convenient to centre the tachometer voltage at earth potential in the rectifier circuit used in the speed control system of the transmission; see Fig.(A3.4). There is also an advantage in reducing distortion as the amplifier is symmetrical. In addition to stabilising the gain, the feedback from the output transformer also ensures a high input resistance and low phase shift.

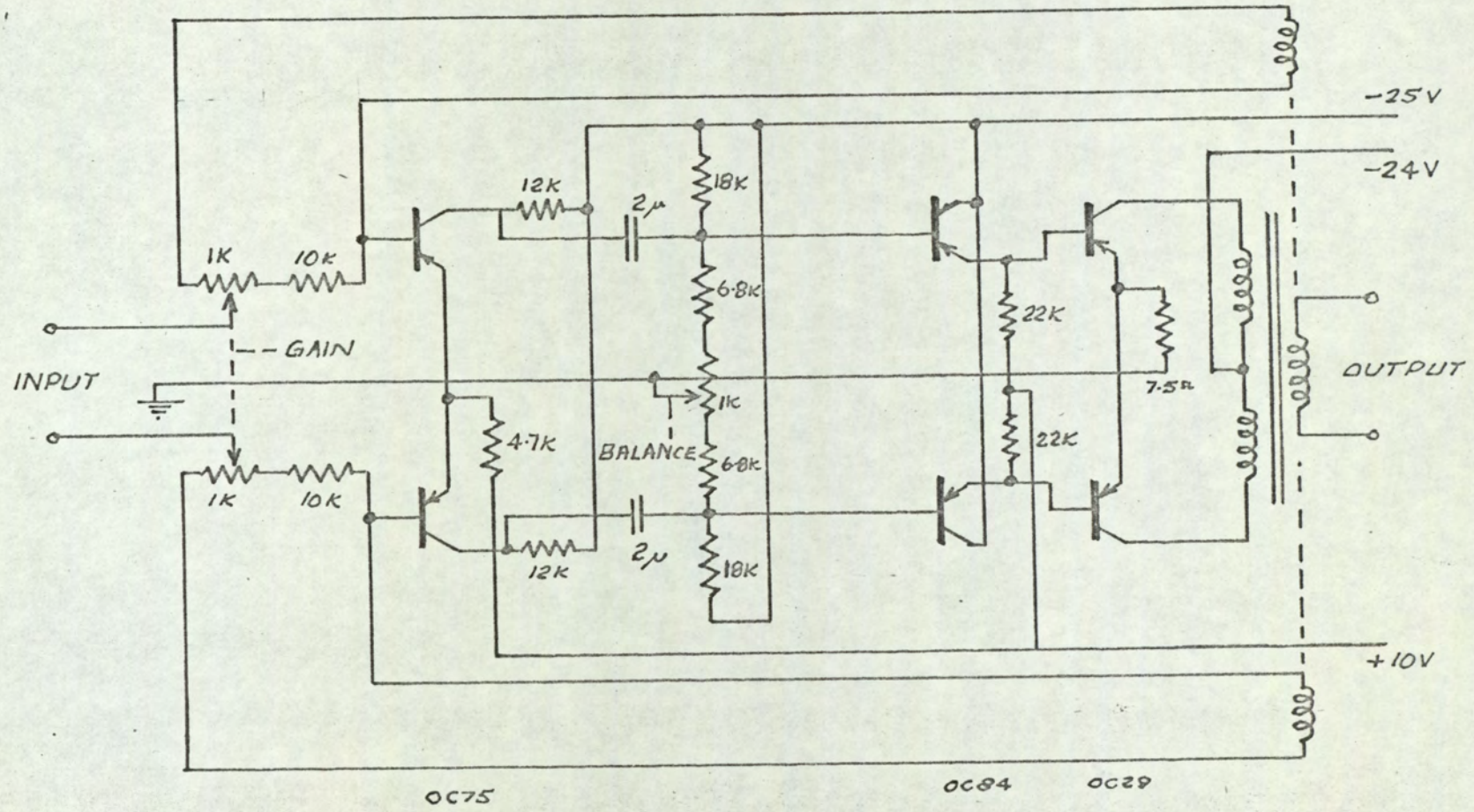

FIG.(A5.8)

SPEED-SIGNAL AMPLIFIER

The circuit gives an undistorted output of 170 Volt with an input signal of 30 mV on open loop. On closed loop the gain is nominally 10 so that the error voltage is 0.2% of the input . This is sufficiently small to ensure consistent performance inspite of changes of the open loop gain with temperature. The phase shift through the amplifier at 50 Hz was too amall to be measured by normal methods.

A means of adjusting the gain is provided by the ganged potentiometers in the input circuit. This adjustment raises the gain by reducing the feedback gain.

5.7 SETTING-UP PROCEDURE.

A number of adjustments were necessary to set up the efficiency measuring system ensuring accurate operation.

(a) Balancing adjustment.

The strain gauge bridges were first balanced with the resistance and capacitance adjustment under zero torque conditions. During this adjustment the bridges were supplied through their respective speed-signal amplifiers, since the stray capacitance of the amplifier output transformer can affect the bridge balance.

The resistance RV3 in Fig.(A5.4) was set to equalise the resistance in the two arms of the servo-bridge circuit. A Wheatstone Bridge was used to compare the resistance values. The need for this setting was identified in Section (A5.4).

(b) Amplifier gain adjustment.

Each of the strain gauge bridges has been designed to give an open circuit voltage proportional to the mechanical power. The efficiency measurement is made by comparing the voltages of the two bridges. For the efficiency value to be correct the proportionality constant, relating voltage to power, for each bridge must be the same. The proportionality constant involves the tachometer-generator constant, the strain gauge constant, the torque/strain constant of the torque-tube and the gain of the speed signal amplifier. Of these the amplifier gain is the most readily adjustable to compensate for differences in the other constants between the two channels.

Differences in the tachometer-generator constants were compensated first. The relative gain of the two amplifiers was adjusted to equalise the voltages supplied to the two bridges, when the pump and motor were running at precisely the same speed. In this the speeds were compared stroboscopically. At the same time the relative phase of the two voltages was checked, by backing off the output of one amplifier against the other to form a difference signal. The phase error was found to be less than 2^{o} and this is adequate.

The differences in the strain gauge and torque-tube constants were next compensated, by a further adjustment of the amplifier gain. To do this the

input of each amplifier was transferred to a reference supply. The two reference supplies were then adjusted to equalise the output voltages of the amplifiers. With the pump and motor rotating slowly, torque was applied to the motor sufficient to raise the hydraulic pressure to 3000 p.s.i.. In this condition it may be assumed that the torque on the two machines is the same when both are set to maximum stroke, as the flow in the system is small. The relative gain of the amplifiers was adjusted to equalise the bridge output voltages, i.e. so that the balancing servo found the 100% position.

5.8 GENERAL OBSERVATIONS.

In designing the efficiency measuring system efforts were made to obtain as accurate a measurement as possible. It should be noted however that extreme accuracy is not important in this application. The optimising system seeks to locate the point of maximum efficiency and in this it is necessary only to detect a change of efficiency, i.e. the absolute value is not important. The chief requirement is the repeatability of results.

The main factor affecting the repeatability of the measurements is drift in the balance of the strain gauge bridges. A change of balance can be caused by temperature variations, particularly if the temperature is not the same round the torque-tube. The temperature will change with the power input to the gauges and this in turn depends on the pump and motor speeds.

To ensure consistent operation in this respect the bridges were energised at their nominal working voltage for half an hour before running the rig. The bridge balancing adjustment was then repeated before taking measurements. With these precautions it is expected that the results would be repeatable within 1% of efficiency.